

**GREEN TECHNOLOGY FOR WATER PURIFICATION:  
INVESTIGATIONS ON SOLAR PHOTOCATALYSIS FOR THE  
MINERALIZATION OF PESTICIDE POLLUTANTS IN WATER**

*Thesis submitted to  
Cochin University of Science and Technology  
in partial fulfillment of the requirements  
for the award of the degree of  
Doctor of Philosophy  
in  
Environmental Chemistry  
Under the faculty of Environmental Studies*

*By*

**Shibin O. M.  
(Reg. No. 4090)**



**SCHOOL OF ENVIRONMENTAL STUDIES  
COCHIN UNIVERSITY OF SCIENCE AND TECHNOLOGY  
KOCHI - 682 022**

*April 2018*

# **Green Technology for Water Purification: Investigations on Solar Photocatalysis for the Mineralization of Pesticide Pollutants in Water**

*Ph.D. Thesis under the Faculty of Environmental Studies*

*Author*

**Shibin O. M.**  
Research Scholar  
School of Environmental Studies  
Cochin University of Science and Technology  
Kochi – 682 022  
Kerala, India

*Supervising Guide*

**Dr. Suguna Yesodharan**  
Professor (Emeritus)  
School of Environmental Studies,  
Cochin University of Science and Technology  
Kochi – 682 022  
Kerala, India

School of Environmental Studies  
Cochin University of Science and Technology  
Kochi, Kerala, India 682 022

*April 2018*



**SCHOOL OF ENVIRONMENTAL STUDIES**  
**COCHIN UNIVERSITY OF SCIENCE AND TECHNOLOGY**  
KOCHI - 682 022

---

**Dr. Suguna Yesodharan**  
Professor (Emeritus)

---

## Certificate

This is to certify that this thesis entitled "**Green Technology for Water Purification: Investigations on Solar Photocatalysis for the Mineralization of Pesticide Pollutants in Water**" is an authentic record of the research work carried out by **Mr. Shibin O. M.** (Reg. No. 4090), under my guidance at the School of Environmental Studies, Cochin University of Science and Technology in partial fulfillment of the requirements for the award of the degree of Doctor of Philosophy in Environmental Chemistry and no part of this work has previously formed the basis for the award of any other degree, diploma, associateship, fellowship or any other similar title or recognition. All the relevant corrections and modifications suggested by the audience during the pre-synopsis seminar and recommended by the Doctoral committee have been incorporated in the thesis.

Kochi - 22  
-04-2018

**Dr. Suguna Yesodharan**  
(Supervising Guide)



## *Declaration*

I do hereby declare that the work presented in the thesis entitled **“Green Technology for Water Purification: Investigations on Solar Photocatalysis for the Mineralization of Pesticide Pollutants in Water”** is based on the authentic record of the original work done by me, for my Doctoral Degree under the guidance of **Dr. Suguna Yesodharan**, Professor (Emeritus), School of Environmental Studies, Cochin University of Science and Technology in partial fulfillment of the requirements for the award of the degree of Doctor of Philosophy in Environmental Chemistry and no part of this work has previously formed the basis for the award of any other degree, diploma, associateship, fellowship or any other similar title or recognition.

Kochi – 22  
-04-2018

**Shibin O. M.**



---

## *Acknowledgements*

*It gives me immense pleasure to acknowledge all the people who have helped me in different ways for completing my Ph.D. work successfully. I humbly dedicate this work to all those who have helped me in exploring the vast expanses of knowledge.*

*I take immense pleasure to express my sincere thanks and deep sense of gratitude to my supervising guide, Dr. Suguna Yesodharan, Professor (Emeritus), School of Environmental Studies (SES), Cochin University of Science and Technology (CUSAT). I was fortunate to have her support and guidance throughout my research career. The high level of encouragement and personal guidance from her laid the strong foundation for this work. Above all her overwhelming attitude to help her students is the primary reason for the timely completion of this work.*

*I find no words to express my intense gratitude and respect to Dr. E. P. Yesodharan, Professor (Emeritus), School of Environmental Studies (SES), Cochin University of Science and Technology (CUSAT) for his inspiring guidance, heartfelt support and affection. His deep knowledge level, dedication and keen interest helped me for the timely completion of this work. His timely advice, meticulous scrutiny, scholarly inventions and scientific approach have helped me to a very great extent to accomplish this task.*

*I offer my gratitude to the present Director of SES, Prof. Dr. S. Rajathy Sivalingam and the previous Directors Prof. Ammini Joseph and Dr. Harindranathan Nair for providing all the facilities of the school for the smooth conduct of my research. I also wish to place on record my thanks to Prof. I.S. Bright Singh, Dr. Sivanandan Achari and Dr. M. Anand, faculty members of the school, for all their suggestions, help, support and encouragement throughout the period of research. I also thank the non-teaching staff of the school for their help and assistance.*

*I would like to express my sincere and heartfelt gratitude to all the research scholars of our laboratory, Mr. Hariprasad, Ms. Vidya, Mr. Rajeev, Dr. Anju, Dr. K.P. Jyothi, Ms. Sindhu, Ms. Phonsy, Ms. Gayathri, Ms. Deepthi, Ms. Veena and all other research scholars in SES for their timely advice, help and affection, which made my stay in the laboratory a pleasant one.*

*I place on record, my gratitude to the Cochin University of Science and Technology for providing the necessary facilities.*

*I would like to extend my sincere gratitude to the management of Süd-Chemie India Pvt Ltd. (SCIL), for giving permission to do this research work. I am also expressing my gratitude for the help and support given by Dr. Sreekala, Dr. K. Anas, Dr. Rajesh Gopinath, Dr. C.U. Aniz, Dr. K.S. Thushara, Dr. P. Unnikrishnan, Mr. Jithesh, Mr. Kishore Ravindran, Ms. Rekhasree, Mr. Mohammed Saneeb and all the friends and well-wishers of SCIL family.*

*I find no words to express my gratitude and respect to Dr. K.K. Abdul Rashid and Ms. K. H. Khadeeja Beevi for their help and support.*

*I appreciate the encouragement and help given by Dr. V. Babu at every stage of this work.*

*Finally I thank, my parents, my in-laws and above all my wife and son for providing me continuous support and inspiration to carry on with my research.*

*Above all, O' my Lord, this piece of work is accomplished only with your blessings and mercy showered upon me. I bow before O' Lord for all with a sense of humility and gratitude.....*

***Shibin O. M.***

## ||||| Preface |||||

Water scarcity is one of the major threats facing the world today. The problem is aggravated by water pollution, which is the outcome of population growth, industrialization and life style. Extensive use of pesticides for agriculture and public health has been contaminating water bodies. Technology development for waste water treatment (so that it can be reused) is a major field of research today. In this context, Advanced Oxidation Process (AOP) often termed as “treatment process of 21<sup>st</sup> century” for the mineralization of trace amounts of chemical contaminants in polluted waters gains special significance.

AOPs utilize the in-situ generated  $\cdot\text{OH}$  radicals and other reactive oxygen species (ROS) for initiating chemical reactions and degrade the organic and inorganic contaminants present in water. The non-selective  $\cdot\text{OH}$  radical is capable of degrading most of the chemical and biological contaminants. Generation of  $\cdot\text{OH}$  radicals can be achieved by both photochemical and non-photochemical methods. Some of the methods used for the purpose are radiolysis, photolysis, photocatalysis, Fenton oxidation, microwave catalysis, sono-catalysis etc. and their combination. Main advantages of AOP include nonhazardous nature of the end products, absence of sludge formation, simultaneous mineralization of multiple pollutants etc.

In the current study, solar photocatalysis is investigated in detail as an AOP for the removal of pesticide pollutants from water. ZnO is used as the catalyst. Diquat, a herbicide and Carbendazim, a fungicide are chosen as the test pollutants.

Main objectives of the study are:

- Detailed investigation on exploiting the potential of ZnO as a visible light active photocatalyst for the removal of selected pesticide pollutants from water using diquat and carbendazim as the test molecules and sunlight as the energy source.
- Photocatalytic degradation studies of combination of pollutants, evaluation of the mutual effect on the mineralization rate and identification of optimum reaction parameters for eventual field application.
- Investigation on the effect of formulation additives on the photocatalytic degradation and mineralization of diquat and carbendazim.
- Investigation on the role of natural contaminants in water on the efficiency of the process.
- Identification of various intermediates formed during the process, their stability and effect on the mineralization efficiency of the process.
- Elucidation of the kinetics and mechanism of the photocatalytic degradation of the pollutants.
- Application of the laboratory-optimized parameters for the solar photocatalytic removal of carbendazim and diquat from real field water matrix.

The study is the first major investigation on the application of solar energy for the irreversible removal of diquat and carbendazim pesticides from water. The inconsistency in the effect of dissolved salts/anions/cations on the efficiency of the process also has been illustrated in the study. The

study has conclusively established that the natural contaminants in non-saline water bodies (river, well) do not hinder the photocatalytic degradation of diquat and carbendazim. Many other aspects relevant for the commercial application of the process have also been evaluated and reported in this thesis.

The thesis consists of nine chapters and annexures as follows:

Chapter 1 Introduction: Background literature.

Chapter 2 Objectives of the study, Materials and methods, Plan of the thesis.

Chapter 3 Solar photocatalysis mediated by ZnO for the removal of carbendazim fungicide from water.

Chapter 4 Solar photocatalysis mediated by ZnO for the removal of diquat herbicide from water.

Chapter 5 Solar photocatalysis mediated by ZnO for the removal of the combination of diquat and carbendazim from water.

Chapter 6 Solar photocatalysis mediated by ZnO for the removal of carbendazim formulation from water.

Chapter 7 Solar photocatalysis mediated by ZnO for the removal of diquat formulation from water.

Chapter 8 Solar photocatalysis mediated by ZnO for the removal of diquat and carbendazim pollutants from natural water systems.

Chapter 9 Summary and Conclusion.

Annexures:

Annexure 1: List of the abbreviations used in the thesis.

Annexure 2: List of research papers (A) published in peer reviewed journals and (B) presented in conferences.

Annexure 3: Reprints of papers published in journals.



# Contents

## *Chapter 1*

|  |                |
|--|----------------|
| <b>INTRODUCTION: BACKGROUND LITERATURE .....</b>                               | <b>01 - 46</b> |
| 1.1 General.....   | 01             |
| 1.2 Conventional waste water treatment .....                                   | 10             |
| 1.3 Advanced Oxidation processes (AOPs) .....                                  | 12             |
| 1.3.1 Photocatalysis .....   | 16             |
| 1.3.1.1 Homogeneous photocatalysis .....                                       | 17             |
| 1.3.1.2 Heterogeneous Photocatalysis .....                                     | 24             |
| 1.3.1.3 Use of sunlight as energy source in photocatalysis .....               | 33             |
| 1.4 Some typical photocatalytic degradation studies related to pesticides..... | 34             |

## *Chapter 2*

|  |                |
|--|----------------|
| <b>OBJECTIVES OF THE STUDY, MATERIALS AND METHODS, PLAN OF THE THESIS.....</b> | <b>47 - 62</b> |
| 2.1 Introduction.....  | 47             |
| 2.2 Objectives .....   | 49             |
| 2.3 Materials used .....   | 51             |
| 2.3.1 Zinc oxide .....   | 51             |
| 2.3.2 Carbendazim .....  | 53             |
| 2.3.3 Diquat .....   | 54             |
| 2.3.4 Pesticide formulations .....   | 55             |
| 2.3.5 Miscellaneous materials.....   | 57             |
| 2.4 Experimental setup .....   | 58             |
| 2.5 Analytical procedures .....  | 58             |
| 2.6 Plan of the thesis .....   | 58             |

## *Chapter 3*

|   |                 |
|---|-----------------|
| <b>SOLAR PHOTOCATALYSIS MEDIATED BY ZnO FOR THE REMOVAL OF CARBENDAZIM FUNGICIDE FROM WATER. ....</b> | <b>63 - 110</b> |
| 3.1 Introduction.....   | 63              |
| 3.2 Experimental details .....  | 64              |
| 3.2.1 Materials .....   | 64              |
| 3.2.2 Analytical procedures .....   | 64              |
| 3.2.3 Adsorption .....  | 67              |
| 3.2.4 Detection of hydroxyl radicals .....  | 67              |
| 3.2.5 Analysis of reaction products/ intermediates .....  | 68              |

|        |  |     |
|--------|--|-----|
| 3.2.6  | Photocatalytic Experimental set up .....                         | 68  |
| 3.3    | Results and discussion .....                                     | 70  |
| 3.3.1  | Catalyst characterization .....                                  | 70  |
| 3.3.2  | Preliminary experiments .....                                    | 72  |
| 3.3.3  | Effect of catalyst dosage .....                                  | 75  |
| 3.3.4  | Effect of initial concentration of carbendazim, Kinetics .....   | 76  |
| 3.3.5  | Effect of pH .....   | 82  |
| 3.3.6  | Effect of oxidants .....   | 85  |
| 3.3.7  | Effect of salts (anions and cations) .....                       | 89  |
| 3.3.8  | Effect of oxygen .....   | 103 |
| 3.3.9  | Mineralization process .....                                     | 104 |
| 3.3.10 | Identification of reaction intermediates .....                   | 105 |
| 3.4    | Mechanism of the photocatalytic degradation of carbendazim ..... | 108 |
| 3.5    | Conclusion .....   | 110 |

#### **Chapter 4**

#### **SOLAR PHOTOCATALYSIS MEDIATED BY ZnO FOR THE REMOVAL OF DIQUAT HERBICIDE FROM**

#### **WATER..... 111 - 146**

|        |   |     |
|--------|---|-----|
| 4.1    | Introduction .....  | 111 |
| 4.2    | Experimental details .....  | 112 |
| 4.2.1  | Materials .....   | 112 |
| 4.2.2  | Analytical procedures .....                                       | 113 |
| 4.2.3  | Adsorption .....  | 113 |
| 4.2.4  | Detection of hydroxyl radicals .....                              | 113 |
| 4.2.5  | Analysis of reaction products/ intermediates .....                | 113 |
| 4.2.6  | Photocatalytic Experimental set up .....                          | 114 |
| 4.3    | Results and discussion .....                                      | 114 |
| 4.3.1  | Preliminary experiments .....                                     | 114 |
| 4.3.2  | Effect of catalyst dosage .....                                   | 115 |
| 4.3.3  | Effect of initial concentration of diquat, Kinetics .....         | 117 |
| 4.3.4  | Effect of pH .....  | 121 |
| 4.3.5  | Effect of oxidants .....  | 125 |
| 4.3.6  | Effect of added H <sub>2</sub> O <sub>2</sub> .....               | 126 |
| 4.3.7  | Effect of added S <sub>2</sub> O <sub>8</sub> <sup>2-</sup> ..... | 129 |
| 4.3.8  | Effect of anions and cations .....                                | 131 |
| 4.3.9  | Effect of oxygen .....  | 140 |
| 4.3.10 | Identification of reaction intermediates .....                    | 142 |
| 4.4    | Mechanism of the photocatalytic degradation of diquat .....       | 144 |
| 4.5    | Conclusion .....  | 146 |

## **Chapter 5**

### **SOLAR PHOTOCATALYSIS MEDIATED BY ZnO FOR THE REMOVAL OF THE COMBINATION OF DIQUAT AND CARBENDAZIM FROM WATER ..... 147 - 188**

|        |  |     |
|--------|--|-----|
| 5.1    | Introduction.....  | 147 |
| 5.2    | Experimental.....  | 149 |
| 5.2.1  | Materials.....   | 149 |
| 5.2.2  | Analytical procedures.....   | 149 |
| 5.2.3  | Adsorption.....  | 152 |
| 5.2.4  | Detection of hydroxyl radicals.....  | 152 |
| 5.2.5  | Analysis of reaction products/intermediates.....                               | 152 |
| 5.2.6  | Photocatalytic experimental set up.....  | 153 |
| 5.3    | Results and Discussion.....  | 153 |
| 5.3.1  | Preliminary experiments.....   | 153 |
| 5.3.2  | Effect of catalyst loading.....  | 156 |
| 5.3.3  | Effect of initial concentration, Kinetics.....                                 | 158 |
| 5.3.4  | Effect of pH.....  | 168 |
| 5.3.5  | Effect of oxidants.....  | 171 |
| 5.3.6  | In-situ formation of H <sub>2</sub> O <sub>2</sub> .....                       | 175 |
| 5.3.7  | Effect of common inorganic anions and cations.....                             | 176 |
| 5.3.8  | Effect of oxygen.....  | 182 |
| 5.3.9  | Mineralization process.....  | 183 |
| 5.3.10 | Identification of intermediates.....   | 185 |
| 5.4    | Mechanism of the photocatalytic degradation of carbendazim/diquat mixture..... | 187 |
| 5.5    | Conclusion.....  | 188 |

## **Chapter 6**

### **SOLAR PHOTOCATALYSIS MEDIATED BY ZnO FOR THE REMOVAL OF CARBENDAZIM FORMULATION FROM WATER ..... 189 - 213**

|       |  |     |
|-------|--|-----|
| 6.1   | Introduction.....                                | 189 |
| 6.2   | Experimental.....                                | 190 |
| 6.2.1 | Chemicals.....                                   | 190 |
| 6.2.2 | Photocatalytic Experimental set up.....          | 191 |
| 6.2.3 | Analytical procedures.....                       | 191 |
| 6.2.4 | Adsorption.....                                  | 191 |
| 6.2.5 | Analysis of reaction products/intermediates..... | 192 |
| 6.3   | Results and Discussion.....                      | 192 |
| 6.3.1 | Preliminary experiments.....                     | 192 |
| 6.3.2 | Effect of catalyst loading.....                  | 194 |
| 6.3.3 | Effect of initial concentration, Kinetics.....   | 195 |

|       |  |     |
|-------|--|-----|
| 6.3.4 | Effect of pH .....                             | 202 |
| 6.3.5 | Effect of oxidants .....                       | 203 |
| 6.3.6 | Effect of anions and cations .....             | 206 |
| 6.3.7 | Effect of oxygen .....                         | 208 |
| 6.3.8 | Identification of reaction intermediates ..... | 209 |
| 6.4   | Mechanism of the degradation of CZ-F .....     | 212 |
| 6.5   | Conclusion .....                               | 212 |

## ***Chapter 7***

### **SOLAR PHOTOCATALYSIS MEDIATED BY ZnO FOR THE REMOVAL OF DIQUAT FORMULATION FROM WATER.....215 - 242**

|         |  |     |
|---------|--|-----|
| 7.1     | Introduction.....  | 215 |
| 7.2     | Experimental .....   | 216 |
| 7.2.1   | Chemicals .....  | 216 |
| 7.2.2   | Analytical procedures .....  | 216 |
| 7.2.3   | Analysis of reaction products/intermediates .....                      | 217 |
| 7.2.4   | Photocatalytic Experimental set-up .....                               | 218 |
| 7.3     | Results and Discussion .....   | 218 |
| 7.3.1   | Preliminary experiments .....  | 218 |
| 7.3.2   | Effect of catalyst loading .....                                       | 220 |
| 7.3.3   | Effect of initial concentration of diquat in the EC, Kinetics .....    | 222 |
| 7.3.4   | Effect of pH .....   | 226 |
| 7.3.5   | Effect of oxidants .....   | 228 |
| 7.3.5.1 | Effect of H <sub>2</sub> O <sub>2</sub> .....                          | 228 |
| 7.3.5.2 | Effect of persulphate (PS) .....                                       | 230 |
| 7.3.6   | Effect of common inorganic anions and cations .....                    | 231 |
| 7.3.6.1 | Effect of anions .....   | 231 |
| 7.3.6.2 | Effect of cations .....  | 233 |
| 7.3.7   | Effect of oxygen .....   | 235 |
| 7.3.8   | Mineralization of diquat in the formulation .....                      | 238 |
| 7.4     | Mechanism of the photocatalytic degradation of diquat formulation..... | 240 |
| 7.5     | Conclusion .....   | 241 |

## ***Chapter 8***

### **SOLAR PHOTOCATALYSIS MEDIATED BY ZnO FOR THE REMOVAL OF DIQUAT AND CARBENDAZIM POLLUTANTS FROM NATURAL WATER SYSTEMS .....243 - 260**

|       |                    |     |
|-------|--------------------|-----|
| 8.1   | Introduction.....  | 243 |
| 8.2   | Experimental ..... | 244 |
| 8.2.1 | Chemicals .....    | 244 |

|  |     |
|--|-----|
| 8.2.2 Analytical procedures .....              | 245 |
| 8.2.3 Photocatalytic Experimental set up ..... | 245 |
| 8.3 Results and discussion.....                | 246 |
| 8.3.1 Preliminary experiments .....            | 246 |
| 8.3.2 Mineralization .....                     | 257 |
| 8.3.3 Effect of solution turbidity.....        | 258 |
| 8.4 Conclusion .....                           | 259 |

***Chapter 9***

|                                     |                  |
|-------------------------------------|------------------|
| <b>SUMMARY AND CONCLUSION .....</b> | <b>261 - 264</b> |
|-------------------------------------|------------------|

|                         |                  |
|-------------------------|------------------|
| <b>REFERENCES .....</b> | <b>265 - 281</b> |
|-------------------------|------------------|

|                       |                  |
|-----------------------|------------------|
| <b>ANNEXURES.....</b> | <b>283 - 327</b> |
|-----------------------|------------------|

|   |            |
|---|------------|
| Annexure 1: <b>List of Abbreviation .....</b> | <b>283</b> |
|---|------------|

|  |            |
|--|------------|
| Annexure 2: <b>List of Publication .....</b> | <b>285</b> |
|--|------------|

|  |            |
|--|------------|
| Annexure 3: <b>Reprints of Paper Published .....</b> | <b>287</b> |
|--|------------|



## List of Tables

|           |   |     |
|-----------|---|-----|
| Table 1.1 | Photochemical and Non-photochemical AOPs.....   | 13  |
| Table 1.2 | Oxidation Potential of common oxidizing agents.....   | 15  |
| Table 1.3 | Band position of some common semiconductor<br>photocatalysts .....  | 29  |
| Table 2.1 | Physico-chemical properties of ZnO.....   | 52  |
| Table 2.2 | Physico-chemical properties of carbendazim. ....  | 53  |
| Table 2.3 | Physico-chemical properties of diquat. ....   | 55  |
| Table 2.4 | Common pesticide formulations. ....   | 56  |
| Table 3.1 | Pseudo first order rate constants for the photocatalytic<br>degradation of carbendazim over ZnO. pH: 5.5<br>Temp: $29 \pm 1^\circ\text{C}$ .....                    | 80  |
| Table 3.2 | Some of the intermediates formed during the solar<br>photocatalytic degradation of carbendazim. ....  | 107 |
| Table 4.1 | Pseudo first order rate constants for the photocatalytic<br>degradation of diquat over ZnO pH: 5.6 Temp: $29 \pm 1^\circ\text{C}$ .....                             | 120 |
| Table 4.2 | List of possible intermediates formed during the solar<br>photocatalytic degradation of diquat (50% degradation). ....  | 143 |
| Table 5.1 | Pseudo first order rate constants for the photocatalytic<br>degradation of carbendazim over ZnO. pH: 6.2<br>Temp: $29 \pm 1^\circ\text{C}$ .....                    | 165 |
| Table 5.2 | Pseudo first order rate constants for the photocatalytic<br>degradation of diquat over ZnO. pH: 6.2 Temp: $29 \pm 1^\circ\text{C}$ .....                            | 166 |
| Table 6.1 | Pseudo first order rate constants for the photocatalytic<br>degradation of CZ and CZ-F over ZnO. pH: 5.0<br>Temp: $29 \pm 1^\circ\text{C}$ .....                    | 199 |
| Table 6.2 | List of intermediates identified during the solar<br>photocatalytic degradation of carbendazim in the<br>formulated form. ....                                      | 211 |
| Table 7.1 | Pseudo first order rate constants for the photocatalytic<br>degradation of DQ-F at various concentrations over<br>ZnO. pH: 5.2 Temp: $29 \pm 1^\circ\text{C}$ ..... | 225 |
| Table 7.2 | Comparative list of intermediates identified during the<br>photocatalytic degradation of diquat technical and diquat<br>formulation.....                            | 239 |
| Table 8.1 | Different Parameters and the results .....  | 247 |



## ||| List of Figures |||

|            |  |    |
|------------|--|----|
| Figure 1.1 | A comparison of the consumption pattern of pesticides in India and rest of the world .....   | 08 |
| Figure 1.2 | Reaction sequence in the UV/H <sub>2</sub> O <sub>2</sub> process.....   | 19 |
| Figure 1.3 | Reaction sequence in the UV/O <sub>3</sub> process.....  | 21 |
| Figure 1.4 | Reaction sequence in the Photo-Fenton process .....  | 23 |
| Figure 1.5 | Difference between energy bands of (a) insulator, (b) semiconductor and (c) metals.....  | 25 |
| Figure 1.6 | The positions of bands of semiconductor relative to the standard potential of several redox couples (shown at the right hand side of the figure). The positions of the valence and conduction band of semiconductor appear favorable for one or the other of the redox reaction of the cleavage of water ..... | 27 |
| Figure 1.7 | Mechanism of Photocatalysis on a semiconductor .....   | 31 |
| Figure 1.8 | Process on the Photo-excited semiconductor surface and bulk .....  | 32 |
| Figure 1.9 | Spectral composition of sunlight at Earth's surface .....  | 34 |
| Figure 2.1 | Hexagonal wurtzite structure of ZnO (Shaded gray and black spheres denote Zn and O atoms, respectively) .....  | 51 |
| Figure 2.2 | Carbendazim .....  | 53 |
| Figure 2.3 | Diquat dibromide .....   | 54 |
| Figure 2.4 | SEM image of pesticide applied surface (A) without adjuvant and (B) with adjuvant.....   | 56 |
| Figure 3.1 | Ion chromatogram of selected anions .....  | 66 |
| Figure 3.2 | Schematic diagram of the photocatalytic experimental set up .....  | 69 |
| Figure 3.3 | Pore size distribution of ZnO .....  | 70 |
| Figure 3.4 | XRD pattern of ZnO .....   | 71 |
| Figure 3.5 | SEM image of ZnO .....   | 72 |
| Figure 3.6 | TEM image of ZnO.....  | 72 |
| Figure 3.7 | Degradation of carbendazim under various conditions.....   | 73 |
| Figure 3.8 | Photocatalytic degradation of carbendazim .....  | 74 |
| Figure 3.9 | Effect of catalyst dosage on the rate of degradation .....   | 75 |

|             |  |    |
|-------------|--|----|
| Figure 3.10 | Effect of carbendazim concentration on the percentage degradation.....   | 77 |
| Figure 3.11 | Effect of carbendazim concentration on the rate of degradation.....  | 77 |
| Figure 3.12 | Logarithmic plot of pseudo first order kinetics for the degradation of carbendazim .....                                 | 80 |
| Figure 3.13 | Reciprocal plot of initial rate of degradation of carbendazim versus initial concentration .....                         | 81 |
| Figure 3.14 | Effect of pH on the degradation of carbendazim .....   | 83 |
| Figure 3.15 | Formation of H <sub>2</sub> O <sub>2</sub> during the photocatalytic degradation of carbendazim.....                     | 86 |
| Figure 3.16 | Effect of H <sub>2</sub> O <sub>2</sub> at various concentrations on the photocatalytic degradation of carbendazim ..... | 87 |
| Figure 3.17 | Effect of persulphate on the photocatalytic degradation of carbendazim .....   | 88 |
| Figure 3.18 | Effect of chloride on the photocatalytic degradation of carbendazim [Cation: Na+].....                                   | 90 |
| Figure 3.19 | Effect of nitrate on the photocatalytic degradation of carbendazim [Cation: Na+].....                                    | 90 |
| Figure 3.20 | Effect of sulphate on the photocatalytic degradation of carbendazim [Cation: Na+].....                                   | 91 |
| Figure 3.21 | Effect of phosphate on the photocatalytic degradation of carbendazim[Cation:Na+].....                                    | 91 |
| Figure 3.22 | Adsorption of selected anions on ZnO [Cation:Na+] .....  | 92 |
| Figure 3.23 | Effect of concentration of HPO <sub>4</sub> <sup>2-</sup> on its adsorption on the ZnO surface .....                     | 93 |
| Figure 3.24 | FTIR spectral evidence for the adsorption of HPO <sub>4</sub> <sup>2-</sup> on ZnO .....                                 | 93 |
| Figure 3.25 | PL spectral changes observed in the photocatalytic system in presence of various anions .....                            | 95 |
| Figure 3.26 | Effect of Na <sup>+</sup> on the photocatalytic degradation of carbendazim [Anion: SO <sub>4</sub> <sup>2-</sup> ].....  | 96 |
| Figure 3.27 | Effect of K <sup>+</sup> on the photocatalytic degradation of carbendazim [Anion: SO <sub>4</sub> <sup>2-</sup> ].....   | 96 |
| Figure 3.28 | Effect of Ca <sup>2+</sup> on the photocatalytic degradation of carbendazim [Anion: SO <sub>4</sub> <sup>2-</sup> ]..... | 97 |
| Figure 3.29 | Effect of Mg <sup>2+</sup> on the photocatalytic degradation of carbendazim [Anion: SO <sub>4</sub> <sup>2-</sup> ]..... | 97 |

|             |   |     |
|-------------|---|-----|
| Figure 3.30 | Effect of $\text{Al}^{3+}$ on the photocatalytic degradation of carbendazim [Anion: $\text{SO}_4^{2-}$ ]              | 98  |
| Figure 3.31 | PL spectral changes observed in the photocatalytic system in presence of various cations [Anion: $\text{SO}_4^{2-}$ ] | 98  |
| Figure 3.32 | Effect of different chlorides on the photocatalytic degradation of carbendazim  | 99  |
| Figure 3.33 | Effect of different nitrates on the photocatalytic degradation of carbendazim   | 100 |
| Figure 3.34 | Effect of different sulphates on the photocatalytic degradation of carbendazim  | 101 |
| Figure 3.35 | Effect of different phosphates on the photocatalytic degradation of carbendazim                                       | 101 |
| Figure 3.36 | Effect of deaeration with $\text{N}_2$ on the photocatalytic degradation of carbendazim                               | 104 |
| Figure 3.37 | COD of the reaction system after different periods of irradiation   | 105 |
| Figure 3.38 | Mass spectra of degradation products, (A) 50% degradation, (B) 80% degradation  | 106 |
| Figure 3.39 | Mechanism of ZnO mediated photocatalysis for the degradation of carbendazim   | 109 |
| Figure 4.1  | Degradation of diquat under various conditions  | 114 |
| Figure 4.2a | Effect of catalyst dosage on the percentage degradation of diquat   | 116 |
| Figure 4.2b | Effect of catalyst dosage on the rate of degradation  | 116 |
| Figure 4.3  | Effect of initial concentration on the percentage degradation of diquat over ZnO                                      | 117 |
| Figure 4.4  | Effect of initial concentration on the rate of photocatalytic degradation of diquat                                   | 118 |
| Figure 4.5  | Kinetics of photocatalytic degradation (linear transform $\ln C_0/C$ vs time) of diquat over ZnO                      | 119 |
| Figure 4.6  | Effect of pH on the degradation of diquat in dark and under photocatalysis  | 122 |
| Figure 4.7  | Fate of in-situ formed and externally added $\text{H}_2\text{O}_2$ with time  | 125 |
| Figure 4.8a | Effect of added $\text{H}_2\text{O}_2$ at different concentrations on the photocatalytic degradation of diquat        | 127 |
| Figure 4.8b | Effect of added $\text{H}_2\text{O}_2$ on the photocatalytic degradation of diquat at different reaction times        | 127 |

|             |  |     |
|-------------|--|-----|
| Figure 4.9a | Effect of added persulphate on the photocatalytic degradation of diquat .....  | 130 |
| Figure 4.9b | Effect of added persulphate on the photocatalytic degradation of diquat with time .....  | 130 |
| Figure 4.10 | Effect of anions on the photocatalytic degradation of diquat [Cation: Na+] .....   | 132 |
| Figure 4.11 | Effect of $\text{HPO}_4^{2-}$ on the photocatalytic degradation of diquat [Cation: Na+] .....  | 133 |
| Figure 4.12 | Photocatalytic degradation of diquat over $\text{HPO}_4^{2-}$ pre-adsorbed ZnO .....   | 134 |
| Figure 4.13 | Effect of in between addition of $\text{HPO}_4^{2-}$ on the photocatalytic degradation of diquat .....   | 135 |
| Figure 4.14 | UV-Visible spectrum of diquat under photocatalytic condition at different times of irradiation. (A) Standard experimental conditions ([Diquat]: 50mg/L, [ZnO]: 0.6g/L), (B) In presence of $\text{HPO}_4^{2-}$ (Standard conditions + [ $\text{HPO}_4^{2-}$ ]: 50mg/L) ..... | 136 |
| Figure 4.15 | Depletion in the TOC content with time of irradiation during the solar photocatalytic degradation of diquat in the presence as well as absence of $\text{HPO}_4^{2-}$ .....  | 138 |
| Figure 4.16 | Effect of cations on the photocatalytic degradation of diquat [Anion: $\text{SO}_4^{2-}$ ] .....   | 139 |
| Figure 4.17 | Adsorption of selected cations on ZnO [Anion: $\text{SO}_4^{2-}$ ] .....   | 139 |
| Figure 4.18 | PL spectral changes observed in the photocatalytic system in presence of $\text{Al}^{3+}$ at various concentrations .....  | 140 |
| Figure 4.19 | Effect of $\text{N}_2$ and $\text{O}_2$ atmosphere on the photocatalytic degradation of diquat. ....   | 141 |
| Figure 4.20 | Effect of introduction of $\text{O}_2$ into deaerated reaction system on the photocatalytic degradation of diquat.....   | 142 |
| Figure 4.21 | Mass spectrum showing various intermediates formed during the photocatalytic degradation of diquat over ZnO.....   | 142 |
| Figure 4.22 | Mechanism of semiconductor photocatalysis on ZnO for the degradation of diquat .....   | 145 |
| Figure 5.1  | UV-Visible spectrum of carbendazim/diquat mixture in solution.....   | 150 |
| Figure 5.2  | Observed increase in the concentration of carbendazim (7mg/L) with varying concentration of diquat .....   | 151 |

|             |  |     |
|-------------|--|-----|
| Figure 5.3  | The plot for determining the correction factor for carbendazim concentration at various concentrations of diquat in the combination .....                                      | 151 |
| Figure 5.4  | Variation in percentage degradation of carbendazim and diquat individually and in combination with time of irradiation during the photocatalytic reaction .....                | 154 |
| Figure 5.5  | Degradation of diquat and carbendazim in combination under various conditions .....  | 155 |
| Figure 5.6  | Effect of catalyst dosage on the rate of degradation of carbendazim in presence and absence of diquat .....  | 156 |
| Figure 5.7  | Effect of catalyst dosage on the rate of degradation of diquat in presence and in the absence of carbendazim .....   | 157 |
| Figure 5.8  | Percentage degradation of carbendazim at different initial concentrations in presence of diquat.....   | 159 |
| Figure 5.9  | Percentage degradation of diquat at different initial concentrations in presence of carbendazim .....  | 160 |
| Figure 5.10 | Effect of initial concentration of carbendazim on its photocatalytic degradation rate in presence of diquat.....   | 161 |
| Figure 5.11 | Effect of initial concentration of diquat on its photocatalytic degradation rate in presence of carbendazim .....  | 161 |
| Figure 5.12 | Pseudo first order kinetic plot for the degradation of carbendazim at different initial concentrations in the absence and in presence of a fixed concentration of diquat.....  | 163 |
| Figure 5.13 | Pseudo first order kinetic plot for the degradation of diquat at different initial concentrations in the absence and in presence of a fixed concentration of carbendazim ..... | 164 |
| Figure 5.14 | Reciprocal plot of initial rate of degradation of carbendazim versus its initial concentration.....  | 167 |
| Figure 5.15 | Reciprocal plot of initial rate of degradation of diquat versus its initial concentration .....  | 167 |
| Figure 5.16 | Effect of pH on the degradation of carbendazim independently and in combination with diquat (7mg/L) under photocatalysis .....   | 169 |
| Figure 5.17 | Effect of pH on the degradation of diquat independently and in combination with carbendazim (7mg/L) under photocatalysis.....  | 170 |
| Figure 5.18 | Effect of H <sub>2</sub> O <sub>2</sub> and persulphate on the photocatalytic degradation of carbendazim in presence of diquat .....   | 172 |

|             |  |     |
|-------------|--|-----|
| Figure 5.19 | Effect of H <sub>2</sub> O <sub>2</sub> and persulphate on the photocatalytic degradation of diquat in presence of carbendazim. ....   | 172 |
| Figure 5.20 | Effect of H <sub>2</sub> O <sub>2</sub> on the photocatalytic degradation of carbendazim individually as well as in combination with diquat .....  | 173 |
| Figure 5.21 | Effect of persulphate on the photocatalytic degradation of carbendazim individually as well as in combination with diquat .....  | 174 |
| Figure 5.22 | Effect of H <sub>2</sub> O <sub>2</sub> on the photocatalytic degradation of diquat individually as well as in combination with carbendazim .....  | 174 |
| Figure 5.23 | Effect of persulphate on the photocatalytic degradation of diquat individually as well as in combination with carbendazim .....  | 175 |
| Figure 5.24 | Formation of H <sub>2</sub> O <sub>2</sub> during the photocatalytic degradation of diquat/carbendazim, independently and in combination and also in presence of added H <sub>2</sub> O <sub>2</sub> .....           | 176 |
| Figure 5.25 | Effect of anions on the photocatalytic degradation of carbendazim in the carbendazim/diquat combination [Cation:Na <sup>+</sup> , Irradiation time: 30min] .....   | 178 |
| Figure 5.26 | Effect of HPO <sub>4</sub> <sup>2-</sup> at different concentrations on the photocatalytic degradation of carbendazim in the carbendazim/diquat combination [Cation:Na <sup>+</sup> , Irradiation time: 30min] ..... | 178 |
| Figure 5.27 | Effect of anions on the photocatalytic degradation of diquat [Cation:Na <sup>+</sup> , Irradiation time: 30min] in the diquat/carbendazim combination .....  | 179 |
| Figure 5.28 | Effect of HPO <sub>4</sub> <sup>2-</sup> concentration on the photocatalytic disappearance of diquat in the carbendazim/diquat combination [Cation:Na <sup>+</sup> , Irradiation time: 30min] .....                  | 180 |
| Figure 5.29 | Effect of cations on the photocatalytic degradation of carbendazim [Anion:SO <sub>4</sub> <sup>2-</sup> , Irradiation time: 30min] in the carbendazim/diquat system .....  | 181 |
| Figure 5.30 | Effect of cations on the photocatalytic degradation of diquat [Anion:SO <sub>4</sub> <sup>2-</sup> , Irradiation time: 30min] in the diquat/carbendazim system .....   | 181 |
| Figure 5.31 | Effect of deaeration with N <sub>2</sub> on the photocatalytic degradation of carbendazim/diquat system .....  | 183 |

|             |  |     |
|-------------|--|-----|
| Figure 5.32 | Depletion in the TOC content with time of irradiation during the solar photocatalytic degradation of diquat/ carbendazim combination .....             | 184 |
| Figure 5.33 | Mass spectra of degradation products formed during the photocatalytic degradation of the mixture of diquat and carbendazim after 1hr irradiation ..... | 186 |
| Figure 6.1  | Degradation of carbendazim formulation under various conditions .....  | 193 |
| Figure 6.2  | Photocatalytic degradation of carbendazim in formulated and technical forms .....  | 193 |
| Figure 6.3  | Effect of catalyst dosage on the rate of degradation of CZ and CZ-F .....  | 195 |
| Figure 6.4  | Effect of carbendazim concentration on the rate of degradation in formulated and technical forms .....   | 196 |
| Figure 6.5  | Logarithmic plot of pseudo first order kinetics for the degradation of carbendazim formulation .....   | 197 |
| Figure 6.6  | Comparative logarithmic plot of pseudo first order kinetics for the degradation of carbendazim formulation and technical form .....                    | 198 |
| Figure 6.7  | Effect of various adjuvants on the photocatalytic degradation of carbendazim .....   | 200 |
| Figure 6.8  | Comparative depletion in the TOC content with time of irradiation during the solar photocatalytic degradation of CZ and CZ-F .....                     | 201 |
| Figure 6.9  | Effect of pH on the degradation of carbendazim technical (CZ) and formulation (CZ-F) .....   | 203 |
| Figure 6.10 | Formation of H <sub>2</sub> O <sub>2</sub> during the photocatalytic degradation of carbendazim formulation .....                                      | 204 |
| Figure 6.11 | Effect of H <sub>2</sub> O <sub>2</sub> on the photocatalytic degradation of CZ-F .....  | 205 |
| Figure 6.12 | Effect of persulphate on the photocatalytic degradation of CZ-F .....  | 206 |
| Figure 6.13 | Effect of anions on the photocatalytic degradation of CZ-F [Cation: Na <sup>+</sup> ] .....  | 207 |
| Figure 6.14 | Effect of cations on the photocatalytic degradation of CZ-F [Anion: SO <sub>4</sub> <sup>2-</sup> ] .....  | 207 |
| Figure 6.15 | Effect of deaeration with N <sub>2</sub> on the photocatalytic degradation of CZ-F .....   | 208 |

|             |   |     |
|-------------|---|-----|
| Figure 6.16 | Mass spectra of carbendazim formulation before photocatalysis (A), and after photocatalytic degradation (B).....                              | 210 |
| Figure 7.1  | Analysis of diquat 'formulation' and 'technical' at various concentrations .....  | 217 |
| Figure 7.2  | Degradation of diquat in the formulated form under various conditions .....   | 219 |
| Figure 7.3  | Percentage degradation of diquat in the technical and formulated forms at different times of irradiation under photocatalysis.....            | 219 |
| Figure 7.4  | Effect of catalyst dosage on the rate of degradation of diquat in technical and formulation forms .....                                       | 220 |
| Figure 7.5  | Effect of initial concentration on the rate of photocatalytic degradation of diquat in technical and formulated forms.....                    | 223 |
| Figure 7.6  | Kinetics of photocatalytic degradation (linear transform $\ln C_0/C$ vs time) of diquat formulation over ZnO .....                            | 224 |
| Figure 7.7  | Comparative kinetics of photocatalytic degradation of diquat formulation and technical over ZnO .....   | 224 |
| Figure 7.8  | Effect of pH on the degradation of diquat formulation in dark and under photocatalysis.....   | 227 |
| Figure 7.9  | Fate of in-situ formed and externally added H <sub>2</sub> O <sub>2</sub> during the photocatalytic degradation of diquat (formulation) ..... | 229 |
| Figure 7.10 | Effect of added H <sub>2</sub> O <sub>2</sub> on the photocatalytic degradation of diquat formulation .....                                   | 230 |
| Figure 7.11 | Effect of added persulphate on the photocatalytic degradation of diquat formulation .....   | 231 |
| Figure 7.12 | Effect of anions on the photocatalytic degradation of diquat in the formulation [Cation:Na <sup>+</sup> ] .....                               | 232 |
| Figure 7.13 | Effect of HPO <sub>4</sub> <sup>2-</sup> on the photocatalytic degradation of diquat in the formulation [Cation:Na <sup>+</sup> ].....        | 233 |
| Figure 7.14 | Effect of cations on the photocatalytic degradation of diquat in the formulation [Anion:SO <sub>4</sub> <sup>2-</sup> ].....                  | 234 |
| Figure 7.15 | Effect of deaeration by N <sub>2</sub> on the photocatalytic degradation of diquat in the formulation .....                                   | 236 |
| Figure 7.16 | Depletion in the TOC content with time of irradiation during the solar photocatalytic degradation of diquat .....                             | 237 |
| Figure 7.17 | Mass spectrum of diquat formulation before photocatalytic reaction.....   | 238 |

|             |  |     |
|-------------|--|-----|
| Figure 7.18 | Mass spectrum showing various intermediates formed during the photocatalytic degradation of diquat formulation over ZnO after 10hr of irradiation..... | 238 |
| Figure 8.1  | The locations from where the water samples were collected.....   | 244 |
| Figure 8.2  | Degradation of diquat in different water matrices .....  | 248 |
| Figure 8.3  | Degradation of carbendazim in different water matrices .....   | 249 |
| Figure 8.4  | Effect of selected salts at various concentrations on the degradation of carbendazim .....   | 250 |
| Figure 8.5  | Effect of selected salts at various concentrations on the degradation of diquat .....  | 251 |
| Figure 8.6  | Decrease in percentage degradation of diquat in presence of sequentially added salts .....   | 254 |
| Figure 8.7  | Decrease in percentage degradation of carbendazim in presence of sequentially added salts .....  | 254 |
| Figure 8.8  | Effect of changing the salt addition sequence on the percentage degradation of diquat .....  | 256 |
| Figure 8.9  | Effect of changing the salt addition sequence on the percentage degradation of carbendazim.....  | 256 |
| Figure 8.10 | Mineralization of diquat in different water matrices.....  | 257 |
| Figure 8.11 | Mineralization of carbendazim in different water matrices .....  | 258 |
| Figure 8.12 | Effect of solution turbidity on the photocatalytic degradation of (A) diquat and (B) carbendazim .....   | 259 |



## INTRODUCTION: BACKGROUND LITERATURE

|                 |  |
|-----------------|--|
| <b>Contents</b> | 1.1 <i>General</i>   |
|                 | 1.2 <i>Conventional waste water treatment</i>                                    |
|                 | 1.3 <i>Advanced Oxidation processes (AOPs)</i>                                   |
|                 | 1.4 <i>Some typical photocatalytic degradation studies related to pesticides</i> |

### 1.1 General

Water is essential for all living organisms on earth. The presence of water makes earth unique in the solar system. Water covers ~71% of earth, the 'blue planet'. Over 96.5% of total water is distributed in the seas and oceans while ~1.7% is locked up in the glaciers and in the ice caps. Another ~1.7% exists as ground water and other water bodies like rivers and lakes. Even though the planet contains huge resources of water, only ~2.5% of it is fresh water, which is available for drinking and sanitation. The human body contains ~70% water. Water fit for human consumption is known as potable water and that for other sanitation purposes is called safe water. Nowadays, mankind is facing severe problems related to the quality and quantity of fresh water. Due to industrialization and other human activities, the water resources are getting contaminated day by day. Water-borne diseases are the outcome of poor water quality and lack of sanitation. As per World Health Organization, safe water can prevent ~1.4 million child deaths from diarrhea each year. Studies reveal that by

2025, half of the world population will face huge water related vulnerabilities. Agriculture is the largest user of fresh water. ~90% of water drawn from the ground is used for irrigation in some of the developing countries. As the population grows the food requirement also increases demanding high agricultural production rates. Net result is the over exploitation of both the ground and surface water for irrigation and other purposes. Every year world population is expanding by ~80 million people and demand for fresh water increases by ~64 billion m<sup>3</sup>/annum. World water development report warns that by 2050 the global population is expected to be 9 billion and the fresh water consumption will be ~50% more than the current rate [1].

There is enough water for everyone; the insufficiency is often due to the mismanagement and human activities [2]. Water pollution is one of the major reasons for water scarcity. From the beginning of 19<sup>th</sup> century, industrialization spread all over the world and since then tons of chemicals and other effluents are being dumped into the fresh water resources. Over 70% of the untreated industrial wastes in developing countries are dumped into the water sources thereby contaminating the existing water supply. The main industrial pollutants such as chlorinated solvents, heavy metals, oil, synthetic-persistent engineered chemicals, medical drug residues, hormone mimetics and their by-products, radioactive pollution, thermal pollution from industrial cooling etc. contribute to the deterioration of water quality [3]. Most of the major industries have treatment facilities for the effluent. But the enormous investment for the same is beyond what the small scale industries can afford as their profit

margin is very slender. They are the major “point sources” for the industrial water pollution.

Population growth and urbanization are two major factors contributing to the water pollution. Urban runoff from city landscape and landfill sites serve as “non-point sources” and consist of residues, wastes and natural products that are washed from streets and lawns by rain into storm drains. Leachates from landfills are concentrated with metal ions and can pollute both surface and ground water [4]. Population growth increases the demand and use of water. The used waste water is frequently discharged into the drainage system which ultimately reaches the nearby river or lake without proper treatment.

One of the major sources of inorganic and organic chemical pollutants in water is intensive agriculture. According to a report by Environmental Protection Agency (EPA) of USA, over 50% of water pollution of streams and rivers occurs due to leaching and mixing of chemicals from the agricultural practices [5]. Population growth and the consequent need for expanded food production demands the use of synthetic fertilizers and pesticides. The positive aspect of the application of these agricultural inputs is that they enhance crop productivity. Substantial increase in production rate, more than fourfold, is achieved by the use of agricultural chemicals. Pesticides play an important role in agriculture by reducing losses due to the weeds, diseases and insect pests that can markedly reduce the amount of harvestable products. In addition to enhanced crop production, pesticides also have direct benefit to human health. Vector-borne diseases are effectively controlled by the use of

pesticides. The prevalent use of insecticides has decreased the population of insects that spread deadly diseases like malaria. Other diseases that are controlled by the use of pesticides include the bubonic plague, which is carried by rat fleas, and typhus which is transmitted by both fleas and body lice. Insecticides and herbicides are also used for other purposes such as maintenance of the turf on sports pitch, protection of buildings and other wooden structures from damage by termites and wood boring insects [6].

The term pesticide covers a wide range of compounds including, insecticides, fungicides, herbicides, rodenticides, molluscicides, nematocides and plant growth regulators. After the discovery of DDT in 1939, numerous pesticides are developed and used extensively worldwide. In industrialized countries, the ‘green revolution’ in 1960s accelerated the use of pesticides. After 1960, organochlorine pesticides were banned or restricted in most of the technologically advanced countries. Various organophosphorus insecticides, carbamates, pyrethroids, herbicides and fungicides were introduced in the 1970s and 1980s and they greatly contributed to the pest control. The worldwide consumption of pesticides in agriculture showed a steady increase from 0.49 kg/ha in 1961 to 2 kg/ha in 2004 [7]. According to new technical market research report from ‘BCC research’, the global pesticide market valued at \$37.5 billion in 2011 is expected to reach \$65.3 billion in 2017 [8]. Germany, France, United States and China are the largest exporters of pesticides in the global market. Based on the reports, Indian pesticide industry is one of the fastest growing pesticide exporters (up 39.9%) [9]. First pesticide industry in India started in 1952 for the production of BHC near Calcutta. After China, India is the second largest manufacturer

of pesticides in Asia. There are 125 large and medium scale pesticide manufacturers in India producing more than 500 different pesticides including DDT and lindane, which are banned in most of the countries.

Globally ~4.6 million tons of pesticides are applied to the environment. About 99% of these pesticides are discharged into the soil or volatilized into the atmosphere, ultimately contaminating the surface water and air and eventually absorbed by almost every organism [10]. The most susceptible category is the workmen group including the production workers, formulators, agricultural farm workers and those engaged in spraying, mixing, loading, transportation etc. The adverse effects of pesticides include diseases such as cancer, allergies and neurological disorders. The studies conducted on the workmen category reveal neurological and cardiotoxic effects of hexachlorocyclohexane (HCH) and methomyl, a carbamate insecticide. Psychological, neurological, cardiorespiratory and gastrointestinal effects of malathion, DDT, methyl parathion and lindane are observed in the surveillance conducted on the male workers in manufacturing units [11]. Many pesticides are identified as endocrine disruptors, the chemicals that bind to various hormone receptors and mimic the natural hormone action, thereby interfering with the process of synthesis, transport and metabolism. Infants and children are more susceptible than adults. About 105 pesticides including DDT, mancozeb, pentachloronitrobenzene, ziram, endosulfan etc. are identified as endocrine disruptors. [7].

Direct application of pesticides on plants is the major pathway for the pesticide contamination in the food chain. Studies conducted by

European Union on the extent of pesticide contamination in vegetables and fruits found the presence of pesticides in the collected samples. The residual levels are much higher than the accepted Maximum Residual Limits (MRLs) for these pesticides. The first pesticide poisoning in India is reported in 1958 from Kerala. Over 100 people died due to parathion contamination in wheat flour. The presence of DDT was found in the bovine milk samples collected from 12 Indian states. About 82% of the total samples collected have shown 0.05mg/Kg of DDT residue which is much higher than the tolerance limit [12].

The toxicity of pesticide directly kills the targeted insects and weeds, but the indirect victims are the non-target organisms such as beneficial insects, non-target plants, animals, birds and aquatic life forms. The most vulnerable species are the soil microorganisms, which are essential for maintaining the soil structure and providing nutrients for plants. Various pesticides such as sulphonylurea herbicides and chlorothalonil and certain fungicides like mancozeb and maneb are toxic to nitrifying bacteria. Soil fungi and actinomycetes are susceptible to the toxic effects of fungicides. Certain soil invertebrates such as earthworms, nematodes, mites and microarthropods declined primarily due to pesticide exposure [13]. The growth and reproduction of earthworms are detrimentally affected by chlorpyrifos, azinphos methyl and glyphosate [14]. The bioaccumulation of pesticides in fish and other aquatic animals starts from the phytoplankton in which relatively high amount of DDT and its metabolites can occur. Broad spectrum herbicides have devastating effects on the aquatic plants [15]. Pesticide concentration in top predators is magnified as they consume the smaller organisms. Pesticides like DDT and HCH affect the egg mortality

and make embryos defective in fish. These xenobiotic compounds are also toxic to common seal [16]. Studies are showing high accumulation of persistent organic pesticides in aquatic mammals such as dolphins [17]. Symptoms of pesticide toxicity in the sea birds include reduction in fertility and hatch rate as well as egg shell thinning. The accumulation of toxic pesticides in avian species is mainly through the food chain. According to reports ~50% of lethal poisoning of birds is caused by organophosphate pesticides and carbamates [18]. More than ~100,000 bird deaths are reported to be due to the monocrotophos poisoning worldwide [19].

The hazard due to accumulation of pesticides in living organisms starts from contamination of these chemicals in water, air and soil. Pesticides contamination of surface water and ground water is occurring due to the two fundamental processes that are linked to the earth's hydrological cycle, i.e. surface runoff and leaching [20]. The solubility of pesticide, soil structure, weather condition and the distance from the point source are the major factors that contribute to the pesticide pollution in surface and ground water. The occurrence of various types of pesticides in the contaminated water also depends on the pattern of pesticide usage. In India, most of the rivers are contaminated with insecticides, especially the river Ganga [21]. Comparing with the standards of USEPA (United States Environmental Protection Agency), river Ganga is highly polluted with organochlorine pesticides, i.e. thousand times more than the permissible limits [22].

Insecticides are the most widely used pesticides (~76%) in India. Worldwide it is only 44%. Fig. 1.1 shows the comparison of pesticide usage in India and the world. Studies and the surveys conducted on the pesticide contamination levels in various parts of world indicate that most of the surface water and ground water sources are contaminated with pesticides from every major chemical class.

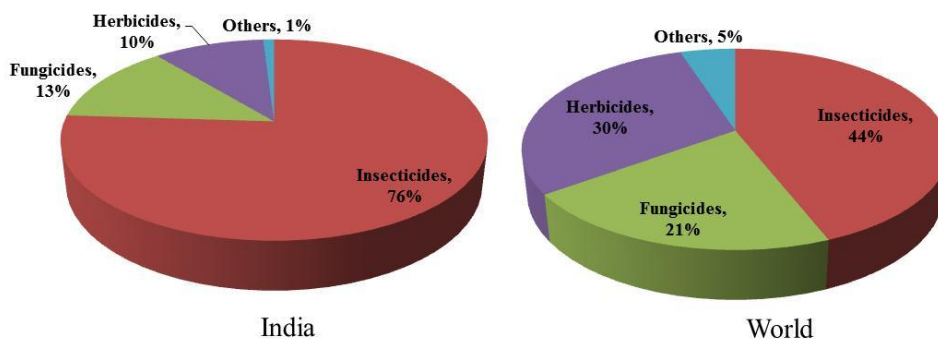


**Fig. 1.1:** A comparison of the consumption pattern of pesticides in India and rest of the world

A 5-year survey for monitoring the pesticide contamination in surface water in Hungary showed that 59% of the samples collected contain acetochlor, atrazine, carbofuran, diazinon, fenoxycarb, metribuzin, phorate, prometryn, terbutryn, and trifluralin [23]. Seasonal variation in pesticide concentration in polluted river and lakes is reported from Greece. Maximum concentration is noticed in the late spring and summer period followed by a decrease during winter [24]. The presence of chlortoluron, atrazine, terbutryn, alachlor, diflufenican and fluazifop-butyl are reported in the ground and surface water near the agricultural areas of Zamora and Salamanca (Spain) [25]. In the last decades of 20<sup>th</sup> century, a major incident that attracted world's attention due to the pesticide pollution was

the endosulfan poisoning in Kasargod district, Kerala. Endosulfan sprayed for years to eradicate the tea mosquito bug in the cashew plantation contaminated the surface and ground water. People who lived inside the plantation and also within 25 km radius were affected by the devastating effect of endosulfan. Children suffer from congenital anomalies, mental retardation, physical deformities, cerebral palsy, epilepsy, hydrocephalus etc. Studies conducted show higher concentration of endosulfan in the well water, rivers and soil in the affected area [26].

The potential source of pesticides in the atmosphere is volatilization. Certain Persistent Organic Pollutants (POPs) such as polychlorinated biphenyls, DDT and HCH are semi-volatile and they enter the atmosphere during the time of application or get volatilized from soil, water or vegetation depending on the atmospheric conditions [27]. Presence of these POPs is found in the environment of most of the industrialized countries where the production and usage were banned decades ago. Air and surface water in the remote polar regions of Arctic and Antarctic contain higher residual levels of these contaminants. The ‘long-range atmospheric transport’ of volatilized pesticides from the point of application is believed to be the reason for the measured levels of POP contamination [28].

In general, enhanced economic growth in terms of increased crop production can be ensured by the use of pesticides in agriculture. The devastating health hazards and degradation of environment are the unwanted consequences of this pesticide based economy.

Treatment of contaminated water is essential for providing clean, safe, healthy and hygienic water. Traditional adsorption methods using

granular activated carbon, clay and other adsorbents are not much efficient for removing trace amounts of toxic chemical contaminants. Also traditional waste treatment systems involve the use of techniques such as coagulation, chlorination or ozonation which utilize potentially hazardous or polluting materials. Chlorination presents a serious problem since it will often generate trihalomethanes as by-products when used to treat water contaminated with organic compounds. An effective treatment system is the one which can degrade the polluting materials safely prior to their discharge into the environment.

## 1.2 Conventional waste water treatment

Conventional waste water treatment normally involves three stages, namely, primary, secondary and tertiary treatments.

**Primary treatment process:** Primary treatment process generally includes the removal of debris and coarse biodegradable material from the waste water and also the stabilization of waste water by the addition of chemicals. In domestic treatment, primary processes remove ~25% of the organic load and virtually complete removal of non-organic solids. Primary process is used to remove items such as rags, grit, sticks, other debris, and foreign objects which can interfere with the operation of the treatment system. Some of the commonly used primary treatment processes are as follows:

- 1) Screening and comminution,
- 2) Grit removal,
- 3) Preaeration,

- 4) pH control,
- 5) Equalization,
- 6) Flootation.

The primary process includes the sedimentation of waste with and without chemical addition. Plain sedimentation is done by the gravity settling of waste in a tank to produce near quiescent conditions. In this facility, settleable solids and suspended solids are removed by sedimentation. About 30 to 40% BOD and 40 to 70% suspended solid removal can be achieved by this method. In industrial sedimentation process, addition of chemical coagulants enhances the removal of BOD and suspended solids.

**Secondary treatment:** This includes the removal of organic contaminants from water using biological methods to coagulate and remove the non-settleable colloidal solids. The biological processes are classified into aerobic and anaerobic treatment processes. Depending on the medium used for the treatment, they are further divided into two categories,

- 1) Suspended growth processes, in which the microorganism and the waste water are in the same reactor and oxygen is passed through the reactor for the biological activity to take place. Treatment ponds, lagoons and activated sludge systems belong to this category.
- 2) Fixed growth processes in which the biological mass is allowed to grow on a medium and the waste water is sprayed over the medium to stabilize the waste over it. The most common methods employed in the fixed growth processes are trickling filters and rotating biological contactors.

**Tertiary treatment:** After primary and secondary treatment, the waste water quality may not be sufficient enough to be discharged or to be used as drinking water. The purpose of tertiary treatment is to improve the water quality before it is discharged into the receiving environment. Many physical and chemical treatment methods are identified for the tertiary treatment of waste water. Activated carbon adsorption is one of the major techniques used in this category. Waste water may contain high level of nutrients such as nitrate and phosphate which can be removed by biological oxidation methods. Ammonia present in the waste water can be biologically converted into nitrate followed by the reduction to nitrogen gas. Phosphate can be removed by both biological and chemical precipitation methods. Chemical oxidations such as chlorination, ozonation and H<sub>2</sub>O<sub>2</sub> oxidation, UV radiation and ionizing radiation are also employed for the tertiary treatment of waste water.

### 1.3 Advanced Oxidation processes (AOPs)

The term Advanced Oxidation Processes (AOPs) include all the chemical treatment processes that are used for the remediation of both organic and inorganic contaminants in water by in-situ generated highly reactive  $\cdot\text{OH}$  radicals. The  $\cdot\text{OH}$  are very powerful non-selective oxidants which react with most of the organic and inorganic species. Various chemical contaminants such as pesticides, pharmaceuticals, chlorinated hydrocarbons, detergents, dyes and inorganic species like cyanides, sulfides and nitrates are effectively removed by the attack of  $\cdot\text{OH}$  to yield the corresponding mineralized end products. Due to its versatility,

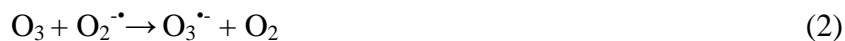
advanced oxidation process is considered as the “treatment process of 21<sup>st</sup> century” [29].

The generation of  $\cdot\text{OH}$  radicals can be achieved chemically or by irradiating the medium with suitable energy source. Based on the method used for the generation of  $\cdot\text{OH}$  radicals, AOPs are generally classified into photochemical and non-photochemical processes.

**Table 1.1:** Photochemical and Non-photochemical AOPs.

| Non-photochemical                                     | Photochemical  |
|---|--|
| $\text{O}_3$ at elevated pH (>8.5)                    | $\text{H}_2\text{O}_2/\text{UV}$                               |
| $\text{O}_3/\text{H}_2\text{O}_2$                     | $\text{O}_3/\text{UV}$   |
| $\text{O}_3/\text{US}$                                | $\text{O}_3/\text{H}_2\text{O}_2/\text{UV}$                    |
| $\text{O}_3$ / Catalyst                               | $\text{Fe}^{2+}/\text{H}_2\text{O}_2/\text{UV}$ (Photo Fenton) |
| $\text{Fe}^{2+}/\text{H}_2\text{O}_2$ (Fenton system) | $\text{TiO}_2/\text{UV}$ , $\text{ZnO}/\text{UV}$              |
| Electro-Fenton  | $\text{H}_2\text{O}_2/\text{TiO}_2/\text{UV}$                  |
| Electron beam irradiation                             | $\text{O}_2/\text{TiO}_2/\text{UV}$                            |
| Ultrasound (US)                                       | $\text{UV}/\text{US}$  |
| $\text{H}_2\text{O}_2/\text{US}$                      |  |

Well-known processes for the generation of  $\cdot\text{OH}$  radicals without using light energy involves the chemical or catalytic acceleration of ozonation reactions and the Fenton system. At elevated pH, the half -life of ozone in water is less than 1min. Reaction of hydroxide ions with ozone produces superoxide anion and hydroperoxy radicals. The superoxide radical further reacts with ozone to form  $\text{O}_3^{\cdot-}$ , which combines with  $\text{H}^+$  to form  $\text{HO}_3^{\cdot}$ . This in turn decomposes immediately giving  $\cdot\text{OH}$  radicals.



Addition of  $\text{H}_2\text{O}_2$  to ozone initiates the decomposition cycle of ozone ultimately leading to the formation of  $\bullet\text{OH}$  radicals.



Several metal oxides and metal ions such as  $\text{Fe}_2\text{O}_3$ ,  $\text{MnO}_2$ ,  $\text{Ru/CeO}_2$ ,  $\text{Fe}^{2+}$ ,  $\text{Fe}^{3+}$  and  $\text{Mn}^{2+}$  catalytically accelerate the ozonation reaction and promote the decomposition of organic contaminants in water. Fenton process involves the generation of  $\bullet\text{OH}$  radicals by the reaction of  $\text{Fe}^{2+}$  with  $\text{H}_2\text{O}_2$  and is found to be an efficient method for treatment of phenols, nitrobenzene and herbicides in water. Photochemical AOPs are generally a combination of strong oxidizing agents (e.g.  $\text{H}_2\text{O}_2$ ,  $\text{O}_3$ ) with catalysts (e.g. transition metal ions) and irradiation (e.g. ultraviolet, visible). These treatment processes are considered very promising for the remediation of contaminated ground, surface and wastewaters containing non-biodegradable organic pollutants.

The general mechanism of AOP involves the production of hydroxyl radicals ( $\bullet\text{OH}$ ) which are highly reactive oxidizing agents with an oxidation potential between 2.8 eV (at pH = 0) and 1.95 eV (at pH = 14) vs. SCE (saturated calomel electrode) [29]. It is also the second strongest oxidant after fluorine.

The oxidation potentials of some common oxidants are given in the Table 1.2.

**Table 1.2:** Oxidation Potential of common oxidizing agents.

| Sl. no. | Oxidant species     | Oxidation potential, eV |
|---------|---------------------|-------------------------|
| 1       | Fluorine            | 3.06                    |
| 2       | Hydroxyl radical    | 2.80                    |
| 3       | Sulphate radical    | 2.60                    |
| 4       | Atomic oxygen       | 2.42                    |
| 5       | Nascent oxygen      | 2.42                    |
| 6       | Ozone               | 2.07                    |
| 7       | Persulphate         | 2.01                    |
| 8       | Hydrogen peroxide   | 1.77                    |
| 9       | Perhydroxyl radical | 1.70                    |
| 10      | Permanganate        | 1.68                    |
| 11      | Hypobromous acid    | 1.59                    |
| 12      | Hypochlorous Acid   | 1.49                    |
| 13      | Hypochlorite        | 1.49                    |
| 14      | Hypoiodous acid     | 1.45                    |
| 15      | Chlorine            | 1.36                    |
| 16      | Chlorine dioxide    | 1.27                    |
| 17      | Oxygen(molecular)   | 1.23                    |
| 18      | Bromine             | 1.09                    |
| 19      | Iodine              | 0.54                    |

Once  $\cdot\text{OH}$  radicals are produced, they can rapidly react with numerous species with rate constants of the order of  $10^8\text{--}10^{10} \text{ M}^{-1} \text{ s}^{-1}$ . Hydroxyl radicals attack organic pollutants through radical addition, hydrogen abstraction and electron transfer.  $\cdot\text{OH}$  radical combination yielding  $\text{H}_2\text{O}_2$  also takes place [30].



R is the organic molecule.

The reaction of  $\cdot\text{OH}$  radicals with organic compounds produce carbon-centered radicals ( $R\cdot$  or  $R\cdot\text{-OH}$ ). These may be transformed to organic peroxy radicals ( $\text{ROO}\cdot$ ) by the addition of  $\text{O}_2$ .



The radicals further react to form more reactive species such as  $\text{H}_2\text{O}_2$  and superoxide radical ( $\text{O}_2^{\cdot-}$ ), leading to chemical degradation and mineralization of organic compounds present. Because hydroxyl radicals have a very short lifetime, they are produced only in-situ during the chemical or photochemical reactions.

Even though AOPs are providing an effective way for the treatment of contaminated water, the high treatment cost, safety aspects and excitation energy input involved are found to be their major drawbacks.

### 1.3.1 Photocatalysis

Photocatalysis is a process in which light energy is used for the activation of relevant substance to undergo a chemical reaction. The photocatalyst increases the rate of reaction without itself being consumed in the process. In photo generated catalysis, ground state of the catalyst and of the substrate are involved in thermodynamically spontaneous

catalytic step [31]. Several photoreactions that take place in the presence of semiconductor and certain oxidants have been termed as photocatalytic reactions. Thus photocatalysis can be described as a change in the rate of chemical reactions or their initiation, under the action of light in the presence of a substance called photocatalyst that absorbs light and takes part in the chemical transformation of the reactants. Photocatalyst is a substance that produces electron-hole pairs by absorption of light quanta and effects chemical transformations of the reactants that come in contact with it, and regains its chemical composition after each cycle of such interactions. Based on the phase of the reactant and the photocatalyst, the reactions can be classified into homogeneous and heterogeneous photocatalysis.

#### **1.3.1.1 Homogeneous photocatalysis**

In homogeneous photocatalysis the reactant and catalyst are in same phase. Certain strong oxidants such as  $\text{H}_2\text{O}_2$  and ozone serve as photocatalysts for the generation of free radicals in presence of light. Conventional treatment methods assisted by the oxidants do not completely oxidize organics to  $\text{CO}_2$  and  $\text{H}_2\text{O}$ . The oxidizing strength of hydrogen peroxide is relatively low. However irradiation by UV light enhances the rate and the strength of oxidation through the production of reactive hydroxyl radicals. For efficient ozone photolysis a maximum radiation output at 254 nm is required. Most of the organic contaminants absorb UV energy in the range of 200-300 nm and decompose or get excited to react with chemical oxidants [32]. The use of UV light for homogeneous photocatalysis of pollutants can result in either (i) direct photo degradation of the pollutant by UV light or (ii) photo-oxidation

initiated by hydroxyl radicals, that are produced by the photolytic cleavage of strong oxidants employed as the photocatalysts.

#### 1.3.1.1.1 UV/Hydrogen peroxide (UV/ H<sub>2</sub>O<sub>2</sub>)

The reaction involves direct photolysis of H<sub>2</sub>O<sub>2</sub> by UV light (200 to 280 nm). UV irradiation photolytically cleaves the O-O bond in the H<sub>2</sub>O<sub>2</sub> to form the <sup>•</sup>OH radicals. The major steps involved in the process are given below:



Of the above reactions, Eq. 12 is the rate limiting step because the rates of other reactions are much higher. Theoretically in UV/H<sub>2</sub>O<sub>2</sub> process, the higher initial hydrogen peroxide concentration produces higher hydroxyl radical concentration (Eq. 12), which decomposes more target compounds. But after an optimal (hydrogen peroxide) concentration, overdosing of hydrogen peroxide would lead to its reaction with hydroxyl radical and formation of less reactive HO<sub>2</sub><sup>•</sup> (Eq. 13).

The mechanism of the reactions of the hydroxyl radical and other Reactive Oxygen Species (ROS) generated in UV/H<sub>2</sub>O<sub>2</sub> process in the presence of the organic substrate is given in Fig. 1.2.

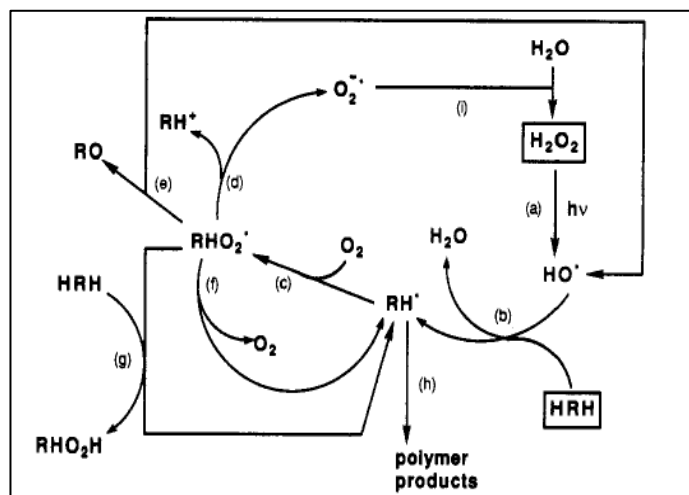


Fig. 1.2: Reaction sequence in the UV/H<sub>2</sub>O<sub>2</sub> process

Hydroxyl radicals generated by hydrogen peroxide photolysis react with organic compounds (HRH) primarily by hydrogen abstraction to produce an organic radical (RH•). This radical further reacts quickly with dissolved oxygen to produce an organic peroxy radical (RHO<sub>2</sub>•) which initiates subsequent thermal oxidation reactions.

UV/H<sub>2</sub>O<sub>2</sub> process is efficient for mineralizing organic pollutants. The major disadvantages of this process are low molar extinction coefficient in the near UV-region and small absorption cross section at 254 nm. Also H<sub>2</sub>O<sub>2</sub> has poor UV absorption characteristics and the reaction system contains water which absorbs a lot of UV light energy. Thus most of the light input to the reactor will be wasted. The major factors affecting this process are:

- Initial concentration of the target compound
- Concentration of H<sub>2</sub>O<sub>2</sub> used for the reaction
- pH of reaction medium
- Reaction time.

The rate constant for UV/H<sub>2</sub>O<sub>2</sub> degradation process is inversely proportional to the initial concentration of the pollutant. As a result, wastewater dilution should be done at an optimum level [33].

#### 1.3.1.1.2. UV/Ozone (UV/O<sub>3</sub>)

Ozone in conjunction with UV light is applied as an AOP for the treatment of a wide range of contaminants in water. Compared to H<sub>2</sub>O<sub>2</sub>, ozone provides a much higher absorption spectrum cross section at 254 nm. The mechanism of UV/O<sub>3</sub> involves light induced homolysis of O<sub>3</sub> and subsequent production of <sup>•</sup>OH radicals by the reaction of O (<sup>1</sup>D) with water [33].



Dissolved ozone is photolytically cleaved to form H<sub>2</sub>O<sub>2</sub> which in turn generates <sup>•</sup>OH radicals.



Detailed chemistry involved in the process is shown in Fig. 1.3.

The generated <sup>•</sup>OH radicals react with organic substrates to produce organic radicals that interact with the molecular oxygen to yield organic peroxy radicals. The peroxy radicals are the true propagators of the thermal chain reactions of oxidative substrate degradation.

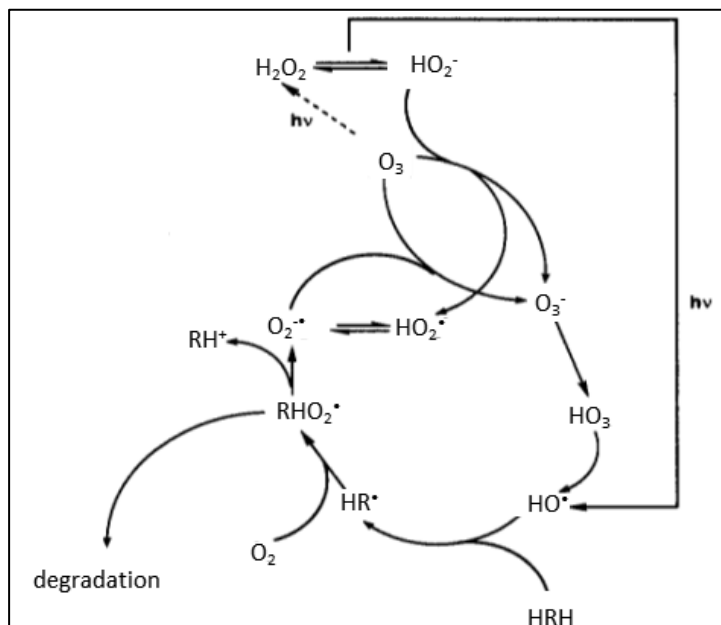
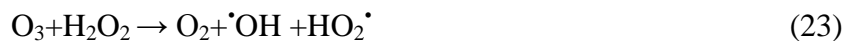


**Fig. 1.3:** Reaction sequence in the UV/O<sub>3</sub> process

The O<sub>3</sub>/UV process can effectively oxidize or decompose pollutants such as refractory organics, bacteria, and viruses in water. One of the major advantages of this process is the improved efficiency compared to the methods which use UV or ozone alone. In many cases, complete mineralization of pollutants is reported. The low ozone solubility in water is a major disadvantage [33].

#### 1.3.1.1.3 UV/ Ozone and Hydrogen peroxide (UV /O<sub>3</sub>/H<sub>2</sub>O<sub>2</sub>)

Addition of H<sub>2</sub>O<sub>2</sub> to the UV/O<sub>3</sub> system enhances the degradation efficiency. The mechanism of the process can be considered to be the same as that of UV/O<sub>3</sub>. In presence of H<sub>2</sub>O<sub>2</sub> the decomposition of ozone gets accelerated, thereby increasing the <sup>•</sup>OH radical generation. The pathway for the generation of <sup>•</sup>OH radical can be summarized as:



Almost 98% degradation efficiency in pilot scale system is reported for the removal of aromatic contaminants in water [33]. The advantage of this process is that, it can be applied to the pollutants that are weak absorbers of UV radiation as the addition of hydrogen peroxide facilitates the reaction at a reduced UV flux.

#### 1.3.1.1.4 Photo-Fenton system (UV/Fe<sup>2+</sup>/H<sub>2</sub>O<sub>2</sub>)

Fenton process involves a homogeneous catalytic system with H<sub>2</sub>O<sub>2</sub> and ferrous ion. It is reported that, in presence of UV irradiation the rate of Fenton reaction increases considerably and can be used for the mineralization of several organic pollutants such as pesticides, phenol etc. [34]. The major reasons for the increased efficiency of the photo-Fenton reaction are:

- 1) UV irradiation of ferric ion produces ferrous ion which reacts with H<sub>2</sub>O<sub>2</sub> to form secondary  $\cdot\text{OH}$  radical and ferric ion and the cycle continues.
- 2) Compared to H<sub>2</sub>O<sub>2</sub>, the absorption spectrum of ferric ion extends further to the near UV/visible region enabling photo-oxidation and mineralization even in visible light [32].

Typical reactions involved in the photo-Fenton system are given in Fig. 1.4.

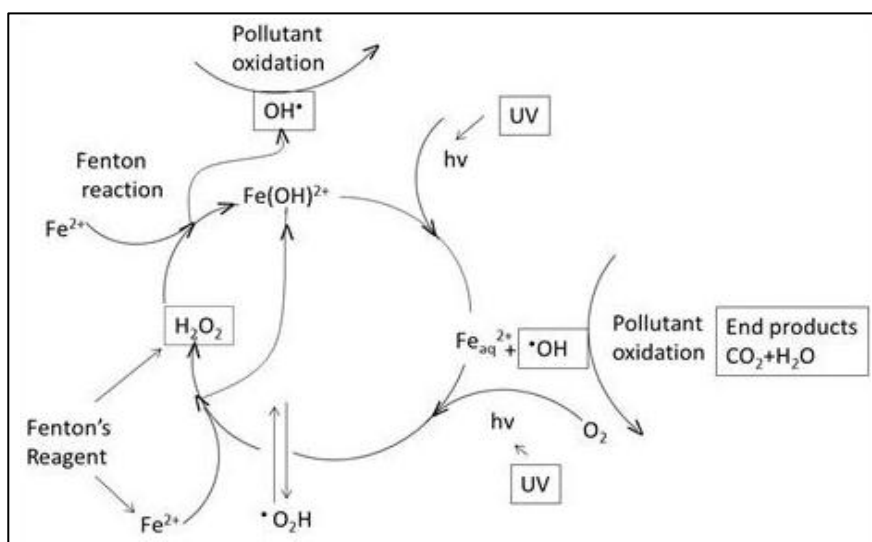


**Fig. 1.4:** Reaction sequence in the Photo-Fenton process

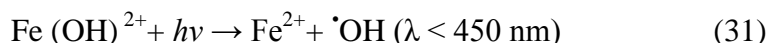
In presence of H<sub>2</sub>O<sub>2</sub> at acidic pH the Fe<sup>2+</sup> gets converted into Fe<sup>3+</sup>



At pH 3, Fe<sup>3+</sup> remains in the complex form which can be represented by Fe(OH)<sup>2+</sup> [34].



When exposed to UV irradiation the complex further decomposes to Fe<sup>3+</sup> and OH<sup>-</sup>.



The generated hydroxyl radicals interact with the organic species present in the solution and initiate chemical decomposition by H- abstraction or addition to the C-C bonds.

### 1.3.1.2 Heterogeneous Photocatalysis

The term, 'Heterogeneous Photocatalysis', is used for the process that contains a light absorbing semiconductor (solid) used as the photocatalyst in contact with liquid or gas phase reactant. Heterogeneous photocatalysis is an emerging field used for a variety of environmental and energy related applications. In recent years, semiconductor based photocatalysis is accepted as an effective tool for the removal of pollutants from water. Complete degradation and mineralization of the target molecules can be ensured by this technique. Major advantages of heterogeneous photocatalysis are:

- The absorption of UV light by the semiconductors can be tuned by metal doping, sensitizing and controlling the morphology of particles.
- The process is facile and the end products are mainly the corresponding inorganic salts, CO<sub>2</sub>, ammonium and nitrate ions depending on the substrate.
- Reaction can be carried out in presence of solar light as the irradiation source.
- The efficiency of the process can be improved by the presence of certain oxidants.

- Also the solid catalyst can be separated easily from the reaction medium and reused without substantial reduction in its photocatalytic activity.
- Less expensive and relatively easy to fabricate.

### 1.3.1.2.1 Semiconductor Photocatalysis

The efficiency of various photo-redox processes is related to the band gap of the semiconductor. According to band model, the highest energy filled band of a conducting material is known as valence band ( $E_v$ ) and the lowest empty energy band is called conduction band ( $E_c$ ). These two are separated by an energy gap, the band gap ( $E_{bg}$ ). The positions of bands and the energy gap of the material are shown in Fig. 1.5.

Semiconductors are electronic conductors with electric resistivity values generally in the range of  $10^{-2}$  to  $10^9$  ohm-cm at room temperature, intermediate between conductors ( $10^{-6}$  ohm-cm) and insulators ( $10^{14}$  to  $10^{22}$  ohm-cm) [35].

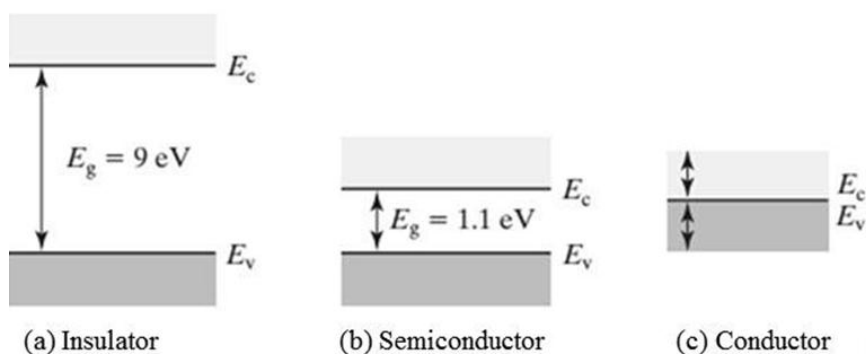


**Fig. 1.5:** Difference between energy bands of (a) insulator, (b) semiconductor and (c) metals

Absorption of light energy,  $E \geq E_{bg}$  by the semiconductor leads to the formation of electrons and holes. Under the influence of an electrical field the electrons and holes will move to the conduction band and valence band respectively. Semiconductor powder based photocatalysis is a redox reaction. The irradiated surface of semiconductor will act as a sink for the electrons (or holes) depending upon the direction of band bending. The effective separation of charge carriers, the electrons and holes determine the efficiency of photocatalytic reaction. The charge separation ability of the semiconductors can be improved by metallization, doping or by coupling two semiconductors.

The energy level of the lower edge of conduction band and the upper edge of the valence band can be considered to be a measure of reduction and oxidation strength of electron and hole generated by the semiconductor. Based on the potential of electron and hole, semiconductors are classified into four groups from the point of view of water splitting [36].

OR type: The oxidation and reduction ability is strong enough to induce both hydrogen and oxygen evolution.

R type: Only the reduction capability is high and strong enough to reduce water.

O type: Only the oxidation capability is strong enough to oxidize water. The valence band is located at a more positive value compared to the  $O_2/H_2O$  level.

X type: The conduction and valence bands are located between  $H^+/H_2$  and  $O_2/H_2O$  levels. Hence, both oxidation and reduction capabilities are weak.

The energy levels of various semiconductors and the redox potentials are given in the Fig. 1.6.

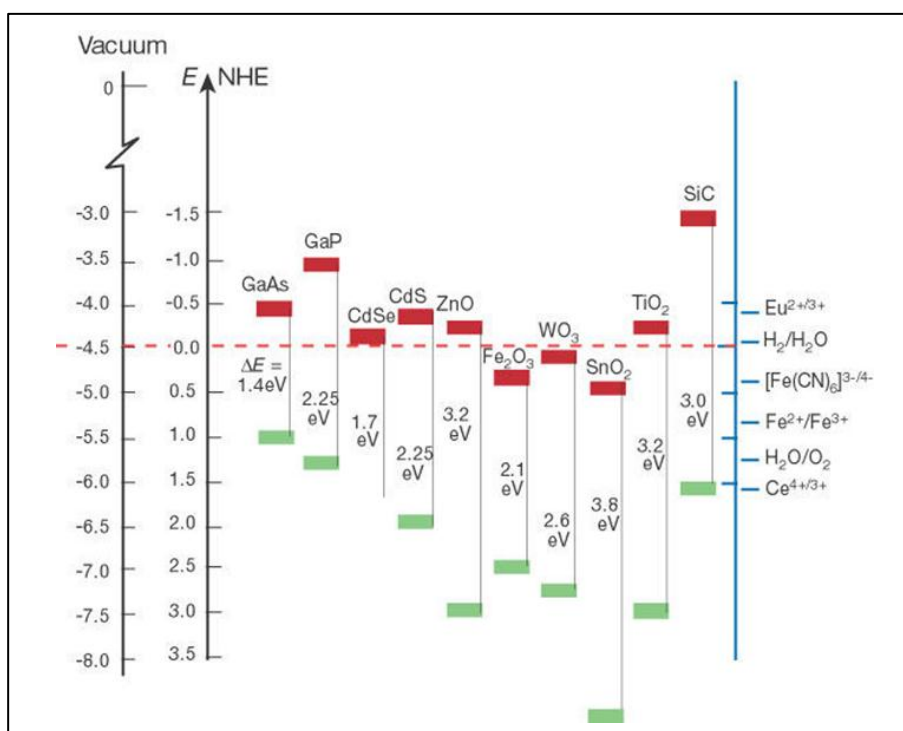


**Fig. 1.6:** The positions of bands of semiconductor relative to the standard potential of several redox couples (shown at the right hand side of the figure). The positions of the valence and conduction band of semiconductor appear favorable for one or the other of the redox reaction of the cleavage of water [36].

### 1.3.1.2.2 Photocatalytic semiconductor material

A single particle of semiconductor can provide both oxidizing and reducing species for the reaction. Semiconductors like  $\text{TiO}_2$ ,  $\text{ZnO}$ ,  $\text{Fe}_2\text{O}_3$ ,  $\text{CdS}$  and  $\text{ZnS}$  can be used as photocatalysts for wastewater treatment and polluted air purification [37-39]. Semiconductor can act as sensitizer for light induced processes. Absorption of a photon of energy greater than or

equal to the band gap energy leads to the formation of an electron-hole pair. In the absence of suitable scavengers, the stored energy is dissipated within few nanoseconds by recombination [40]. If a suitable scavenger or surface defect site is available to trap electron or hole, recombination is prevented and subsequent redox reaction may occur. The valence band holes are powerful oxidants (+1.0 to +3.5 vs. NHE depending on the semiconductor and pH), while the conduction band electrons are good reductants (+0.5 to -1.5 vs. NHE) [41].

Most organic photodegradation reactions utilize the oxidizing power of the holes either directly or indirectly. Semiconductor photocatalysis is an emerging technique valuable for water and air purification and remediation. Fundamental and applied research on this subject have been in progress extensively during the last 30 years all over the world.

Metal oxides and sulphides represent a large class of semiconductor material suitable for photocatalysis [42-44]. Among these listed semiconductors,  $\text{TiO}_2$  is proven to be the most suitable for wide spread environmental applications. In spite of the search for the ideal photocatalyst for more than two decades, titania has remained a benchmark for any material that is introduced as photocatalyst. Titanium dioxide is biologically and chemically inert; it is stable to photo- and chemical corrosion and is inexpensive. Furthermore, it can also be used for solar energy applications. This is because  $\text{TiO}_2$  has an appropriate energetic separation between its valence and conduction bands, which can be excited by the energy of a solar photon. The VB and CB energies of the  $\text{TiO}_2$  are estimated to be +3.1 and -0.1 eV, respectively, which means that its band

gap energy is +3.2eV and therefore absorbs the near UV light ( $\lambda < 388$  nm). Due to faster electron transfer to molecular oxygen, TiO<sub>2</sub> is found to be more efficient for the photocatalytic degradation of pollutants [45]. The band positions of some common semiconductor photocatalysts in aqueous solution at pH=1 are shown in Table 1.3.

**Table 1.3:** Band position of some common semiconductor photocatalysts [46].

| Semiconductor    | Valence Band<br>(V vs NHE)<br>(eV) | Conduction Band<br>(V vs NHE)<br>(eV) | Band gap<br>(eV) | Band gap<br>wavelength (nm) |
|------------------|------------------------------------|---------------------------------------|------------------|-----------------------------|
| TiO <sub>2</sub> | 3.1                                | -0.1                                  | 3.2              | 388                         |
| SnO <sub>2</sub> | 4.1                                | 0.3                                   | 3.9              | 318                         |
| ZnO              | 3                                  | -0.2                                  | 3.2              | 388                         |
| ZnS              | 1.4                                | -2.4                                  | 3.7              | 335                         |
| WO <sub>3</sub>  | 3                                  | 0.2                                   | 2.8              | 443                         |
| CdS              | 2.1                                | -0.4                                  | 1.4              | 496                         |
| CdSe             | 1.6                                | -0.1                                  | 1.7              | 729                         |
| GaAs             | 1                                  | -0.4                                  | 1.4              | 886                         |
| GaP              | 1.3                                | -1                                    | 2.3              | 539                         |

### 1.3.1.2.3 ZnO as semiconductor photocatalyst

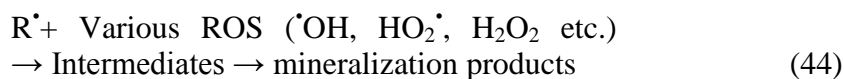
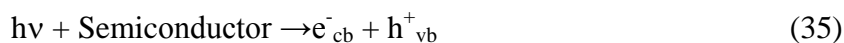
Due to the enhanced photocatalytic efficiency in pure form and in combination with other materials, ZnO is extensively used as a semiconductor photocatalyst. The similarity in charge carrier dynamics upon excitation and generation of reactive oxygen species makes ZnO a true alternative for TiO<sub>2</sub>. ZnO absorbs wide range of solar spectrum and is proven to be a better catalyst for the solar energy applications [47].

The photocorrosion, formation of inert Zn(OH)<sub>2</sub> under photocatalytic condition and dissolution at very low and high pH are the major disadvantages of ZnO.



#### 1.3.1.2.4. General mechanism of semiconductor photocatalysis

When semiconductor photocatalyst is irradiated with light having energy (hν) higher than the band gap energy, an electron is promoted to the conduction band (CB) leaving a hole in the valence band (VB). The electron and hole can then diffuse and/or migrate to the semiconductor's surface. Various steps involved in semiconductor photocatalysis are:



Schematic presentation of the mechanism is given in Fig. 1.7.

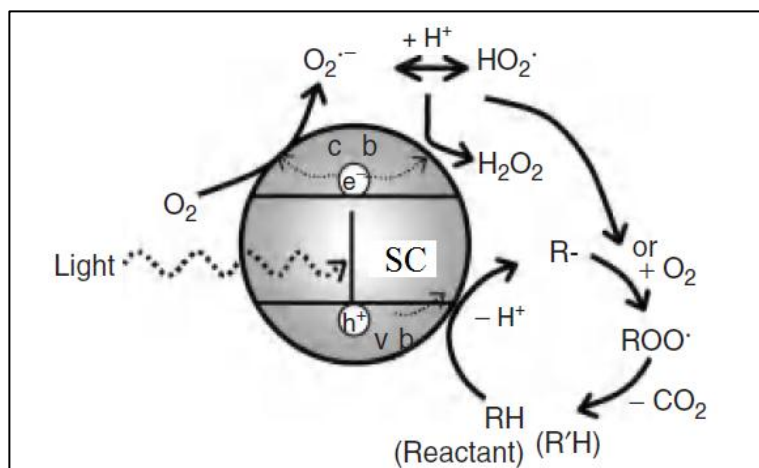


**Fig. 1.7:** Mechanism of Photocatalysis on a semiconductor [48]

The photogenerated electron-hole pairs may undergo several reactions like:

- Recombination in the bulk
- Recombination at the surface
- Reduction of a suitable electron acceptor adsorbed on the surface by photogenerated electron.
- Oxidation of a suitable electron donor adsorbed on the surface by the photogenerated hole.

Electron-hole recombination is promoted by defects in the semiconductor material and thus most amorphous materials show little photo activity. The photogenerated electron and hole are able to make their separate ways on to the surface of the semiconducting material where it is possible for them to interact with surface species as shown in Fig. 1.8.

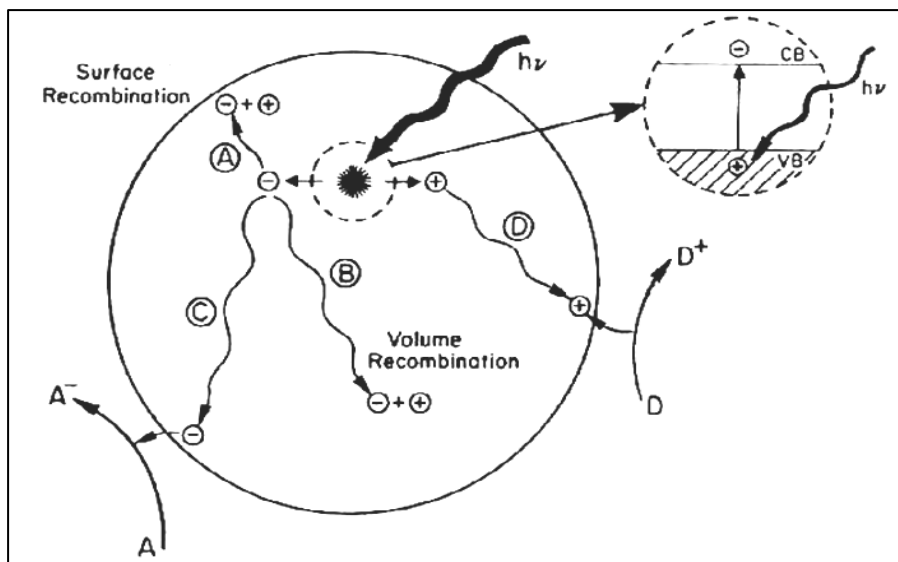
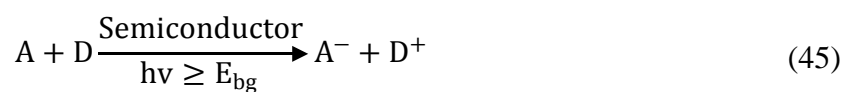


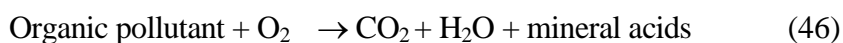
**Fig. 1.8:** Process on the Photo-excited semiconductor surface and bulk [49]

In the presence of electron donor D molecules such as ethanol, methanol, and EDTA (Ethylenediaminetetraaceticacid), the photogenerated hole can react with them to generate their oxidized product,  $D^+$ . Similarly, if there are electron acceptor molecules (A) present at the surface, such as oxygen or hydrogen peroxide, the photogenerated electrons can react with them to generate corresponding reduced product,  $A^-$ .

The overall reaction can be summarized as follows;



Many of the current commercial systems that utilize reaction (45) employ a semiconductor photocatalyst such as  $TiO_2$  to drive the oxidation of organic pollutants by oxygen i.e., photomineralization of pollutants [49].



Mineral acids as in reaction (46) are generated only if there are hetero atoms such as sulphur, nitrogen or chlorine in the original organic pollutant. In photomineralization, ultra band gap generates electron-hole pairs. Photogenerated holes that make to the surface can react with surface hydroxyl groups to generate adsorbed hydroxyl radicals ( $\cdot\text{OH}$ ) which in turn can oxidize the pollutant molecules such as dyes. Photogenerated electrons that make to the surface can react with adsorbed oxygen to generate superoxide anion ( $\text{O}_2^{\cdot-}$ ) which can be subsequently reduced to hydrogen peroxide and then water. The intermediate species hydroperoxides ( $\text{HO}_2^{\cdot}$ ) produced can act as further source of hydroxyl radicals. In photo mineralization of organic materials sensitized by  $\text{TiO}_2$ , the photogenerated electrons reduce water to oxygen and the holes mineralize the organics.

### **1.3.1.3 Use of sunlight as energy source in photocatalysis**

Major part of the cost for the photocatalytic water treatment process is the artificial generation of photons required for the degradation of pollutants. Replacing the artificial irradiation source with sunlight will make the photocatalytic process less expensive. The solar spectrum consists of UV rays in the range of 200 to 400 nm, visible light in the range 390 to 740 nm and the infrared in the range 700 nm to 1 mm (Fig. 1.9). The total radiation falling on the earth's surface contains 3.5-8% UV radiation. With a typical UV-flux of  $20\text{-}30 \text{ Wm}^{-2}$  near the surface of the earth the sun provides  $0.2\text{-}0.3 \text{ mol photons m}^{-2}\text{h}^{-1}$  in the 300-400 nm range [50]. The excitation ranges of many photocatalysts match with the UV and visible region of solar spectrum and can be used

as effective sensitizers for inducing photochemical reactions for the detoxification of pollutants in water.

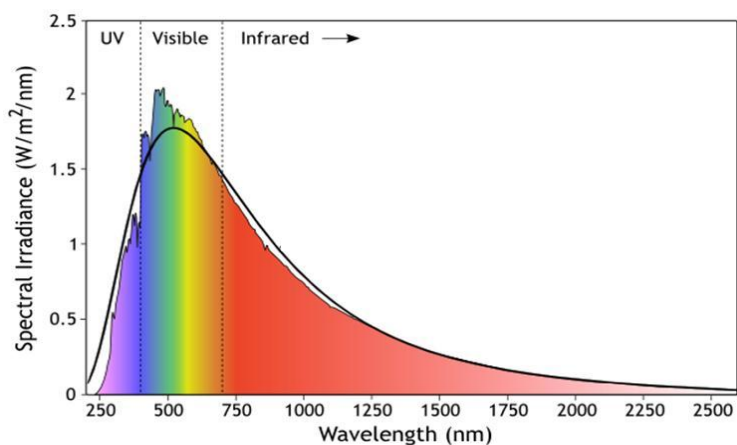


**Fig. 1.9:** Spectral composition of sunlight at Earth's surface

#### **1.4 Some typical photocatalytic degradation studies related to pesticides**

The application of photocatalytic degradation of organic pollutants in water has been widely demonstrated in recent years [45,50,51]. Various toxic compounds like dyes, pharmaceuticals, industrial organic-inorganics and pesticides are reported to be photocatalytically mineralized into simple compounds such as  $\text{CO}_2$ ,  $\text{N}_2$  and corresponding inorganic salts [45,50,52]. Most of the investigations relate to the effect of certain catalytic properties such as surface area, particle size, crystalline size, doping with metals and non- metals and also some process parameters such as pH, temperature, light intensity, catalyst loading, substrate concentration and the presence of inorganic ions on the photocatalytic degradation efficiency of the semiconductors. Many studies demonstrated the use of various light sources such as UV, visible, LED and natural

sunlight for the photo-excitation of the semiconductors [53]. Recent investigations indicate a general trend towards solar light utilization for photocatalysis which will make the process more cost-effective. This possibility also makes photocatalysis a green technology for the removal of toxic pollutants from water.

Extensive studies have been carried out using ZnO as photocatalyst in its pure form and in combination with other materials. Improvement in photocatalytic activity of ZnO by doping with transition metals such as Pt, Pd, Cu, Co, Fe, Mn, Ni, Ag, Au, Mo, Zr, La, Dy and Eu is reported by many researchers [54-61]. ZnO doped with metals such as Sn, Sb, Li, Na, and K are also tested as photocatalysts for the degradation of organic pollutants in water. Application of ZnO composites like Nb<sub>2</sub>O<sub>5</sub>/ZnO, Fe/ZnO/SiO<sub>2</sub>, Pt/Co/ZnO, Cu/Zn/ZnO, N-doped In<sub>2</sub>Ga<sub>2</sub>ZnO<sub>7</sub>, AgBr/ZnO, Ag/AgBr/ZnO, Zr/Ag/ZnO, graphite-like-C<sub>3</sub>N<sub>4</sub>/ZnO, α-Fe<sub>2</sub>O<sub>3</sub>/ZnO, CoFe<sub>2</sub>O<sub>4</sub> and TiO<sub>2</sub>/ZnO as photocatalysts also has been reported. It is reported that ZnO supported on various mesoporous materials such as MCM-41, SBA-15 etc. and supports like activated carbon, sepiolite, kaolin and diatomaceous earth shows better photocatalytic activity than its pure form. ZnO with different morphologies like nano wires, nano flower, nano mesh, tetrapodes, sheets, dumbbell and hexagonal are synthesized and studied to identify the effect of particle morphology on the photocatalytic performance [62-74]. It is reported that the oxygen vacancy and defect structure of ZnO crystals improve the visible light photo excitation [75].

Recent reviews on the photocatalytic degradation studies using TiO<sub>2</sub> as photocatalyst reveal the effectiveness of this technique for the removal or mineralization of pesticides in water from every major chemical class. Many of the researchers identified ZnO as an alternative for TiO<sub>2</sub> and extensively used it for the photocatalytic degradation of pesticides in water.

Trevino et al. [76] studied the photocatalytic degradation of Dicamba (3,6-Dichloro-2-methoxybenzoic acid) and 2,4-D (2,4-dichlorophenoxyacetic acid) using ZnO-Fe<sub>2</sub>O<sub>3</sub> composite prepared by sol-gel method in presence of solar light simulator. The prepared catalyst showed slight displacement in the band gap energy (3.14 eV) compared to pure ZnO (3.2 eV). The dechlorination of Dicamba is completed in 300min. In the case of 2,4-D only 70% dechlorination is observed for the same time.

Navarro et al. [77] investigated the photocatalytic degradation of 8 pesticides from different chemical groups (azoxyxtrobin, kresoxim-methyl, hexaconazole, tebuconazole, triadimenol, pyrimethanil, primicarb and propyzamide) using ZnO in presence of natural sun light. A pilot scale photoreactor is used for the studies. The added oxidant Na<sub>2</sub>S<sub>2</sub>O<sub>8</sub> is enhancing the degradation, while in presence of another oxidant H<sub>2</sub>O<sub>2</sub>, no increase in degradation rate was observed. The complete mineralization was achieved within 2 hr of irradiation.

A comparative study of the photocatalytic activity of ZnO and TiO<sub>2</sub> is made by Mahalakshmi et al. [78] using Carbofuran (2,3-dihydro-2,2-dimethylbenzofuran-7-yl methylcarbamate) as the target molecule in presence of UV light. Different process parameters such as initial

concentration of Carbofuran, pH of the solution and catalyst loading also are studied. Complete mineralization of Carbofuran was achieved within 7 hr of treatment. Also it is concluded that the degradation efficiency is much higher in the case of TiO<sub>2</sub> than ZnO. A similar comparative study for the degradation of Carbofuran is reported by Fenoll et al. [79] in presence of natural sunlight. They used different mixed phases of TiO<sub>2</sub> (anatase/ rutile) and ZnO for the investigation. The residual level of Carbofuran in the contaminated water after 240 min was much less for the reaction system sensitized by ZnO. The photocatalytic activity of the catalysts was in the order: ZnO >> TiO<sub>2</sub> (P25 Degussa) > TiO<sub>2</sub> rutile, TiO<sub>2</sub> anatase.

Kanmoni et al. [80] investigated the photocatalytic activity of prepared nano ZnO and TiO<sub>2</sub> for the degradation of Chlorpyrifos (O,O-diethyl O-3,5,6-trichloro-2 pyridyl phosphorothioate) in presence of sunlight. The prepared catalysts are having smaller particle size and hence they are very active in presence of sunlight. Also it is reported that the prepared nano TiO<sub>2</sub> is more efficient than the nano ZnO. Various free radicals generated during the degradation process interact with the in-situ formed intermediates at a faster rate.

Direct and indirect photodegradation of cyhalofop, an aryloxyphenoxy propionic herbicide and its primary metabolite (2R)-2-[4-(4-cyano-2-fluorophenoxy)phenoxy]propanoic acid was studied by Pinna et al. [81] using UV and simulated sunlight in presence of TiO<sub>2</sub> and ZnO. Both cyhalofop and its metabolite degrade in presence of UV and simulated sunlight to corresponding stable intermediates. The complete mineralization

was achieved only in presence of photocatalysts. It was observed that the degradation efficiency is higher for ZnO in presence of simulated sunlight. The mineralization was completed after 4 hr for TiO<sub>2</sub>, while in presence of ZnO mineralization was achieved within 75 min.

Fenoll et al. [82] extensively studied the photocatalytic degradation of various pesticides using ZnO and TiO<sub>2</sub> as catalysts in presence of simulated and natural sunlight. All the studies concluded that ZnO is a better photocatalyst than TiO<sub>2</sub>. The degradation follows pseudo first order kinetics for most of the pesticides selected. Studies conducted on the degradation of fungicides cyprodinil and fludioxonil in leaching water reported complete degradation of both within 4 hr of irradiation. In another study, they compared the photocatalytic degradation efficiencies of ZnO, TiO<sub>2</sub>, WO<sub>3</sub>, SnO<sub>2</sub> and ZnS for the degradation of 8 miscellaneous pesticides i.e. ethoprophos, isoxaben, metalaxyl, metribuzin, pencycuron, pendimethalin, propanil and tolclofos-methyl in drinking water [83]. 99% of the initially present pesticides are degraded within 4 hr irradiation in presence of ZnO. Compared to ZnO and TiO<sub>2</sub> all other studied catalysts are less active. But complete mineralization was not observed in presence of any of the catalysts used in the study. Complete mineralization of Fenamiphos, an organophosphorous pesticide in leaching water, is achieved within 240 min of irradiation in presence of natural sunlight. Major intermediates like fenamiphos-sulfoxide and fenamiphos sulfone formed during the photocatalytic condition were identified. The percentage degradation after 10 min of irradiation for selected photocatalysts was, ZnO= 99.9%, SnO<sub>2</sub>= 59%, WO<sub>3</sub>= 68%, TiO<sub>2</sub> anatase:rutile (1:3)= 99.4%, TiO<sub>2</sub>(anatase)= 99.7% and TiO<sub>2</sub>(P25 Degussa)= 99.9% [84]. Studies

conducted on the degradation of sixteen substituted phenyl herbicides, i.e. Chlorbromuron, Chloroxuron, Chlortoluron, Difenoxuron, Dimefuron, Diuron, Fenuron, Fluometuron, Isoproturon, Linuron, Metobromuron, Metoxuron, Monolinuron, Monuron, Neburon and Thidiazuron present in water showed complete disappearance of all compounds after 120 min irradiation in presence of artificial light (300-460 nm). Various steps involved in the degradation process were also proposed. The efficiency of the catalyst/oxidant system used under the optimized conditions is in the order:  $\text{ZnO}/\text{Na}_2\text{S}_2\text{O}_8 > \text{ZnO} > \text{TiO}_2/\text{Na}_2\text{S}_2\text{O}_8 > \text{TiO}_2$ . A similar work conducted for 30 sulfonylurea herbicides in water showed incomplete mineralization of the organic species present. Average time required for 90% degradation was 3 and 30 min for  $\text{ZnO}/\text{Na}_2\text{S}_2\text{O}_8$  and  $\text{TiO}_2/\text{Na}_2\text{S}_2\text{O}_8$  respectively [85-86].

Daneshvar et al. [87] studied the photocatalytic degradation of diazinon over prepared nano ZnO. 80% degradation was observed after 80 min of UV irradiation. The degradation was also followed by using commercial ZnO. It is found that the degradation efficiency increases as the crystalline size of ZnO decreases. The crystalline size of the prepared ZnO is 14 nm and it is found to be more efficient than commercial ZnO with 33 nm crystalline size.

Naman et al. [88] investigated the photodegradation of dichlorovos in presence of various semiconductor photocatalysts like  $\text{TiO}_2$ , ZnO and the effect of addition of organic sensitizers such as p-nitrophenol, hydroquinone and riboflavine. Increase in photocatalytic activity is observed in presence of  $\text{TiO}_2$  sensitized by riboflavine. The photocatalytic

efficiency of the catalysts in presence of UV light is in the order: TiO<sub>2</sub> sensitized by riboflavine > TiO<sub>2</sub> anatase > ZnO > TiO<sub>2</sub> rutile. A similar study done by Evgenidou et al. [89] reported complete disappearance of dichlorovos within 20 min of irradiation in presence of TiO<sub>2</sub>. In this case the degradation rate increases in presence of added oxidants such as H<sub>2</sub>O<sub>2</sub> and K<sub>2</sub>S<sub>2</sub>O<sub>8</sub>. For ZnO, complete removal of dichlorovos is observed only after 120 min of irradiation. In presence of H<sub>2</sub>O<sub>2</sub> slight decrease in degradation efficiency was observed. Complete mineralization was observed in presence of TiO<sub>2</sub> only. Increase in toxicity of aqueous solution was observed during the treatment, indicating the inefficient detoxification capacity of the process.

Comparative study of the photodegradation efficiency of TiO<sub>2</sub> and ZnO for the degradation of dimethoate in aqueous solution is reported by Evgenidou et al. [90]. In presence of ZnO and TiO<sub>2</sub> complete mineralization was not achieved. But the addition of H<sub>2</sub>O<sub>2</sub> in presence of TiO<sub>2</sub> improves the degradation rate and eventually leads to complete mineralization. The dissolution of zinc under photocatalytic condition was observed when ZnO was employed as photocatalyst. The concentration of Zn<sup>2+</sup> in water increased with the irradiation time and then stabilized.

Sathiyarayanan et al. [91] studied the photocatalytic degradation of insecticides imidacloprid and spirotetramat residue in water using prepared ZnO nanorods as catalyst. The ZnO nanorods with 100-250 nm diameter and 1 to 2 μm length were prepared from zinc acetate and triethanolamine using ultrasonic irradiation. The degradation rate of both imidacloprid and spirotetramat increases as the solution pH is increased.

The photodegradation of imidacloprid was more rapid than spirotetramat under the optimized conditions.

The photocatalytic degradation of metaldehyde, a selective molluscicide, was studied by Doria et al. [92] using nano-sized ZnO composite in presence of UV light. The nano-sized composite contained ZnO and trace amount of laponite, a silica based adsorbent clay and polyvinyl alcohol as binder. Maximum degradation was observed at pH 10.4 and the degradation kinetics followed modified first order kinetics.

Mijin et al. [93] studied the photocatalytic degradation of metamitron herbicide using ZnO in presence of UV light irradiation. The maximum degradation rate was observed in the alkaline medium. The effect of some common salts such as NaCl, Na<sub>2</sub>CO<sub>3</sub> and Na<sub>2</sub>SO<sub>4</sub> on degradation process was also studied. It was found that Na<sub>2</sub>CO<sub>3</sub> inhibited the degradation. Under optimized conditions 56% total organic carbon and 34% total nitrogen removal was observed within 4 hr of irradiation. The results also showed the presence of ammonia, nitrate and nitrite ions in the reaction medium after mineralization process.

Photocatalytic degradation of metasystox R, an organophosphorus pesticide was investigated by Korake et al. [94] on prepared La doped ZnO in presence of UV irradiation. Results showed reduction in the crystalline size of ZnO with increasing La content. It was found that the degradation efficiency increased up to 0.5% La loading, but a decreasing tendency was observed as the doping level increased beyond 0.5%. Maximum reduction in COD level was obtained after 150 min irradiation. Compared to pure ZnO, shorter irradiation time was required for La

doped ZnO for completing the mineralization of metasytox present in the aqueous solution.

Tomasevic et al. [95] reported the photocatalytic degradation of methomyl using commercial ZnO as photocatalyst in presence of UV light. It was found that ZnO is a better catalyst than TiO<sub>2</sub> for the degradation of methomyl present in the aqueous solution. The presence of chloride ion in the photocatalytic system negatively affected the degradation process. Also they compared the photocatalytic process in three different aqueous media such as, distilled water, deionized water and sea water and found that the ions present in the aqueous solution affected the degradation rate. The reaction rate increased as the temperature of the system increased. The ion chromatographic analysis of aqueous solution after mineralization process showed the presence of sulfate, nitrate and ammonium ions.

Evgenidou et al. [96] reported the photocatalytic degradation of methyl parathion over ZnO and TiO<sub>2</sub> in presence of UV irradiation. The degradation process is facile and complete mineralization was reported in the case of both catalysts used for the study. The addition of persulphate increased the reaction rate for both systems catalyzed by ZnO and TiO<sub>2</sub>. Complete degradation was achieved within 45 and 150 min in presence of TiO<sub>2</sub> and ZnO respectively.

Anandan et al. [97] studied the photocatalytic degradation of monocrotophos over La doped ZnO. The prepared catalyst showed absorbance band shifts towards lower wavelength region as the La doping increased. Maximum degradation under optimized conditions was observed for the catalyst containing 0.8% La loading. They

concluded that the smaller particle size and higher porous nature are reasons for the better performance of the catalyst for the degradation of trace amount of monocrotophos in aqueous solution. Also they compared the degradation of monocrotophos over ZnO supported on various zeolites (Y,  $\beta$  and ZSM-5). The zeolite improves the adsorptive nature and hence the photocatalytic degradation efficiency of the catalysts. Compared to other supported catalysts, ZnO supported on  $\beta$  zeolite showed maximum efficiency at optimized conditions [98].

Rabindranathan et al. [99] reported the degradation of phospamidon over TiO<sub>2</sub> and ZnO in presence of UV and sunlight. It was observed that TiO<sub>2</sub> is a better catalyst for the sunlight application. The mineralization of phospamidon in presence of sunlight and TiO<sub>2</sub> was complete after 75 hr irradiation. They also reported the simultaneous formation and decomposition of in-situ formed H<sub>2</sub>O<sub>2</sub> during the photocatalytic reaction. Korake et al. [100] showed that Ag-doped ZnO nano rods are effective catalysts for the visible light photocatalytic degradation of phospamidon in aqueous solution.

The photocatalytic degradation of quinalphos and monocrotophos over heterostructured nano ZnO/TiO<sub>2</sub> in presence of UV light is reported by Kaur et al. [101]. The average crystalline size of the catalyst was found to be 21.48 nm and was more active than TiO<sub>2</sub> and ZnO in their pure form.

Muneer et al. [102] studied the photocatalytic degradation of pentachlorophenol (PCP) using ZnO nano particles in presence of sunlight. About 99.6% removal of PCP was achieved within 2 hr of

irradiation. Highest degradation efficiency was observed for ZnO nano particles of 20 nm size with a band gap of 3.198 eV.

Mazellier et al. [103] studied the degradation of carbendazim by UV/H<sub>2</sub>O<sub>2</sub>. The transformation was very efficient. The presence of HCO<sub>3</sub><sup>-</sup> and CO<sub>3</sub><sup>2-</sup> quenched the ·OH radical production. The carbonate radicals formed in presence of HCO<sub>3</sub><sup>-</sup> also reacted with carbendazim to induce the photodegradation.

Enhanced photocatalytic efficiency of Cu doped ZnO was reported by Siboni et al. [104] for the removal of diazinon in presence of UV light. The degradation efficiency (~96.97%) for Cu doped ZnO/ UV was much higher than the ZnO/UV (~58.22%). Complete removal of diazinon was achieved after 120 min irradiation.

The radiolytic degradation of carbendazim using γ-irradiation was investigated by Bojanowska-Czajka et al. [105] Compared to the photolytic process, the irradiation time needed was less for the degradation of carbendazim. The mechanism of decomposition involves numerous parallel reactions. Four times reduction in toxicity was observed after 24 hr irradiation.

Kalwasinska et al. [106] reported the biodegradation of carbendazim by homogenous culture of epiphytic and neustonic bacteria. The results indicated that the epiphytic bacteria are more efficient for carbendazim degradation. Reduction of 50% in carbendazim concentration was observed after 60 day incubation.

Saien et al. [107] studied the photocatalytic decomposition of carbendazim using UV/TiO<sub>2</sub>. Over 90% degradation was observed after 70 min irradiation. They also studied the effect of temperature on the degradation efficiency in the range 25- 45°C. The results showed only moderate difference in degradation efficiency at elevated temperature.

The degradation of diquat in aqueous medium was investigated by Ghalwa et al. [108] using electrochemical method assisted by C/PbO<sub>2</sub> electrode. Complete mineralization was achieved in 210 min of electrolysis. The degradation was carried out under optimized conditions at 5-10°C.

Florencio et al. [109] investigated the photodegradation of diquat in presence of TiO<sub>2</sub> and reported that the type of catalyst and pH are major determinants of the degradation profile. The reaction intermediates identified are mainly carbonyl compounds. They observed that the degradation does not take place in acidic medium while it is fast in the alkaline solution.

Thus it is seen that extensive research is being done on the photocatalytic degradation of organic pesticide pollutants present in water. Both TiO<sub>2</sub> and ZnO are efficient for the complete degradation and also for the mineralization of the contaminants. The degradation efficiency in presence of UV and sunlight was also compared using various photocatalysts. It may be seen that the photocatalytic degradation of two widely used pesticides in India i.e. diquat and carbendazim is not investigated in detail except for the limited studies mentioned in this chapter. Similarly the sunlight induced photodegradation of these two pesticides in presence of ZnO is not reported so far. Hence, in the current

study, a detailed investigation of the solar photocatalytic degradation of both carbendazim and diquat in water is undertaken. The effect of additives in the formulation of these two pesticides on the photocatalytic degradation and the various intermediates formed during the process are also investigated. The salts/ions present in natural water can affect the degradation efficiency. The effect of some common ions likely to be present in water on the degradation profile of carbendazim and diquat was also studied. Various other parameters relevant for the efficiency of the degradation are also examined in detail and optimized.

*.....✪.....*

### OBJECTIVES OF THE STUDY, MATERIALS AND METHODS, PLAN OF THE THESIS

|                 |                                  |
|-----------------|----------------------------------|
| <i>Contents</i> | 2.1 <i>Introduction</i>          |
|                 | 2.2 <i>Objectives</i>            |
|                 | 2.3 <i>Materials used</i>        |
|                 | 2.4 <i>Experimental setup</i>    |
|                 | 2.5 <i>Analytical procedures</i> |
|                 | 2.6 <i>Plan of thesis</i>        |

#### 2.1 Introduction

Identification and optimization of efficient and environment friendly methods for the removal of organic and inorganic contaminants from water is essential for effective pollution control. The extensive use of pesticides and other organic compounds for agricultural purposes is contributing to a large extent to the contamination of natural water resources. Conventional methods like adsorption and chemical treatments for decontamination of water have certain limitations. These processes are not degrading the pollutants to simple harmless compounds. In recent years, advanced oxidation processes (AOPs) are proven to be efficient for the removal of toxic species from contaminated water. Semiconductor based heterogeneous photocatalysis is identified as an effective AOP for treatment of polluted water. Compared to other treatment methods, AOP is more viable and the pollutants are completely mineralized into simple harmless compounds like  $\text{CO}_2$ ,  $\text{NH}_4^+$  etc. Various semiconductor based

photocatalytic systems are evaluated for the degradation of pollutants like dyes, pesticides, pharmaceutical and inorganic compounds. Semiconductor oxides such as TiO<sub>2</sub> and ZnO in presence of UV, visible or sunlight have attracted much attention as photocatalytic systems for the remediation of toxic species in water due to their low cost, non-toxic and non-selective nature.

In most of the photocatalytic studies for the treatment of contaminated water, TiO<sub>2</sub> is used as the catalyst due to the high photocatalytic activity, non-toxicity and high resistance to photo corrosion. ZnO has almost the same band gap energy (3.2 eV) as TiO<sub>2</sub> which makes it an alternative candidate for the photocatalytic applications.

The mode of illumination for the photoexcitation is a major factor that determines the cost effectiveness of photocatalytic processes. Variety of irradiation sources such as UV light, visible light, laser and LED (Light-Emitting Diode) are reported. Use of natural sunlight as the source of energy will make the process more viable for pollution control. ZnO has a wider sunlight absorption range compared to TiO<sub>2</sub> which makes it a better solar photocatalyst. The limiting factors like the dissolution and the fast recombination rate of electron-hole pair can be overcome by optimizing the reaction conditions (addition of electron scavengers, pH etc.).

As mentioned in Chapter 1, extensive use of pesticides for agricultural purpose is contaminating the water resources. Carbendazim (fungicide) and diquat (herbicide) are two commonly used pesticides. The photodegradation of these pollutants in presence of UV light, TiO<sub>2</sub>, ozone and H<sub>2</sub>O<sub>2</sub> under different conditions has been reported. However, the

reaction/degradation of carbendazim and diquat in presence of sunlight as the energy source and/or ZnO as the photocatalyst has not been reported.

Unlike in the case of controlled laboratory conditions, in real life, water may contain a variety of pollutants, including multiple pesticide contaminants. The degradation and removal of trace pollutants in such a situation is complicated due to a number of factors including the interaction among the contaminants and various intermediates formed from them. The possibility of using photocatalysis as an effective tool for the removal of combination of pollutants from water is also important for effective water treatment.

Pesticides for field application are often available as formulations. The formulations contain various additives such as inert carriers, emulsifiers, wetting agents, solvents, stabilisers, thickeners, anticaking agents etc. in addition to the active ingredient (A.I.) pesticide. Along with pesticides, these additives also enter the natural water resources and contaminate them. They can also influence the photocatalytic degradation of the pesticide active ingredient.

## **2.2 Objectives**

The main objectives of the study are:

- Detailed investigation on exploiting the potential of ZnO as a visible light active photocatalyst for the removal of selected pesticide pollutants from water using diquat and carbendazim as test molecules and sunlight as the energy source.

- Photocatalytic degradation studies of combination of pollutants and evaluation of the mutual effect on the mineralization rate.
- Investigation on the effect of formulation additives on the photocatalytic degradation and mineralization of diquat and carbendazim.
- Application of the laboratory-optimized parameters for the solar photocatalytic removal of carbendazim and diquat from real field water matrix.
- Elucidation of the kinetics and mechanism of the photocatalytic degradation of the pollutants.

Specific activities to achieve the objectives will include:

- Characterization of the selected catalyst, i.e. ZnO
- Optimization of reaction parameters i.e. catalyst loading, reactant concentration, pH, dissolved oxygen, dissolved salts etc. on the photocatalytic degradation of diquat and carbendazim.
- Investigation on the effect of various contaminant anions and cations in water on the efficiency of degradation of carbendazim and diquat.
- Identification of reaction intermediates formed during the photocatalytic degradation of carbendazim and diquat.
- Determination of chemical oxygen demand (COD) and total organic carbon (TOC) at various intervals of irradiation and their correlation with the degradation.
- Evaluation of the role of O<sub>2</sub> in the photocatalytic process.

## 2.3 Materials used

### 2.3.1 Zinc oxide

ZnO has many important applications such as in luminescent materials, electro acoustic transducers, electro photography, gas sensors, hetero junction solar cells, conductors, heat mirrors etc. It also has versatile application in many fields such as catalysis. Of these, application of ZnO as an efficient photocatalyst has been the subject of intensive investigation.

ZnO is present in the earth's crust as zincite. The main crystal structures of ZnO are hexagonal wurtzite, zinc blende and rocksalt. Under ambient conditions, wurtzite phase is thermodynamically the most stable. The zinc blende ZnO structure can be stabilized only by growth on cubic substrates. Rocksalt or Rochelle salt (NaCl) structure may be obtained at relatively high pressures [110].

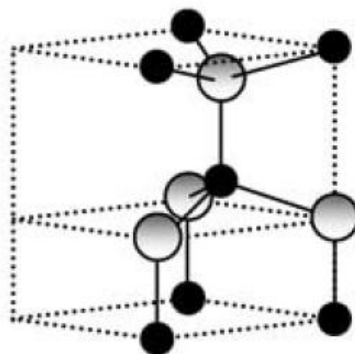


**Fig. 2.1:** Hexagonal wurtzite structure of ZnO (Shaded gray and black spheres denote Zn and O atoms, respectively)

Wurtzite structure (Fig. 2.1) has characteristic properties of semiconductors and is the hardest of the II-VI family (zinc and oxygen

belong to the 2<sup>nd</sup> and 6<sup>th</sup> group of the periodic table respectively). It is an n-type semiconductor and is more resistant to radiation damage than other common semiconductor materials, such as Si, GaAs, CdS, and even GaN. The high excitation binding energy (60 meV) gives it a very high potential for room temperature light emission [111].

ZnO is insoluble in water, but soluble in most inorganic acids. ZnO also dissolves in alkalis to give soluble zincates.



Various physico-chemical properties of ZnO are shown in Table 2.1.

**Table 2.1:** Physico-chemical properties of ZnO.

|                            |  |
|----------------------------|--|
| Molecular mass             | 81.37 g/mol                                  |
| Crystal structure          | Wurtzite                                     |
| Density                    | 5.606 g/mL                                   |
| Meting point               | 1975°C                                       |
| Boiling point              | 2360°C                                       |
| Solubility in water        | 0.16 g/100 mL                                |
| Thermal conductivity       | 0.6, 1-1.2 Wcm <sup>-1</sup> K <sup>-1</sup> |
| Energy gap                 | 3.4 eV                                       |
| Excitation binding energy  | 60 mV  |
| Static dielectric constant | 8.656  |
| Refractive index           | 2.008, 2.029                                 |

ZnO is commercially produced by direct and indirect oxidation of zinc vapor or by wet chemical process. Nanostructures of ZnO with variety of morphologies like nanowires, nanorods, tetrapods, nanobelts, nanoflowers, nanoparticles etc. and also defect structures are obtained by the above-mentioned techniques, under certain conditions [112-114].

### 2.3.2 Carbendazim

Carbendazim is a systemic benzimidazole fungicide that has extensive application. It is used to control diseases in cereals, fruits, vegetables and ornamental plants. It is also used for seed pre-planting treatment and post-harvest food storage. It is also a degradation product of the widely used fungicide benomyl [115].

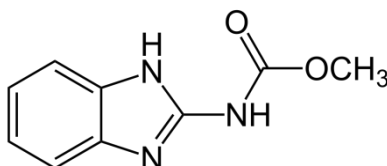


Fig. 2.2: Carbendazim

The fungicidal action of carbendazim involves the inhibition of the development of the fungi by interfering with spindle formation at mitosis (Mitosis is a process where a single cell divides into two identical daughter cells). The physico-chemical properties of carbendazim are shown in Table 2.2.

Table 2.2: Physico-chemical properties of carbendazim.

| IUPAC Name          | Methyl <i>1H</i> -benzimidazol-2-ylcarbamate                |
|---------------------|---|
| Chemical formula    | C <sub>9</sub> H <sub>9</sub> N <sub>3</sub> O <sub>2</sub> |
| Molar mass          | 191.187 g/mol   |
| Appearance          | Light gray powder   |
| Density             | 1.45 g/cm <sup>3</sup>                                      |
| Melting point       | 302 to 307 °C (576 to 585 °F; 575 to 580 K) (decomposes)    |
| Solubility in water | 8 mg/L  |

Carbendazim is identified as an endocrine disruptor. It can also damage the development of mammals in the womb. It also affects the

number of chromosomes in human even at low exposures by inhibition of polymerization of tubulin, the protein that is essential for segregation of chromosome during cell division. Carbendazim gets strongly adsorbed to sediments thereby affecting the aquatic organisms. It is toxic to earthworm and non-target plants.

### 2.3.3 Diquat

Diquat is a herbicide that is commercially available in different trade names such as, Aquacide, Dextrone, Reglone, Reglox, Weedtrine-D, Aquakill, Vegetrole, Deiquat, Reglon, Tag etc. It is also used as a plant growth regulator. Diquat is a quick acting non-selective herbicide and can affect the non-target plants also. It is known as a desiccant because diquat dries out quickly the entire plant or leaf where it is applied. Normally it is used for controlling the aquatic weeds [116].

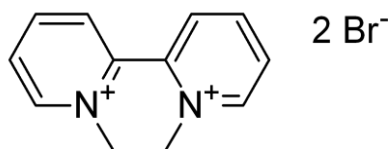


**Fig. 2.3:** Diquat dibromide

Diquat is a moderately toxic chemical and can cause kidney failure and liver damage. Also it is acutely toxic if absorbed through the skin. It will not get degraded by microbes and binds with the organic matter and sediments and remains without significant degradation for years. It is known to be toxic to fish.

The pesticidal activity of diquat is by interfering with the photosynthesis, especially the photosystem I (PS I) thereby leading to the

destruction of cell membrane. The physico-chemical properties of diquat are as follows:

**Table 2.3:** Physico-chemical properties of diquat.

| <b>IUPAC Name</b>   | <b>6,7-Dihydrodipyrido[1,2-a:2',1'-c]pyrazinediium dibromide</b> |
|---------------------|--|
| Chemical formula    | $C_{12}H_{12}Br_2N_2$  |
| Molar mass          | 344.05 g/mol   |
| Appearance          | Yellow crystals  |
| Density             | 1.22 - 1.27 g/cm <sup>3</sup>                                    |
| Melting point       | 335 °C (635 °F; 608 K)   |
| Boiling point       | Decomposes   |
| Solubility in water | 70g/100mL  |

#### **2.3.4 Pesticide formulations**

Pesticides are originally manufactured as technical grade (active ingredient or A.I.). In this form they are unsuitable for direct use because of the following reasons:

- They have unsuitable physical characteristics.
- They are generally waxy or lumpy solids or viscous liquids and difficult to be applied in the field in this form.
- They have high purity and hence it is difficult to disperse in the required dose which is quite small. Since they are toxic, the dosage has to be more or less precise and it is difficult to disperse the pesticide in the AI form evenly and effectively.
- The toxicity is very high and hence its direct application is hazardous and the handling also needs specialised training and skill.

Various ingredients that are added to the active ingredient to improve its pesticidal activity are collectively known as adjuvants. Adjuvants are added to the pesticide A.I. for better mixing and application characteristics thereby enhancing the biological performance and promoting better uptake (of pesticide) [117]. Some of the commonly available formulations are shown in Table 2.4.

**Table 2.4:** Common pesticide formulations.

| <b>Dry</b>                 | <b>Liquid</b>                    |
|----------------------------|----------------------------------|
| Dusts                      | Emulsifiable concentrate         |
| Granules                   | Ultra low volume                 |
| Wettable powder            | Technical concentrates           |
| Soluble powder             | Flowables                        |
| Pellets                    | Aerosols                         |
| Feed formulations          | Liquefied gas/Fumigant solutions |
| Baits                      | Paints                           |
| Fertilizer combinations    |                                  |
| Water dispersable granules |                                  |
| Dry Flowables              |                                  |

The adjuvant helps the pesticide to form a uniform layer and stick to the surface when sprayed. Fig. 2.4 shows the SEM image of the pesticide sprayed surface with and without adjuvant. When pesticide is applied without adjuvant, the pesticide crystals are segregated outside the droplet and form a coffee ring pattern. In presence of adjuvants, the pesticides form a uniform layer inside the droplet thereby enhancing the surface coverage of the pesticide [118].

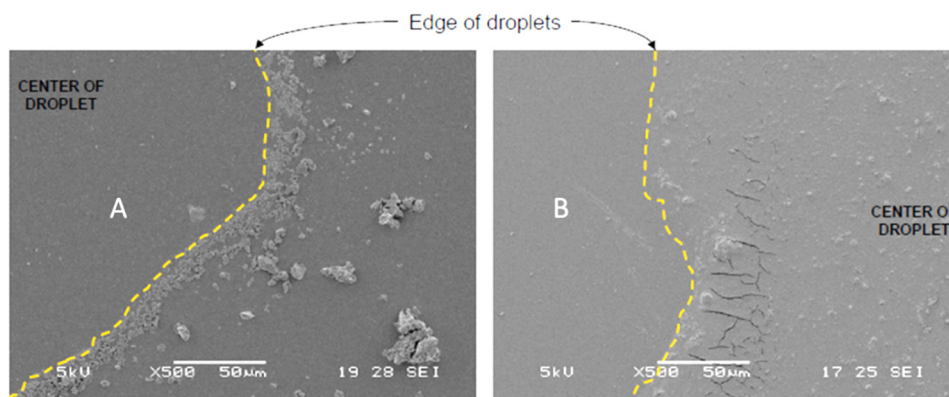


**Fig. 2.4:** SEM image of pesticide applied surface (A) without adjuvant and (B) with adjuvant[118]

The most commonly used formulation of carbendazim is wettable powder (A.I.= 5-75%). A wettable powder is basically a solid formulation which contains micronized powder of active ingredient along with dispersing agent, an anionic species and a wetting agent which is anionic or non-ionic. Normally surfactants are used as wetting and dispersing agents. When wettable powder is mixed with water it forms a uniform suspension of particles dispersed in water. Diquat formulation is available as wettable powder and emulsifiable concentrate. Emulsifiable concentrate of pesticide contains 0.1-40% A.I. It contains an emulsifying agent and water-insoluble organic solvent along with the pesticide. When mixed with water it forms an emulsion. Basically, the emulsifying agent is a surfactant which is anionic or non-ionic species. The amount of surfactant added to the formulation is normally below its critical micelle concentration [118].

### 2.3.5 Miscellaneous materials

Relevant details of various other materials used in the study are provided in the respective chapters.

## **2.4 Experimental setup**

The experimental set up and the procedures are described in the respective chapters.

## **2.5 Analytical procedures**

The analytical procedures used in the study include spectroscopy, chromatography, microscopy, XRD, conventional wet methods etc. These are described in relevant sections in the respective chapters.

## **2.6 Plan of the thesis**

The thesis is divided into nine chapters. Each chapter which is dealing with the results of the current study (from chapter 3 onwards) has its own specific objectives, experimental procedures, results, discussion and conclusions.

Chapter 1 entitled “Introduction: Background literature” gives an overview of the recent relevant literature and discussions on pesticide pollution and various types of advanced oxidation processes (AOPs) with special focus on the application of solar photocatalysis for water treatment.

Chapter 2 entitled “Objectives of the study, Materials and methods, Plan of the thesis” explains the main objectives of the study and specific activities undertaken to accomplish the objectives. The chapter also explains the characteristics of the important materials such as ZnO, carbendazim, diquat and their formulations used in the study. The chapter also provides the general plan and layout of the thesis.

Chapter 3 entitled “Solar photocatalysis mediated by ZnO for the removal of carbendazim fungicide from water.” deals with the studies on solar photocatalytic degradation of carbendazim in presence of ZnO under different reaction conditions. Details of the experimental procedure, catalyst characterization, analytical procedures etc. are provided. This chapter explains the effect of various process parameters, dissolved salts, oxidants and oxygen on the photocatalytic degradation of carbendazim in contaminated water. The results are discussed and a mechanism for the photocatalytic process is proposed.

Major findings reported in this chapter were published in the following original peer reviewed research paper:

Paper 1. “Green technology in wastewater treatment: Solar photocatalysis mediated by ZnO for the removal of trace amounts of carbendazim fungicide from water”, *IOSR Journal of Applied Chemistry*, e-ISSN:2278-5736 (2016) 71-86.

Some of the findings presented in this chapter were also presented in the “International Conference on Emerging Trends in Engineering & Management (ICETEM-2016)”, held at Kadayirippu, Ernakulam (2016).

Chapter 4 entitled “Solar photocatalysis mediated by ZnO for the removal of diquat herbicide from water” deals with the studies on solar photocatalytic degradation of diquat herbicide in water in the presence of ZnO under different reaction conditions. Details of

the experimental procedure, catalyst characterization, analytical procedures etc. are provided. This chapter explains the effect of various process parameters, anionic and cationic species, oxidants, oxygen etc. on the photocatalytic degradation of diquat in contaminated water. The results are discussed in detail and probable mechanism is proposed.

Part of the findings presented in this chapter are published as two peer reviewed research papers in international journals.

Paper 2. “ZnO Photocatalysis Using Solar Energy for the Removal of Trace Amounts of Alfa-Methylstyrene, Diquat and Indigo Carmine from Water”, *J. Adv. Oxid. Technol.* 17 (2014) 297-304.

Paper 3. “Sunlight induced photocatalytic degradation of herbicide diquat in water in presence of ZnO”, *J. Env. Chem. Eng.* 3 (2015) 1107-1116.

Chapter 5 entitled “Solar photocatalysis mediated by ZnO for the removal of the combination of diquat and carbendazim from water” deals with the studies on solar photocatalytic degradation of the combination of diquat and carbendazim when they are simultaneously present in the contaminated water. The chapter explores the possibility of using ZnO as photocatalyst for the degradation of mixed contaminants in water. Details of the experimental procedure, catalyst characterization, analytical procedures etc. are provided. The effect of one component on

the degradation and mineralization of the other is also experimentally verified and discussed in detail. The effect of various process parameters as well as various contaminants likely to be present in water on the photocatalytic degradation of diquat/carbendazim combination is also verified and discussed.

Chapter 6 entitled “Solar photocatalysis mediated by ZnO for the removal of carbendazim formulation from water” deals with the studies on solar photocatalytic degradation of carbendazim formulation in presence of ZnO under different reaction conditions. Details of the experiments, analytical procedures etc. are also explained and discussed. The effect of various process parameters, adjuvants and salts on the photocatalytic degradation of carbendazim in the formulated form is investigated in detail.

Chapter 7 entitled “Solar photocatalysis mediated by ZnO for the removal of diquat formulation from water” deals with the studies on solar photocatalytic degradation of diquat in the form of its formulation in presence of ZnO under different reaction conditions. Details of the experiments, analytical procedures etc. are discussed. The effect of various process parameters and formulation adjuvants as well as the presence of natural water contaminants on the photocatalytic degradation of diquat formulation is investigated in detail and the results are discussed.

Chapter 8 entitled “Solar photocatalysis mediated by ZnO for the removal of diquat and carbendazim pollutants from natural water systems” examines the possibility of the application of ZnO mediated solar photocatalysis for the removal of pesticide pollutants from the actual field water. Water collected from different natural water resources such as sea, river and well is used as the medium. The water samples are analyzed for various contaminants and physico-chemical characteristics. The influence of these factors on the degradation and mineralization of both pollutants is evaluated and discussed.

Chapter 9 entitled “Summary and Conclusion” summarizes the findings of the study and highlights the conclusions.

Annexure 1: List of the abbreviations used in the thesis.

Annexure 2: Provides the list of research papers (A) published in peer reviewed journals and (B) presented in conferences.

Annexure 3: Provides the reprints of papers published in peer reviewed journals.

.....❧.....

**SOLAR PHOTOCATALYSIS MEDIATED BY ZnO FOR THE  
REMOVAL OF CARBENDAZIM FUNGICIDE FROM WATER**

- 3.1 Introduction
- 3.2 Experimental details
- 3.3 Results and discussion
- 3.4 Mechanism of the photocatalytic degradation of carbendazim
- 3.5 Conclusion

**3.1 Introduction**

It has been reported that extensive usage of carbendazim results in contamination of various water bodies [115,119]. It is relatively stable, having a half-life of 6-25 weeks in water. Details on the chemistry and fungicidal characteristics of carbendazim are described in Chapter 2 section 2.3.2. Reports on the photodegradation of carbendazim in presence of UV light in combination with TiO<sub>2</sub>, ozone and H<sub>2</sub>O<sub>2</sub> are available in the literature [119,120]. However, to the best of our knowledge, no investigations have been made so far on the application of solar energy and/or ZnO catalyst for the removal of traces of carbendazim from water. In this chapter, the results of our study on the solar photocatalytic degradation of carbendazim in water are presented and discussed. Various process parameters affecting the degradation are evaluated in detail and optimum reaction conditions are identified. Some of the major reaction intermediates are also identified by LC/MS technique.

## 3.2 Experimental details

### 3.2.1 Materials

ZnO (99.5%) used in the study was supplied by Merck India Limited. The surface area, as determined by the Brunauer–Emmett–Teller (BET) method is  $\sim 12\text{m}^2/\text{g}$ . The physicochemical characteristics of ZnO used in the study were confirmed by X-ray diffraction (XRD), Scanning Electron Microscopy (SEM), Transmission Electron Microscopy (TEM), particle size and adsorption measurements.

Carbendazim (99.9%) obtained from Sigma-Aldrich was used as such without further purification.  $\text{H}_2\text{O}_2$  and  $\text{Na}_2\text{S}_2\text{O}_8$  (both LR grade) were from Nice chemicals, India.  $\text{Na}_2\text{SO}_4$ ,  $\text{K}_2\text{SO}_4$ ,  $\text{CaSO}_4$ ,  $\text{MgSO}_4$ ,  $\text{Al}_2(\text{SO}_4)_3$ ,  $\text{NaCl}$ ,  $\text{NaNO}_3$  and  $\text{Na}_2\text{HPO}_4$  were from Merck Chemical Company (India). Terephthalic acid was from Rolex, India.

The solutions were prepared in Millipore water. The solubility of carbendazim in water at  $25^\circ\text{C}$  is  $8\text{mg/L}$ . Saturated stock solution of carbendazim in water was prepared by adding the required quantity of the solute to the solvent in a glass conical flask at  $60^\circ\text{C}$  and stirring for 1hr. The solution was cooled to room temperature and then filtered through Whatmann No.1 filter paper to remove suspended micro particles, if any. The clear solution remains stable for a minimum of two days, as is confirmed by spectrophotometric analysis.

### 3.2.2 Analytical procedures

The degradation of carbendazim was followed by spectrophotometry using a Perkin-Elmer Lambda 650 Spectrophotometer. At periodic

intervals, samples were drawn from the reactor and filtered through 0.45 $\mu$ m syringe filter. The absorbance of the clear solution was measured at 284 nm. Millipore water, used for the preparation of the solution was used as the reference.

Chemical Oxygen Demand (COD) of the samples was determined using open reflux method [121]. 50 ml of the sample was pipetted out into a refluxing flask. HgSO<sub>4</sub> (1g) was added to the sample. 5 ml of sulphuric acid reagent (Ag<sub>2</sub>SO<sub>4</sub> + H<sub>2</sub>SO<sub>4</sub>) was added slowly with mixing to dissolve HgSO<sub>4</sub>. The sample was cooled while mixing to avoid the possible loss of volatile material. 25 ml of 0.05N K<sub>2</sub>Cr<sub>2</sub>O<sub>7</sub> solution was also added and mixed well. 15 ml sulphuric acid reagent was added through the open end of the condenser. The whole mixture was refluxed for 2 hr and cooled thereafter to room temperature. It was then diluted to 150 ml and the excess K<sub>2</sub>Cr<sub>2</sub>O<sub>7</sub> was titrated against 0.05N ferrous ammonium sulphate (FAS) solution. The end point was sharp change of color from blue-green to reddish brown. A blank experiment was also carried out under identical conditions using the reagents and distilled water in place of the sample.

COD is calculated using the following equation:

$$\text{COD as mg } \frac{\text{O}_2}{\text{L}} = \frac{(A - B) \times M \times 8000}{\text{Sample volume (in ml)}} \quad (49)$$

where

A = ml FAS used for blank

B = ml FAS used for sample

M = molarity of FAS

8000 = milli equivalent weight of oxygen x 1000 ml/L

H<sub>2</sub>O<sub>2</sub> was analyzed by standard iodometry. The oxidation of iodide ions by H<sub>2</sub>O<sub>2</sub> was carried out in 1N sulphuric acid in presence of a few drops of saturated ammonium molybdate solution, which acts as a catalyst. The reaction was allowed to go to completion (5 min) in the dark. The liberated iodine was then titrated against a standard solution of sodium thiosulphate, usually of the order of 5 x 10<sup>-3</sup>N prepared freshly from 0.1N stock solution. Freshly prepared starch was used as the indicator.

The anion concentration was determined by ion chromatography using Metrohm 861 advanced compact IC equipped with Metrosep A sup 5-250/4.0 column. A mixture of 3.2mM Na<sub>2</sub>CO<sub>3</sub> and 1.0mM NaHCO<sub>3</sub> solution was used as the eluent. Typical chromatogram for the selected ions is shown in Fig. 3.1.

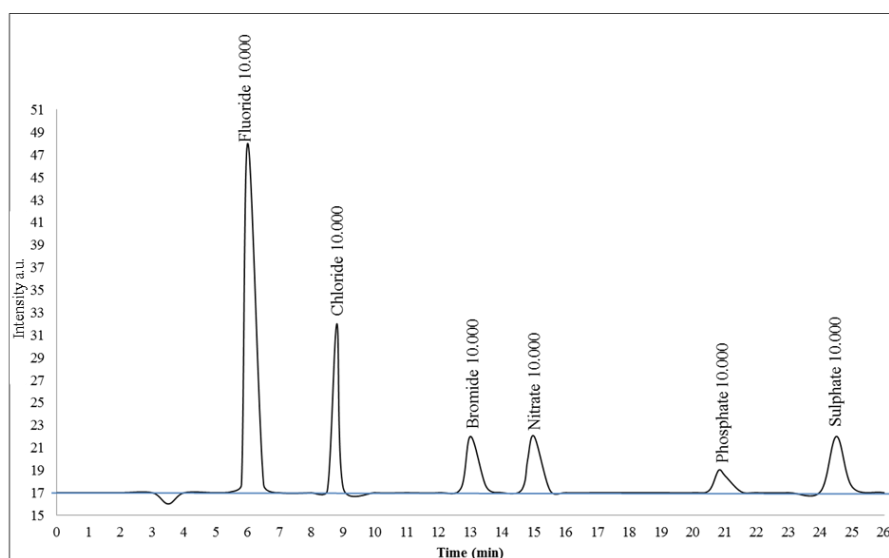


**Fig. 3.1:** Ion chromatogram of selected anions

The concentration of cations was determined by ICP/MS technique using Agilent Technologies 7900 ICP MS.

### **3.2.3 Adsorption**

The adsorption of carbendazim on ZnO was determined by dispersing a fixed amount (0.1g) of ZnO in 100 ml carbendazim solution of required concentration in a 250 ml reaction flask. The suspension was agitated continuously for 2 hr. The temperature was maintained at  $29 \pm 1^\circ\text{C}$ . After 2 hr, the stirring was stopped and suspension was kept undisturbed for 2 hr. Then it was filtered through 0.45 $\mu\text{m}$  Millipore syringe filter. The concentration of carbendazim remaining in the supernatant was determined using spectrophotometer. No significant change in concentration was observed by keeping the suspension overnight indicating that 2 hr is sufficient for maximum adsorption. The adsorption was calculated using the equation.

$$q_e = (C_0 - C_e)V/W \quad (50)$$

where  $q_e$  is adsorption capacity i.e. the quantity adsorbed in mg/g of the adsorbent.  $C_0$  is the initial adsorbate concentration (mg/L),  $C_e$  is the equilibrium adsorbate concentration in solution (mg/L),  $V$  is the volume of the solution in litre (L) and  $W$  is the mass of the adsorbent in gram.

The same procedure was used for measuring the adsorption of various ions using respective salt solutions under required conditions.

### **3.2.4 Detection of hydroxyl radicals**

The formation of hydroxyl radicals in presence of ZnO during solar irradiation is verified by the photoluminescence (PL) technique using terephthalic acid (TPA) as the probe molecule [122,123]. The hydroxyl radicals formed in-situ in the system react with TPA and form 2-hydroxyl

terephthalic acid (HTPA). The fluorescence intensity of HTPA formed is proportional to the concentration of  $\cdot\text{OH}$  radicals in the system. In this method, ZnO (0.03 g) is suspended in a mixed aqueous solution of TPA ( $2 \times 10^{-4}\text{M}$ ) and NaOH ( $2 \times 10^{-3}\text{M}$ ) and irradiated by sunlight. The PL spectrum of the product HTPA is recorded in the range of 400 -450 nm after every 5min of irradiation. The excitation wavelength was 315 nm. The PL intensity at 425 nm corresponds to the concentration of HTPA. Shimadzu model RF-5301PC fluorescence spectrophotometer is used for recording the spectrum. The hydroxyl radical formation in presence of cations and anions is monitored by adding 20 ml (8mg/L) of the respective ion/salt solutions to ZnO and stirring for 10min before adding TPA solution. After adding TPA to the suspension, the whole system is irradiated with sunlight for 10 min and the PL spectrum is recorded as mentioned above.

### 3.2.5 Analysis of reaction products/ intermediates

The reaction intermediates were identified by using Agilent 6460 Triple quad LC/MS equipped with an ESI interface operating in positive polarity mode. The LC column was C18 of 150 mm x 4.6 mm and  $5\mu\text{m}$  particles (Phenomenex). The mobile phase was acetonitrile - formic acid (0.1%) in the ratio 20:80. The scanning was done by multiple reactions monitoring (MRM) in the range of 50-250 amu.

### 3.2.6 Photocatalytic Experimental set up

Photocatalytic experiments in presence of sunlight were performed using a glass reactor. The carbendazim solution (50 ml) of the required

concentration together with ZnO was taken in the reactor. Cooling water from a thermostat ( $29 \pm 1^\circ\text{C}$ ) was continuously circulated through the water bath in which the reactor was placed. Solar experiments were performed by placing the reaction system on the roof-top of our laboratory at Kochi, Kerala, India ( $9^\circ 57' 51''$  N,  $76^\circ 16' 59''$  E) during sunny days in February-May 2013 and November-December 2014.

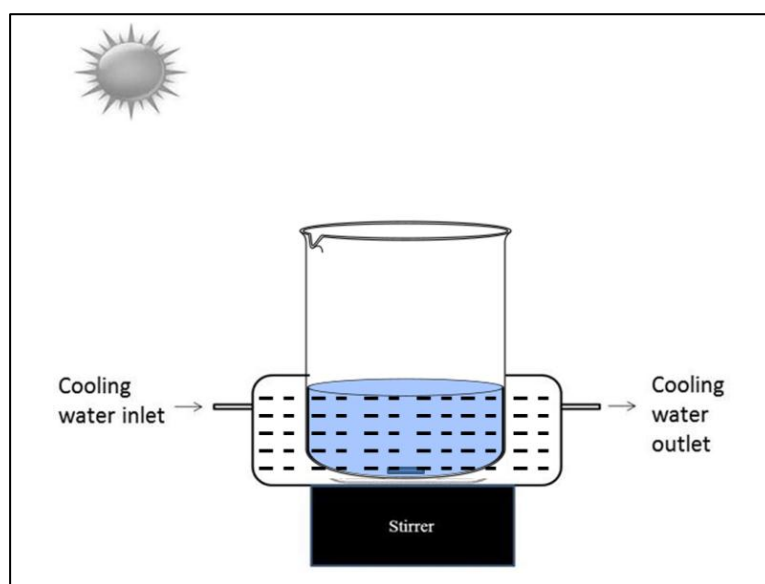


**Fig. 3.2:** Schematic diagram of the photocatalytic experimental set up

The average intensity of solar light during the experiments was  $1.25 \times 10^5$  Lux, as calculated from the measurements using Digital Lux meter (LT-Lutron LX-101A). The suspension was stirred frequently to ensure uniform mixing. Samples were drawn at regular intervals. Suspended catalyst was removed by filtration and concentration of carbendazim remaining in the solution was analyzed as explained under

analytical procedure. Samples were also drawn for analyzing the H<sub>2</sub>O<sub>2</sub> present in the system and also for the identification of reaction intermediates at specified time intervals. Suspension prepared and kept under identical conditions in the dark was used as the reference in each case to eliminate the contribution from adsorption and dark reaction.

### 3.3 Results and discussion

#### 3.3.1 Catalyst characterization

Various techniques such as surface area measurement, particle size analysis, pore size distribution, X-Ray Diffraction (XRD), Scanning Electron Microscopy (SEM) and Transmission Electron Microscopy (TEM) were used for the characterization of ZnO. The pore size distribution of ZnO is measured using Micrometrics Tristar surface area and porosity analyser and the results are shown in Fig. 3.3. The distribution of pore size is in the range 30-180 Å. The average pore width and pore volume are 139Å and 0.035 cm<sup>3</sup>/g respectively.

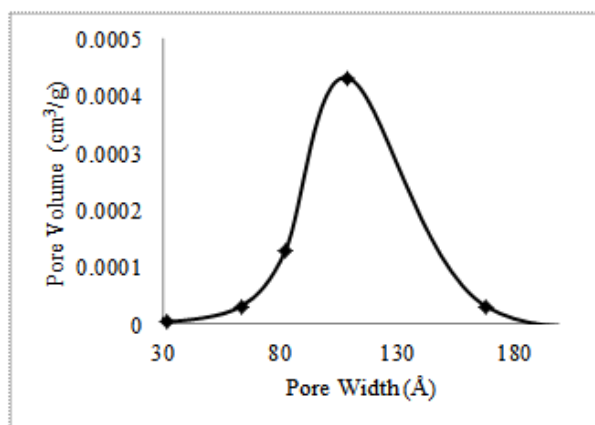


**Fig. 3.3:** Pore size distribution of ZnO

XRD analysis of the ZnO powder using Bruker D2 PHASER X-Ray powder analyzer within the diffraction angle ( $2\theta$ )  $5-65^\circ$  shows highly crystalline phase of pure hexagonal wurtzite structure with crystalline size of  $290\text{\AA}$ . The profile is matching with the reference provided by the International Centre for Diffraction Data (ICDD PDF # 00-003-0888) for ZnO. 100% intensity peak was found at  $2\theta$  of  $36.04^\circ$  and is often used for the calculation of crystalline size using Diffrac Eva V2.1 software. Other major characteristic peaks are at  $2\theta$ s  $31.36^\circ$ ,  $34.21^\circ$ ,  $47.32^\circ$  and  $56.37^\circ$  (Fig. 3.4).

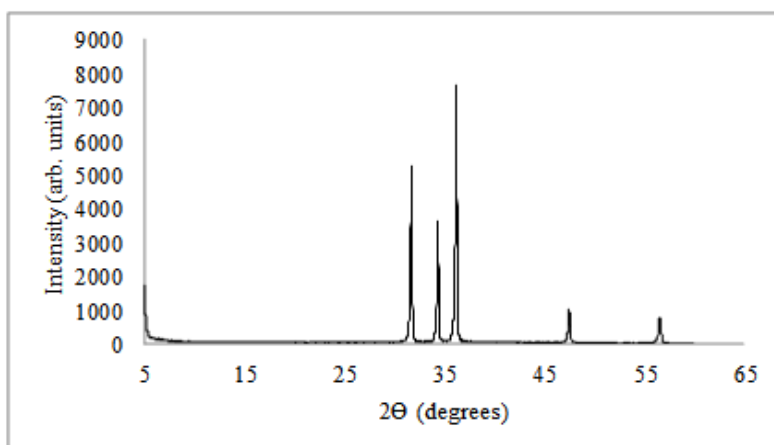


**Fig. 3.4:** XRD pattern of ZnO

The SEM image of ZnO recorded using JEOL Model JSM - 6390LV is shown in the Fig. 3.5. The particles were rod-shaped with size approximately in the range of  $0.1$  to  $0.2\mu\text{m}$ . The morphology of ZnO is further verified by TEM (JEOL JEM-2100). The TEM image of ZnO used is given in Fig. 3.6.

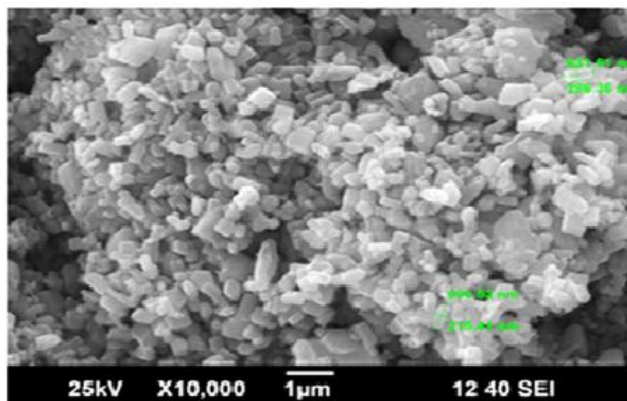


**Fig. 3.5:** SEM image of ZnO

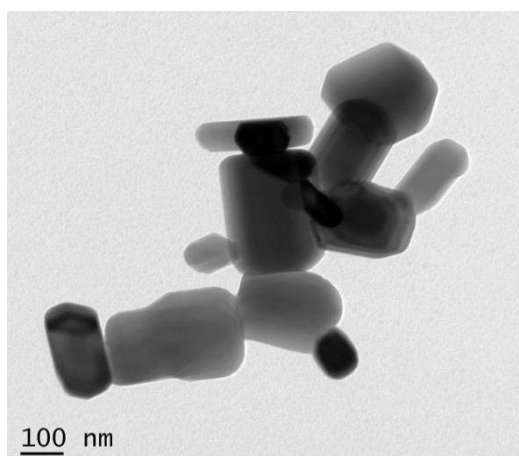


**Fig. 3.6:** TEM image of ZnO

The particles are rod-shaped with an average particle size of 0.09 to 0.2µm. In general, the particle size of ZnO, as measured using various techniques as above can be considered to be in the range of 0.1 to 0.2µm.

### 3.3.2 Preliminary experiments

Preliminary investigations on the solar photocatalytic degradation of carbendazim (CZ=7mg/L) using zinc oxide (0.1g/L) as catalyst showed

that the process is very efficient and ~80% degradation occurred in 30 min at the natural pH (5.5) of the solution (Fig. 3.7). Adsorption studies showed practically negligible adsorption of carbendazim on the surface of ZnO. No degradation was observed in parallel experiments conducted in presence of sunlight without catalyst and in dark with catalyst. This showed that both sunlight and ZnO are essential to effect the degradation of carbendazim.

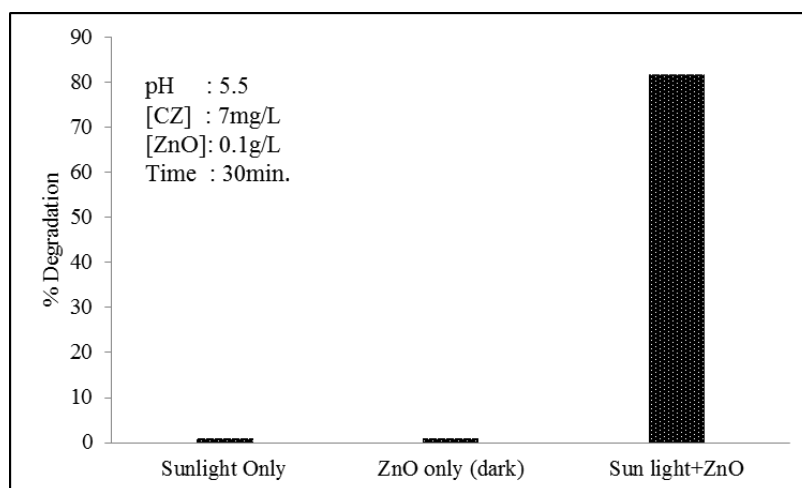
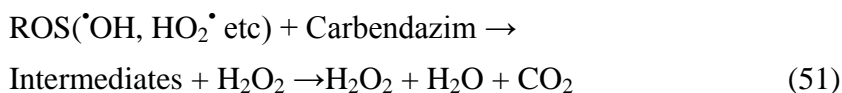


**Fig. 3.7:** Degradation of carbendazim under various conditions

The degradation can be explained based on the general mechanism of photocatalysis. When a semiconductor is irradiated with light of wavelength greater than or equal to the band gap, the valence band electrons get excited to the conduction band creating electron-hole pairs. The photogenerated electron-hole pairs can migrate to the catalyst surface or can recombine. The migrated species can initiate redox reactions leading to the formation of reactive oxygen species (ROS). The electrons reduce the adsorbed oxygen to produce  $O_2^{\cdot-}$  and the positively charged holes oxidize water to form OH radical. The OH radicals which are strong oxidants ( $E^{\circ}=2.8$  eV) can

oxidize most of the organic pollutants [38,124,125]. The reactive  $\cdot\text{OH}$  free radicals can also combine together and form  $\text{H}_2\text{O}_2$ .



Details of the mechanism are discussed in section 3.4 and other respective sections later in this chapter.

The percentage degradation of carbendazim increases with time and stabilizes eventually (Fig. 3.8), probably due to saturation of the catalyst surface, decreasing concentration of the substrate and interference/competition by the intermediates for surface sites as well as the reactive free radicals.

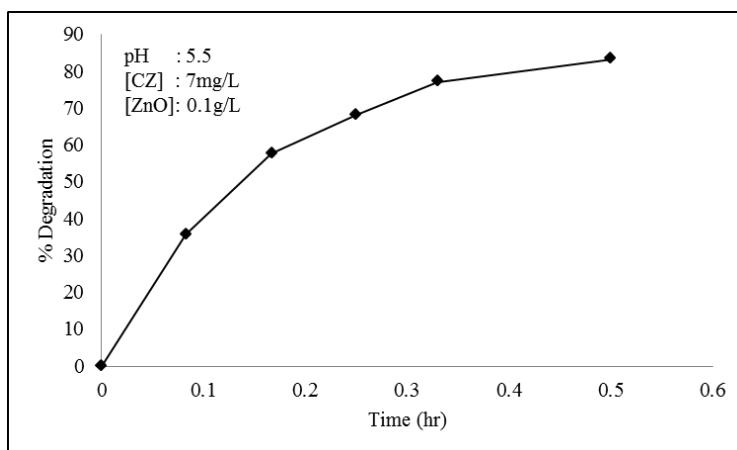


**Fig. 3.8:** Photocatalytic degradation of carbendazim

The effect of various reaction parameters on the degradation of carbendazim is investigated in detail and the results are as follows:

### 3.3.3 Effect of catalyst dosage

The catalyst loading is known to influence the rate of semiconductor oxide mediated photocatalytic reactions in aqueous phase. The optimum catalyst loading for a particular system depends on a number of parameters such as concentration of substrate species, area/volume ratio of the photoreactor and the intensity of the light used [45,126]. The effect of catalyst loading on the rate of degradation of carbendazim, keeping all other parameters constant, is investigated and the result is shown in Fig. 3.9. With increase in catalyst loading, the reaction rate also increases, reaches an optimum at 0.1g/L and stabilizes thereafter. The increase in reaction rate is proportional to the number of active sites which increases with the catalyst loading. At higher loadings the effective absorption of light will be better and this leads to the generation of more reactive oxygen species such as  $\cdot\text{OH}$  radical and consequently enhanced degradation. Beyond the optimum dosage, any further increase in catalyst concentration can only lead to scattering and reduced passage of light through the sample.

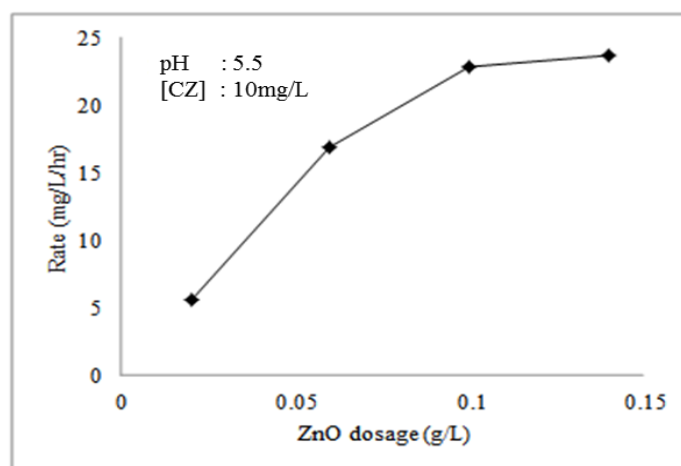


**Fig. 3.9:** Effect of catalyst dosage on the rate of degradation

Higher loading may also cause aggregation of catalyst particles resulting in decreased number of active surface sites available for adsorption/reaction. The particles cannot be fully and effectively suspended beyond a particular loading in a particular reactor which also leads to suboptimal penetration of light and reduced adsorption of the substrate on the surface. (In the case of carbendazim, the adsorption is not significant as explained earlier). Another possibility is that at higher loading, at least a part of the originally photoactivated zinc oxide collides with ground state catalyst and get deactivated as follows [127]:



(where MO represents the semiconductor oxide ZnO)

MO\* and MO<sup>#</sup> are the activated and deactivated forms respectively.

The optimum loading identified here, i.e. 0.1g/L was used for all further studies, unless indicated otherwise.

### 3.3.4 Effect of initial concentration of carbendazim, Kinetics

The photocatalytic degradation rate of organic molecules in aqueous medium varies with the initial concentration. This is verified in the present context by varying the initial concentration of carbendazim from 3-10mg/L under otherwise identical reaction conditions. The percentage degradation of carbendazim decreases as the concentration is increased (Fig. 3.10). However the rate of degradation increases with increase in concentration up to 7mg/L and stabilizes thereafter (Fig. 3.11). Since the solubility of carbendazim in water is only~8mg/L, it is possible that at least a fraction of the substrate in solution prepared at higher temperature

(as explained in section 3.2.1) may be thrown out of solution at lower temperature at which the experiments are carried out. However, this is not observed at the highest concentration tested here, i.e. 10mg/L though the possibility cannot be ruled out.

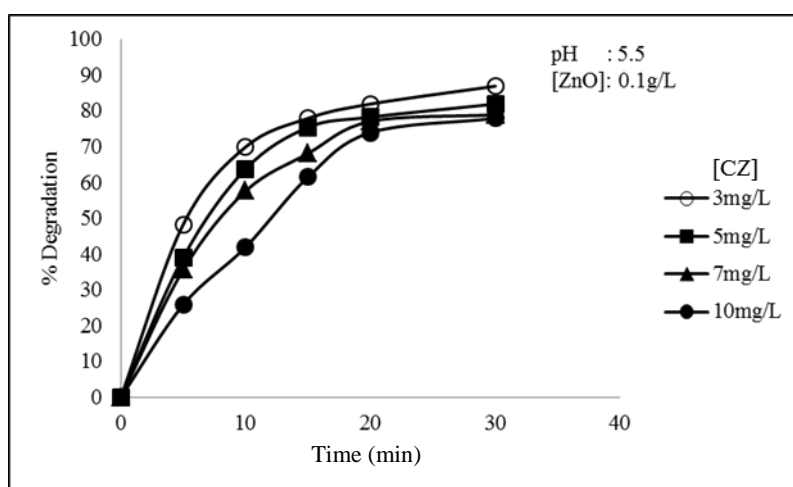


**Fig. 3.10:** Effect of carbendazim concentration on the percentage degradation

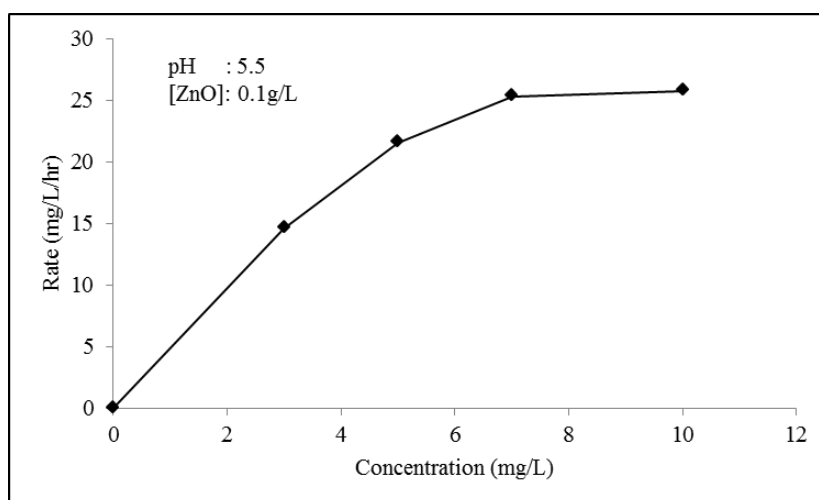


**Fig. 3.11:** Effect of carbendazim concentration on the rate of degradation

The optimum degradation rate attained is ~25.4 mg/L/hr. The results clearly show that the degradation follows variable kinetics, with pseudo first order at lower concentration (3-7mg/L) and zero order at higher concentration (> 7mg/L). Similar kinetics is reported in many other cases of photocatalytic degradation [89,91,93]. The pseudo first order kinetics is rationalized in terms of the modified Langmuir-Hinshelwood model (L-H model) which accommodates the reactions occurring at solid-liquid interface as well. The applicability of the model is based on the assumption that the reaction is in dynamic equilibrium and there is no competition between the substrate and the reaction intermediates for the surface sites as well as the ROS.

The simplest L-H kinetic model applicable to photocatalytic degradation of chemical contaminants is proposed as follows [79,128-130].

$$r_0 = -dC/dt = kKC_0/(1 + KC_0) \quad (55)$$

where

$r_0$  = initial rate of degradation of the contaminant (mg/L/min)

$C_0$  = initial concentration of the contaminant (mg/L)

$C$  = concentration (mg/L) remaining after time  $t$ .

$t$  = irradiation time (min)

$k$  = limiting reaction rate at maximum coverage for the experimental conditions ( $\text{min}^{-1}$ ) and

$K$  = equilibrium adsorption constant of the contaminant

At higher concentration of the substrate when the concentration is more than the saturation coverage for the surface of the catalyst, i.e.  $KC_0 \gg 1$ , the equation simplifies to zero order rate equation as

$$-dC/dt = k \quad (56)$$

When the concentration of the contaminant is very small ( $KC_0 \ll 1$ ), the equation can be simplified as

$$-dC/dt = kKC_0 = k'C_0 \quad (57)$$

where  $k'$  is the pseudo first order rate constant.

Rearranging and integrating the above equation yields a typical pseudo first order model as follows:

$$C = C_0 e^{-k't} \quad (58)$$

$$\ln(C_0/C) = k't \quad (59)$$

Plot of  $\ln(C_0/C)$  vs  $t$  will yield straight line for first order reactions. The slope of the straight line will be the pseudo first order rate constant.

The half-life ( $t_{1/2}$ ), (the time required for 50% degradation) is calculated by replacing  $C$  by  $C_0/2$  and  $t$  by  $t_{1/2}$  in the Eq. (59):

$$t_{1/2} = \ln 2/k = 0.693/k \quad (60)$$

The plot of  $\ln(C_0/C)$  vs  $t$  for the photocatalytic degradation of carbendazim at different concentrations is shown in the Fig. 3.12. The linearity of the plot confirms that the degradation fits well with the L-H model for the pseudo first order kinetics. The calculated value for the pseudo first order rate constants are given in the Table 3.1.

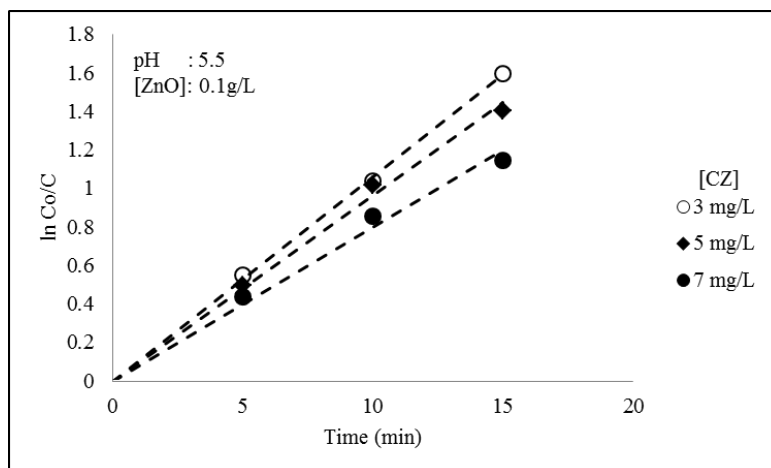


**Fig. 3.12:** Logarithmic plot of pseudo first order kinetics for the degradation of carbendazim

**Table 3.1:** Pseudo first order rate constants for the photocatalytic degradation of carbendazim over ZnO. pH: 5.5 Temp:  $29 \pm 1^\circ\text{C}$

| Experiment | ZnO (g/L) | Carbendazim (mg/L) | $k'$ ( $\text{hr}^{-1}$ ) | $t_{1/2}$ (hr) |
|------------|-----------|--------------------|---------------------------|----------------|
| 1          | 0.1       | 3                  | 6.29                      | 0.11           |
| 2          | 0.1       | 5                  | 5.44                      | 0.13           |
| 3          | 0.1       | 7                  | 4.22                      | 0.16           |

It is evident that the value of  $k'$  decreases as the concentration of carbendazim is increased. For a particular amount of catalyst loading, the active surface sites and the reactive species generated will be constant. At the same time, the number of substrate molecule increases as the concentration increases. The effective interaction between the substrate and the reactive species generated will be finite. The relative percentage fraction of interacting substrate will be less at higher concentrations and this leads to the lowering of the rate constant with concentration.

The  $t_{1/2}$  for the reaction in the selected concentration range increases with increase in concentration, which is expected since the reaction rate constant decreases as the concentration is increased.

Rearranging equation (55) yields equation (61) as follows:

$$1/r_0 = (1/kK)(1/C_0) + 1/k \quad (61)$$

Validity of L-H model for the reaction is further confirmed by the inverse plot of  $1/r_0$  vs  $1/C_0$  as shown in Fig. 3.13. The excellent linearity in the concentration range studied here reconfirms the pseudo first order kinetics. The values of  $k$  and  $K$  can be calculated from the intercept of the straight line and from the slope respectively based on equation (61) [129,130]. At higher concentration, the substrate as well as the intermediates formed may absorb some of the incident photons thereby reducing the availability of light for the activation of ZnO. Also it is possible that the higher concentration of intermediates formed from the higher concentration of substrate may get adsorbed or loosely attached to the ZnO surface and thus hinder the approach of fresh reactant molecules to the active site.

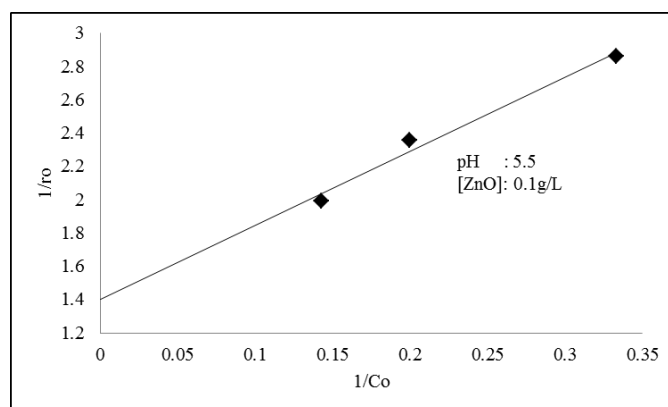


**Fig. 3.13:** Reciprocal plot of initial rate of degradation of carbendazim versus initial concentration

However, the optimum concentration of 7mg/L computed experimentally is applicable only under the present conditions. The optimum will be different under a different set of experimental conditions such as light intensity, catalyst loading, reactor size and geometry etc. Hence, for every set of reaction conditions, respective optimum parameters have to be identified experimentally.

### **3.3.5 Effect of pH**

The pH of the aqueous medium has significant role in the semiconductor mediated photocatalytic degradation reactions. The surface characteristics of the semiconductors change with the pH of the dispersing medium. For semiconductors, the net electric charge on the surface in aqueous medium is characterized in terms of the point of zero charge (PZC). The surface is positively charged below the PZC while it will be negatively charged above the PZC [93]. The PZC of ZnO is approx.9.3. Since the catalytic reactions are mostly surface mediated, the net charge on the surface will play an important role in determining the rate and mechanism of the reaction. The adsorption of the reactant species on the catalyst surface which in turn directly contributes to the rate of the reaction is an important pH dependent parameter in this respect.

The effect of pH on the photocatalytic degradation of carbendazim is studied by varying the pH of the solution while other reaction parameters are kept constant. The results are plotted in Fig. 3.14. Parallel studies conducted in the dark without catalyst in the pH range 3-11 showed no change in the carbendazim concentration. The degradation increases with increase in the solution pH and reaches a maximum at pH 4-5. Thereafter

it remains steady upto pH~9 and decreases at pH > 9. The lower degradation at pH< 4 may be at least partly due to ZnO corrosion and consequent decrease in the amount of catalyst.

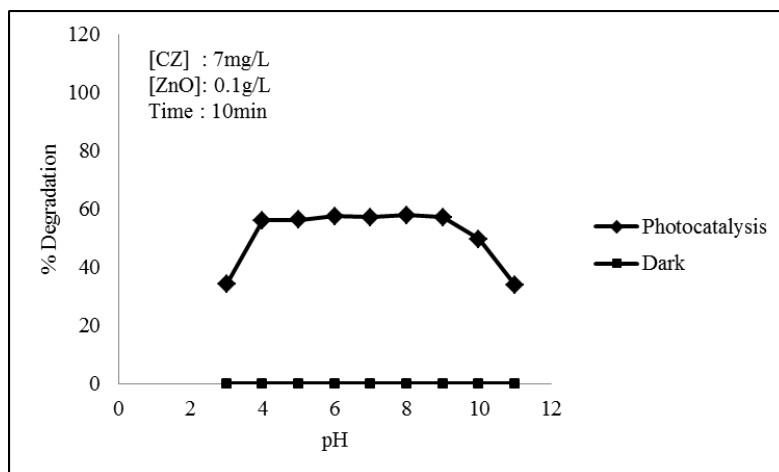


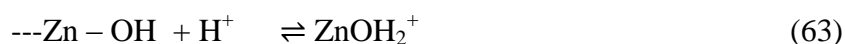
**Fig. 3.14:** Effect of pH on the degradation of carbendazim

Below the  $pK_a$  value of 4.2, carbendazim exists in the protonated form. Similarly, below the PZC of ~9.0, the surface of ZnO is positively charged. The electrostatic repulsion between the protonated form of carbendazim and the positively charged surface of ZnO may be another reason for the low degradation rate at pH < 4.2. Above pH 4.2 carbendazim in the neutral form can access or be in proximity to the surface which contributes to the increase in the percentage degradation at higher pH. However, it is observed that the adsorption of carbendazim on ZnO is negligible at all pH. Hence, the interaction between the ROS and carbendazim may be occurring in the bulk or nearer to the ZnO surface. At alkaline pH > 9, the ZnO is negatively charged and once again, the repulsion of carbendazim from the surface leads to decreased degradation.

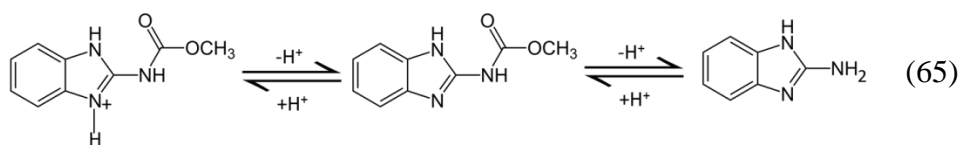
The possibility of alkaline dissolution of ZnO as in reaction (62) also cannot be ruled out.



In the case of ZnO, the effect of pH can also be explained at least partially based on its amphoteric behavior and surface charge. The acid-base property of metal oxides is known to have considerable influence on their photocatalytic activity [99]. Solution pH influences the ionization state of ZnO surface according to the reaction:



In aqueous medium, depending on the pH, carbendazim exists in protonated ( $\text{pH} < \text{p}K_a \sim 4.2$ ) or in neutral form ( $\text{pH} > \text{p}K_a$ ). Three nitrogen atoms are present in the molecule and hence there are three possible sites for protonation. Transformation of carbendazim to aminobenzimidazole at higher pH ranges (Eq. 65) has also been reported [131].



Since the degradation is optimum at the normal pH of the reaction suspension, i.e. 5.5, all further studies are carried out without adjustment of the pH, unless indicated otherwise.

### **3.3.6 Effect of oxidants**

The photocatalytic degradation rate of many organic pollutants in aqueous medium is enhanced by certain oxidants. They can act as electron scavengers thereby preventing the electron-hole recombination on the irradiated catalyst.  $\text{H}_2\text{O}_2$ ,  $\text{O}_3$  and  $\text{S}_2\text{O}_8^{2-}$  have been reported to accelerate the photocatalytic degradation of organic pollutants in aqueous medium [80,89,99,103,120,132]. The degradation is initiated and propagated by  $\cdot\text{OH}$  radical formed during the irradiation. Combination of  $\text{H}_2\text{O}_2$  with semiconductor oxide catalysts enhances the degradation of many pollutants [89,99,132], though instances of inhibition also are reported at higher concentrations.  $\text{H}_2\text{O}_2$  is formed as an intermediate and/or end product in many photocatalytic reactions. Recently Jyothi et al. [133] demonstrated the concurrent decomposition of in-situ formed  $\text{H}_2\text{O}_2$  leading to oscillation in its concentration. Formation of  $\text{H}_2\text{O}_2$  is observed in the current instance also. However, the concentration of  $\text{H}_2\text{O}_2$  increases with the degradation of carbendazim and eventually stabilizes and increases again (Fig. 3.15). Based on the previous reports, it may be inferred that the stabilization occurs when the rates of formation and decomposition balance, especially towards the later stages of degradation. Once the degradation of carbendazim to various intermediates is over, the latter will begin to degrade further and eventually mineralize resulting in another increase in the concentration of  $\text{H}_2\text{O}_2$ .

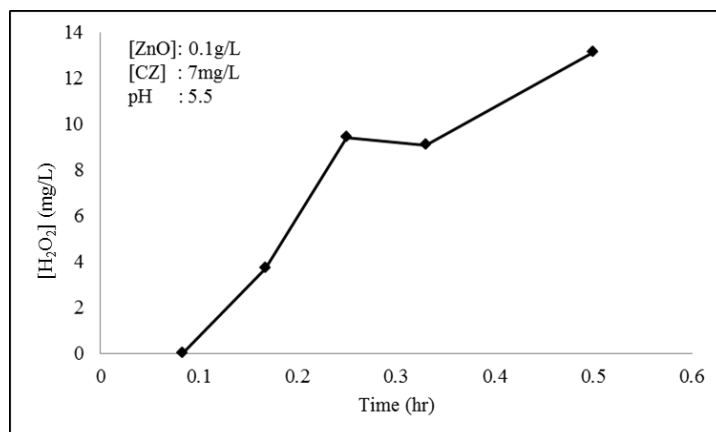
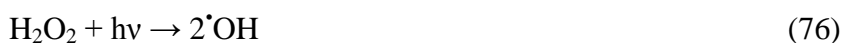
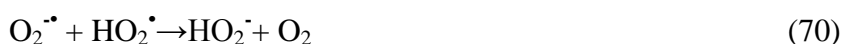
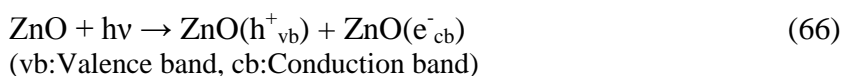


**Fig. 3.15:** Formation of H<sub>2</sub>O<sub>2</sub> during the photocatalytic degradation of carbendazim

Various steps involved in the concurrent formation and decomposition of H<sub>2</sub>O<sub>2</sub> are as follows [133]:



Since H<sub>2</sub>O<sub>2</sub> is a good oxidant by itself and also a good electron scavenger, addition of small amount of H<sub>2</sub>O<sub>2</sub> to the photocatalytic system

is expected to influence the degradation of carbendazim. This possibility is investigated with the addition of small quantity (1, 4 and 8mg/L) of H<sub>2</sub>O<sub>2</sub> to the reaction system. The results are presented in Fig. 3.16. Marginal enhancement in the degradation of carbendazim is observed in all cases.

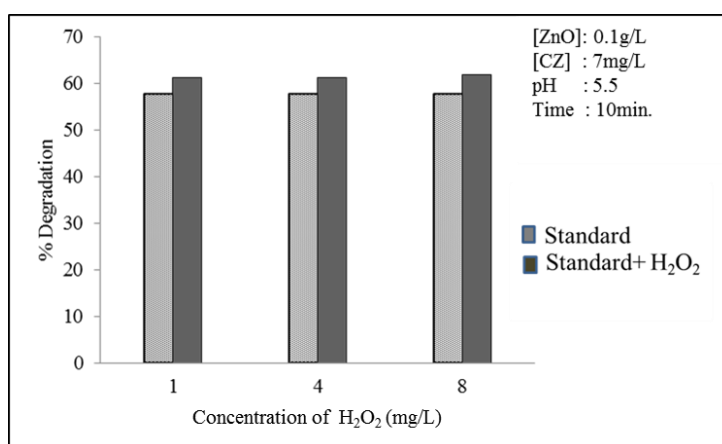


**Fig. 3.16:** Effect of H<sub>2</sub>O<sub>2</sub> at various concentrations on the photocatalytic degradation of carbendazim

Effect of increase in the concentration of H<sub>2</sub>O<sub>2</sub> on the percentage degradation of carbendazim is negligible. This may be because, the in-situ formed H<sub>2</sub>O<sub>2</sub> has already played the enhancing role and the higher concentration by extra addition predominantly results in concurrent decomposition and re-formation of H<sub>2</sub>O<sub>2</sub> without any specific effect on the degradation of carbendazim. The reaction sequence, in addition to that explained above, involves the interaction of H<sub>2</sub>O<sub>2</sub> with the in-situ formed highly reactive  $\cdot\text{OH}$  radicals as follows:



Compared to  $\cdot\text{OH}$  ( $E^\circ=2.8$  eV) radical,  $\text{HO}_2\cdot$  ( $E^\circ=1.06$  eV) is a weak oxidant. The added  $\text{H}_2\text{O}_2$  can also absorb sunlight and undergo self-photolysis which reduces the amount of incident radiation available for the activation of ZnO. Since the population of  $\text{H}_2\text{O}_2$  molecules in the bulk and also in the vicinity of the catalyst is more at higher concentrations, the photo-generated  $\cdot\text{OH}$  radical can easily react with  $\text{H}_2\text{O}_2$  rather than with carbendazim molecule. The overall effect of these factors limits the enhancement in the degradation of carbendazim by added  $\text{H}_2\text{O}_2$ . This explains the 'nil' or 'insignificant' effect on the photocatalytic degradation of carbendazim in the case of added  $\text{H}_2\text{O}_2$ .

Another powerful oxidant persulphate (PS) is also investigated for its potential for enhancing the degradation of carbendazim. It is observed that PS enhances the degradation significantly compared to  $\text{H}_2\text{O}_2$  as seen in Fig. 3.17. Sodium salt, i.e.  $\text{Na}_2\text{S}_2\text{O}_8$  is used in these experiments.

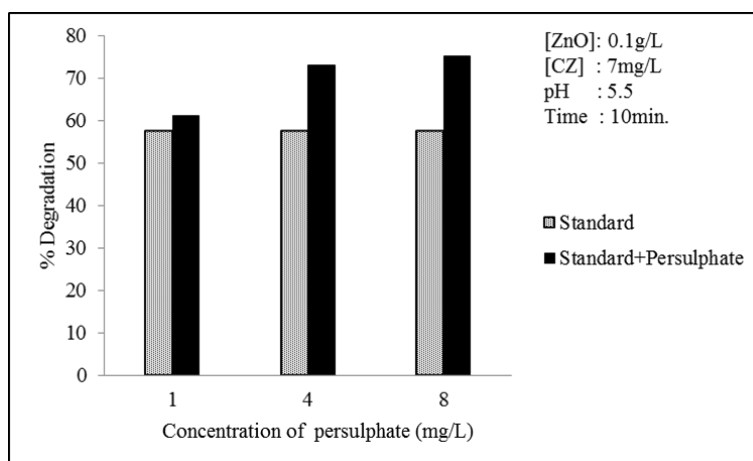
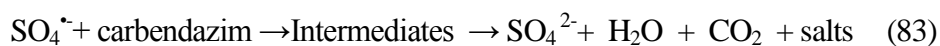


**Fig. 3.17:** Effect of persulphate on the photocatalytic degradation of carbendazim

The degradation is enhanced by about ~20% in presence of PS. The enhancing effect of PS is attributed to the electron scavenging ability thereby reducing the electron-hole recombination as in the case of H<sub>2</sub>O<sub>2</sub>. It also produces a very strong oxidant such as sulfate radical, SO<sub>4</sub><sup>•-</sup> (*E*<sup>o</sup> = 2.6 eV) [79] which can interact directly with carbendazim and oxidise it. Further the SO<sub>4</sub><sup>•-</sup> radicals can interact with H<sub>2</sub>O generating equally reactive <sup>•</sup>OH radicals which also enhance the degradation of carbendazim. Various steps involved in the process are [129]:



### 3.3.7 Effect of salts (anions and cations)

Natural water contains considerable amount of different types of dissolved salts. Any viable technology for the mineralization of pollutants in water must take the effect of these salts on the efficiency also into consideration. The inorganic ionic species present in the medium can affect the photocatalytic degradation in many ways, the most important being the competitive adsorption on the active surface sites of the catalyst. This will prevent the pollutant molecules from adsorption and consequent activation. Other effects of salts include; reducing the solar radiation reaching the catalyst surface, deactivation of the ROS, formation of unwanted byproducts which may influence the efficiency of photocatalysis and mineralization etc. [86,87,93,99,134]. Factors such as pH, nature of

catalyst and substrate, concentration of ionic species etc. also influence the nature of anion effect on the photocatalytic efficiency.

The effect of salts on the degradation need to be evaluated both in terms of anions and cations. The effect of four typical anions,  $\text{Cl}^-$ ,  $\text{NO}_3^-$ ,  $\text{SO}_4^{2-}$ ,  $\text{HPO}_4^{2-}$  on the degradation of carbendazim is evaluated at various concentrations keeping the cation the same, i.e.  $\text{Na}^+$  (Figs. 3.18 - 3.21).

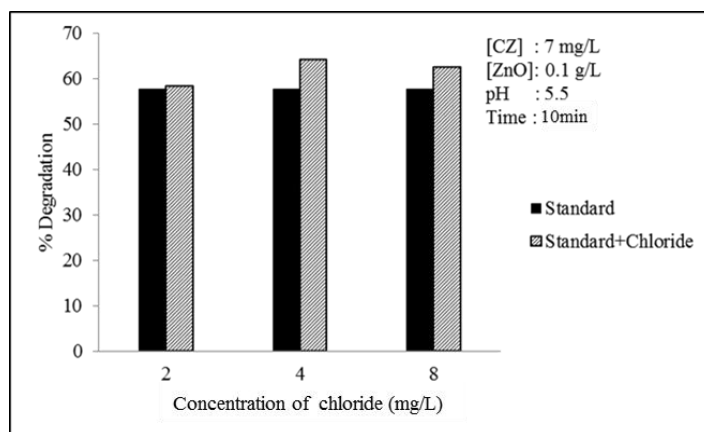


**Fig. 3.18:** Effect of chloride on the photocatalytic degradation of carbendazim [Cation:  $\text{Na}^+$ ]

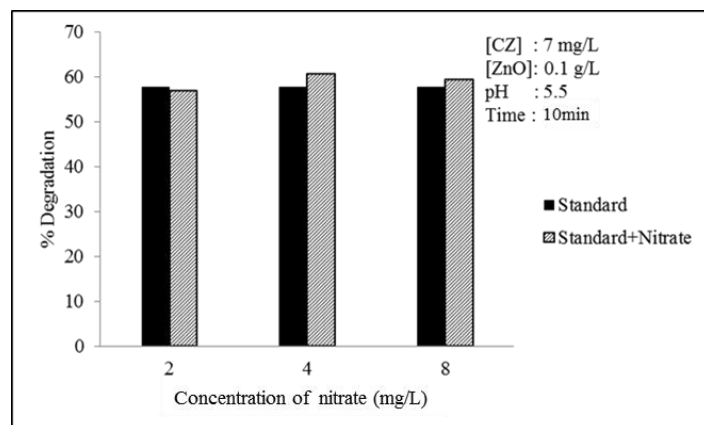


**Fig. 3.19:** Effect of nitrate on the photocatalytic degradation of carbendazim [Cation:  $\text{Na}^+$ ]

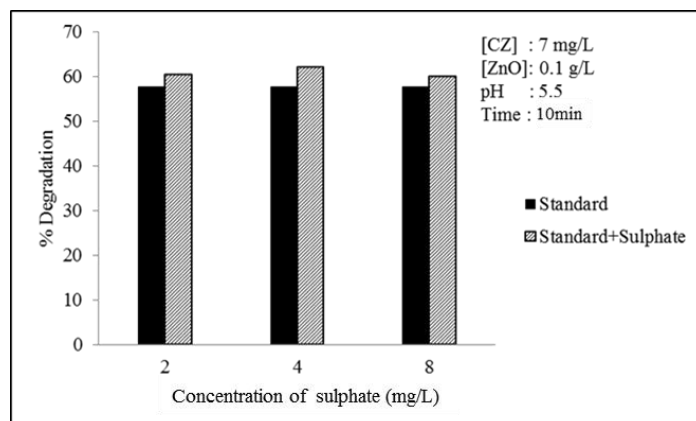


**Fig. 3.20:** Effect of sulphate on the photocatalytic degradation of carbendazim [Cation: Na+]

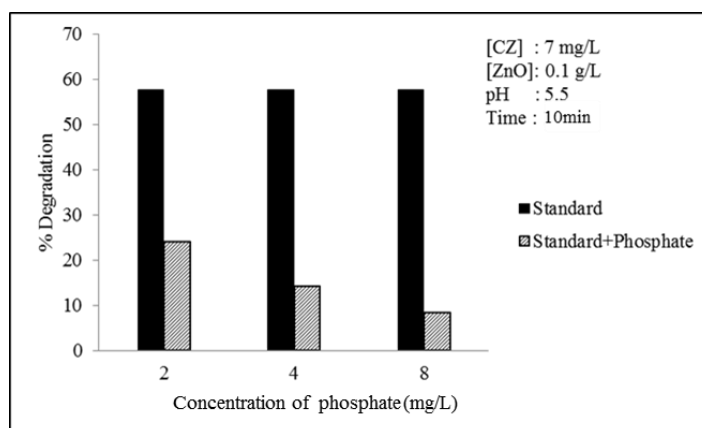


**Fig. 3.21:** Effect of phosphate on the photocatalytic degradation of carbendazim [Cation:Na+]

Except phosphate, other anions tested here have either ‘no effect’ or ‘mild enhancing effect’ on the degradation, at least in the concentration range of 2-8mg/L. The detrimental effect of  $\text{HPO}_4^{2-}$  on the photocatalytic degradation has been reported in the case of both ZnO and  $\text{TiO}_2$  catalysts [135]. Preferential adsorption by  $\text{HPO}_4^{3-}$  on the surface of ZnO and consequent decrease in the adsorption of substrate, prevention of activation

of the sites and reduction in the number of ROS etc. are possible causes of inhibition. However, the adsorption of carbendazim itself on ZnO is negligible and hence inhibition of its adsorption is not a cause for the anion effect. Possible prevention of the activation of the surface by adsorbed anion is tested by measuring the adsorption of various anions on ZnO (decrease in the concentration of anions in presence of ZnO) as explained in section 3.2.3. The adsorption of selected anions, except phosphate, is negligible on the surface of ZnO.

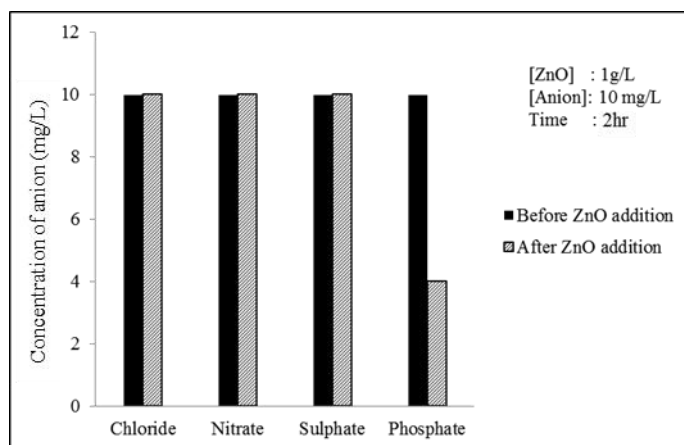


**Fig. 3.22:** Adsorption of selected anions on ZnO [Cation:Na<sup>+</sup>]

It is observed that  $\text{HPO}_4^{2-}$  is getting adsorbed on to the surface of ZnO (Fig. 3.22) with the adsorption increasing with increasing concentration (Fig. 3.23). Eventually the adsorption is stabilized probably when the surface is fully covered. The adsorption is further confirmed from FTIR spectra of  $\text{NaHPO}_4$ , ZnO and ZnO treated with  $\text{NaHPO}_4$  solution (Fig. 3.24). Spectral bands corresponding to  $\text{HPO}_4^{2-}$

can be clearly seen in the case of ZnO, which was pretreated with  $\text{HPO}_4^{2-}$ .

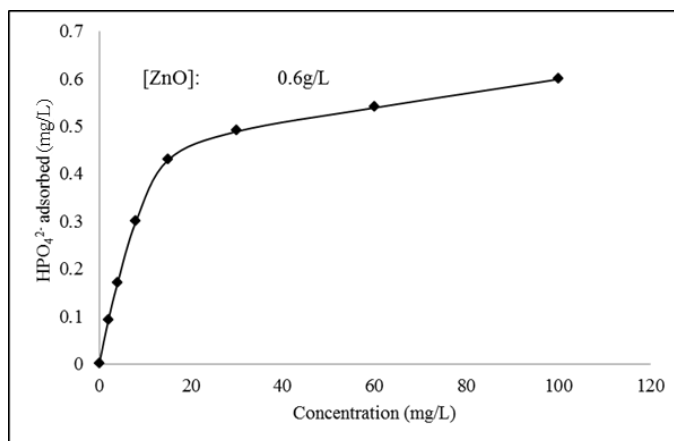


**Fig. 3.23:** Effect of concentration of  $\text{HPO}_4^{2-}$  on its adsorption on the ZnO surface

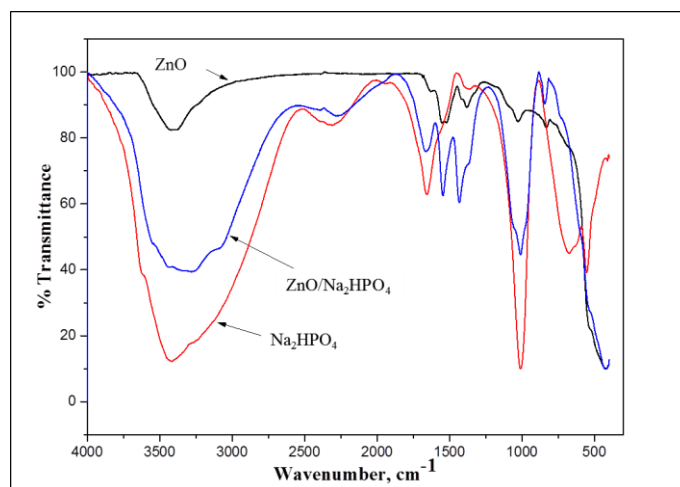


**Fig. 3.24:** FTIR spectral evidence for the adsorption of  $\text{HPO}_4^{2-}$  on ZnO

The adsorption of other anions on ZnO is practically negligible at least in the concentration range studied here. This explains the absence of inhibition by  $\text{Cl}^-$ ,  $\text{NO}_3^-$  and  $\text{SO}_4^{2-}$  ions. Mild enhancement by these anions

can be explained by the formation of reactive radical anion by interaction with  $\cdot\text{OH}$  as follows:



These radical anions are also oxidising agents, though relatively less efficient compared to  $\cdot\text{OH}$ . However, unlike in the case of  $\cdot\text{OH}$  which gets deactivated by other interactions, the radical anions are exclusively available for the substrate thereby making them equally or more effective oxidants. Compared to  $\cdot\text{OH}$  radicals, these radical anions will undergo slower recombination and deactivation. Hence the radical anions can react with substrate molecules more effectively than  $\cdot\text{OH}$  radicals [136,137] resulting in enhanced rate of degradation.

The decrease in the concentration of  $\cdot\text{OH}$  radicals in presence of anions is verified by measuring the actual quantity of the radicals generated using the TPA procedure (section.3.2.4). The intensity of photoluminescence (PL) spectrum of the 2-hydroxy TPA formed during the experiments is proportional to the concentration of  $\cdot\text{OH}$  radical generated [122,123]. The intensity of PL remains more or less unaffected in the presence of the anions  $\text{Cl}^-$ ,  $\text{NO}_3^-$  and  $\text{SO}_4^{2-}$  indicating that they do not inhibit the surface initiated formation of the  $\cdot\text{OH}$  radicals, except for the formation of small quantities of radical anions as explained earlier. In the presence of  $\text{HPO}_4^{2-}$  which is found to get strongly adsorbed on the surface, the relative concentration of the  $\cdot\text{OH}$  radicals is much less as seen

from the lower PL intensity (Fig. 3.25). This is more due to the poor generation of the radical rather than their scavenging. The detrimental effect of anions on the  $\cdot\text{OH}$  radical formation is in the order  $\text{HPO}_4^{2-} \gg \text{SO}_4^{2-} \approx \text{NO}_3^- > \text{Cl}^-$ . This also confirms that the surface processes on irradiated catalyst are not affected much by  $\text{SO}_4^{2-}$ ,  $\text{NO}_3^-$  and  $\text{Cl}^-$  which are not adsorbed on the surface.

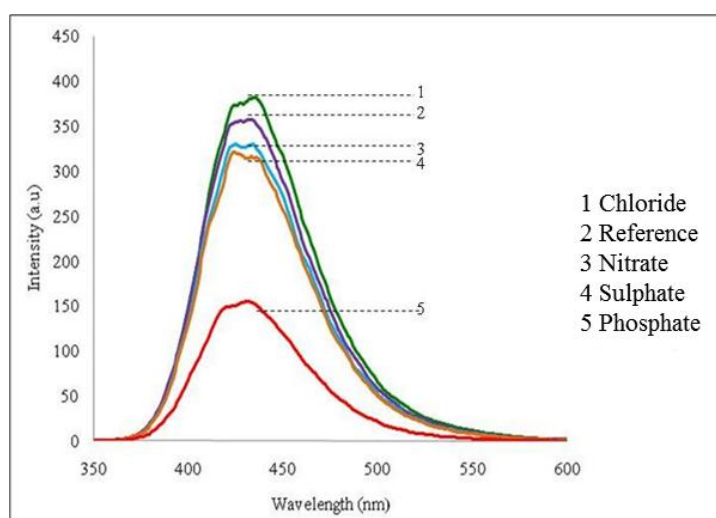


**Fig. 3.25:** PL spectral changes observed in the photocatalytic system in presence of various anions

Similarly, the effect of cations on the photocatalytic degradation of carbendazim is evaluated by keeping the anion the same, i.e.  $\text{SO}_4^{2-}$  (Figs. 3.26 - 3.30). As the results show, the cations  $\text{Na}^+$ ,  $\text{K}^+$ ,  $\text{Ca}^{2+}$ ,  $\text{Mg}^{2+}$  have no noticeable effect on the degradation of carbendazim. The mild enhancing effect in the case of the salts may be due to the common anion  $\text{SO}_4^{2-}$ , which is a mild enhancer as demonstrated earlier. However, when the cation is  $\text{Al}^{3+}$  the degradation is inhibited significantly, with the inhibition increasing with increase in the concentration of the salt (Fig. 3.30). Since

the  $\text{SO}_4^{2-}$  has little or no effect on the degradation, the inhibition in this case can be exclusively attributed to the  $\text{Al}^{3+}$ .

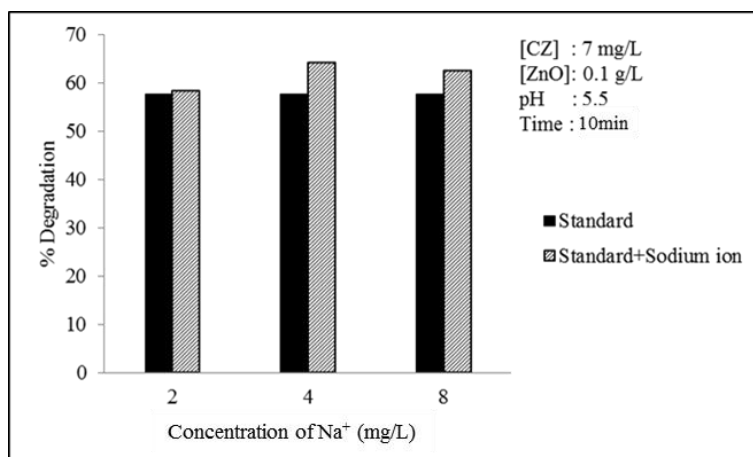


**Fig. 3.26:** Effect of  $\text{Na}^+$  on the photocatalytic degradation of carbendazim [Anion:  $\text{SO}_4^{2-}$ ]

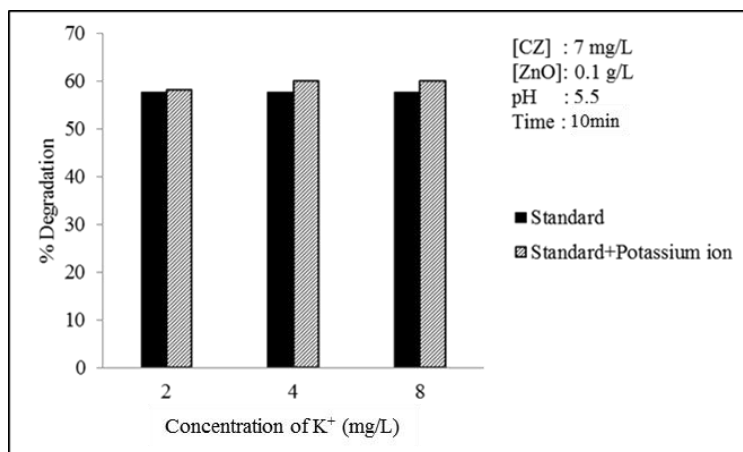


**Fig. 3.27:** Effect of  $\text{K}^+$  on the photocatalytic degradation of carbendazim [Anion:  $\text{SO}_4^{2-}$ ]

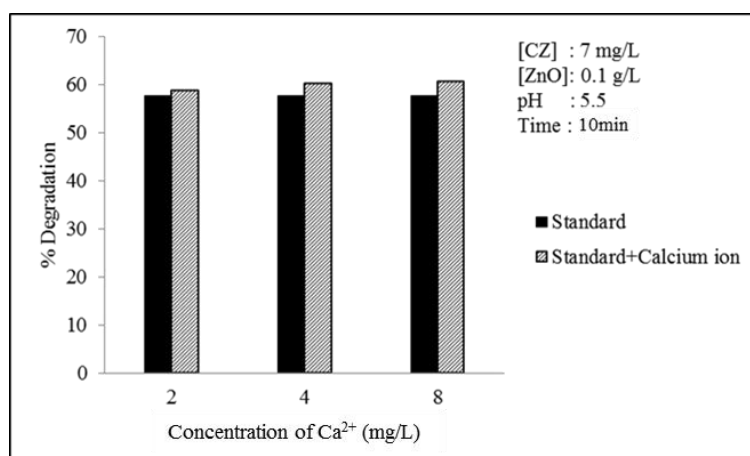


**Fig. 3.28:** Effect of Ca<sup>2+</sup> on the photocatalytic degradation of carbendazim [Anion: SO<sub>4</sub><sup>2-</sup>]

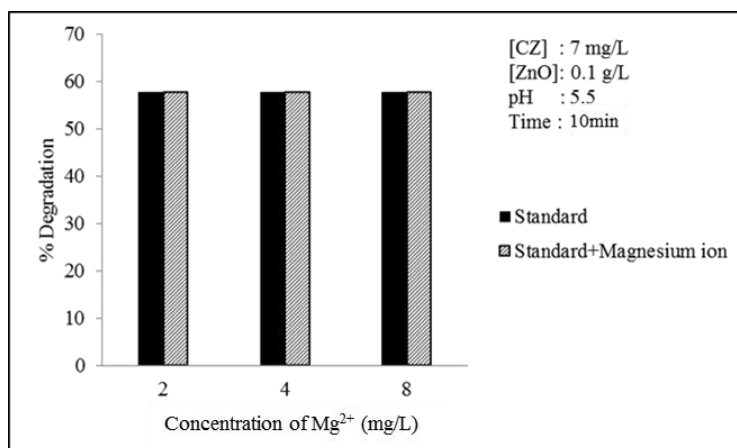


**Fig. 3.29:** Effect of Mg<sup>2+</sup> on the photocatalytic degradation of carbendazim [Anion: SO<sub>4</sub><sup>2-</sup>]

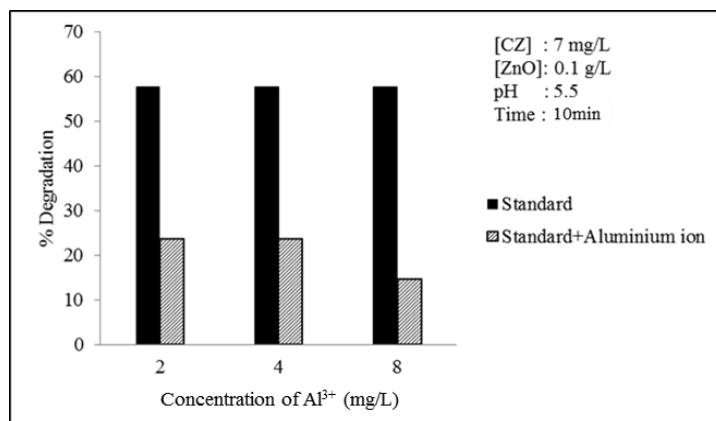


**Fig. 3.30:** Effect of Al<sup>3+</sup> on the photocatalytic degradation of carbendazim [Anion: SO<sub>4</sub><sup>2-</sup>].

In the presence of the different cations (anion SO<sub>4</sub><sup>2-</sup> is constant), the in-situ formed <sup>•</sup>OH concentration in the photocatalytic system is tested as earlier by the PL method. The results show that <sup>•</sup>OH radical formation is inhibited significantly in the presence of Al<sup>3+</sup> (Fig. 3.31). The slightly enhanced concentration of <sup>•</sup>OH radicals in presence of Ca<sup>2+</sup> ion is not adequate to effect any significant increase in the degradation of carbendazim as seen from the results in Fig. 3.28.

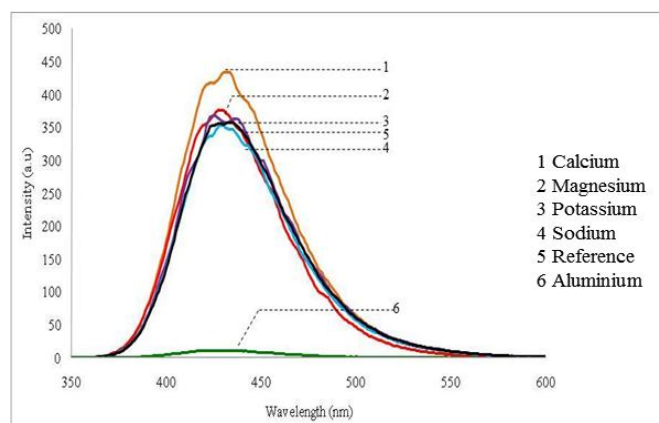


**Fig. 3.31:** PL spectral changes observed in the photocatalytic system in presence of various cations [Anion: SO<sub>4</sub><sup>2-</sup>]

The results clearly show that the inhibition caused by specific anions and cations is due to their detrimental effect on the activation of the catalyst and surface initiated processes resulting in a decrease in the availability of  $\cdot\text{OH}$  radicals. Further, the  $\cdot\text{OH}$  radicals formed in-situ also get competitively scavenged by the anions reducing their availability for the degradation of the substrate carbendazim.

The above results show that the effect of a salt on the photocatalytic degradation of carbendazim over ZnO depends on the nature of its cation and anion.  $\text{Al}^{3+}$  is a clear inhibiting cation while  $\text{HPO}_4^{2-}$  is a clear inhibiting anion.

Salts with different combination of cations and anions were investigated for their effect on the degradation of carbendazim. The results are summarized in Figs. 3.32-3.35. The following salts were used for the study.

- $\text{Cl}^-$  : NaCl, KCl,  $\text{CaCl}_2$ ,  $\text{MgCl}_2$ ,  $\text{AlCl}_3$
- $\text{SO}_4^{2-}$  :  $\text{Na}_2\text{SO}_4$ ,  $\text{K}_2\text{SO}_4$ ,  $\text{CaSO}_4$ ,  $\text{MgSO}_4$ ,  $\text{Al}_2(\text{SO}_4)_3$
- $\text{NO}_3^-$  :  $\text{NaNO}_3$ ,  $\text{KNO}_3$ ,  $\text{Ca}(\text{NO}_3)_2$ ,  $\text{Mg}(\text{NO}_3)_2$ ,  $\text{Al}(\text{NO}_3)_3$
- $\text{PO}_4^{3-}$  :  $\text{Na}_2\text{HPO}_4$ ,  $\text{K}_2\text{HPO}_4$

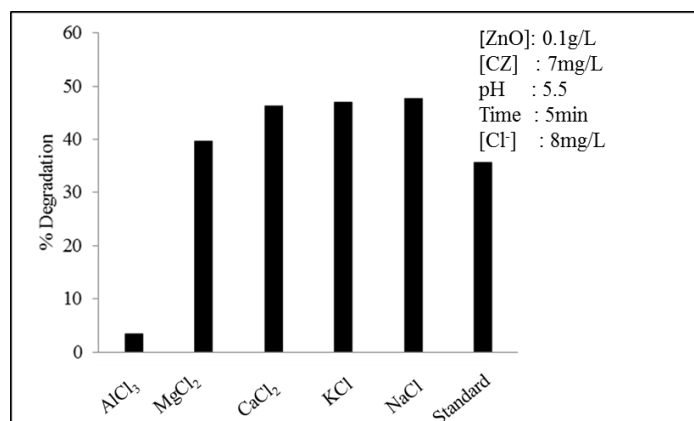


**Fig. 3.32:** Effect of different chlorides on the photocatalytic degradation of carbendazim

Mild to moderate enhancement is seen in the presence of  $\text{Cl}^-$  ions irrespective of the nature of the cation, except in the case of  $\text{Al}^{3+}$ . The results clearly show that cations also do play a role in the effect of the salt, as seen from the variation in the degree of enhancement with nature of the cation.

The enhancement effect of cations, with  $\text{Cl}^-$  as the common anion, is in the order  $\text{Na}^+ \approx \text{K}^+ \approx \text{Ca}^{2+} > \text{Mg}^{2+}$ .  $\text{Al}^{3+}$  is a strong inhibitor.

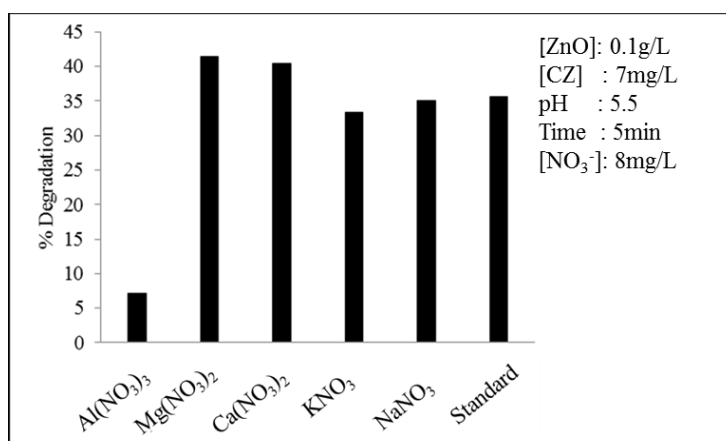


**Fig. 3.33:** Effect of different nitrates on the photocatalytic degradation of carbendazim

With  $\text{NO}_3^-$  as the anion,  $\text{Na}^+$  and  $\text{K}^+$  have practically no effect.  $\text{Ca}^{2+}$  and  $\text{Mg}^{2+}$  are mild enhancers.  $\text{Al}^{3+}$  is a strong inhibitor.

Enhancement:  $\text{Mg}^{2+} \approx \text{Ca}^{2+}$

No effect:  $\text{K}^+$ ,  $\text{Na}^+$

Inhibition:  $\text{Al}^{3+}$

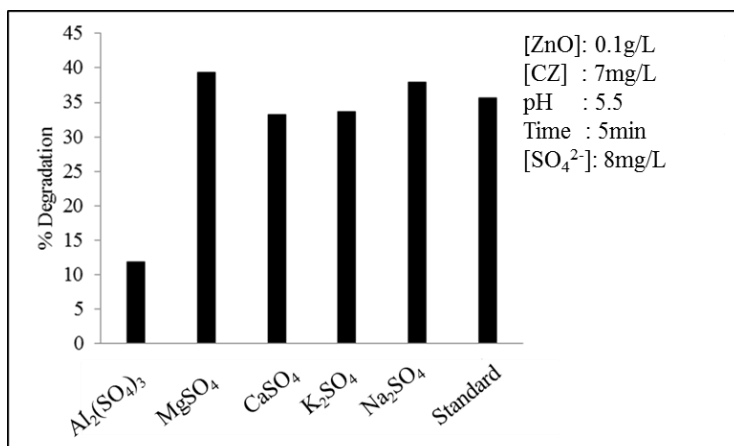


**Fig. 3.34:** Effect of different sulphates on the photocatalytic degradation of carbendazim

With  $\text{SO}_4^{2-}$  as the anion,  $\text{Na}^+$  and  $\text{Mg}^{2+}$  enhance the degradation slightly.  $\text{Ca}^{2+}$  and  $\text{K}^+$  have practically no effect.  $\text{Al}^{3+}$  is a clear inhibitor.

Enhancement:  $\text{Mg}^{2+} \geq \text{Na}^+$

No effect:  $\text{K}^+$ ,  $\text{Ca}^{2+}$

Inhibition:  $\text{Al}^{3+}$

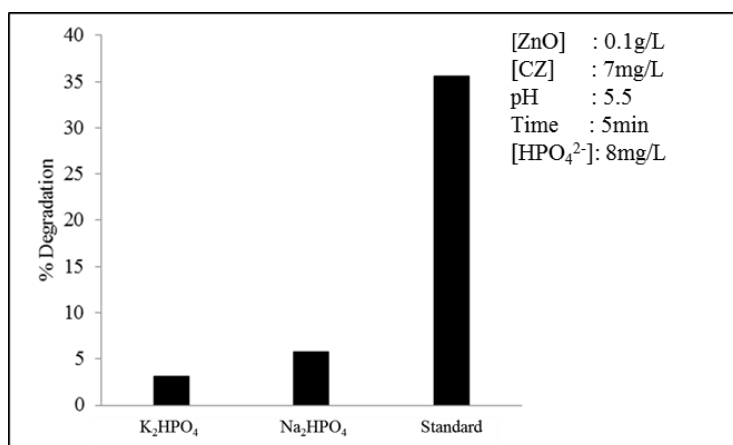


**Fig. 3.35:** Effect of different phosphates on the photocatalytic degradation of carbendazim

In the case of  $\text{HPO}_4^{3-}$  as the anion, only two salts were tested since more salts were not readily available. Both salts tested here are strong inhibitors. This proves that irrespective of the nature of the cation,  $\text{PO}_4^{3-}$  is a strong inhibitor of photocatalytic processes.

Jyothi et al. [137] correlated the inhibition of photocatalytic processes by  $\text{Al}^{3+}$ , partially with the relatively lower ionic radius of the ion.  $\text{Al}^{3+}$  can cover the surface of the ZnO more effectively than other cations due to its favorable size. This results in strong inhibition of the absorption of light and consequently decreased formation of  $\cdot\text{OH}$  radicals.

In short, all the salts except those of  $\text{Al}^{3+}$  (with various anions) and  $\text{HPO}_4^{2-}$  (with various cations) have either no effect or mild enhancement on the photocatalytic degradation of carbendazim. In the case of  $\text{Al}^{3+}$  and  $\text{HPO}_4^{2-}$  all the salts tested here are very efficient inhibitors. The relative enhancement is not consistent in the case of cations, possibly due to the influence of the anions, Hence rather than evaluating the effect of anions or cations as such, it may be more appropriate to study the effect of the salt on the degradation of the pollutants.

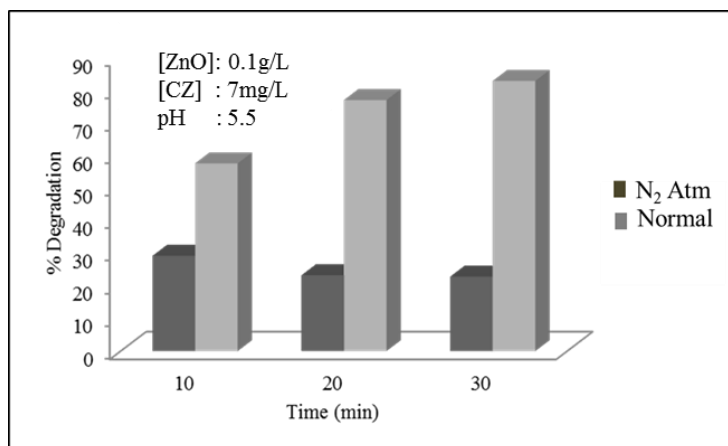
Zhen et al. reported that at 298K maximum adsorption of phosphate on the ZnO surface is 163.4mg/g at pH  $6.2\pm 0.1$  [138]. Under the present experimental conditions also the ZnO surface is significantly covered by phosphate ions. Remaining surface can absorb the light and lead to the generation of OH radicals. The decrease in the percentage degradation in presence of  $\text{HPO}_4^{2-}$  as well as  $\text{Al}^{3+}$  may be mainly due to the decrease in

the  $\cdot\text{OH}$  radical formation even though there may be other factors, which need to be investigated in depth.

### **3.3.8 Effect of oxygen**

$\text{O}_2$  either in dissolved form in reaction medium or on the solid catalyst surface is a key factor in semiconductor mediated photocatalytic reactions.  $\text{O}_2$  is a good electron scavenger that can prevent the recombination of photogenerated electron/hole pair. Further the electron scavenging by oxygen generates superoxide radical anion which facilitates the formation of other reactive species.  $\text{O}_2$  also enhances the amount of  $\text{H}_2\text{O}_2$  and in turn the formation of  $\cdot\text{OH}$  radicals as in reactions (67-75).

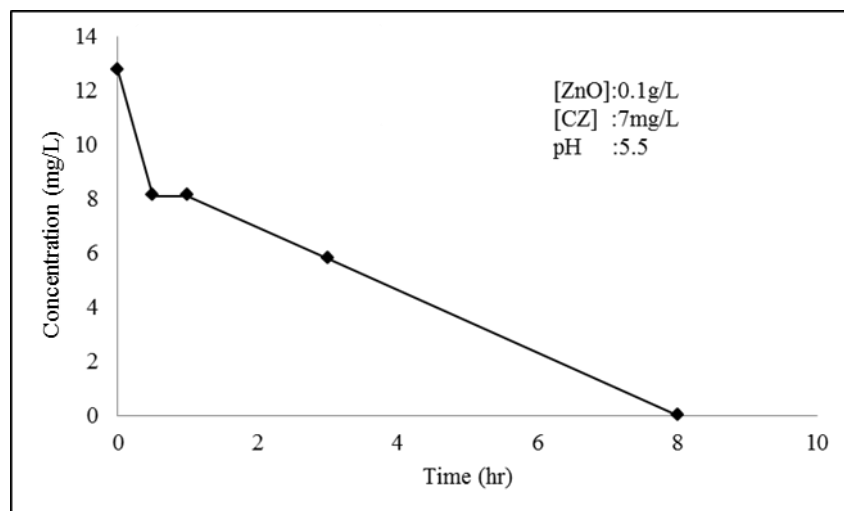
To confirm the effect of dissolved oxygen on the photocatalytic degradation of carbendazim, the reaction medium is deaerated with  $\text{N}_2$  and the experiments are carried out under identical optimized conditions. As shown in the Fig. 3.36; the percentage degradation of carbendazim is much less in the deaerated system. The relatively smaller percentage degradation may be effected by the adsorbed surface oxygen and small fraction of dissolved oxygen that cannot be removed by  $\text{N}_2$  deaeration. The decrease in the percentage degradation of carbendazim with time and the eventual stabilization in the deaerated system clearly indicate that once the remaining available oxygen has been fully consumed, the degradation will not proceed further.



**Fig. 3.36:** Effect of deaeration with N<sub>2</sub> on the photocatalytic degradation of carbendazim

### 3.3.9 Mineralization process

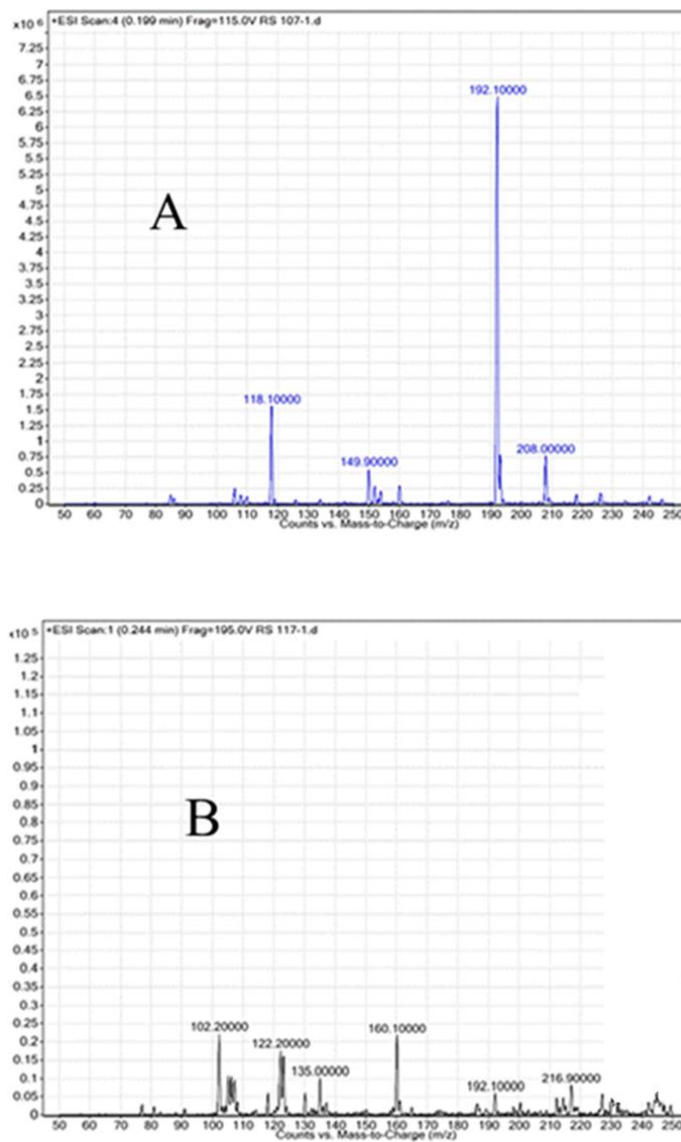
Polluted water after treatment is reusable only when the pollutant and the degradation products are completely mineralized into harmless products such as CO<sub>2</sub>, H<sub>2</sub>O and salts. Complete removal of the organic pollutants can be verified by measuring the TOC/COD of the system at various stages during the treatment. Decrease in chemical oxygen demand (COD) also confirms the fragmentation of various intermediates and eventual mineralization. The COD of the solution containing carbendazim at different times of irradiation is shown in the Fig. 3.37. The initial steep fall in COD corresponds to the degradation of carbendazim forming various intermediates, some of them getting mineralized faster. The steady state during a short period of irradiation shows the accumulation of more stable intermediates which get mineralized later. Complete mineralization of carbendazim is achieved in presence of sunlight in 8hr.



**Fig. 3.37:** COD of the reaction system after different periods of irradiation

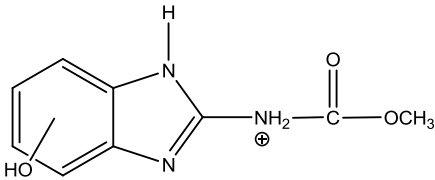
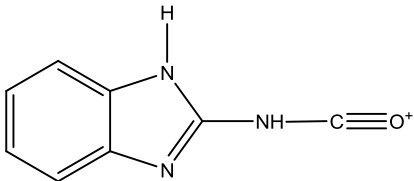
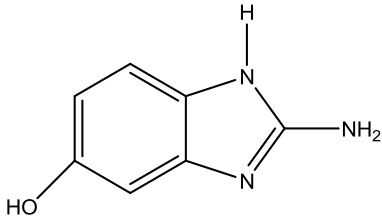
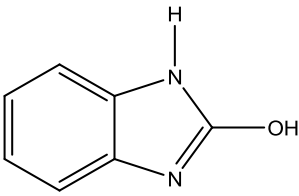
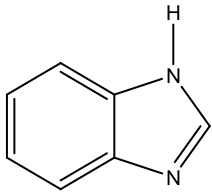
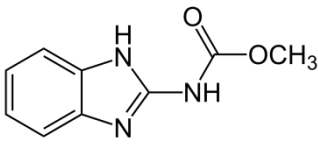
### 3.3.10 Identification of reaction intermediates

The gradual decrease in COD shows that the mineralization process is slow and the degradation proceeds through different stages. In this context, reaction intermediates have been identified by LC/MS. The reaction system at two different stages, i.e. 50% and 80% degradation is chosen for the analysis of intermediates. The mass spectra are shown in Fig. 3.38 A and B. The difference in the mass spectra at two time intervals of irradiation shows that the intermediates are getting transformed further into more compounds before mineralization. Some of the intermediates identified are shown in Table 3.2. The presence of intermediates like protonated carbendazim with added hydroxyl group ( $m/z = 208$ ) confirms reaction between the substrate molecule and the OH radicals formed in-situ.



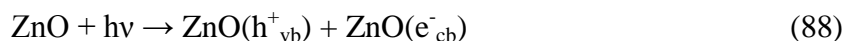
**Fig. 3.38:** Mass spectra of degradation products, (A) 50% degradation, (B) 80% degradation

**Table 3.2:** Some of the intermediates formed during the solar photocatalytic degradation of carbendazim.

| Molecular or Cationic mass | Intermediates/Reaction products  |
|----------------------------|--|
| 208                        |    |
| 160                        |    |
| 149                        |   |
| 135                        |  |
| 118                        |  |
| 192                        |  |

### 3.4 Mechanism of the photocatalytic degradation of carbendazim

Specific processes taking place during the photocatalytic degradation are discussed in respective sections above. The overall mechanism can be generally presented as follows: When ZnO is irradiated with sunlight, it absorbs radiation of energy greater than or equal to its band gap (3.2 eV). The valence band electron gets excited to its conduction band leaving a hole ( $h^+$ ) behind in the valence band. This leads to the formation of electron-hole pair. The photogenerated electron-hole pair can migrate to the catalyst surface or can recombine.



vb: Valence band, cb: Conduction band

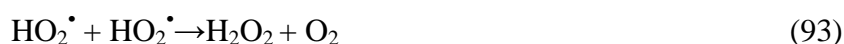
The photo induced hole can oxidize a donor molecule (D) [carbendazim (CZA), in this case] adsorbed on the ZnO surface.



The strong oxidation power of the  $h^+$  can also oxidize water to produce hydroxyl radical ( $\cdot\text{OH}$ ).



The electron can reduce the  $\text{O}_2$  present in the system and generate superoxide radical, which results in the formation of more ROS as follows:



Reduction of H<sub>2</sub>O<sub>2</sub> produces hydroxyl radical (·OH).



The ·OH radicals being strong oxidants ( $E^0=2.8$  eV) can oxidize carbendazim present in the reaction medium to various intermediate products as identified earlier. Ultimately these intermediates also get completely mineralized, leading to COD of ‘0’ as observed in this study.

The schematic representation of various steps involved in the solar photocatalytic degradation of carbendazim in presence of ZnO is shown in the Fig. 3.39.

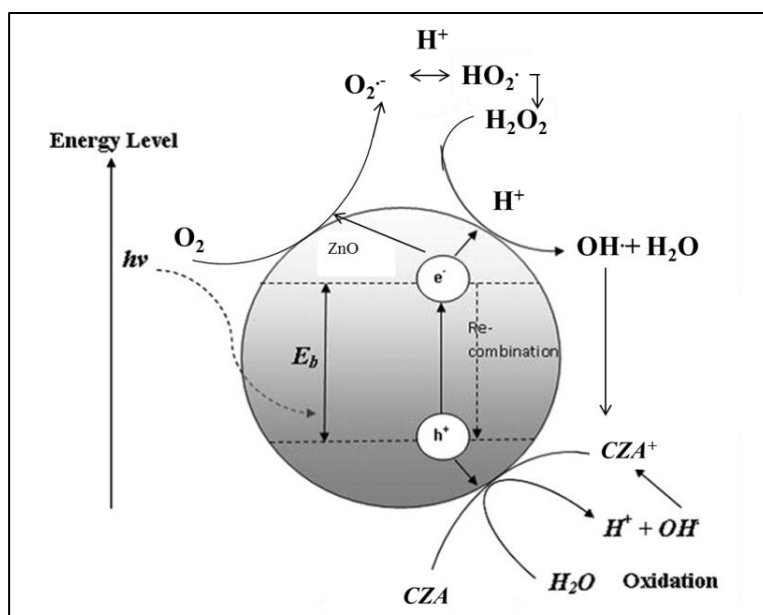


**Fig. 3.39:** Mechanism of ZnO mediated photocatalysis for the degradation of carbendazim

Various steps involved in the simultaneous formation and decomposition of H<sub>2</sub>O<sub>2</sub> are discussed earlier in the chapter.

### 3.5 Conclusion

Sunlight induced photocatalysis in presence of ZnO is an effective technique for the complete degradation and mineralization of small amounts of carbendazim pollutant present in water. The degradation follows pseudo first order kinetics. Added oxidant persulphate (in the selected concentration range) enhances the degradation slightly while another oxidant H<sub>2</sub>O<sub>2</sub> has no effect. Some of the ions present in natural water systems such as Na<sup>+</sup>, K<sup>+</sup>, Ca<sup>2+</sup> and Mg<sup>2+</sup> (cations) as well as Cl<sup>-</sup>, SO<sub>4</sub><sup>2-</sup> and NO<sub>3</sub><sup>-</sup>(anions) have no effect on the degradation. However Al<sup>3+</sup> cation and HPO<sub>4</sub><sup>2-</sup> anion adversely affect the degradation. These ions (Al<sup>3+</sup> and HPO<sub>4</sub><sup>2-</sup>) influence the degradation by inhibiting the formation of the reactive <sup>•</sup>OH radicals. The preferential adsorption of anions and layer formation by anion/cation resulting in poor activation of the catalyst may be another reason for the inhibition. Oxygen is essential for the degradation as seen from the experiments with the deaerated system. Major intermediates formed during the degradation have been identified by LC/MS. Complete mineralization of carbendazim is achieved in presence of sunlight in 8 hr. The study conclusively demonstrated that solar photocatalysis is an efficient and environment-friendly advanced oxidation process for the removal of even recalcitrant pollutants like carbendazim fungicide. Relevant reaction mechanism of the process is also discussed.

.....❧.....

**SOLAR PHOTOCATALYSIS MEDIATED BY ZnO  
FOR THE REMOVAL OF DIQUAT HERBICIDE FROM WATER**

- 4.1 Introduction
- 4.2 Experimental details
- 4.3 Results and discussion
- 4.4 Mechanism of the photocatalytic degradation of diquat
- 4.5 Conclusion

**4.1 Introduction**

Herbicides constitute a significant proportion of pesticide pollutants in water globally. As explained in Chapter 2, one of the most widely used herbicides across the world is diquat which is a non-selective contact herbicide and crop desiccant. It is also used (at or below 1mg/L) as an aquatic herbicide for the control of free-floating and submerged aquatic weeds in ponds, lakes and irrigation ditches. The possibility of contamination of water by diquat is high and hence development of an appropriate reaction system and parameters capable of mineralizing the pollutant is essential. Use of sunlight as the source of energy will be a major step towards decontamination and purification of water economically. Diquat is a bipyridylium herbicide generally marketed as a dibromide salt. The physical properties of diquat such as crystalline nature (ease of handling), low vapour pressure (minimal fumes), high water solubility of 700 g/L at

20°C (better efficacy), high binding potential (soil binding causes deactivation and immobilization) and fast working (once photosynthesis begins) make it comparatively more suitable than many other herbicides for agricultural use. Due to the double positive charge on the diquat cation it can be strongly adsorbed to the negatively charged clay minerals present in the soil.

Diquat is applied in the open field and hence its facile degradation in presence of sunlight as the energy source will be important from the environmental decontamination angle. Florencio et al. [109] investigated the photodegradation of diquat in presence of TiO<sub>2</sub> and reported that the type of catalyst and pH are major determinants of the degradation profile. However, no detailed studies on the solar degradation of diquat have been reported so far. In this chapter, the photocatalytic mineralization of trace amounts of diquat pollutant in water using sunlight as the energy source is investigated. Application of widely available ZnO as the catalyst and sunlight as the energy source makes it a perfect viable economical tertiary technique for the complete removal of diquat from water and achieve zero pollution.

## **4.2 Experimental details**

### **4.2.1 Materials**

Diquat dibromide monohydrate (99.9%) obtained from Sigma-Aldrich was used as such without further purification. ZnO and other chemicals used are the same as mentioned in Chapter 3 section 3.2.1.

#### **4.2.2 Analytical procedures**

The concentration of diquat in the solution was analyzed by spectrophotometry (310 nm).

The mineralization of diquat is followed by analyzing the TOC content of the solution after photocatalytic treatment using Shimadzu TOC-L analyzer.

Analysis of H<sub>2</sub>O<sub>2</sub>, anion and cation concentrations are done by the procedure given in Chapter 3 section 3.2.2.

#### **4.2.3 Adsorption**

Adsorption of diquat on ZnO was tested by dispersing a fixed amount (0.1g) of ZnO in 100 ml diquat solution of required concentration in a 250 ml reaction flask. The experimental procedure and the calculation are similar to those given in the Chapter 3 section 3.2.3

The same procedure was used for measuring the adsorption of various ions using respective salt solutions under required conditions.

#### **4.2.4 Detection of hydroxyl radicals**

The ·OH radicals in the reaction system are detected by the same procedure as mentioned in Chapter 3 section 3.2.4

#### **4.2.5 Analysis of reaction products/ intermediates**

The reaction intermediates were identified using Agilent 6460 Triple quad LC/MS equipped with an ESI interface operating in positive polarity mode. The LC column was C18 of 150 mm x 4.6 mm and 5µm particles (Phenomenex). The mobile phase was acetonitrile - formic acid

(0.1%) in the ratio 20:80. The scanning was done by multiple reactions monitoring (MRM) in the range 50-250 amu.

#### 4.2.6 Photocatalytic Experimental set up

The experimental setup is the same as described in Chapter 3 section 3.2.6, with the substrate carbendazim being replaced by diquat.

### 4.3 Results and discussion

#### 4.3.1 Preliminary experiments

The photocatalytic degradation of diquat (50mg/L) in presence of sunlight, using ZnO (0.6g/L) as the catalyst, was investigated under various reaction conditions. The natural pH of the suspension was 5.6. The degradation was ~58% in 5 hr of irradiation. No degradation was observed in parallel experiments under identical conditions in the absence of catalyst. Adsorption studies of diquat at different concentrations and at different loadings of ZnO showed that there is no significant adsorption in the dark.

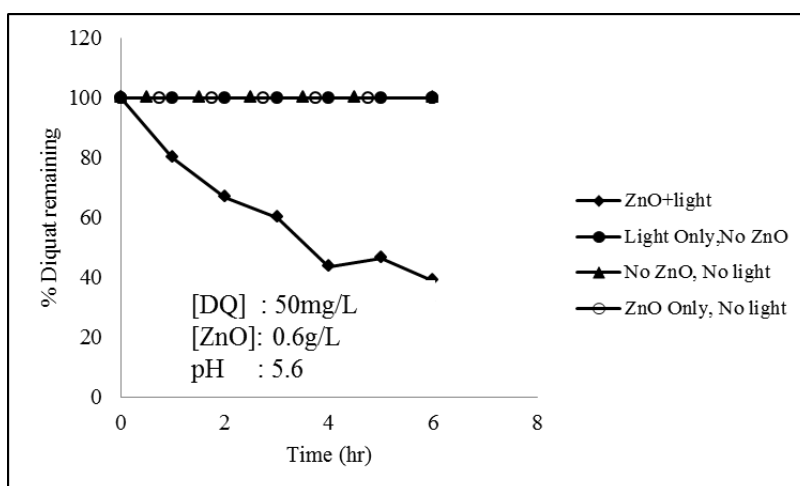


Fig. 4.1: Degradation of diquat under various conditions

Hence, the decrease in concentration in presence of catalyst is not due to simple adsorption. The degradation of diquat is achieved only under photocatalytic conditions in presence of both light and catalyst. The rate of degradation decreases with time possibly due to decrease in the concentration of diquat and the competition between various reaction intermediates and diquat for reactive free radicals.

The effect of various reaction parameters on the degradation is investigated in detail as follows:

#### **4.3.2 Effect of catalyst dosage**

The effect of catalyst dosage on the degradation of diquat is investigated by varying the loading of zinc oxide (0.1 to 2.0g/L) while maintaining other parameters identical (Diquat: 50mg/L, pH: 5.6, Reaction time: 2 hr). The percentage degradation as well as the rate of degradation of diquat increases steadily with increase in catalyst loading, reaches an optimum at 0.6g/L and slows down thereafter (Figs. 4.2a and 4.2b). Eventually, the rate is stabilized. The increase in degradation efficiency with increase in catalyst dosage may be attributed primarily to the availability of higher number of interaction sites on the surface. More catalyst leads to more quanta of light absorption which will result in the formation of higher number of reactive  $\cdot\text{OH}$  and other ROS. Consequently, there will be more frequent and effective interaction of the ROS with the pollutant and enhanced degradation. Beyond the optimum dosage, the observed stabilization trend can be explained on the basis of factors that are discussed in Chapter 3 section 3.3.3. Further increase in catalyst concentration beyond the optimum loading will only lead to

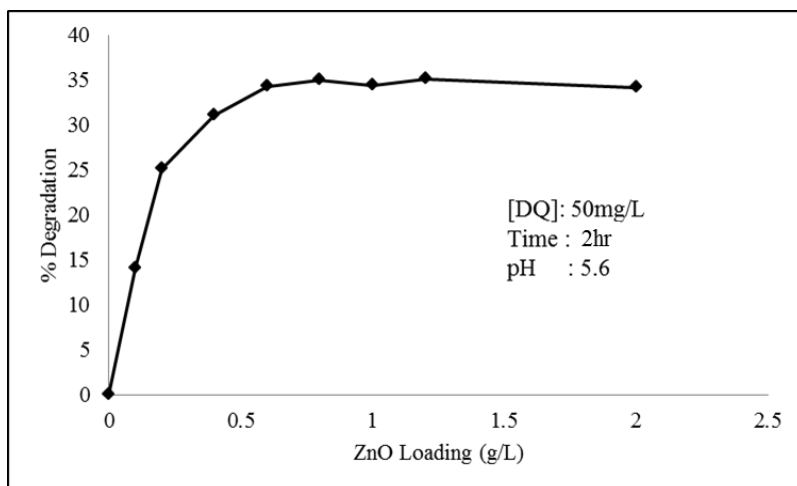


**Fig. 4.2a:** Effect of catalyst dosage on the percentage degradation of diquat

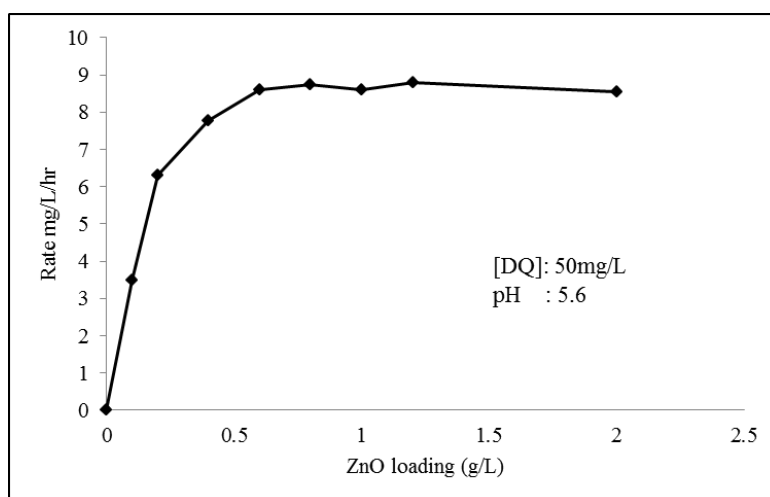


**Fig. 4.2b:** Effect of catalyst dosage on the rate of degradation

scattering and reduced passage of light through the sample. Higher loading may also cause aggregation of catalyst particles resulting in decreased number of active surface sites available for adsorption/reaction. The particles cannot be fully and effectively suspended beyond a particular loading in a particular reactor which also leads to suboptimal

penetration of light. Another possibility is that at higher loading, at least a part of the originally photo-activated zinc oxide will collide with ground state catalyst and get deactivated as discussed in the previous chapter.

The size, shape and geometry of the reactor are also known to influence the optimum catalyst loading. Hence, the optimization has to be made separately for each reactor configuration. Under the present experimental conditions, the optimum loading of ZnO for the photocatalytic degradation of diquat is 0.6g/L. Hence, all further investigations were carried out with this loading, unless indicated otherwise.

### 4.3.3 Effect of initial concentration of diquat, Kinetics

The effect of varying initial concentration of diquat on its solar photocatalytic degradation is investigated in the range 30-70mg/L. The percentage degradation of diquat decreases with increase in its concentration (Fig. 4.3).

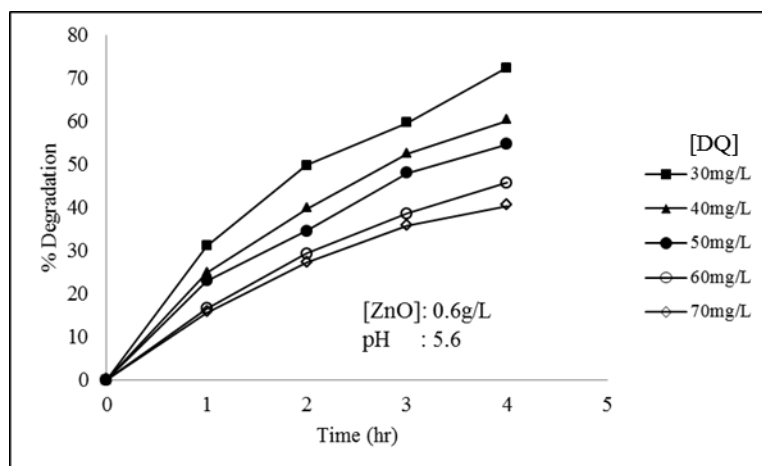


**Fig. 4.3:** Effect of initial concentration on the percentage degradation of diquat over ZnO

On the other hand, the rate of degradation increases steadily with increase in the initial concentration of diquat and stabilizes eventually (Fig. 4.4). As is evident from the figure, the rate follows first order kinetics in the range 30-50mg/L concentration of diquat. The optimum degradation rate of ~8.5mg/L/hr is reached at 50mg/L of diquat. Further increase in concentration does not influence the degradation rate significantly implying a decrease in the order of the reaction and eventual zero order kinetics.

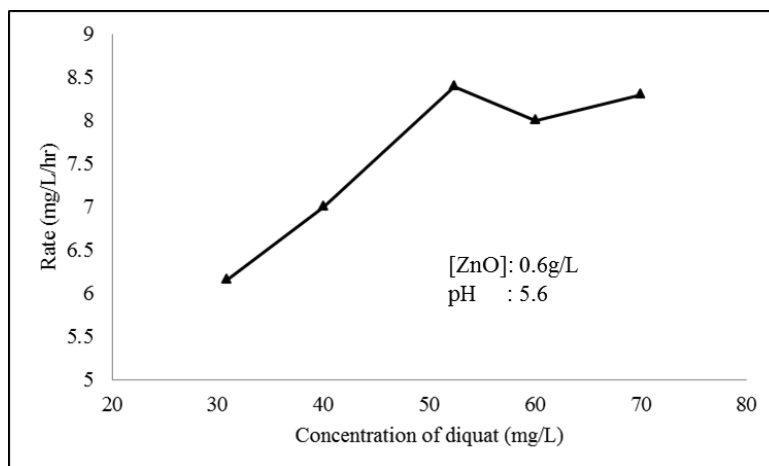


**Fig. 4.4:** Effect of initial concentration on the rate of photocatalytic degradation of diquat

The pseudo first order kinetics is verified and rationalized in terms of the modified Langmuir-Hinshelwood model (L-H model) which accommodates the reactions occurring at solid-liquid interface as well. The simplest L-H kinetic model applicable to photocatalytic degradation of chemical contaminants is proposed and explained under section 3.3.4 in Chapter 3.

As explained, the pseudo first order kinetics model for this process is as follows:

$$\ln(C_0/C) = k't \quad (95)$$

$C_0$  = initial concentration of diquat

$C$  = concentration of diquat (mg/L) remaining after time  $t$

$k'$  = pseudo first order rate constant

Plot of  $\ln(C_0/C)$  vs  $t$  will yield straight line for first order reactions. The slope of the straight line will be the pseudo first order rate constant. The linear plot in Fig. 4.5 thus shows that the degradation of diquat follows first order kinetics in the concentration range 30-50mg/L.

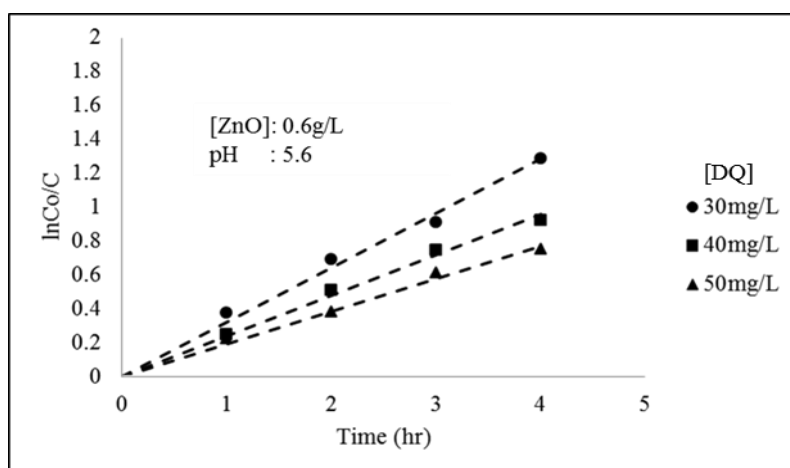


**Fig. 4.5:** Kinetics of photocatalytic degradation (linear transform  $\ln C_0/C$  vs time) of diquat over ZnO

The pseudo first order rate constants for the three concentrations considered in Fig. 4.5 are computed and given in Table 4.1. The rate constant for the degradation decreases with increase in concentration of diquat. This may be explained as already done in the previous chapter, as

follows: For a fixed amount of catalyst and intensity of irradiation, under otherwise identical conditions (excluding the concentration of substrate), the number of surface-generated active species available for interaction is finite. However, the number of substrate molecules is excessive at higher concentrations and this reduces the relative % fraction of substrate which can successfully interact with the ROS. This leads to decrease in the rate constant. However, the quantitative rate constant value applies only under the current experimental conditions and has no absolute meaning as such for another set of parameters.

**Table 4.1:** Pseudo first order rate constants for the photocatalytic degradation of diquat over ZnO. pH: 5.6 Temp:  $29 \pm 1^\circ\text{C}$

| Experiment | ZnO (g/L) | Diquat (mg/L) | $k' \times 10^{-1}$ (hr <sup>-1</sup> ) |
|------------|-----------|---------------|---|
| 1          | 0.6       | 30            | 2.97                                    |
| 2          | 0.6       | 40            | 2.25                                    |
| 3          | 0.6       | 50            | 1.83                                    |

Decrease in the rate of photocatalytic degradation and hence in the order of the reaction at higher concentration of the reactant has been reported earlier [89,99,139]. Variation in the kinetics of degradation with variation in the concentration of substrate has been reported in the case of semiconductor mediated sonophotocatalysis also [132]. The adsorption of diquat on ZnO is not significant and hence increase in the rate of degradation with increase in concentration is not due to increased adsorption or activation of the substrate on the surface sites. At the same time, there will be more diquat molecules available in the bulk as well as in the proximity of the catalyst surface for interaction with the surface-generated ROS such as the  $\cdot\text{OH}$ ,  $\text{HO}_2\cdot$ ,  $\text{O}_2\cdot^-$ ,  $\text{H}_2\text{O}_2$  etc.

Once the concentration of the substrate is adequate to interact with the optimum available ROS and/or other reactive free radicals, any further increase does not result in enhanced reaction and the rate of diquat removal becomes independent of its concentration. This results in an optimum value for the concentration of diquat. It is also possible that at higher substrate concentration, more reaction intermediates are formed and some of them may remain in the system or even get loosely attached/adsorbed to the surface for relatively longer period. This also results in less frequent interaction between fresh diquat molecules and the ROS. Higher substrate concentration and the intermediates formed from them can also absorb more photons unproductively thereby decreasing the photons available for ZnO activation. Complete domination of the system/surface by the reactant/intermediate products by direct adsorption and/or by sheer population in the immediate neighborhood of the catalyst particles can also result in suppression of the generation of surface-initiated reactive free radicals and hence the degradation of the pollutant. However, the absolute value of the optimum concentration, i.e. 50mg/L in the present context is applicable only under the specific experimental conditions employed. For every different set of reaction parameters, including reactor size and geometry, the optimum concentration will be different and has to be determined experimentally.

#### **4.3.4 Effect of pH**

It is observed that an aqueous solution of diquat is stable up to pH 8 and undergoes hydrolysis at higher pH even in the absence of catalyst and light. The effect of pH on the photocatalytic degradation of diquat is

investigated by varying the pH of the medium while other parameters are kept constant. The results are presented in Fig. 4.6. As the pH of the medium increases, the degradation increases and reaches a maximum at pH 5. Thereafter it remains steady or starts decreasing slowly. As is evident from the results, there is natural degradation of diquat even in the absence of irradiation as the pH is raised above 8. Hence the effect of alkaline pH exclusively on the ZnO - photocatalysed degradation cannot be precisely measured due to the complex interplay of a number of parameters. The point of zero charge of ZnO is  $\sim 9.3$  and the ZnO surface is positively charged below pH 9.3 [47,140]. Since diquat is a quaternary ammonium compound, its adsorption on to the catalyst surface will be less below pH  $\sim 9.3$ . The concentration of diquat in the immediate vicinity of the catalyst also will be less.

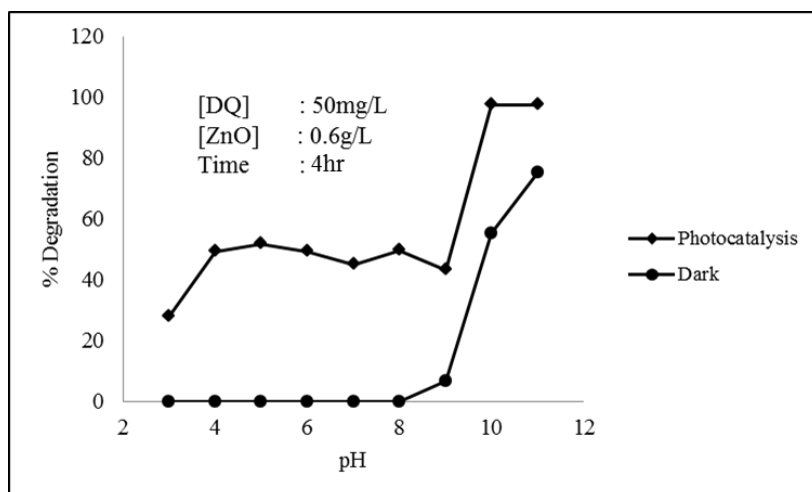


**Fig. 4.6:** Effect of pH on the degradation of diquat in dark and under photocatalysis

Adsorption measurements done as explained in section 4.2.3 show that the adsorption of diquat on ZnO is quite less. Variation in the pH also does not help the adsorption. Hence, at least in the case of diquat, adsorption is not a major precondition for the photocatalytic degradation in presence of ZnO. The photogenerated ROS at the surface interact with the substrate primarily in the bulk resulting in its degradation.

Florencio et al.[109] reported that the major intermediates formed during the photocatalytic degradation of diquat on TiO<sub>2</sub> are carbonyl compounds. They observed that the degradation does not take place in acidic medium while it is faster in an alkaline solution. In the current instance also maximum degradation is observed in the alkaline pH, though at least part of it is attributed to the self-destruction of diquat as explained earlier. The intermediate products of degradation which have negatively charged atoms, i.e. oxygen atoms of the carbonyl group, may have the tendency to be competitively better adsorbed on or come closer to the positively charged surface as the reaction proceeds, even though the adsorption of diquat is not significant as discussed earlier. Hence, the interaction of ROS with the diquat will be less and this may be another reason for the lower degradation rate of diquat below pH 5. At the same time, such adsorption (of intermediates) can lead to faster degradation and eventual mineralization making the surface available for the adsorption of more intermediate molecules as well as for the formation of reactive free radicals. Hence, there is reasonable amount of degradation even below the optimum pH of 5. The significantly low degradation at extremely low pH (<3) may also be due to the corrosion of ZnO and consequent depletion in the number of active sites available for generation of sufficient ROS. In

the alkaline medium, the reaction is further enhanced by the increased number of hydroxyl radicals generated from the abundant OH ions present in the system.

In the alkaline pH range above 9.3 where ZnO is negatively charged, diquat is expected to be closer to the surface. Hence the interaction with surface initiated active species will proceed faster. The self-degradation of diquat also takes place at pH >9. However under acidic conditions, diquat will remain mainly in the solution and its degradation will proceed by interaction with the ROS and/or bulk hydroxyl radicals produced in the aqueous phase [141]. In the alkaline range the possibility of dissolution of ZnO [142] as mentioned in Chapter 3 section 3.3.5 also cannot be ruled out. This decrease in catalyst concentration may be another factor responsible for the lack of significant increase (over the natural increase at alkaline pH) in ZnO catalyzed photodegradation at pH>10.

Unlike in the case of many semiconductor mediated photocatalytic degradation of organics, the current study does not show any direct correlation between the PZC of ZnO and the degradation of the pollutant. Poor adsorption of diquat on ZnO as discussed above may be one reason. Further, the PZC itself is known to depend on a number of factors including the size and nature of dispersion of the particles and the type of catalyst itself. The complexity and lack of correlation of the pH or PZC with the rate of reactions in semiconductor catalyzed photodegradation is reported by other authors [143] also.

Since the optimum pH is observed to be around 5, all further studies, unless indicated otherwise, were carried out at the natural pH of the reaction system, i.e. 5.6.

#### 4.3.5 Effect of oxidants

H<sub>2</sub>O<sub>2</sub> is formed as a by-product/intermediate in many photocatalytic reactions. As discussed in previous chapter, in the current study also H<sub>2</sub>O<sub>2</sub> formation is observed (Fig. 4.7). After initial increase, its concentration remains stable for some time before increasing again slowly even though the photocatalytic degradation of diquat continues unabated. Thus the stabilization/oscillation of H<sub>2</sub>O<sub>2</sub> reported in many earlier studies [132,133,144] is observed in this case also.

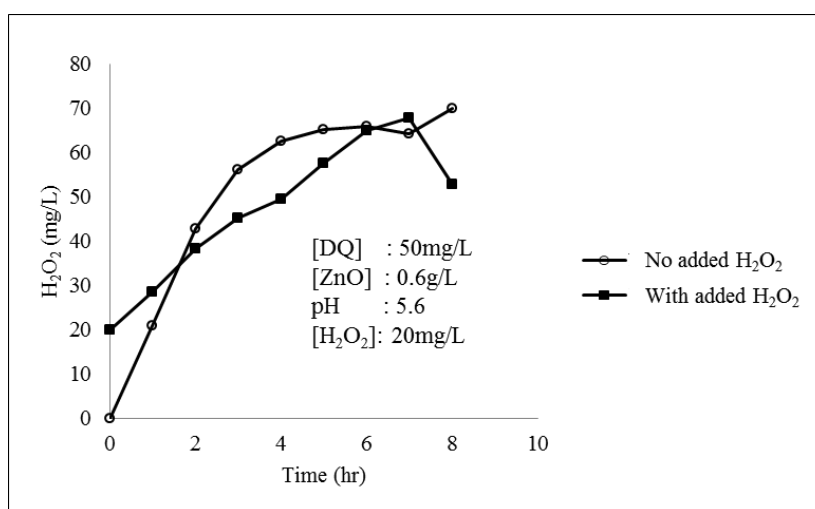


**Fig. 4.7:** Fate of in-situ formed and externally added H<sub>2</sub>O<sub>2</sub> with time

#### 4.3.6 Effect of added H<sub>2</sub>O<sub>2</sub>

In order to test the effect of concentration of H<sub>2</sub>O<sub>2</sub> on its rate of formation/decomposition, experiments were conducted by adding H<sub>2</sub>O<sub>2</sub> externally to the system in the beginning itself. In this case, the net concentration of H<sub>2</sub>O<sub>2</sub> (including the H<sub>2</sub>O<sub>2</sub> formed in-situ) does not increase beyond a limit and starts decreasing eventually (Fig. 4.7) thus confirming the concurrent formation and decomposition under photocatalytic condition. The result also shows that the concentration of H<sub>2</sub>O<sub>2</sub> does not increase beyond a particular maximum, possibly due to the balancing of formation and decomposition rates at this stage. Depending on the domination of either formation or decomposition at any point in reaction time, the net concentration of H<sub>2</sub>O<sub>2</sub> will increase or decrease.

The effect of added H<sub>2</sub>O<sub>2</sub> at different concentrations of 10, 20 and 50mg/L on the degradation of diquat is investigated and the results are shown in Fig. 4.8a. The effect at different time periods as the reaction proceeds is also studied and the results are given in Fig. 4.8b. The degradation is slightly inhibited initially. The inhibition does not increase with increase in concentration of H<sub>2</sub>O<sub>2</sub> and the degradation becomes more or less steady. This might be because, after the initial stage, the H<sub>2</sub>O<sub>2</sub> formed in-situ is fairly sufficient and may have already played the inhibiting role so that the effect of added H<sub>2</sub>O<sub>2</sub> becomes superfluous and indistinguishable. Further, the H<sub>2</sub>O<sub>2</sub> itself may get involved in its own concurrent decomposition and re-formation thereby making its contribution towards the degradation of diquat less significant.

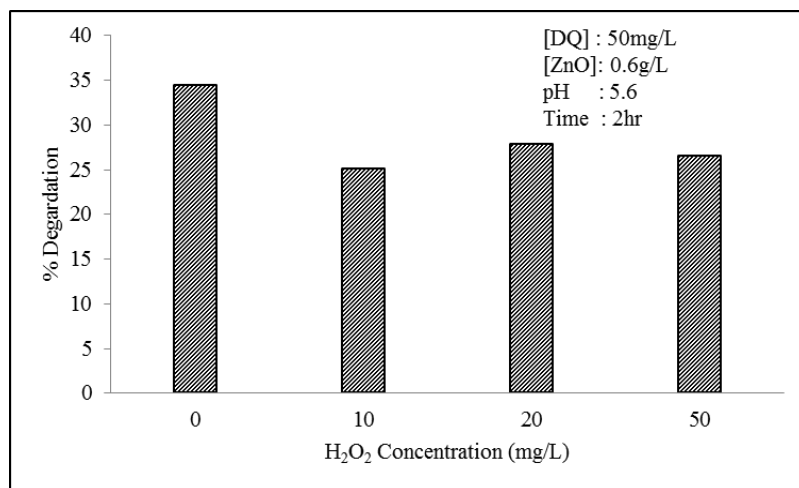


**Fig. 4.8a:** Effect of added H<sub>2</sub>O<sub>2</sub> at different concentrations on the photocatalytic degradation of diquat

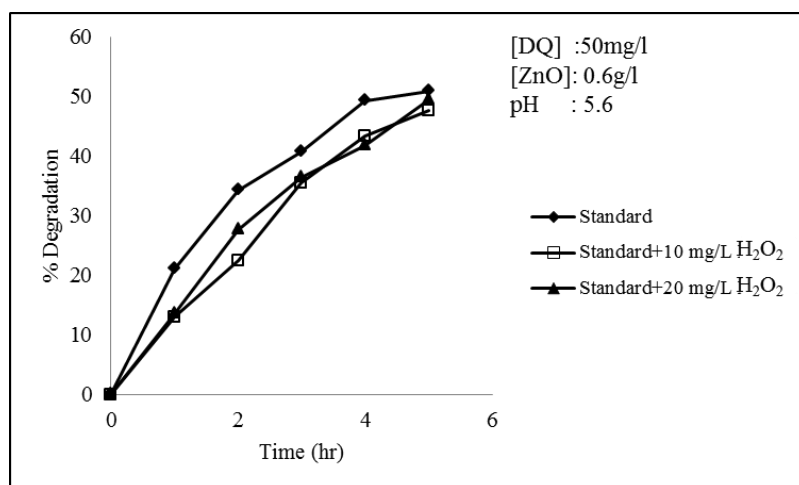


**Fig. 4.8b:** Effect of added H<sub>2</sub>O<sub>2</sub> on the photocatalytic degradation of diquat at different reaction times

Experiments showed that addition of H<sub>2</sub>O<sub>2</sub> to an aqueous solution of diquat does not induce degradation of the latter in the absence or even in the presence of sunlight. Even in the presence of ZnO, H<sub>2</sub>O<sub>2</sub> does not

contribute to the degradation of diquat in the absence of light. The concentration of added H<sub>2</sub>O<sub>2</sub> in the system also remains the same in the absence of light and ZnO. Thus it is confirmed that both sunlight and ZnO are essential for the creation of more ROS and subsequently the degradation of diquat irrespective of the presence of H<sub>2</sub>O<sub>2</sub>. Since higher concentration of H<sub>2</sub>O<sub>2</sub> does not lead to enhanced inhibition, it is clear that all the reactive species generated in-situ in the system (such as <sup>•</sup>OH, HO<sub>2</sub><sup>•</sup> etc.) are not scavenged by H<sub>2</sub>O<sub>2</sub> and some of the ROS do participate in the degradation of diquat also. This will lead to a steady inhibition/enhancement process irrespective of the concentration of added H<sub>2</sub>O<sub>2</sub> or the reaction time.

The adsorption of H<sub>2</sub>O<sub>2</sub> on ZnO is observed to be negligible under the current reaction condition. Hence the deactivation of surface sites by adsorbed H<sub>2</sub>O<sub>2</sub> is not the cause for the inhibition and most of the H<sub>2</sub>O<sub>2</sub> will be in solution. H<sub>2</sub>O<sub>2</sub> is known to serve as a precursor of many reactive free radicals in addition to being a good oxidant by itself under photocatalytic conditions. ROS such as H<sub>2</sub>O<sub>2</sub>, hydroxyl radicals, superoxides and hydroperoxyl radicals formed in presence of irradiated ZnO can interact with the pollutant diquat leading to its degradation. It is also known that H<sub>2</sub>O<sub>2</sub> is a better electron acceptor than O<sub>2</sub> [145] as in reaction (96).



This will reduce the electron-hole recombination in irradiated ZnO, which in turn can also lead to enhancement in the formation of ROS and

resultant degradation of the substrate. In view of these factors, the inhibition effect by  $\text{H}_2\text{O}_2$  in the present context is surprising, though not unusual.

As explained in previous chapter in detail, the concentration of  $\text{H}_2\text{O}_2$  does not increase beyond a particular maximum in most photocatalytic reactions due to the phenomenon of oscillation in its concentration resulting from concurrent formation and decomposition. At relatively higher concentration,  $\text{H}_2\text{O}_2$  can also serve as a scavenger for the reactive  $\cdot\text{OH}$  radicals (as discussed in Chapter 3 section 3.3.6) which are mainly responsible for the degradation of diquat. Further, at higher concentrations,  $\text{H}_2\text{O}_2$  may absorb at least part of the incident solar radiation which reduces its availability for activation of the catalyst [146]. These factors can contribute to decline in the relative concentration of  $\cdot\text{OH}$  radicals and consequent inhibition of the degradation of diquat in presence of added  $\text{H}_2\text{O}_2$ . Even in those cases where  $\text{H}_2\text{O}_2$  is not added externally, once the concentration of in-situ formed  $\text{H}_2\text{O}_2$  reaches a particular maximum it becomes a major competitor to the substrate for the ROS in the system. This will lead to the decomposition of  $\text{H}_2\text{O}_2$  and correspondingly decreased degradation of diquat. When the system is already having adequate concentration of  $\text{H}_2\text{O}_2$ , the effect of extra addition of  $\text{H}_2\text{O}_2$  may not be prominent.

#### **4.3.7 Effect of added $\text{S}_2\text{O}_8^{2-}$**

The effect of added persulphate (PS) on photocatalytic degradation of diquat under optimized condition is tested and the results are shown in Figs. 4.9a and 4.9b. Contrary to many earlier reports according to which

PS is a good enhancer of photocatalytic reaction, it is observed that the addition of PS to the system has no effect on the degradation of diquat.

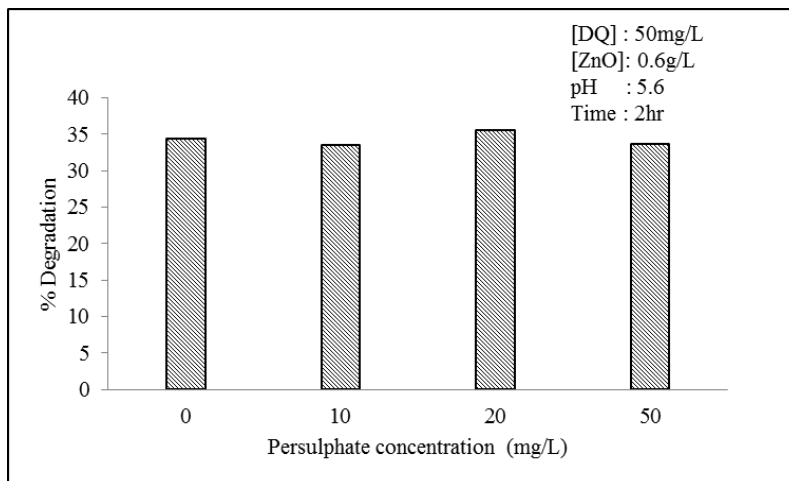


**Fig. 4.9a:** Effect of added persulphate on the photocatalytic degradation of diquat

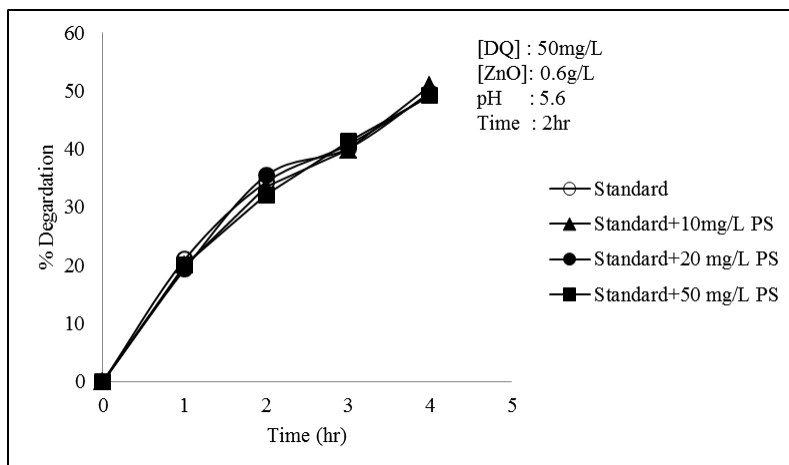


**Fig. 4.9b:** Effect of added persulphate on the photocatalytic degradation of diquat with time

The electron scavenging ability of PS is well known. Consequently, the electron-hole recombination is expected to be inhibited and correspondingly the formation of ROS is expected to be enhanced. As mentioned in Chapter 3, during the interaction of PS with electrons more sulphate radical anions are produced which are also better ROS. But in the present study the effect of PS is practically 'nil'. The absence of any enhancement by persulphate (PS) shows that the formation of the highly reactive  $\text{SO}_4^{\cdot-}$  radicals is not facilitated by sunlight in presence of diquat. The influence of the substrate as well as the chemical composition of the reaction system on the oxidation efficiency of PS under solar irradiation needs further in depth investigation.

#### **4.3.8 Effect of anions and cations**

The effect of various ions on the degradation of diquat under the optimized conditions was examined using four selected common anions i.e. chloride, nitrate, sulphate and phosphate. The corresponding sodium salts of these were used in the experiments. Similarly the effect of cations is tested for sodium, potassium, calcium, magnesium and aluminium keeping the anion the same i.e.  $\text{SO}_4^{2-}$ . Fig. 4.10 shows the influence of selected anions at different concentrations on the photocatalytic degradation diquat in solution. Except  $\text{HPO}_4^{2-}$ , other anions show no effect on the degradation process in the selected concentration range. In presence of  $\text{HPO}_4^{2-}$ , the degradation appears to be enhanced. The 'enhancement' increases as the concentration of  $\text{HPO}_4^{2-}$  increases. This is quite unusual and contrary to the detrimental effects of phosphate ions on photocatalytic process reported in many

earlier studies [137]. Hence the effect of  $\text{HPO}_4^{2-}$  on the degradation of diquat may be different from that of other photocatalytic reactions and more complex which need further in-depth investigation.

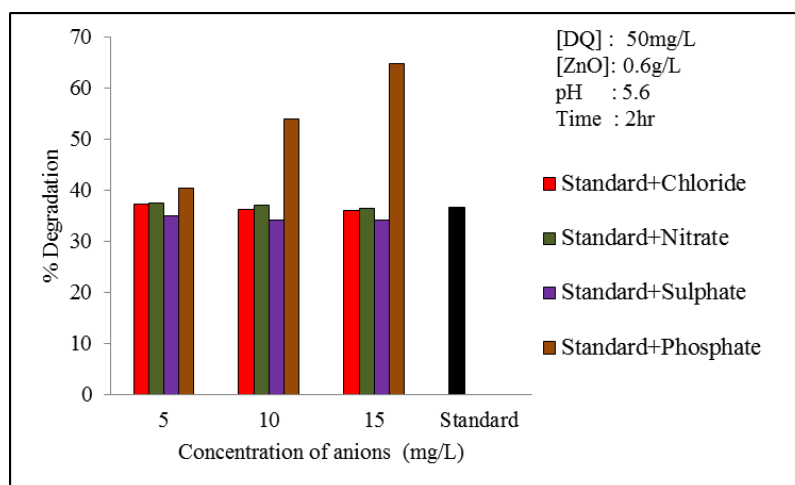


**Fig. 4.10:** Effect of anions on the photocatalytic degradation of diquat [Cation:  $\text{Na}^+$ ]

More detailed investigation on the effect of varying concentration of  $\text{HPO}_4^{2-}$  on the degradation of diquat is made and the results are shown in Fig. 4.11. Clearly, the degradation appears to be increasing with increase in concentration of  $\text{HPO}_4^{2-}$ . As explained in Chapter 3 section 3.3.7, phosphate ions are known to have high affinity for the ZnO surface, thereby preventing the substrate molecules from interacting with the catalyst surface.

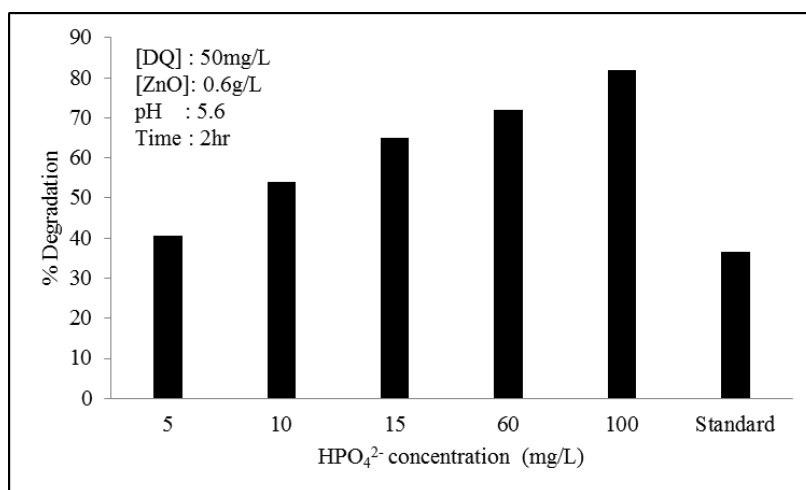


**Fig. 4.11:** Effect of HPO<sub>4</sub><sup>2-</sup> on the photocatalytic degradation of diquat [Cation: Na<sup>+</sup>]

However, in the case of the degradation of diquat, the effect of HPO<sub>4</sub><sup>2-</sup> is ‘enhancement’ and hence other mechanisms have to be explored. One possibility is the facilitation of the adsorption of diquat on ZnO by pre-adsorbed HPO<sub>4</sub><sup>2-</sup> ions (assisted adsorption) and consequently enhanced interaction of the substrate and ROS. However, study of the adsorption of diquat on fresh ZnO as well as HPO<sub>4</sub><sup>2-</sup> pre-adsorbed ZnO shows that there is no change in the adsorption. Previous study has shown that [137] HPO<sub>4</sub><sup>2-</sup> does not cover ZnO surface absolutely and few sites are left vacant where the substrate molecules can get adsorbed. However, in the current instance diquat adsorption is not affected by HPO<sub>4</sub><sup>2-</sup> and hence enhanced adsorption in presence of HPO<sub>4</sub><sup>2-</sup> is not the cause of the increased degradation of diquat.

This is further verified in another set of experiments in which the photocatalytic degradation of diquat is done under the optimized

condition using  $\text{HPO}_4^{2-}$  pre-adsorbed ZnO (Ph-Z) as catalyst (Fig. 4.12). It is observed that the degradation of diquat in presence of Ph-Z is slightly less compared to the standard experiment with pure ZnO as catalyst. From these studies it can be concluded that the apparent enhancement in the photocatalytic degradation of diquat is not due to enhancement in the adsorption of diquat on the catalyst surface or the surface modification by the  $\text{HPO}_4^{2-}$ .

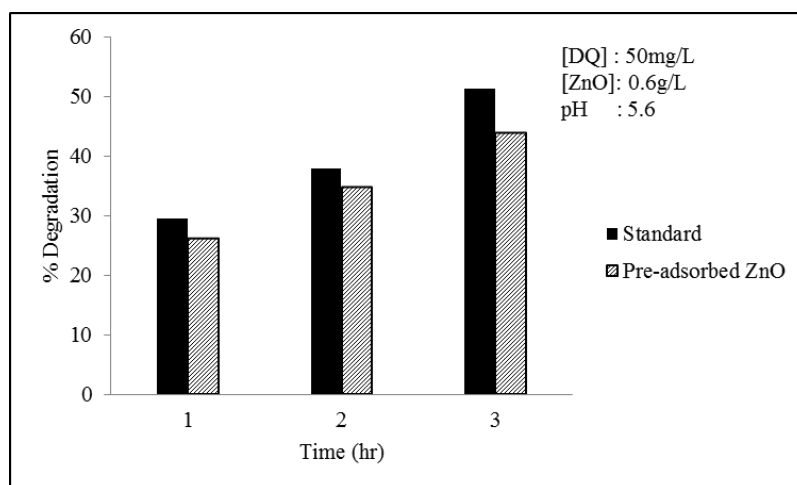


**Fig. 4.12:** Photocatalytic degradation of diquat over  $\text{HPO}_4^{2-}$  pre-adsorbed ZnO

The apparent or real enhancement in the photocatalytic degradation of diquat in presence of  $\text{HPO}_4^{2-}$  is again verified by ‘in between’ addition of  $\text{HPO}_4^{2-}$  to the reaction system under the optimized photocatalytic conditions. The results are presented in Fig. 4.13.

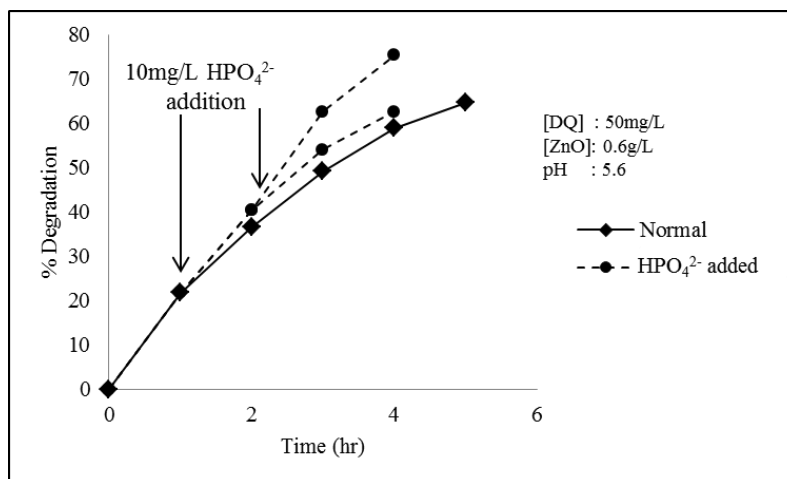


**Fig. 4.13:** Effect of in between addition of  $\text{HPO}_4^{2-}$  on the photocatalytic degradation of diquat

Addition of 10mg/L  $\text{HPO}_4^{2-}$  to the reaction system after 1hr of irradiation increases the disappearance of diquat. After 2 hr of irradiation 10mg/L  $\text{HPO}_4^{2-}$  is added again to the same reaction medium. This results in further increase in the rate of disappearance of diquat.

As the concentration of  $\text{HPO}_4^{2-}$  is increased in the reaction medium the rate of disappearance of diquat also increases. As explained earlier, this cannot be attributed to any of the well-known characteristics of anions or their interaction with the catalyst/substrate under similar conditions.

Another possibility is the formation of an intermediate compound by the reaction between diquat and  $\text{HPO}_4^{2-}$  which will reduce the net concentration of diquat in the system and gives the false indication of its degradation. At high concentrations of  $\text{HPO}_4^{2-}$  (>50mg/L) a yellow colouration of the reaction mixture is observed after 1hr irradiation, which is not observed at low  $\text{HPO}_4^{2-}$  concentrations and also under otherwise identical

condition without  $\text{HPO}_4^{2-}$ . Such colouration is not observed in presence of other substrates such as carbendazim, phenol etc. under similar conditions in presence of  $\text{HPO}_4^{2-}$ , ZnO and sunlight. The intensity of colour increases as the concentration of  $\text{HPO}_4^{2-}$  in the medium increases. Also it is noted that the yellow colouration fades as the irradiation is continued and disappears in about  $\sim 3$  hr. Experiments conducted without catalyst, but with  $\text{HPO}_4^{2-}$  in presence of sunlight as well as in the dark do not show any colour formation or any decrease in the diquat concentration. Thus, it is clear that the reaction leading to the colouration of the system is catalysed by ZnO. The UV-visible spectrum of the reaction solution at different times of irradiation with and without  $\text{HPO}_4^{2-}$  shows that the reaction pathways are different for the degradation of diquat in presence of  $\text{HPO}_4^{2-}$  (Fig. 4.14). As shown in the figure, under standard conditions, the intensity of  $\lambda_{\text{max}}$  at 310 nm decreases with time of irradiation showing degradation of diquat.

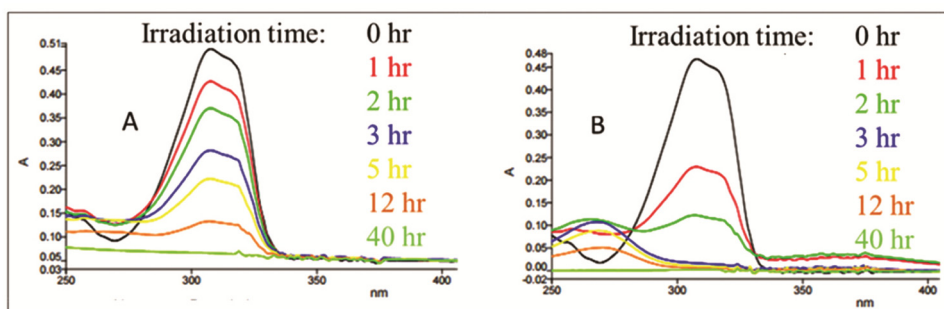


**Fig. 4.14:** UV-Visible spectrum of diquat under photocatalytic condition at different times of irradiation. (A) Standard experimental conditions ([Diquat]: 50mg/L, [ZnO]: 0.6g/L), (B) In presence of  $\text{HPO}_4^{2-}$  (Standard conditions +  $[\text{HPO}_4^{2-}]$ : 50mg/L)

Also the spectrum contains only a single peak at 310 nm which corresponds to the diquat in solution. But in the reaction system, in presence of  $\text{HPO}_4^{2-}$ ,

initially the spectrum contains the peak corresponding to diquat only. As the irradiation progresses, an additional peak at 264 nm appears along with that at 310 nm. The intensity of the peak at 264 nm increases with irradiation time and after attaining a maximum it decreases.

Removal of diquat is faster in presence of  $\text{HPO}_4^{2-}$ . However, the removal is not only due to the degradation but also due to the formation of a coloured compound. In presence of  $\text{HPO}_4^{2-}$  the degradation of diquat and the formation of the coloured intermediate are complete within 40 hr irradiation. Even though these systems are following different pathways and intermediates are different, ultimately diquat and the intermediate formed with  $\text{HPO}_4^{2-}$  are degraded almost within the same duration. Hence the net effect is that just as in the case of other anions,  $\text{HPO}_4^{2-}$  also does not inhibit the degradation of diquat even though the reaction pathway is different. The effect of  $\text{HPO}_4^{2-}$  on the mineralization of diquat is tested by measuring the TOC at different times of irradiation. The results are plotted in Fig. 4.15. It is observed that in the initial stages the rate of TOC removal is same for both systems. Later on,  $\text{HPO}_4^{2-}$  inhibits the mineralization moderately, probably due to the formation of an intermediate compound by interaction with diquat. Eventually the mineralization is complete in both cases. Hence it may be concluded that  $\text{HPO}_4^{2-}$  does not inhibit or enhance the photocatalytic degradation of diquat. The faster disappearance of diquat in presence of  $\text{HPO}_4^{2-}$  is not due to the enhanced degradation/mineralisation of the pesticide. Comparison of the TOC of the system under irradiation in the presence as well as absence of  $\text{HPO}_4^{2-}$  reconfirms this.

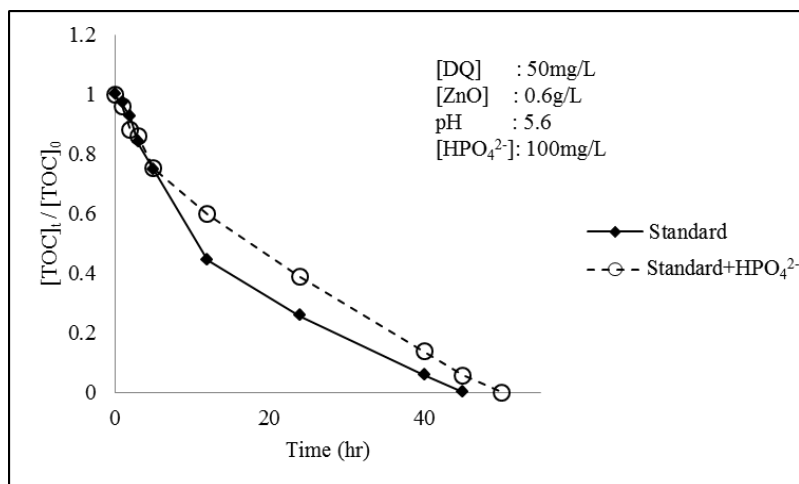


**Fig. 4.15:** Depletion in the TOC content with time of irradiation during the solar photocatalytic degradation of diquat in the presence as well as absence of  $\text{HPO}_4^{2-}$

Any study of the effect of anions will be meaningful only when the effect of corresponding cations also is analyzed. The effect of selected cations (keeping the anion same; i.e.  $\text{SO}_4^{2-}$ ) on the degradation is investigated and the results are shown in Fig. 4.16. The results show fairly comparable percentage degradation in the selected concentration range for all cations, except for  $\text{Al}^{3+}$ . In the case of  $\text{Na}^+$  there is slight enhancement, while  $\text{Al}^{3+}$  shows significant inhibition. The detrimental effect of  $\text{Al}^{3+}$  in the case of  $\text{TiO}_2$  as photocatalyst is already reported [147].  $\text{Al}^{3+}$  has high affinity for both the  $\text{TiO}_2$  and  $\text{ZnO}$  surface and can remain on or in close proximity of the surface. This will shield the incident light from the surface of  $\text{ZnO}$  and subsequent activation. Parallel experiments conducted on the adsorption of selected cations as described in section 4.2.3 also shows the complete adsorption of  $\text{Al}^{3+}$  on  $\text{ZnO}$  surface (Fig. 4.17). But the other selected cations are poorly adsorbed on  $\text{ZnO}$ . The effect of

cations on the formation of  $\cdot\text{OH}$  radicals in the reaction system was verified by PL studies as explained in Chapter 3, section 3.3.7. The PL spectra at various concentrations of  $\text{Al}^{3+}$  are shown in Fig. 4.18.

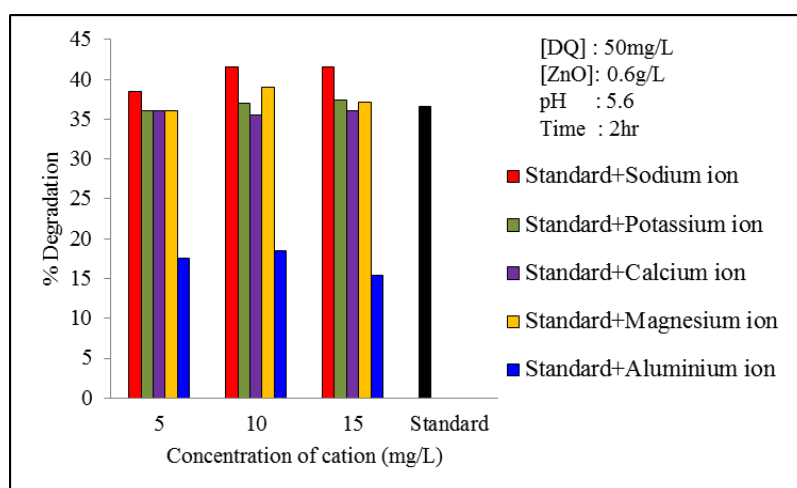


**Fig. 4.16:** Effect of cations on the photocatalytic degradation of diquat [Anion: $\text{SO}_4^{2-}$ ]

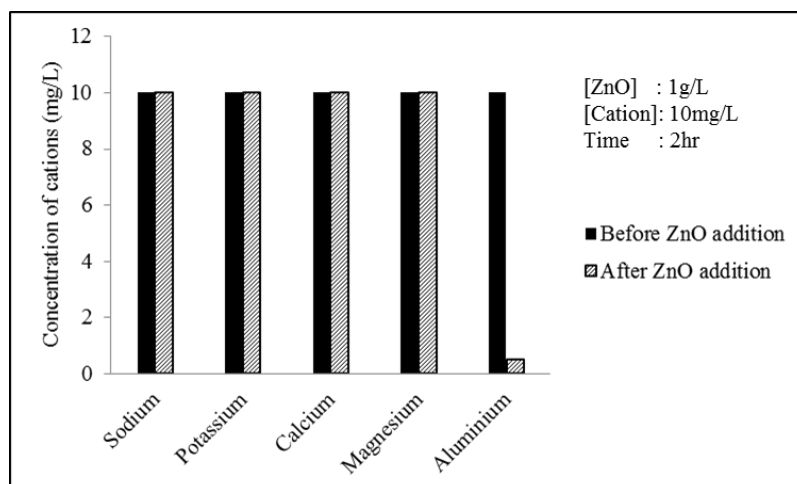


**Fig. 4.17:** Adsorption of selected cations on ZnO [Anion: $\text{SO}_4^{2-}$ ]

It was shown in Chapter 3 also (Fig. 3.31) that  $\text{Al}^{3+}$  inhibits the formation of  $\cdot\text{OH}$  radicals, while other cations do not have much effect. The inhibition increases with increase in the concentration of  $\text{Al}^{3+}$  (Fig. 4.18). Since  $\text{Al}^{3+}$  gets strongly adsorbed on ZnO, the exposed surface area (of ZnO) is less resulting in decreased photo-activation. Consequently, the generation of ROS is also less. Hence it is possible that the inhibition of the degradation of diquat in presence of  $\text{Al}^{3+}$  is mainly due to the decreased generation of  $\cdot\text{OH}$  radicals.

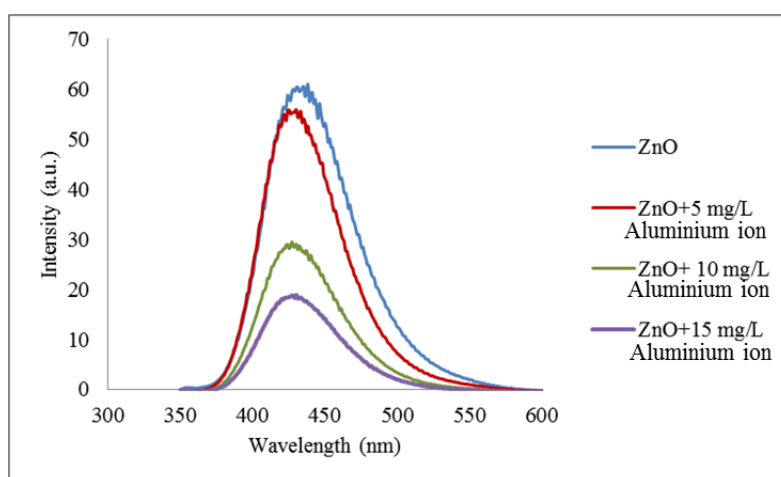
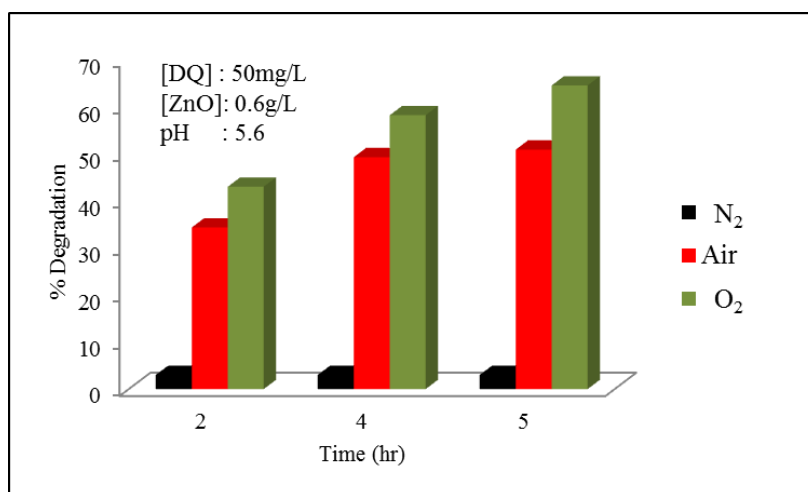


**Fig. 4.18:** PL spectral changes observed in the photocatalytic system in presence of  $\text{Al}^{3+}$  at various concentrations

#### 4.3.9 Effect of oxygen

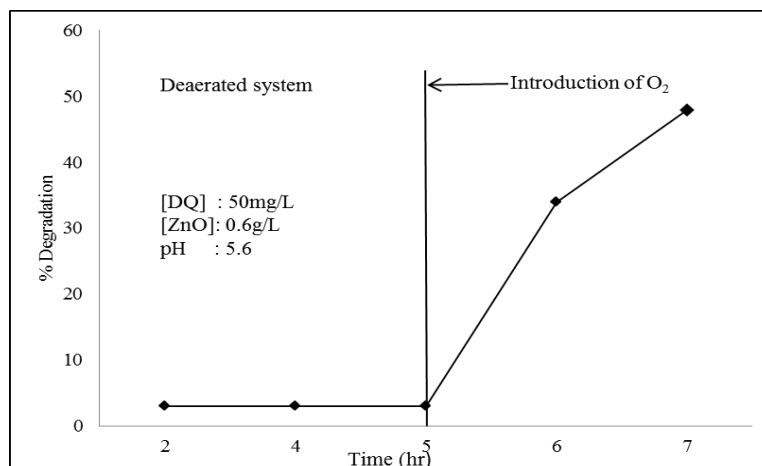
In order to confirm the effect of  $\text{O}_2$  on the photocatalytic degradation of diquat, the reaction system is deaerated with  $\text{N}_2$  and the experiments were carried out under otherwise identical conditions. The degradation is almost fully inhibited in deaerated system. The slight

degradation observed is effected possibly by the adsorbed as well as dissolved O<sub>2</sub> which cannot be fully removed by deaeration. Once the available O<sub>2</sub> is consumed fully, the degradation does not proceed further. In another set of experiments, the system is enriched with extra O<sub>2</sub> (by bubbling O<sub>2</sub> for 1hr) and irradiated. The results shown in Fig. 4.19 clearly illustrate that O<sub>2</sub> (and ROS resulting from it) is essential for the photocatalytic degradation of diquat.



**Fig. 4.19:** Effect of N<sub>2</sub> and O<sub>2</sub> atmosphere on the photocatalytic degradation of diquat.

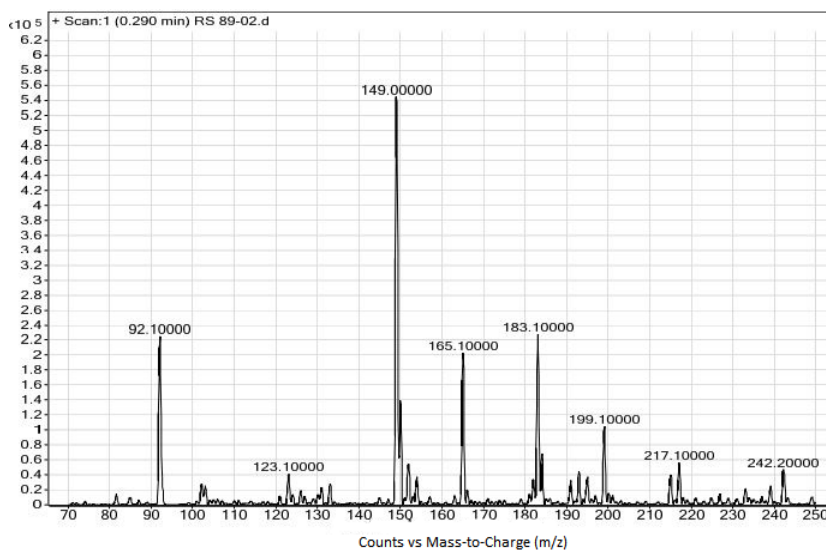
The formation of H<sub>2</sub>O<sub>2</sub> also is negligible in the deaerated system. The role of O<sub>2</sub> is further reconfirmed from the sudden significant enhancement in the degradation of diquat when O<sub>2</sub> was reintroduced into the reaction system that was previously deaerated with N<sub>2</sub> (Fig. 4.20).



**Fig. 4.20:** Effect of introduction of O<sub>2</sub> into deaerated reaction system on the photocatalytic degradation of diquat

#### 4.3.10 Identification of reaction intermediates

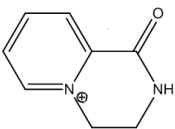
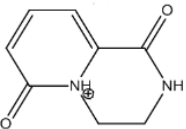
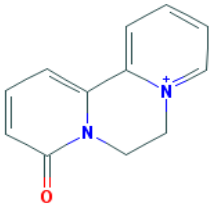
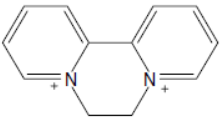
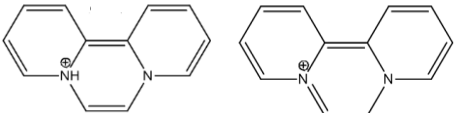
The reaction intermediates formed during the degradation of diquat at approximately 50% conversion are analyzed by LC/MS. Typical mass spectrum is shown in Fig. 4.21.



**Fig. 4.21:** Mass spectrum showing various intermediates formed during the photocatalytic degradation of diquat over ZnO

Possible intermediates are identified and listed in Table 4.2. Eventually these intermediates also get degraded and mineralized as seen from the depleting total organic carbon content (TOC) with time of irradiation.

**Table 4.2:** List of possible intermediates formed during the solar photocatalytic degradation of diquat (50% degradation).

| Molecular or Cationic mass | Intermediates/Reaction products   | Chemical nomenclature                                    |
|----------------------------|---|--|
| 149                        |                    | 1,2,3,4-tetrahydro-oxopirido[1,2]-5-pyrazinium ion       |
| 165                        |                   | Protonated 3,4-dihydro-2H-pyrido[1,2a]pyrazine-1,6-dione |
| 217                        | <br>(Hydrolysed) | Hydrolysed product of Diquatmonopyridone                 |
| 184                        |                  | Diquat Cation  |
| 183                        |                  | (M <sup>+·</sup> -H) <sup>+</sup>                        |

#### 4.4 Mechanism of the photocatalytic degradation of diquat

The general mechanism of photocatalysis discussed in Chapter 3 is applicable in this case also and may be briefly presented as follows:

When ZnO is irradiated with sunlight, it absorbs radiation of wavelength greater than or equal to its band gap (3.2 eV). The valence band electron of the ZnO gets excited to its conduction band leaving a hole (h<sup>+</sup>) behind in the valence band. The photogenerated electron-hole pair can migrate to the catalyst surface and participate in various reactions. They can also recombine unproductively generating only heat.



vb:Valence band, cb:Conduction band

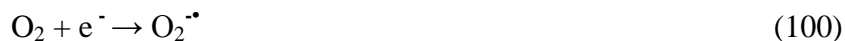
The photo induced hole can oxidize a donor molecule (D) [diquat (DQ), in this case].



Or the strong oxidation power of the h<sup>+</sup> can oxidise the water to produce hydroxyl radical (<sup>•</sup>OH).



The electron can reduce the O<sub>2</sub> present in the system to produce superoxide radical, which results in the formation of more ROS as follows:





Reduction of  $\text{H}_2\text{O}_2$  produces hydroxyl radical ( $^\bullet\text{OH}$ ).



The  $^\bullet\text{OH}$  radicals which are strong oxidants ( $E^\circ=2.8 \text{ eV}$ ) can oxidize diquat present in the reaction medium to various intermediate products as identified earlier. Ultimately these intermediates also get completely mineralized, leading to TOC of '0' as observed in this study.

The schematic representation of various steps involved in the solar photocatalytic degradation of diquat in presence of ZnO is shown in the Fig. 4.22.

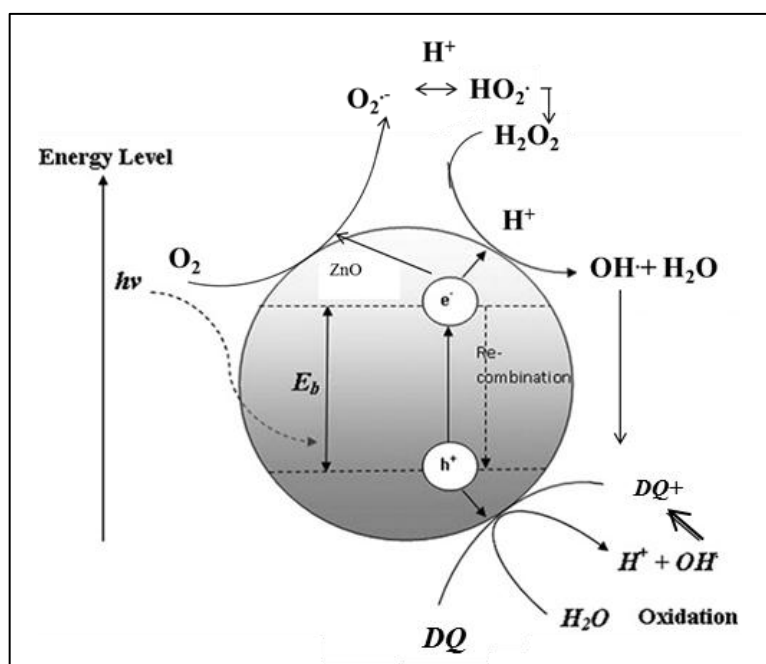


**Fig. 4.22:** Mechanism of semiconductor photocatalysis on ZnO for the degradation of diquat

## 4.5 Conclusion

Sunlight induced photocatalytic degradation of diquat in presence of ZnO is an efficient tool for the complete mineralization of small amounts of diquat present in water. The degradation follows pseudo first order kinetics. Added oxidants such as  $\text{H}_2\text{O}_2$  and persulphate (in the selected concentration range) have negligible effect on the degradation. Some of the ions likely to be present in natural polluted water systems such as cations  $\text{Na}^+$ ,  $\text{K}^+$ ,  $\text{Ca}^{2+}$  and  $\text{Mg}^{2+}$  as well as anions  $\text{Cl}^-$ ,  $\text{SO}_4^{2-}$  and  $\text{NO}_3^-$  have no effect on the degradation. However  $\text{Al}^{3+}$  adversely affects the degradation. The effect of  $\text{HPO}_4^{2-}$  on the degradation is complex and needs further in-depth investigations. In this case, it is observed that in presence of  $\text{HPO}_4^{2-}$ , the degradation proceeds through a different pathway probably by initial interaction between diquat and the anion. In the initial stages the TOC removal rate is same for both normal and  $\text{HPO}_4^{2-}$  containing systems. Later, the rate slows down in presence of  $\text{HPO}_4^{2-}$ . Eventually the mineralization is completed in both cases. Presence of dissolved and/or adsorbed oxygen is essential for maintaining the rate of degradation. The mineralization proceeds through the formation of various intermediates. Some of these intermediates have been identified by LC/MS. The study demonstrates that solar photocatalysis can be an efficient environmental-friendly technique for the mineralization of even recalcitrant pollutants such as herbicides.

.....✪.....

## SOLAR PHOTOCATALYSIS MEDIATED BY ZnO FOR THE REMOVAL OF THE COMBINATION OF DIQUAT AND CARBENDAZIM FROM WATER

- 5.1 Introduction
- 5.2 Experimental details
- 5.3 Results and discussion
- 5.4 Mechanism of the photocatalytic degradation of carbendazim/diquat mixture
- 5.5 Conclusion

### 5.1 Introduction

The application of solar photocatalysis for the removal of two widely used pesticides; i.e. carbendazim and diquat was examined in previous Chapters 3 and 4 respectively. The individual pesticide carbendazim/diquat was the sole contaminant in the synthetically prepared polluted water. However, in real life, water may contain a variety of pollutants, including multiple pesticide contaminants. The degradation and removal of trace pollutants in such a situation is complicated due to a number of factors including the interaction among the contaminants and various intermediates formed from them.

The possibility of using photocatalysis as an effective tool for the removal of multiple pesticide pollutants from water in which they are concurrently present is examined using a combination of diquat and carbendazim. The semiconductor oxide ZnO was used as the catalyst. Many factors can affect the degradation rate of mixed contaminants. These include the physico-chemical characteristics of various components present in the system, interaction between the pollutants and the intermediates, competition between the reactants and various components for the catalyst surface and consequent effect on the generation of ROS during the photocatalytic reaction, penetration of radiation through the medium etc. Multiple contaminants may result in decrease in the reaction rate and/or inhibition of the degradation of one component by the other. The reaction parameters standardized for individual components (as in earlier chapters) also may be different when they are present together. The effect of the presence of oxidants or salts on the reaction rate also can be different in the mixed system.

The photocatalytic degradation of various mixed organic contaminants is already reported. Fenoll et al. [86,148] studied the photocatalytic degradation of different combination of pesticides such as substituted phenyl urea herbicides, sulfonyl urea herbicides and eight miscellaneous pesticides in water in presence of ZnO. Both natural and artificial sunlight were used as the irradiating source. The photocatalytic degradation of a mixture of four pharmaceutical formulations in water is reported by Rimoldi et al. [149]. The degradation studies of a binary mixture of the dyes Basic red 46 and Basic yellow 28 in presence of TiO<sub>2</sub> were carried out by Gozmen et al. [150]. Most of the studies report that, even in the

mixed solutions also, the photocatalytic degradation of contaminants in water follows pseudo first order kinetics. In some instances, the complete mineralization of the contaminants is reported.

Current chapter presents the results of the study on the photocatalytic degradation of a mixture of carbendazim and diquat in water using ZnO in presence of sunlight. Various process parameters which are known to affect the photocatalytic degradation are evaluated in detail. The effectiveness of the process for the complete mineralization of the pollutants also is examined.

## **5.2 Experimental**

### **5.2.1 Materials**

Materials and their specifications are the same as explained in sections 3.2.1 and 4.2.1 of Chapters 3 and 4 respectively.

### **5.2.2 Analytical procedures**

The concentration of diquat and carbendazim remaining in solution after photocatalytic treatment was analyzed by spectrophotometry at wavelengths 310 nm and 284 nm respectively. The interference, if any, of one with the other during the analysis is tested by conducting the analysis at various concentrations of each in presence of the other. The results have shown that the absorbance at 284 nm for carbendazim increases linearly even when its concentration is maintained constant, as the concentration of diquat in the mixture is increased (Fig. 5.1).

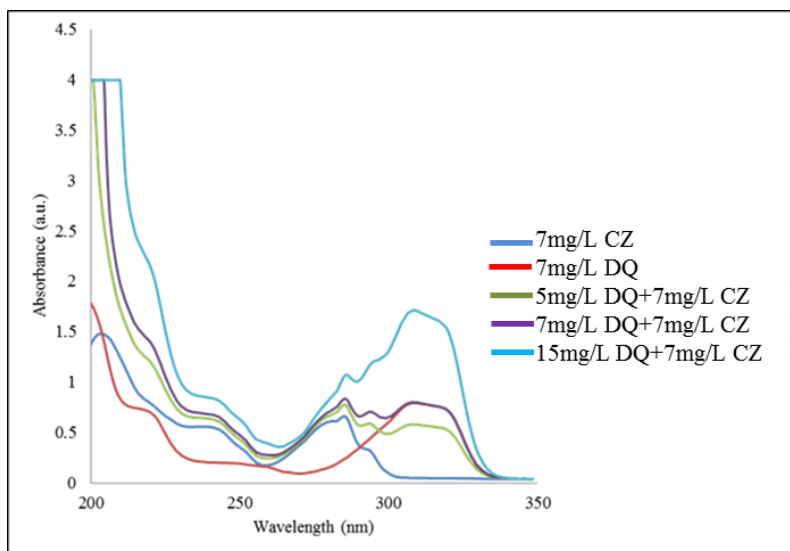


**Fig. 5.1:** UV-Visible spectrum of carbendazim/diquat mixture in solution

Hence it is necessary to standardize the analysis of carbendazim when it is present together with diquat in water. Solutions of the mixture of carbendazim and diquat were prepared with varying concentration of the latter (1-16mg/L), keeping the concentration of the former constant (7mg/L). The mixture was analyzed by spectrophotometer. It is seen that the absorbance corresponding to carbendazim increases steadily even though its concentration is maintained constant. Fig. 5.2 shows the trend when the concentration of carbendazim is maintained constant at 7mg/L with the concentration of diquat varying up to 16mg/L in the mixture. The concentration of carbendazim in presence of different concentrations of diquat in the combination solution is determined by applying a correction factor. The respective correction factor is calculated from the plot in Fig. 5.3. The precision in the analysis of diquat is not affected by carbendazim and hence no correction factor was needed.

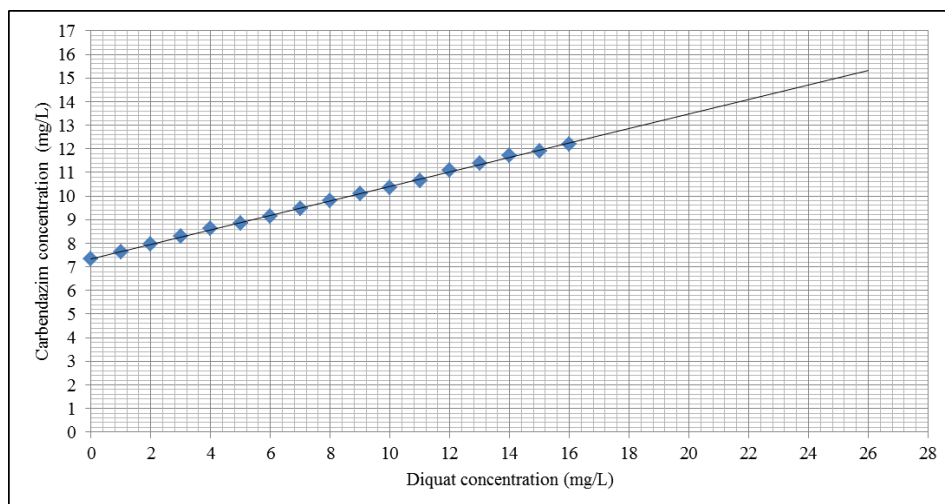


**Fig. 5.2:** Observed increase in the concentration of carbendazim (7mg/L) with varying concentration of diquat

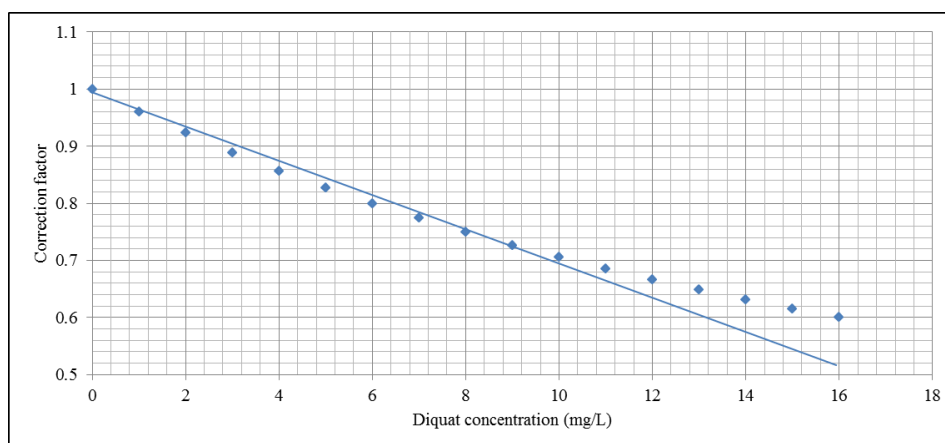


**Fig. 5.3:** The plot for determining the correction factor for carbendazim concentration at various concentrations of diquat in the combination

The mineralization of the combination of diquat and carbendazim is followed by analyzing the TOC content of the solution at specific time periods using Shimadzu TOC-L analyzer.

### 5.2.3 Adsorption

The adsorption of diquat and carbendazim on ZnO was determined by dispersing a fixed amount (0.1g) of ZnO in 100 ml solution of a mixture of diquat and carbendazim of required concentration in a 250 ml reaction flask. The suspension was agitated continuously for 2 hr. The temperature was maintained at  $29 \pm 1^\circ\text{C}$ . The suspension was kept undisturbed for 2 hr and then filtered through  $0.45\mu\text{m}$  Millipore syringe filter. The concentration of diquat and carbendazim remaining in the supernatant was determined using a spectrophotometer. No significant change in concentration was observed by keeping the suspension overnight indicating that 2 hr period is sufficient for optimum adsorption.

The adsorption was calculated as shown in the section 3.2.3 of Chapter 3.

### 5.2.4 Detection of hydroxyl radicals

$\cdot\text{OH}$  radical formation in the system is tested as explained in section 3.2.4 of Chapter 3.

### 5.2.5 Analysis of reaction products/ intermediates

The reaction intermediates were identified using Agilent 6460 Triple quad LC/MS equipped with an ESI interface operating in positive polarity mode. The LC column was C18 of  $150\text{ mm} \times 4.6\text{ mm}$  and  $5\mu\text{m}$  particles (Phenomenex). The mobile phase was acetonitrile - formic acid (0.1%) in the ratio 20:80. The scanning was done by multiple reactions monitoring (MRM) in the range 50-250 amu.

## **5.2.6 Photocatalytic experimental set up**

Photocatalytic experiments in presence of sunlight were performed using a glass reactor (as explained in section 3.2.6 of Chapter 3). Solution of carbendazim and diquat mixture (50 ml) of the required concentration together with ZnO was taken in the reactor. Cooling water from a thermostat ( $29 \pm 1^\circ\text{C}$ ) was continuously circulated through the water bath in which the reactor was placed. Solar experiments were performed by placing the reaction system at the roof top of our laboratory at Kochi, Kerala, India ( $9^\circ 57' 51''$  N,  $76^\circ 16' 59''$  E) during sunny days in February-May 2015. The suspension was stirred periodically to ensure constant mixing. Samples were drawn at regular intervals, the suspended catalyst was removed by filtration and concentrations of carbendazim and diquat remaining in the solution were determined as explained under section 5.2.2. Samples were also drawn for analyzing the  $\text{H}_2\text{O}_2$  present in the system and also for the identification of reaction intermediates at specified time intervals.

## **5.3 Results and Discussion**

### **5.3.1 Preliminary experiments**

Solar photocatalytic decontamination of water containing carbendazim and diquat (CZ=7mg/L, DQ= 7mg/L) using zinc oxide as catalyst (0.2g/L) was investigated under standardized conditions, initially with individual components. As already demonstrated in previous chapters, the method is efficient for the degradation of either of them. However, carbendazim is degraded quickly (100%) in 1hr while it takes about 3 hr in the case of diquat. The degradation of each pollutant, when they are present together

also is tested (Fig. 5.4). The degradation increases with increase in the irradiation time. The rate slows down at later stages of reaction probably due to the formation of intermediates which will compete with the parent molecules for ROS and other interactions.

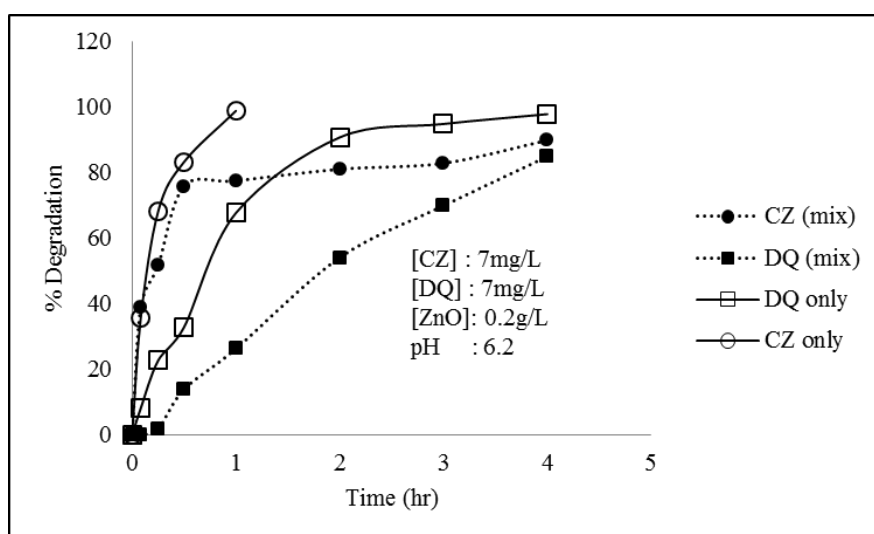


**Fig. 5.4:** Variation in percentage degradation of carbendazim and diquat individually and in combination with time of irradiation during the photocatalytic reaction

In the case of carbendazim, the initial rate of degradation is not affected by the presence of diquat. However, after about 75% degradation, the rate slows down and is stabilized. In the case of diquat, the degradation is severely inhibited in the presence of carbendazim. However, the degradation is not stabilized and proceeds steadily eventually attaining almost the same percentage of degradation after 4 hr. Initially the degradation of diquat is practically negligible in presence of carbendazim, at least until about 25% of the latter is degraded. Thereafter the degradation of diquat also starts and proceeds concurrently. No degradation of either is observed in

presence of sunlight but without catalyst. The experiment conducted in dark with and without catalyst also has not shown any degradation (Fig. 5.5). Hence both light and catalyst are essential for the degradation. The adsorption of carbendazim and diquat is negligible when tested individually. When the adsorption of the components is tested using a combination of the two at equimolar concentration, no adsorption of either is observed on the surface of ZnO, just as in the case of individual components. Hence there is no ‘assisted’ adsorption in this case as is observed in our laboratory in the case of certain hydrocarbons.

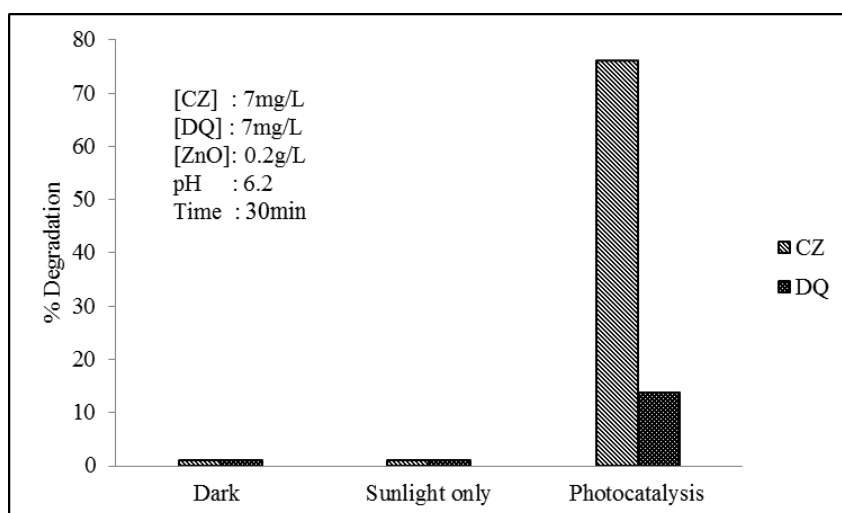


**Fig. 5.5:** Degradation of diquat and carbendazim in combination under various conditions

The influence of various reaction parameters on the removal of the combination of pollutants is investigated and the results are presented below.

### 5.3.2 Effect of catalyst loading

The effect of catalyst loading on the degradation of carbendazim and diquat in their mixture is investigated by varying the loading of ZnO (0.1-0.8g/L) keeping other parameters constant. The rate of degradation of both substrates, individually as well as in presence of one another, at various catalyst loadings is experimentally evaluated and the results are plotted in Figs. 5.6 and 5.7. In the case of carbendazim the degradation is inhibited in presence of diquat. After reaching the optimum loading (0.4g/L) no further increase in the reaction rate is observed. In the absence of diquat, the optimum dosage for the degradation of carbendazim is 0.1g/L. In the case of diquat, in presence of carbendazim, the degradation which was very slow initially, pick up momentum and stabilizes at 0.6g/L. The optimum is same in the absence of carbendazim also (Fig. 5.7), even though the rate in this case is much higher compared to that in the presence of carbendazim.

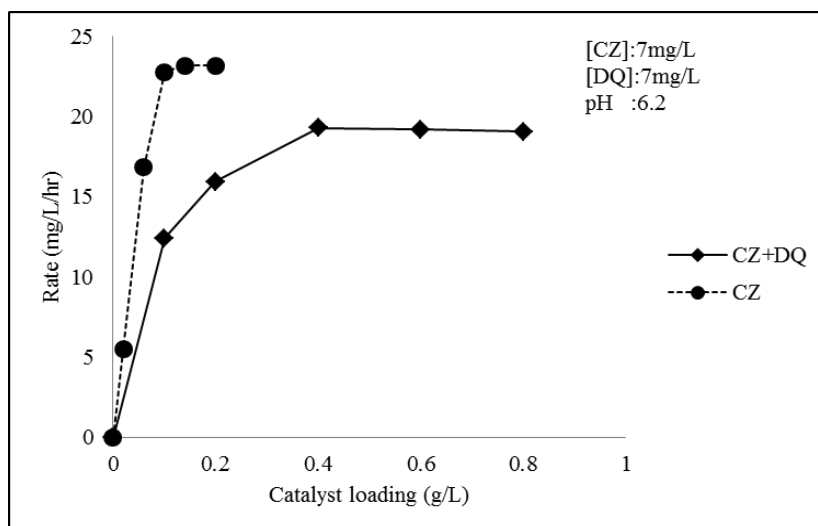


**Fig. 5.6:** Effect of catalyst dosage on the rate of degradation of carbendazim in presence and absence of diquat

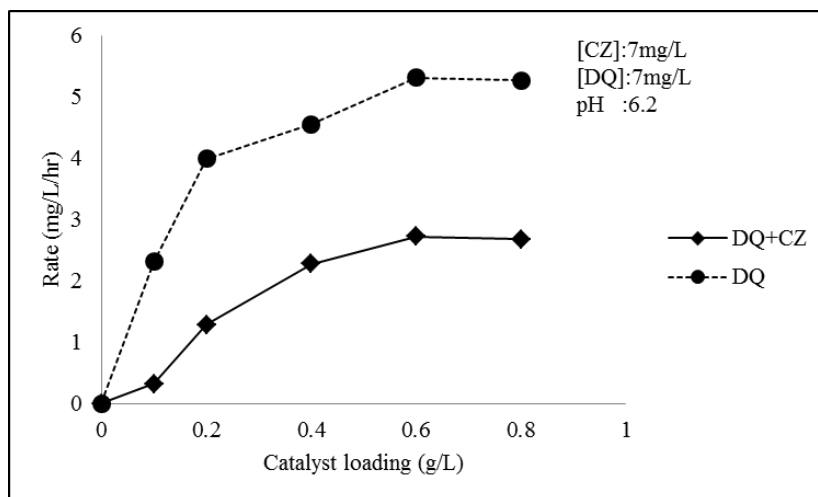


**Fig. 5.7:** Effect of catalyst dosage on the rate of degradation of diquat in presence and in the absence of carbendazim

The observed trend in the ‘effect of catalyst dosage on the degradation rate’ in the case of both components is more or less similar to many photocatalytic systems already reported in literature. The optimum loading of catalyst depends on many factors such as the nature of the catalyst, substrate, presence of other components, geometry of the reactor and irradiation source. Further increase in the catalyst loading above the optimum dosage has no effect on the degradation rate. The rate of degradation slows down with increase in catalyst loading and is stabilized eventually. The stabilization effect is attributed to a number of factors such as hindrance or the scattering of the incident radiation by ZnO, limitation in the availability of ROS as well as various other factors which are already discussed in earlier chapters. The collision between the photo-excited ZnO with the ground state catalyst is also resulting in the deactivation at higher loading.

The competition between carbendazim and diquat for the catalyst surface sites and/or the ROS generated in-situ is evident in the lower degradation rate of either in presence of the other at all catalyst loadings. The reactivity of carbendazim is much more compared to diquat. But the increasing trend in degradation with catalyst dosage continues for both the substrates irrespective of the competition for the ROS. As the catalyst loading increases, more active species are generated which facilitate the degradation of carbendazim and diquat. Once a substantial part of carbendazim is degraded, the competition is less and the rate of degradation of diquat is accelerated (Fig. 5.7). Since the rate of degradation of diquat is slower more catalyst sites are required to sustain the degradation. Hence the optimum ZnO loading is more in this case compared to carbendazim.

### 5.3.3 Effect of initial concentration, Kinetics

To investigate the effect of initial concentration of carbendazim and diquat in the mixed system on the respective degradation kinetics, studies are conducted by varying the concentration of one component carbendazim [in this case (3-9mg/L)] keeping the diquat concentration (7mg/L) and other reaction parameters constant. Another set of experiments were conducted by varying the initial concentration of diquat (3-16mg/L) and keeping carbendazim concentration (7mg/L) and other reaction parameters constant. The optimum catalyst dosage for carbendazim/diquat mixed system is 0.4g/L based on the results in section 5.3.2. At this particular loading the percentage degradation of carbendazim at 15 min is ~80% when it is the lone compound and ~ 75% in presence of diquat.

However, to study the reaction rate and kinetics of degradation, it is better to follow the reaction at lower conversion ranges. At lower conversion the number as well as the concentration of intermediates formed during the reaction will be minimum and hence the interference from these also will be minimal. The percentage degradation of diquat at lower catalyst dosage is very low compared to the degradation of carbendazim. Considering these factors, the catalyst dosage is fixed at 0.2g/L for further studies, keeping other parameters constant.

The percentage degradation of carbendazim in presence of diquat and that of diquat in presence of carbendazim at different concentrations of the variable component is shown in Figs. 5.8 and 5.9 respectively. As expected, the percentage degradation decreases with increasing concentration of respective substrates.

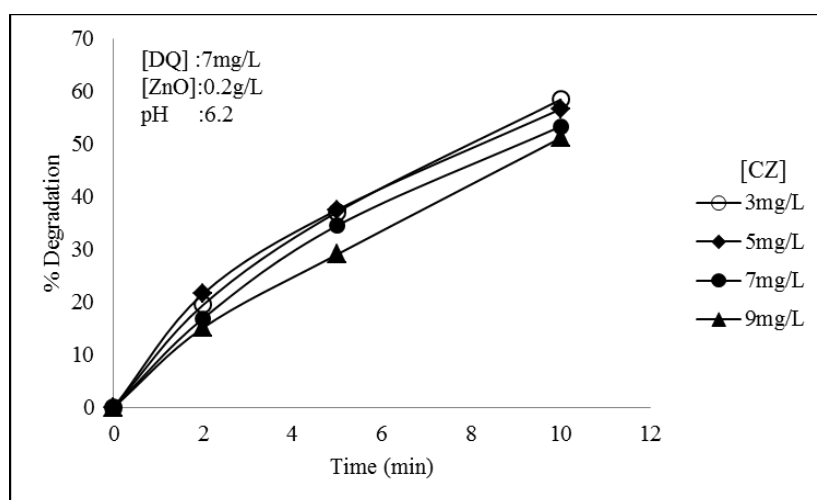


**Fig. 5.8:** Percentage degradation of carbendazim at different initial concentrations in presence of diquat

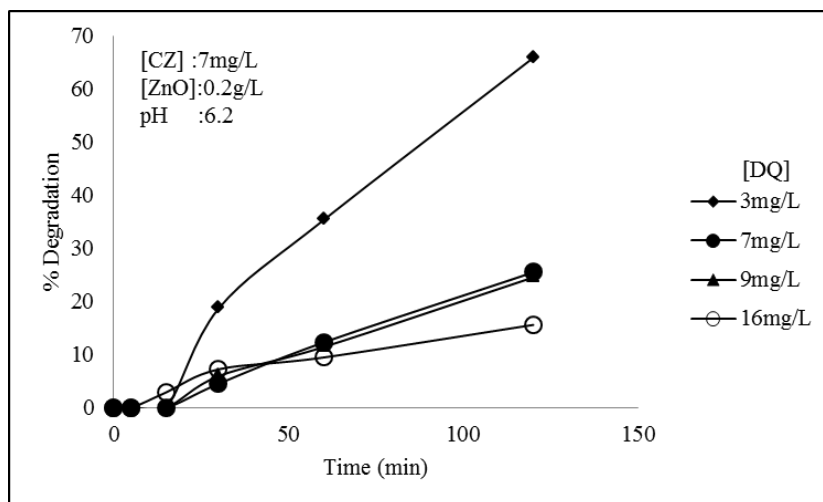


**Fig. 5.9:** Percentage degradation of diquat at different initial concentrations in presence of carbendazim

In both cases, it is observed that the rate of degradation increases with increase in the concentration of respective substrate (Figs. 5.10 and 5.11). The degradation of carbendazim proceeds smoother at all concentrations. However, in presence of carbendazim the degradation of diquat proceeds at reasonable rates only after ~50% of carbendazim is degraded (Fig. 5.4). At normal pH of 6.2 of this combination system, carbendazim is in the neutral form and can easily come in the proximity of positively charged ZnO surface, compared to the doubly positive charged diquat which may get repelled. As shown earlier, this may be a major reason for the slower degradation rate of diquat in presence of carbendazim.

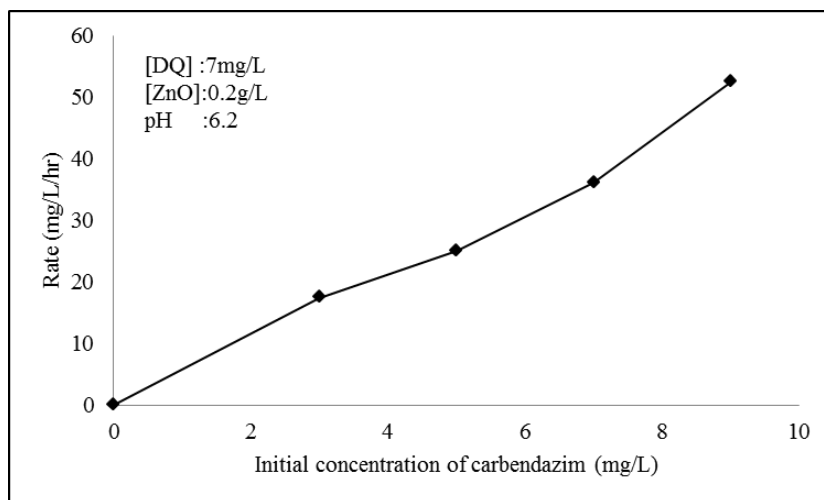


**Fig. 5.10:** Effect of initial concentration of carbendazim on its photocatalytic degradation rate in presence of diquat

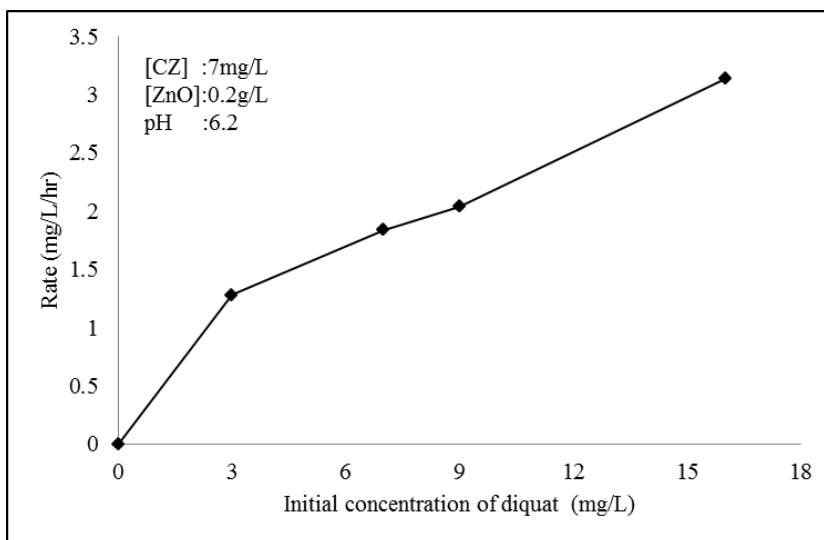


**Fig. 5.11:** Effect of initial concentration of diquat on its photocatalytic degradation rate in presence of carbendazim

Photocatalytic degradation of most of the organic contaminants in water follows pseudo first order kinetics and modified Langmuir-Hinshelwood model (L-H model) as explained earlier. For both the pollutants used in the current study, in their pure form, the kinetics follows the L-H model which is based on the assumptions that reaction is in dynamic equilibrium and there is no competition between the substrate and the reaction intermediates for the surface sites. In the present case of combination of the two substrates, there is competition between them for the reactive free radicals from the beginning itself. However, since the adsorption is relatively negligible in both cases, it may be presumed that the model is applicable. Hence the pseudo first order plot of  $\ln(C_0/C)$  vs  $t$  is made for different concentrations of carbendazim (3-7mg/L), keeping the concentration of diquat constant at 7mg/L (Fig. 5.12). Similar plots were made for different concentrations of diquat (3-9mg/L), keeping the concentration of carbendazim at 7mg/L (Fig. 5.13). The plot gives straight lines in the case of both carbendazim and diquat at lower concentration and earlier reaction times in presence of one another. This indicated that the pseudo first order kinetics of degradation is not affected by the presence of the other component at least at lower concentration range when the influence of intermediates is not critical. Since the two components are poor adsorbates on ZnO, it may be presumed that there is no competition between the substrates for the active sites. Hence, the effect of one on the degradation of the other may be due to the competition for the in-situ generated  $\cdot\text{OH}$  and other reactive radicals. In the initial stages the degradation of diquat is suppressed by carbendazim because the latter interacts more effectively with the ROS.

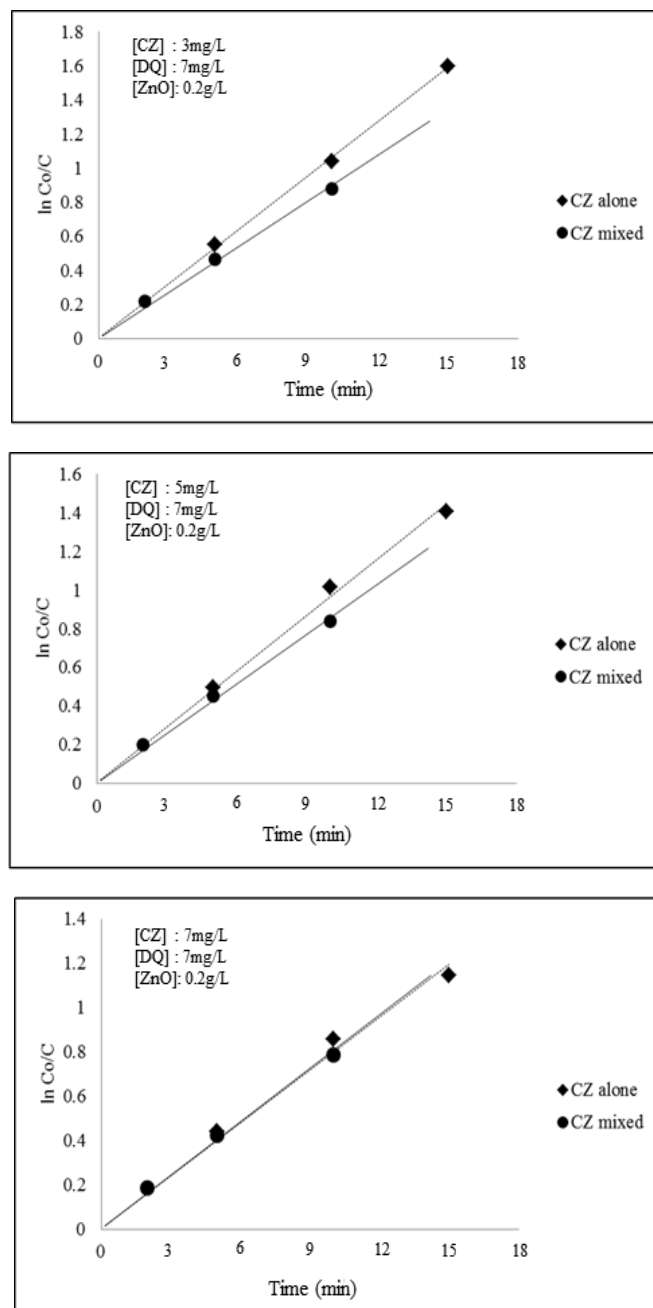


**Fig. 5.12:** Pseudo first order kinetic plot for the degradation of carbendazim at different initial concentrations in the absence and in presence of a fixed concentration of diquat

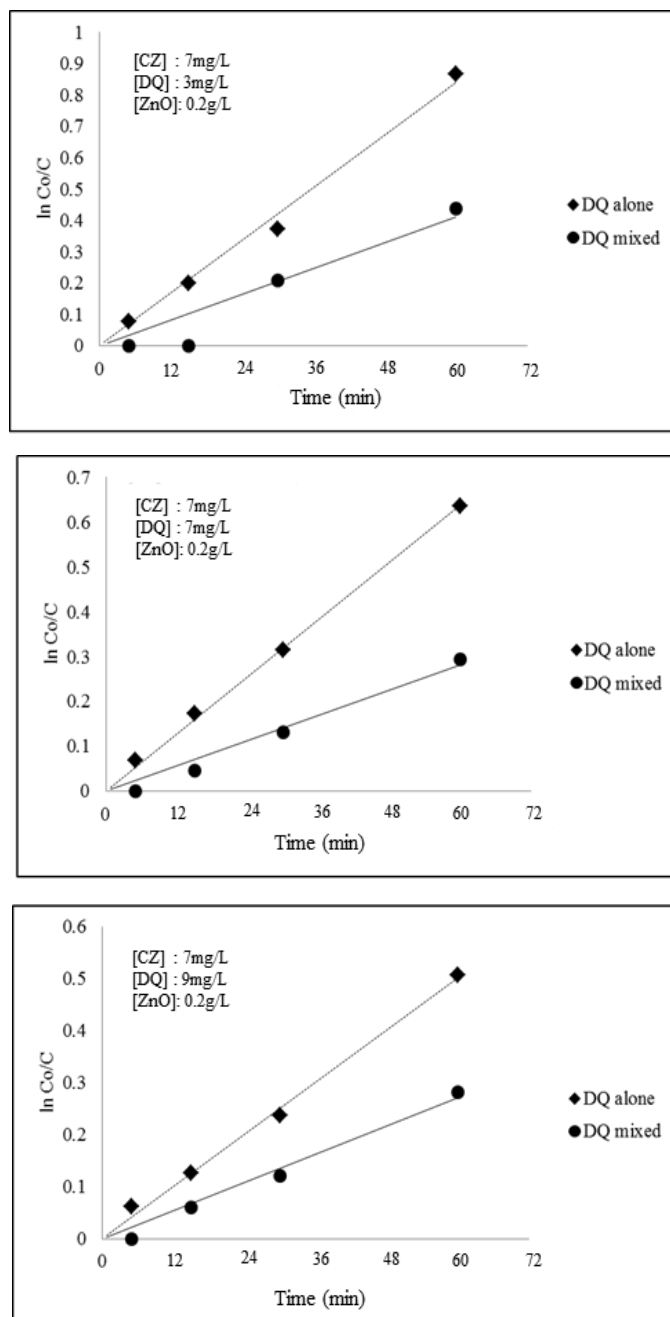


**Fig. 5.13:** Pseudo first order kinetic plot for the degradation of diquat at different initial concentrations in the absence and in presence of a fixed concentration of carbendazim

The degradation of diquat commences only after considerable amount (~50%) of carbendazim is removed from the system. Once the degradation of diquat starts the rate of degradation of carbendazim slows down. Once the degradation of carbendazim is almost complete/stabilised, a sudden increase in the degradation of diquat is observed.

Fig. 5.12 also gives the comparative plot of  $\ln(C_0/C)$  vs  $t$  for carbendazim in the absence of diquat under optimized conditions. As the figure clearly shows, the degradation follows pseudo first order kinetics in the presence as well as absence of diquat. The pseudo first order rate constant is calculated from the slope of the logarithmic plot. The value decreases as the concentration increases (Table 5.1.). The observed rate constant for carbendazim degradation in the mixed system is lower than that for the system containing carbendazim only. But the rate constant values are more or less the same in the presence as well as absence of diquat at higher concentration of carbendazim indicating the dominance of carbendazim in interacting with the ROS. Fig. 5.13 which shows the comparative plot of  $\ln(C_0/C)$  vs  $t$  for diquat in the presence and absence of carbendazim also reveals similar trend.

**Table 5.1:** Pseudo first order rate constants for the photocatalytic degradation of carbendazim over ZnO. pH: 6.2 Temp:  $29 \pm 1^\circ\text{C}$

| Experiment | ZnO (g/L) | Carbendazim (mg/L) | k' (hr <sup>-1</sup> ) |          |
|------------|-----------|--------------------|------------------------|----------|
|            |           |                    | CZ alone               | CZ mixed |
| 1          | 0.2       | 3                  | 6.29                   | 4.95     |
| 2          | 0.2       | 5                  | 5.44                   | 4.74     |
| 3          | 0.2       | 7                  | 4.22                   | 4.49     |

As in the case of carbendazim in this case also, the rate constant for the degradation of diquat in pure form as well as in combination is calculated from the logarithmic plot. The rate constant is higher for the degradation when diquat is treated individually, compared to that when diquat is in combination with carbendazim. But in both cases the rate constant decreases as the concentration of diquat in the system is increased (Table 5.2).

**Table 5.2:** Pseudo first order rate constants for the photocatalytic degradation of diquat over ZnO. pH: 6.2 Temp:  $29 \pm 1^\circ\text{C}$

| Experiment | ZnO (g/L) | Diquat (mg/L) | $k' \times 10^{-1} \text{ (hr}^{-1}\text{)}$ |          |
|------------|-----------|---------------|--|----------|
|            |           |               | DQ alone                                     | DQ mixed |
| 1          | 0.2       | 3             | 8.66   | 5.11     |
| 2          | 0.2       | 7             | 6.16   | 3.24     |
| 3          | 0.2       | 9             | 4.89   | 3.03     |

Validity of L-H model for the reaction at lower concentration ranges is further verified by the inverse plot of  $1/r_0$  vs  $1/C_0$  as shown in Figs. 5.14 and 5.15. The linearity for the degradation of carbendazim in both mixed and pure form in comparable concentration range (3-7mg/L) reconfirms the pseudo first order kinetics. Similar results are obtained in the case of diquat also (concentration range: 3-9mg/L) in both mixed and pure forms (Fig. 5.15) thereby reconfirming the pseudo first order kinetics for its degradation.

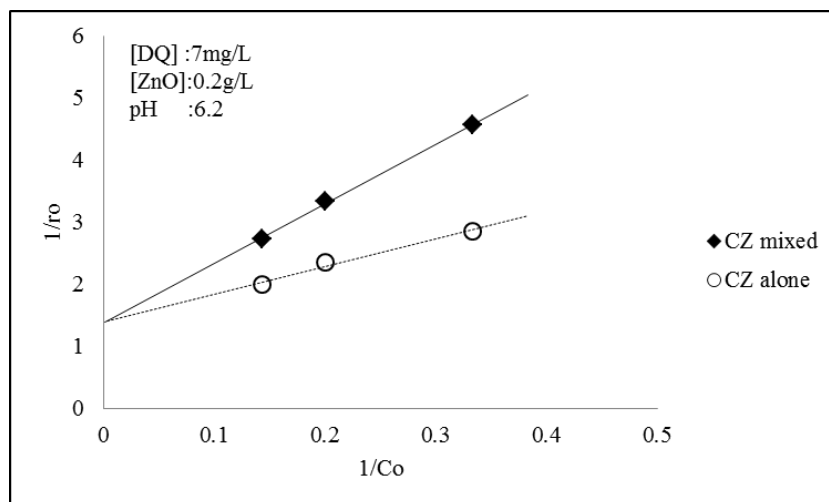


**Fig. 5.14:** Reciprocal plot of initial rate of degradation of carbendazim versus its initial concentration

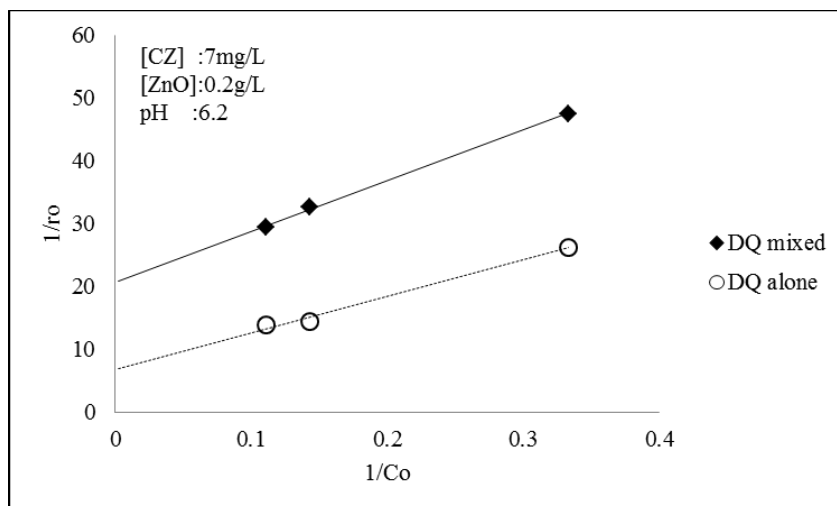


**Fig. 5.15:** Reciprocal plot of initial rate of degradation of diquat versus its initial concentration

### 5.3.4 Effect of pH

As explained earlier, the pH of the reaction medium has significant role in the photocatalytic degradation of organic compounds in solution. The physico-chemical nature of both substrate and catalyst varies as the pH of the solution changes. The extent of electrostatic repulsion or attraction of substrates on the catalyst surface as well as the rate of generation of reactive free radicals depends on the pH of the reaction medium. In the case of systems containing multiple reactants one or more of the compounds present can be preferentially adsorbed on the catalyst depending on the net electronic charge of the substrate and the catalyst surface. As the solution pH changes, the adsorption of the substrate as well as the in-situ formed intermediates on the catalyst surface may get modified thereby affecting the overall rate of the reaction. In this context, the effect of pH on the photocatalytic degradation of carbendazim/diquat combination is investigated by varying the solution pH keeping other parameters unchanged. Preferential adsorption of diquat or carbendazim is not observed at any solution pH. The effect of pH on the degradation of carbendazim in presence of diquat is given in the Fig. 5.16. Similarly, the effect of pH on the degradation of diquat in presence of carbendazim is given in Fig. 5.17. At very low pH (<3) the photocatalytic degradation of carbendazim is less. As the solution pH increases the percentage degradation also increases and then gets stabilized above pH 5.0. Only negligible reduction is observed in the carbendazim concentration in the parallel reaction conducted in dark with and without catalyst. The lower degradation rate of carbendazim at extreme acidic conditions may be due to the electrostatic repulsion between the protonated form of carbendazim

and the positively charged catalyst surface. Also the ROS generated at low pH range is very less due to ZnO corrosion. Above pH 4.0 carbendazim is in the neutral form and can easily access the catalyst surface or be in close proximity to the surface which mainly contributes to the increase in the percentage degradation. The trend of pH effect remains the same in the presence as well as absence of diquat. The relatively lower degradation in presence of diquat can be attributed to the competition between the two substrates for ROS. In the case of diquat, the sudden increase in the percentage degradation at alkaline pH is due to its hydrolysis as explained earlier. No degradation is observed for diquat in the low pH range in the dark, with or without catalyst (Fig. 5.17).

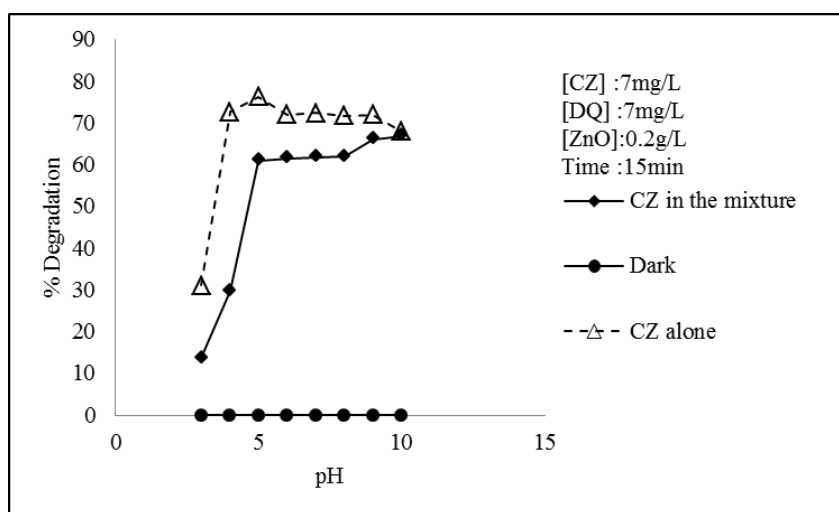


**Fig. 5.16:** Effect of pH on the degradation of carbendazim independently and in combination with diquat (7mg/L) under photocatalysis

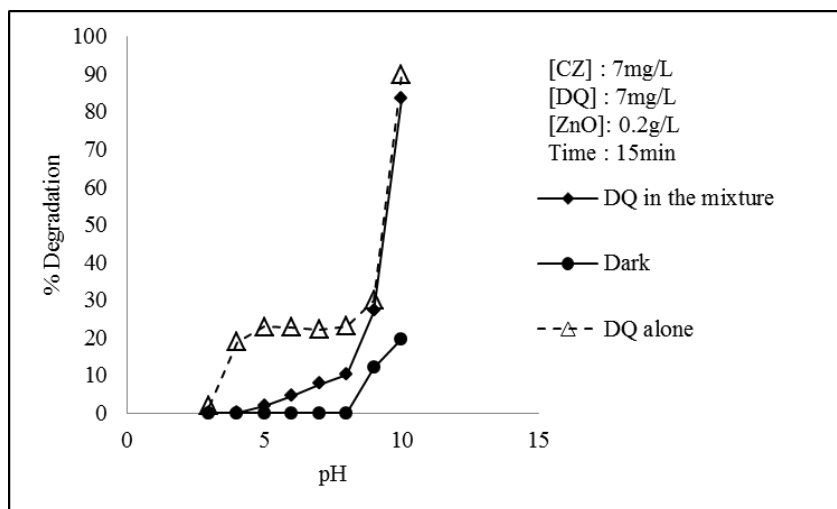


**Fig. 5.17:** Effect of pH on the degradation of diquat independently and in combination with carbendazim (7mg/L) under photocatalysis

As already noticed, the degradation rate of diquat in the initial stages is inhibited in presence of carbendazim up to pH ~9. In the acidic pH range, the degradation of diquat becomes significant only after carbendazim concentration has diminished substantially. No degradation of diquat is observed in presence of carbendazim at pH below 5. As the solution pH increases the percentage degradation/hydrolysis also increases. The degradation due to hydrolysis is evident from the experiments conducted in the dark. The combined effect of the presence of highly reactive carbendazim and the corrosion of ZnO plays a key role in the poor photocatalytic degradation of diquat in the low pH ranges. The diquat degradation picks up momentum as the carbendazim concentration decreases with time. The inhibiting effect of carbendazim is noticeable at all pH ranges selected for the study.

At higher pH (>9) the ZnO surface is negatively charged, since the PZC of ZnO is approx. 9.3. At this pH>9 the positively charged diquat can approach the catalyst surface which increases the interaction with the surface generated ROS and consequently, the percentage degradation. Together with the alkaline hydrolysis, the degradation of diquat will be higher at higher pH, so much so that the degradation is more or less the same in the presence as well as absence of carbendazim. In the mixed system also, the pH effect on the photocatalytic degradation rate of carbendazim and diquat is the same as in the case of individual system even though there is quantitative difference. As explained earlier, the competition for the in-situ generated reactive species between carbendazim and diquat and also the in-situ formed intermediates from both of them is responsible for the lower degradation of both components in presence of each other.

### **5.3.5 Effect of oxidants**

Previous chapters have shown that certain oxidants such as H<sub>2</sub>O<sub>2</sub> and S<sub>2</sub>O<sub>8</sub><sup>2-</sup> can act as electron scavengers and thereby enhance the photocatalytic degradation rate of organic pollutants by preventing the electron-hole recombination. Both detrimental and enhancing nature of H<sub>2</sub>O<sub>2</sub> are reported in many photocatalysis studies. In photocatalytic systems containing more than one component, the effect of these oxidants may be different from that in the case of individual components, which will depend on the chemical nature of the reactants as well as the intermolecular interaction. In this context, the effect of oxidants on the degradation of carbendazim and diquat, when they are present together, is

tested using  $\text{H}_2\text{O}_2$  and  $\text{S}_2\text{O}_8^{2-}$ . Fig. 5.18 shows the effect of these oxidants on the photocatalytic degradation of carbendazim (7mg/L) in presence of 7mg/L diquat. As mentioned earlier, carbendazim is a fast degrading molecule and hence the effect of  $\text{H}_2\text{O}_2$  and  $\text{S}_2\text{O}_8^{2-}$  on the degradation is not quite distinct. In the case of slow degrading diquat also the oxidants  $\text{H}_2\text{O}_2$  and  $\text{S}_2\text{O}_8^{2-}$  show mild inhibition or 'nil' effect (Fig. 5.19).

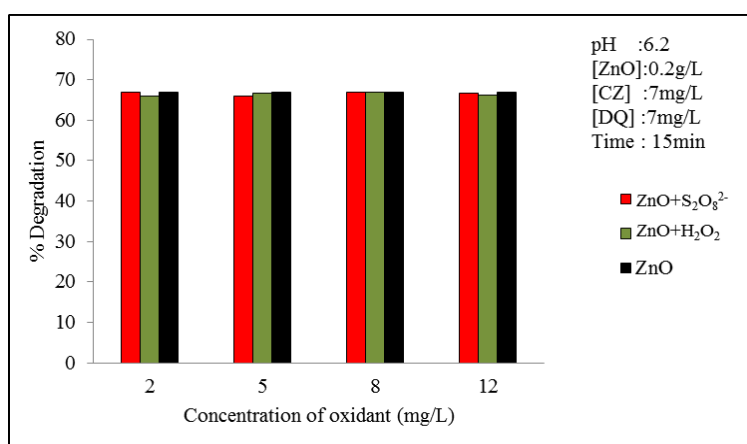


**Fig. 5.18:** Effect of  $\text{H}_2\text{O}_2$  and persulphate on the photocatalytic degradation of carbendazim in presence of diquat

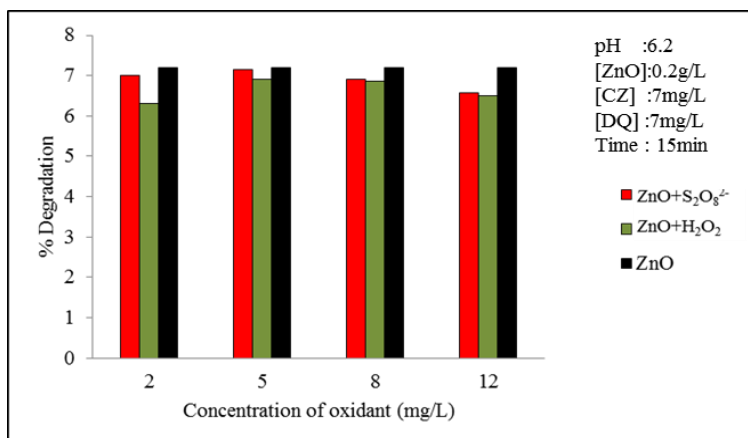


**Fig. 5.19:** Effect of  $\text{H}_2\text{O}_2$  and persulphate on the photocatalytic degradation of diquat in presence of carbendazim.

The enhancing effect of  $H_2O_2$  on the photocatalytic degradation of many organics has already been reported. But in the case of carbendazim/diquat mixed system, the enhancing effect of  $H_2O_2$  is not seen in the selected concentration range (2-8mg/L) for both components. As already reported, when these two reactants are individually studied in presence of  $H_2O_2$  and persulphate ( $S_2O_8^{2-}$ ) the enhancement in photocatalytic degradation is very small. Comparative effect of  $H_2O_2$  and persulphate on the degradation of diquat and carbendazim when they are present individually as well as in combination is presented in Figs. 5.20-5.23. As the figures show, the effect of oxidants on the degradation carbendazim and diquat is very small in all cases, irrespective of whether the substrates are present individually or in combination. The mild inhibition of the degradation of CZ by DQ and the strong inhibition of the degradation of DQ by CZ also remain practically unaffected by the presence of the oxidants.

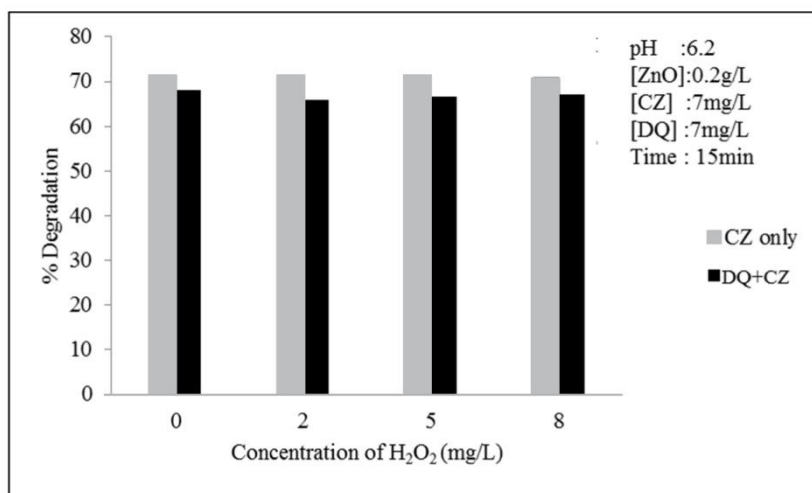


**Fig. 5.20:** Effect of  $H_2O_2$  on the photocatalytic degradation of carbendazim individually as well as in combination with diquat

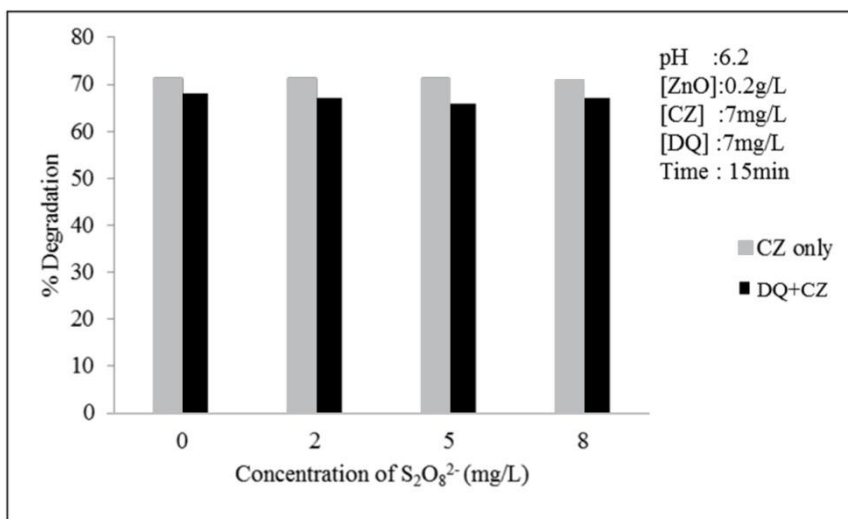


**Fig. 5.21:** Effect of persulphate on the photocatalytic degradation of carbendazim individually as well as in combination with diquat

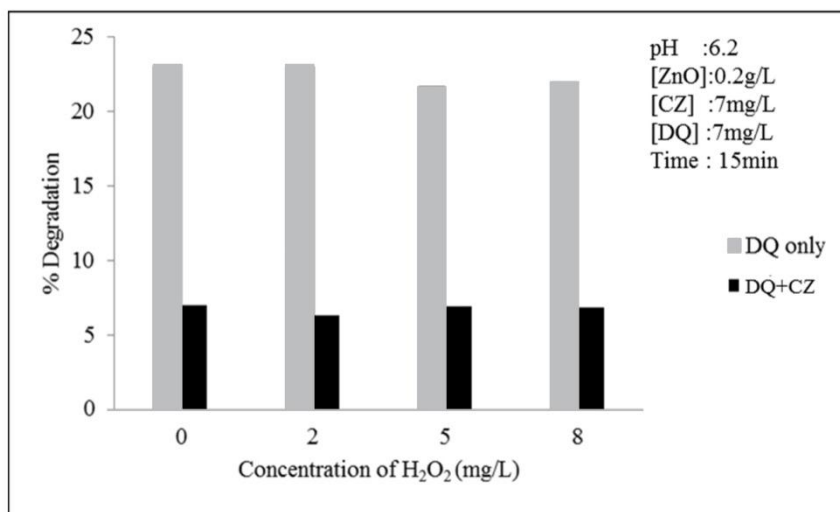


**Fig. 5.22:** Effect of  $H_2O_2$  on the photocatalytic degradation of diquat individually as well as in combination with carbendazim

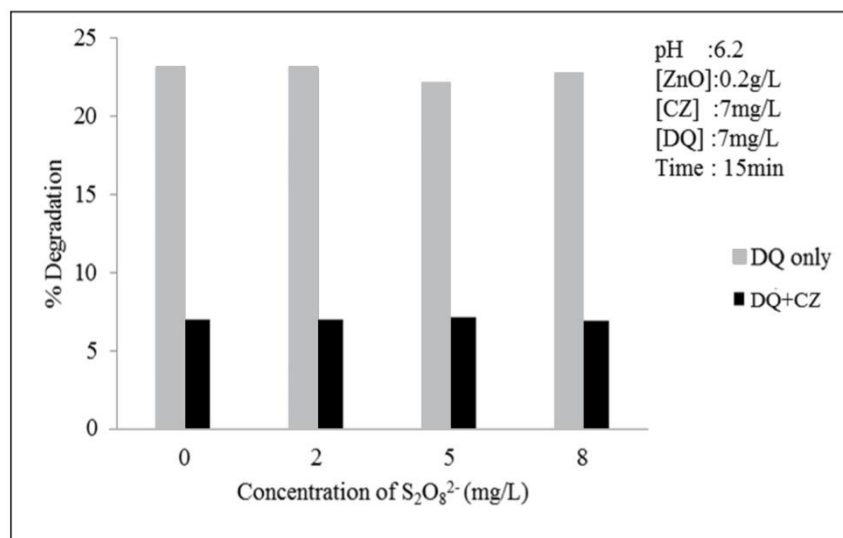


**Fig. 5.23:** Effect of persulphate on the photocatalytic degradation of diquat individually as well as in combination with carbendazim

### 5.3.6 In-situ formation of $H_2O_2$

As in the case of the degradation of diquat and carbendazim independently, the formation of  $H_2O_2$  is noticed also during the photocatalytic degradation of the combination of the two substrates over ZnO.  $H_2O_2$  concentration increases initially, the rate slows down with time and stabilizes thereafter in the case of the diquat/carbendazim mixture as well as the components individually. Even in the case where  $H_2O_2$  is added externally, its concentration does not increase correspondingly or beyond a particular limit. This has been explained as due to the simultaneous formation and decomposition of  $H_2O_2$  under photocatalysis, which results in the phenomenon of oscillation in the concentration of  $H_2O_2$ . However no oscillatory behavior is seen here probably because the formation and decomposition of  $H_2O_2$  balance

each other. The stabilized concentration of  $\text{H}_2\text{O}_2$  is same in the case of the system with and without added  $\text{H}_2\text{O}_2$ . This suggests that every system has an optimum concentration of  $\text{H}_2\text{O}_2$  at which the rate of formation and decomposition can be more or less same.

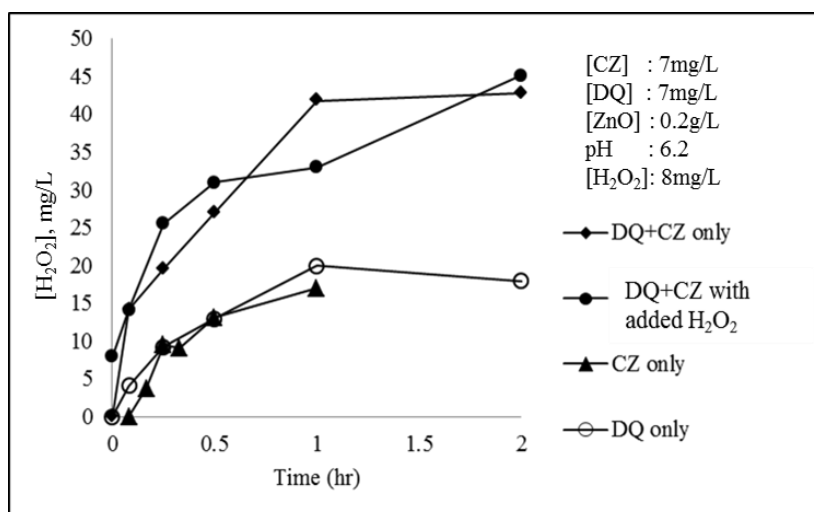


**Fig. 5.24:** Formation of  $\text{H}_2\text{O}_2$  during the photocatalytic degradation of diquat/carbendazim, independently and in combination and also in presence of added  $\text{H}_2\text{O}_2$

### 5.3.7 Effect of common inorganic anions and cations

It has been proven earlier that the presence of different inorganic salts in water can interfere with the photocatalytic degradation of organic pollutants. Natural water contains various inorganic salts in dissolved form. The effect of these salts will be the net effect of the respective anion and cation of those salts and will depend upon the nature of catalyst, pH, the reactant as well as other components present. To study the effect of commonly present anions and cations in natural

water on the photocatalytic degradation of carbendazim/diquat mixed system, experiments were conducted with different concentrations of selected cations and anions.

The effect of various anions on the degradation of diquat and carbendazim is studied at different concentrations of the salts. The cation is kept the same i.e.  $\text{Na}^+$  which, as seen from the results in previous chapters, does not have any effect on the rate of degradation of the pollutants. As in the 'carbendazim alone' system, the  $\text{HPO}_4^{2-}$  inhibits the degradation. In the case of the mixture of carbendazim and diquat also,  $\text{HPO}_4^{2-}$  is a strong inhibitor of the degradation of carbendazim and inhibition increases with increasing concentration of the anion (Figs. 5.25 and 5.26), similar to the observations made when carbendazim was subjected to photocatalysis individually. The effect of other anions is not much significant.

The detrimental effect of  $\text{HPO}_4^{2-}$  on the degradation of organic pollutants is already reported, especially in the case of ZnO as photocatalyst. However in the case of certain substrates such as phenol, the effect of  $\text{HPO}_4^{2-}$  depended on the concentration of the anions and the duration of the reaction, indicating the influence of reaction parameters including in-situ formed intermediates on the anion effect [137].

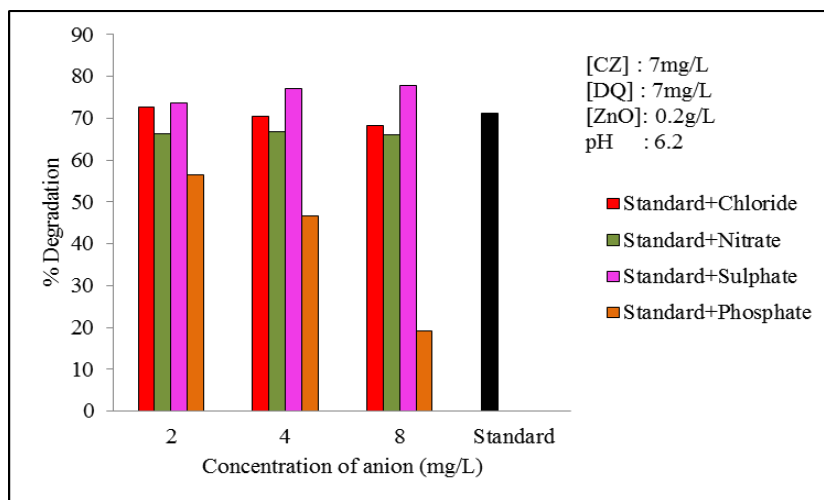


**Fig. 5.25:** Effect of anions on the photocatalytic degradation of carbendazim in the carbendazim/diquat combination [Cation:Na<sup>+</sup>, Irradiation time: 30min]

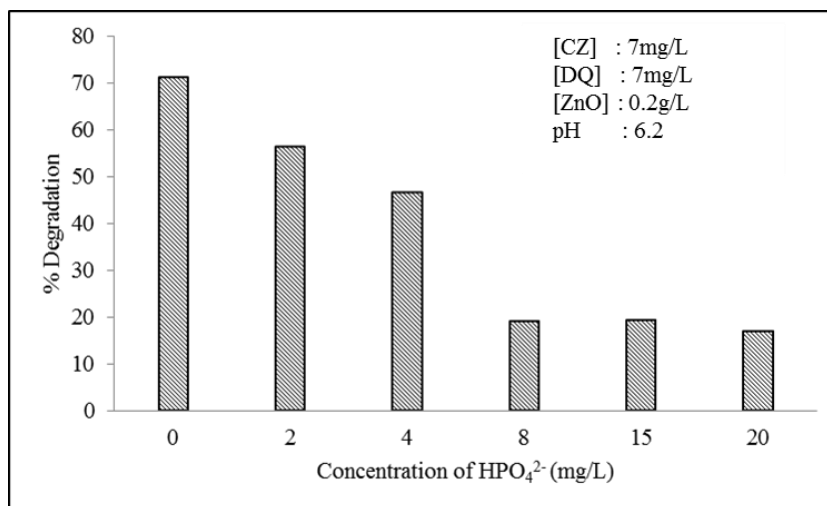


**Fig. 5.26:** Effect of HPO<sub>4</sub><sup>2-</sup> at different concentrations on the photocatalytic degradation of carbendazim in the carbendazim/diquat combination [Cation:Na<sup>+</sup>, Irradiation time: 30min]

In the case of diquat, even when it is present as the diquat/carbendazim mixture, the degradation appeared to be enhanced in presence of  $\text{HPO}_4^{2-}$  (Fig. 5.27). This is similar to the observations made with the system containing only diquat. However as demonstrated earlier, this apparent increase in the removal of diquat is not due to  $\text{HPO}_4^{2-}$ -induced enhancement in the catalytic activity of ZnO or enhanced free radical generation. This is due to the formation of a coloured complex between diquat and  $\text{HPO}_4^{2-}$ . Details are discussed in Chapter 4 section 4.3.8. The effect of increase in the concentration of  $\text{HPO}_4^{2-}$  over a wide range on the disappearance of diquat is shown in the Fig. 5.28. Since the formation of the complex takes place only in presence of ZnO and diquat, it is difficult to delineate the effect from the parallel photocatalytic degradation. Hence the effect of  $\text{HPO}_4^{2-}$  on the photocatalytic degradation of diquat under the current reaction conditions cannot be precisely determined and needs further in-depth investigation.

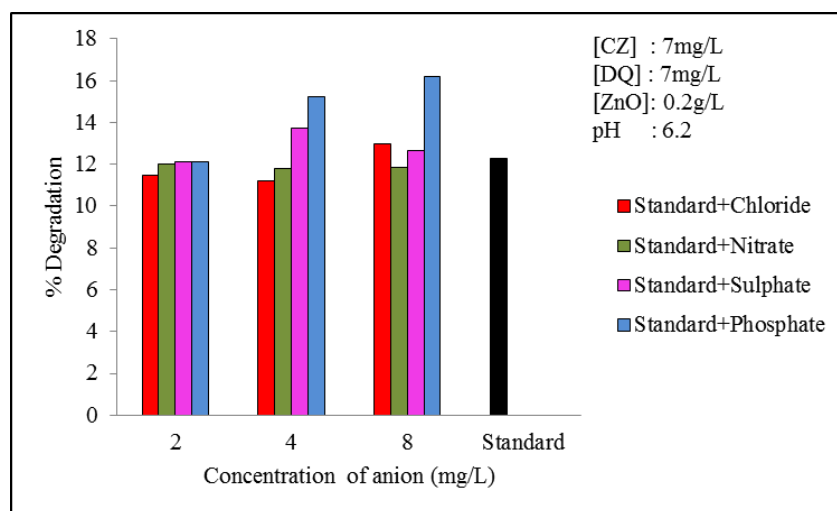


**Fig. 5.27:** Effect of anions on the photocatalytic degradation of diquat [Cation: $\text{Na}^+$ , Irradiation time: 30min] in the diquat/carbendazim combination

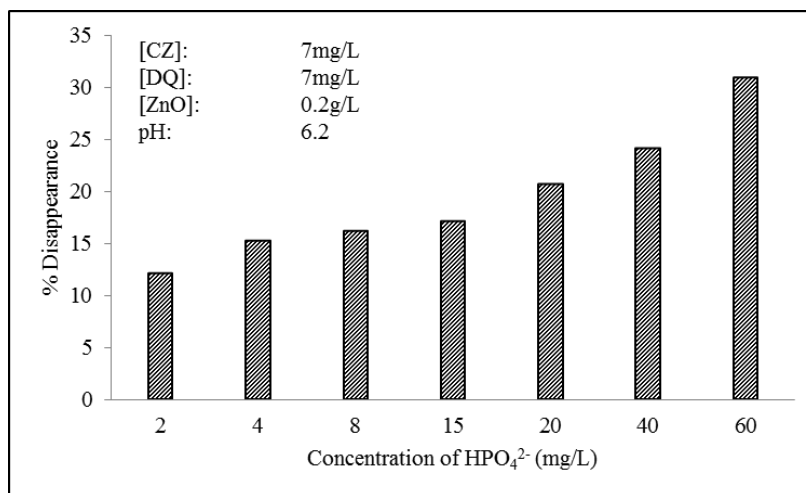


**Fig. 5.28:** Effect of  $\text{HPO}_4^{2-}$  concentration on the photocatalytic disappearance of diquat in the carbendazim/diquat combination [Cation: $\text{Na}^+$ , Irradiation time: 30min]

Figs. 5.29 and 5.30 show the effect of selected cations on the photocatalytic degradation of carbendazim and diquat respectively in the mixed system.  $\text{SO}_4^{2-}$  anion which does not have much effect on the degradation of diquat or carbendazim as demonstrated earlier is chosen for the purpose as the common anion of the salts. Most of the cations do not have any effect on the degradation. However, the degradation is inhibited by  $\text{Al}^{3+}$  and the inhibition increases with increase in the concentration of the salt/cation. In the case of diquat where the degradation is very small, the inhibition by  $\text{Al}^{3+}$  is more significant (Fig. 5.30). At 8mg/L of the salt, the degradation of diquat is almost fully inhibited. Other salts (and hence the respective cations) have very little inhibition at least in the concentration range studied here.

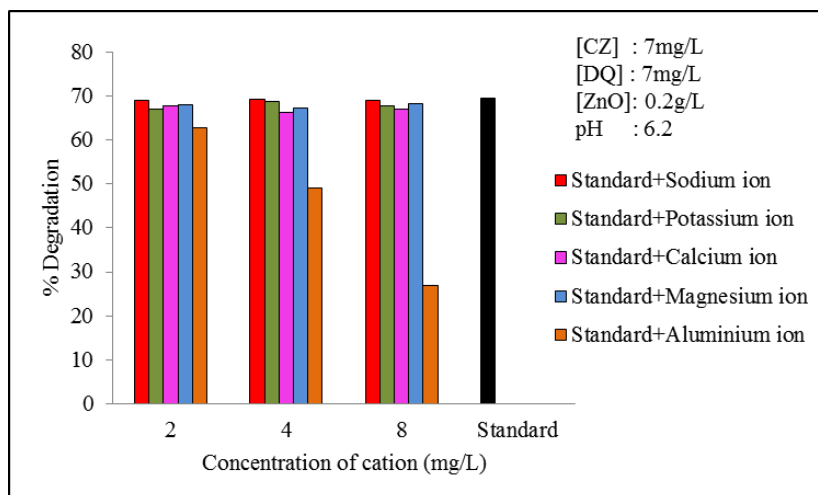


**Fig. 5.29:** Effect of cations on the photocatalytic degradation of carbendazim [Anion:SO<sub>4</sub><sup>2-</sup>, Irradiation time: 30min] in the carbendazim/diquat system

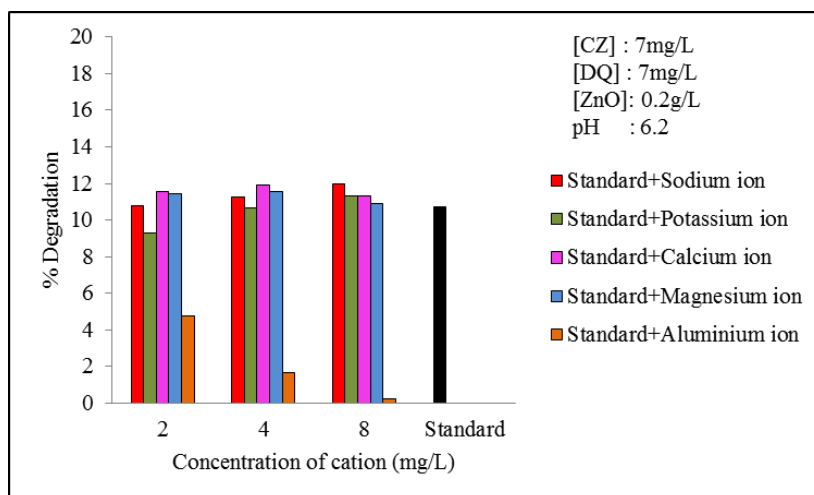


**Fig. 5.30:** Effect of cations on the photocatalytic degradation of diquat [Anion:SO<sub>4</sub><sup>2-</sup>, Irradiation time: 30min] in the diquat/carbendazim system

As reported in previous chapters, all the selected cations except aluminum have negligible effect on the degradation of carbendazim and diquat in the selected concentration range. The detrimental effect of aluminum is primarily due to adsorption  $\text{Al}^{3+}$  on the surface of ZnO. The adsorption of aluminium ion is confirmed by ICP analysis of the  $\text{Al}^{3+}$  solution before and after the addition of ZnO to it (Chapter 4 section 4.3.8). The coverage of aluminum ions on the surface of the catalyst hinders the generation of ROS by blocking the surface sites from the incident radiation. The experiment conducted with the TPA system also shows suppression of the generation of  $\cdot\text{OH}$  radical by  $\text{Al}^{3+}$  (Chapter 3 section 3.3.7). In short, the effect of salts (anions/cations) on the photocatalytic degradation of diquat and carbendazim remains the same irrespective of whether the two pollutants are present individually or in combination.

### 5.3.8 Effect of oxygen

In the carbendazim/diquat mixed system also the effect of oxygen is studied by deaerating the system with  $\text{N}_2$  and carrying out the photocatalytic reaction under optimized conditions. In the case of carbendazim it is observed that (Fig. 5.31) the percentage degradation is less in the absence of oxygen. As already mentioned the reaction with the ROS and carbendazim is very fast and hence, the available dissolved/adsorbed oxygen which is difficult to be removed completely by purging with nitrogen, contributes to the degradation of carbendazim in the initial stage. As the reaction proceeds, this residual oxygen will get fully consumed and the degradation ceases. But in the case of diquat which is a slow degrading

compound, complete suppression of the reaction is observed. Even under normal reaction conditions in the case of the mixture of carbendazim and diquat, as reported earlier, the diquat degradation starts only after half of the carbendazim has degraded. In the deaerated system the removal efficiency is very low and the complete suppression of diquat degradation is expected, since the available O<sub>2</sub> is fully consumed by the carbendazim in the beginning itself. Thus it is reconfirmed that the presence of oxygen is essential for the photocatalytic degradation of pollutants from water using ZnO as catalyst, irrespective of the chemical nature of the pollutants.

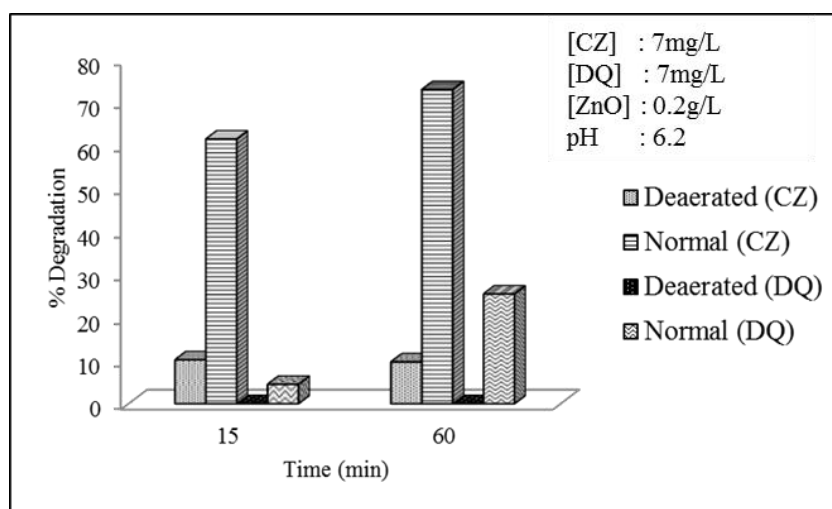


**Fig. 5.31:** Effect of deaeration with N<sub>2</sub> on the photocatalytic degradation of carbendazim/diquat system

### 5.3.9 Mineralization process

The effectiveness of the removal of any organic chemical pollutant from water depends on the complete removal of pollutants as well as their

degradation intermediates. For this, the pollutants must be fully transformed into harmless  $\text{CO}_2$ ,  $\text{H}_2\text{O}$  and salts. For the mixed system with many components, the number of intermediates formed also will be more. The half-life of these intermediates will vary with the reaction conditions and also the chemical nature of the components. Even after the basic pollutants are completely removed, some of the intermediates can persist for longer time which limits the efficiency of the treatment method. To study the mineralization process of the carbendazim/diquat system, experiments were conducted under the optimized conditions discussed earlier. The degree of mineralization with time is followed by measuring the TOC content at different times of irradiation. Fig. 5.32 shows the results.

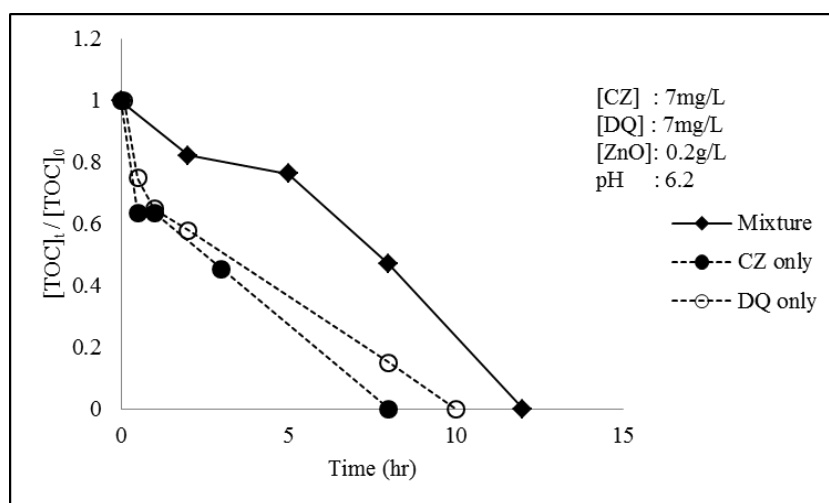


**Fig. 5.32:** Depletion in the TOC content with time of irradiation during the solar photocatalytic degradation of diquat/carbendazim combination

The TOC gradually decreases as the reaction proceeds, stabilizes for a while and then eventually reaches zero. The complete mineralization of carbendazim and diquat occurs after 12 hr irradiation which confirms that the intermediates formed also get mineralized under the solar photocatalytic condition. Comparison of the mineralization of systems with only carbendazim or diquat individually is also shown in the figure. The time taken for complete mineralization is more for the carbendazim/diquat mixture. However, it is less than the sum of the times taken by individual components, thereby suggesting the possibility of a kind of synergy at least in terms of time.

#### **5.3.10 Identification of intermediates**

The reaction intermediates which are formed during the photocatalytic degradation of the combination of carbendazim and diquat are identified by LC/MS. Fig. 5.33 shows the mass spectra of the intermediates formed during the photocatalytic reaction after 1hr of solar irradiation. The complete conversion of carbendazim at this stage can be confirmed by the disappearance of peak at  $m/z$  192 which corresponds to carbendazim. The strong peak at  $m/z$  =118 may be the most stable reaction intermediate of carbendazim. The  $m/z$  at 183 confirms the presence of diquat in the system at this stage. The presence of hydrolysed product of diquatmonopyridone at  $m/z$  =217 also confirms the photocatalytic cleavage of diquat. The presence of many of these intermediates formed from the mixture of carbendazim and diquat is also detected when the two reactants are subjected to photocatalysis individually. This indicates the similarity in the pathway for the

photocatalytic degradation of carbendazim and diquat in the mixed condition as well as individually.

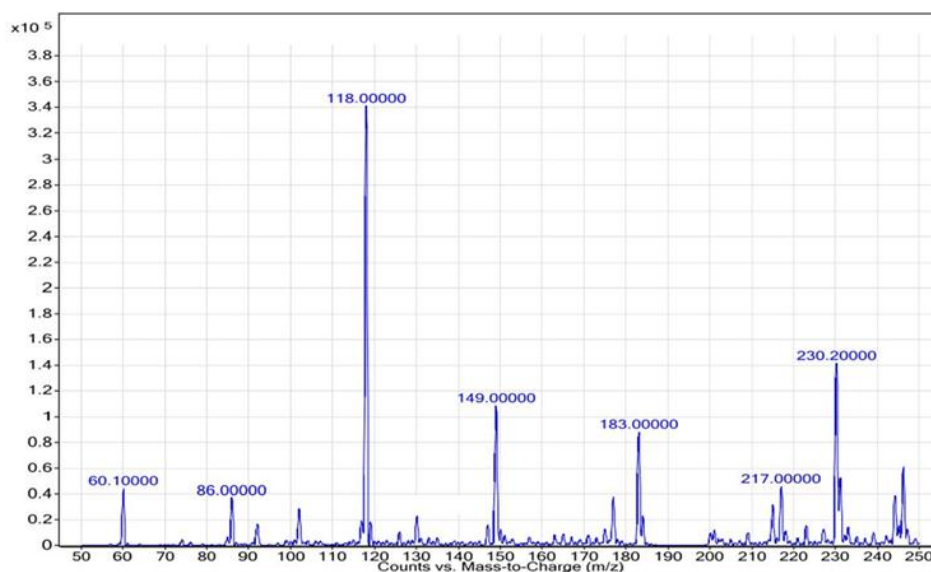
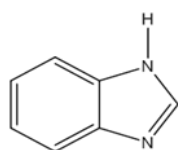
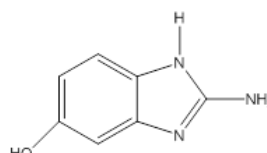


**Fig. 5.33:** Mass spectra of degradation products formed during the photocatalytic degradation of the mixture of diquat and carbendazim after 1hr irradiation

The following major intermediates in the carbendazim/diquat combination after 1hr irradiation are presumably from carbendazim.

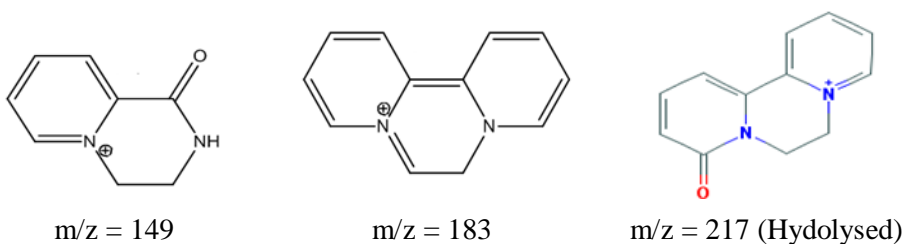


m/z = 118



m/z = 149

Similarly, the following intermediates observed during the photocatalytic degradation may be from diquat:



Since the photocatalytic degradation of the combination carbendazim and diquat is likely to yield a number of intermediates before ultimate mineralization, intensive investigations are needed to identify all of them. Since such an investigation is beyond the scope of the current study, only the most likely intermediates are listed here. In any case detailed investigation on the nature and chemistry of the intermediates will throw more light on the mechanism of the process.

#### **5.4 Mechanism of the photocatalytic degradation of carbendazim/diquat mixture**

Since most of the intermediates identified during the reaction of the carbendazim/diquat mixture over ZnO are similar to those from the photocatalytic degradation of carbendazim and diquat individually, it may be concluded that the reaction mechanism also will be similar to those explained in Chapters 3 & 4 (section 3.4 and 4.4). The relatively lower rate in the degradation of the two components in combination under different conditions is explained earlier in respective sections based on the competition between them for reactive oxygen species and other free radicals.

## 5.5 Conclusion

Sunlight induced photocatalysis in presence of ZnO is proven to be effective for the complete mineralization of small amounts of carbendazim/diquat combination present in water. The degradation in the case of each pollutant follows pseudo first order kinetics even in the combination. Added oxidants such as H<sub>2</sub>O<sub>2</sub> and persulphate (in the selected concentration range) show practically 'nil' effect on the photocatalytic degradation. The effect of various salts likely to be present in water on the rate of degradation is investigated and analysed in terms of respective anions and cations. Cations such as Na<sup>+</sup>, K<sup>+</sup>, Ca<sup>2+</sup> and Mg<sup>2+</sup> have no effect, while Al<sup>3+</sup> inhibits the degradation. Similarly anions such as Cl<sup>-</sup>, SO<sub>4</sub><sup>2-</sup> and NO<sub>3</sub><sup>-</sup> have no effect on the degradation of both carbendazim and diquat. However, HPO<sub>4</sub><sup>2-</sup> inhibits the degradation of carbendazim. HPO<sub>4</sub><sup>2-</sup> forms an intermediate complex with diquat which leads to a decrease in the concentration of the latter giving the false impression of degradation. This makes a systematic study of the effect of this anion on the photocatalytic degradation of diquat difficult. However, eventually both pollutants get completely mineralized in about 12 hr. The study reconfirms that photocatalysis induced by sunlight and mediated by ZnO is an efficient method for the decontamination of water from diquat and carbendazim.

.....✻.....

**SOLAR PHOTOCATALYSIS MEDIATED BY ZnO FOR THE  
REMOVAL OF CARBENDAZIM FORMULATION  
FROM WATER**

|                 |  |
|-----------------|--|
| <b>Contents</b> | 6.1 <i>Introduction</i>  |
|                 | 6.2 <i>Experimental</i>  |
|                 | 6.3 <i>Results and discussion</i>                              |
|                 | 6.4 <i>Mechanism of the photocatalytic degradation of CZ-F</i> |
|                 | 6.5 <i>Conclusion</i>  |

**6.1 Introduction**

Carbendazim in wettable powder (WP) form is its most widely used formulation. Wettable powder does not dissolve in water. When mixed with water, it forms a suspension. When this formulation is sprayed on the target, 100% of the active ingredients are left on the surface, while other forms like emulsifiable concentrate will get partially absorbed or evaporated. A typical wettable powder formulation consists of the active ingredient combined with wetting agents, dispersing agents and sometimes bulking agents and stabilizers.

After the detailed investigation on the solar photocatalytic degradation of the active ingredient carbendazim in pure form (reported in Chapter 3) as well as in combination with diquat (Chapter 5), the influence of various formulation adjuvants on the degradation is examined. Since pesticides

are normally applied as formulations in the field, the rate of degradation of the formulations is more relevant from the environmental angle. In this chapter, the result of our study on the solar photocatalytic degradation of carbendazim W.P formulation in water is discussed. Typical carbendazim wettable powder formulation contains additives such as alkyl aryl sulphonates, alkyl naphthyl sulphonates, carboxy methyl cellulose (CMC) and china clay. The added ingredients can influence the environmental degradation of carbendazim in presence of sunlight. Various process parameters that can affect the photocatalytic degradation of WP formulation are evaluated in detail and optimum conditions are identified.

Carbendazim in its pure form (technical) is represented as CZ and the formulated form is represented as CZ-F throughout this chapter.

## **6.2 Experimental**

### **6.2.1 Chemicals**

Commercially available carbendazim 50% wettable powder (trade name: Tagstin) formulation manufactured by Tropical agro system India Pvt. Ltd. was used for the study. The chemical composition as declared by the manufacturer consists of carbendazim technical 51% w/w (based on 98% A.I. w/w), alkyl aryl sulphonate 2% w/w, alkyl naphthyl sulphonate 2% w/w, CMC/Glu 2% w/w and china clay 43% w/w. The formulation was in fine powder form and the particle size was in the range 2-29 $\mu$ m.

Saturated stock solution of carbendazim formulation in water was prepared by adding the required quantity of wettable powder form to distilled water at 60°C in a glass beaker and stirring it for 1hr. The solution

was then cooled to room temperature and filtered to remove water insoluble clay. The filtrate was used for the detailed studies. Various other chemicals/reagents used are the same as discussed in earlier chapters.

### **6.2.2 Photocatalytic Experimental set up**

The experimental setup is same as mentioned in section 3.2.6 of Chapter 3. All other reaction methodologies are also the same, unless indicated otherwise.

### **6.2.3 Analytical procedures**

The degradation of carbendazim was followed by spectrophotometry using a Perkin-Elmer Lambda 650 Spectrophotometer. At periodic intervals of irradiation, samples were drawn from the reactor and filtered through 0.45 $\mu$ m syringe filter. The absorbance of the clear solution was measured at 284 nm. Millipore water used for the preparation of the solution was used as the reference.

The mineralization of carbendazim (in the formulation) was followed by analyzing the TOC content in the solution after photocatalytic treatment using Shimadzu TOC-L analyzer.

Analysis of H<sub>2</sub>O<sub>2</sub>, anion and cation concentrations were done by the procedure given in section 3.2.2 of Chapter 3.

### **6.2.4 Adsorption**

The adsorption of CZ-F on ZnO was tested by dispersing a fixed amount (0.1g) of ZnO in 100 ml carbendazim formulation solution of required concentration in a 250 ml reaction flask. The experimental

procedure and the calculation are similar to those mentioned in section 3.2.3 of Chapter 3.

The procedure used for measuring the adsorption of various ions is same as discussed earlier using respective salt solutions under required conditions.

### **6.2.5 Analysis of reaction products/ intermediates**

The reaction intermediates were identified using Agilent 6460 Triple quad LC/MS equipped with an ESI interface operating in positive polarity mode. The LC column was C18 of 150 mm × 4.6 mm and 5µm particles (Phenomenex). The mobile phase was acetonitrile - formic acid (0.1%) in the ratio 20:80. The scanning was done by multiple reactions monitoring (MRM) in the range of 50-500 amu.

## **6.3 Results and Discussion**

### **6.3.1 Preliminary experiments**

Preliminary studies conducted on the solar photocatalytic degradation of CZ-F in presence of ZnO as photocatalyst showed that the technique is effective for the removal of the active ingredient from water. Just as in the case of the technical (CZ) form, the adsorption of carbendazim (formulation) on the surface of ZnO also is negligible. Irradiation by sunlight without catalyst shows only negligible degradation. In presence of both sunlight and catalyst about 73% of carbendazim gets degraded within 30 min of irradiation (Fig. 6.1).

The percentage degradation of carbendazim increases with irradiation time (Fig. 6.2). The degradation is relatively less in the case of the

formulation (CZ-F) compared to that in the case of carbendazim technical (CZ), under identical conditions. The lower rate of degradation can be attributed to the presence of added ingredients (such as wetting agents, surfactants etc.) in the formulation.

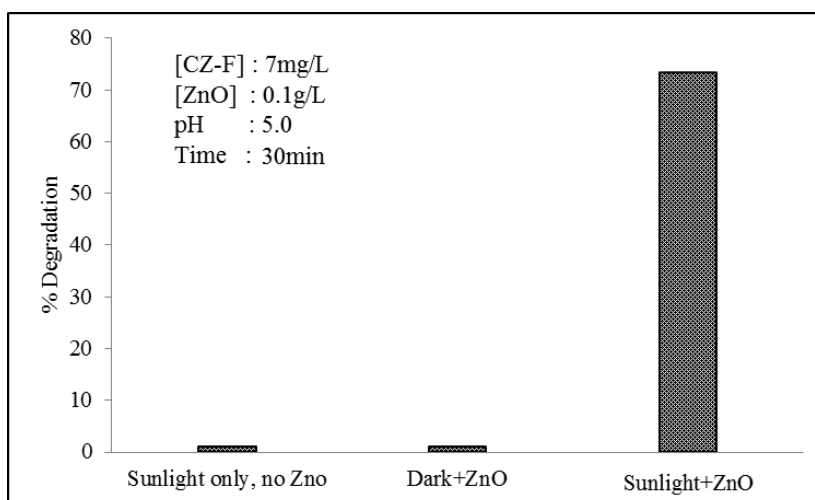


**Fig. 6.1:** Degradation of carbendazim formulation under various conditions

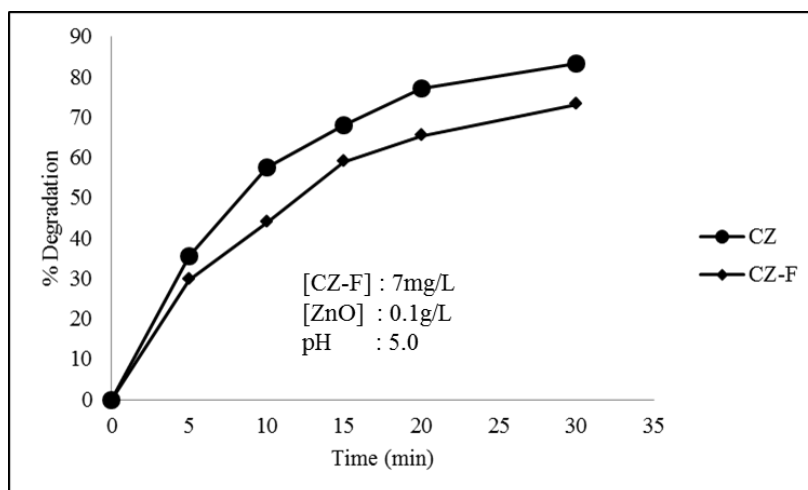


**Fig. 6.2:** Photocatalytic degradation of carbendazim in formulated and technical forms

The influence of various reaction parameters on the photocatalytic degradation is investigated and the results are discussed below.

### 6.3.2 Effect of catalyst loading

The optimum catalyst loading for the photocatalytic degradation of carbendazim in the formulation form is determined by conducting the experiments at various catalyst loadings from 0.02 - 0.18g/L keeping other parameters constant. Degradation rate increases as the catalyst loading increases, reaches an optimum at 0.1g/L and then stabilizes (Fig. 6.3). The optimum catalyst loading is the same as that for carbendazim in pure form under comparable experimental conditions.

As the catalyst loading increases, the ROS species generated by the catalyst surface increases under the photocatalytic reaction conditions. At higher catalyst loading there will be more  $\cdot\text{OH}$  and other ROS formation which will enhance the degradation efficiency. However compared to CZ, the relatively low rate of degradation of CZ-F can be attributed to the presence of added ingredients/wetting agents. At a particular catalyst loading the ROS species generated will be finite and at least a part of these can be consumed for the oxidation of additives. Also some of the active sites may be occupied by the wetting agents and other additives, thereby reducing the adsorption sites available for the substrate. This will also result in decreased rate of ROS generation. The stabilization effect after the optimum loading will be due to various factors which were discussed in the earlier chapters. The factors include: deactivation of ZnO

by the collision between the excited and ground state ZnO, scattering of light by the excess ZnO after the optimum loading and equilibrated adsorption-desorption of the substrate.

In the present experiment, the optimum catalyst loading for the degradation of CZ-F under specified condition is 0.1g/L. Hence, all further investigations were carried out with this dosage unless indicated otherwise.

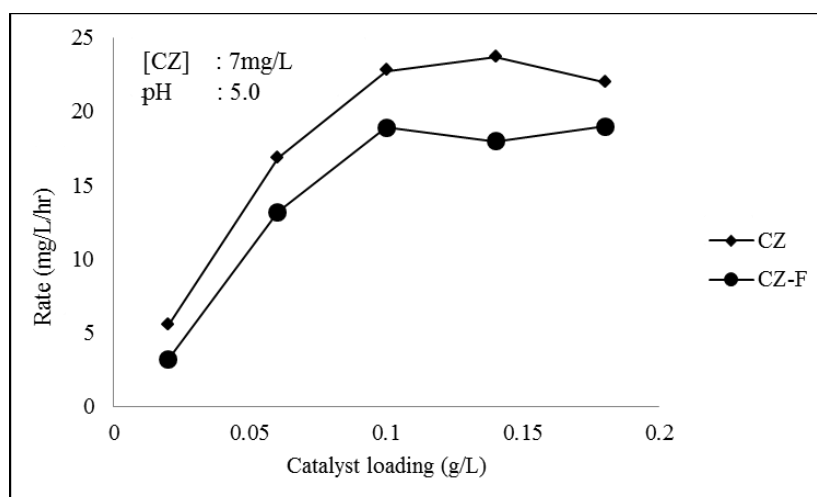


**Fig. 6.3:** Effect of catalyst dosage on the rate of degradation of CZ and CZ-F

### 6.3.3 Effect of initial concentration, Kinetics

In order to study the effect of initial concentration of CZ-F on its degradation, experiments were conducted by varying the initial concentration of carbendazim from 3-10mg/L keeping other parameters constant. As observed in the case of CZ, the rate increases as the initial

concentration increases, reaches an optimum and then stabilizes. But the observed rate of degradation for CZ-F is lower than CZ under same experimental conditions at all selected concentrations. The observed decrease in the rate of degradation may be due to the effect of added ingredients in the formulation. The optimum concentration observed for CZ-F under specified conditions is 7mg/L. Same optimum concentration is observed for CZ also.

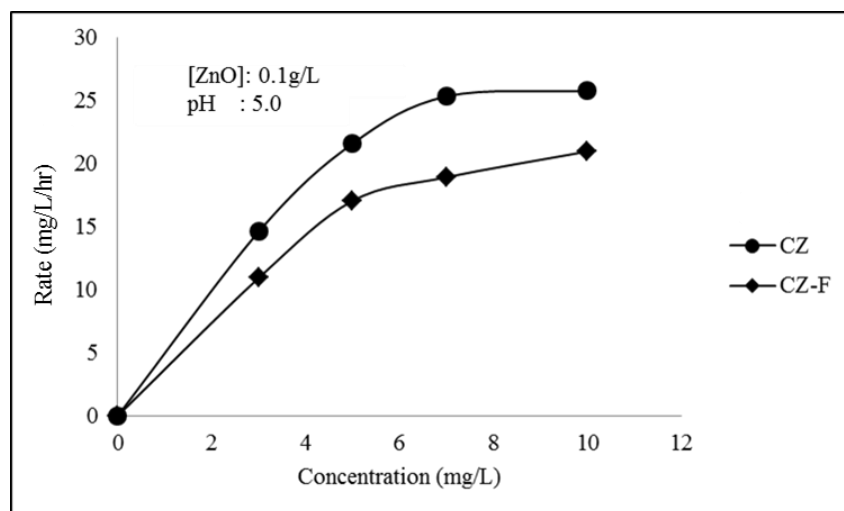


**Fig. 6.4:** Effect of carbendazim concentration on the rate of degradation in formulated and technical forms

The application of L-H model and the pseudo first order kinetics, which are common for most of the photocatalytic processes in presence of ZnO, is tested for the degradation of CZ-F also in the selected concentration range by plotting  $\ln C_0/C$  vs *time*. Linear trend observed (Fig. 6.5), confirms the applicability of pseudo first order kinetics. The

comparative plot of  $\ln C_0/C$  vs time for carbendazim at various concentrations in the technical and formulated forms is given in Fig. 6.6. The slope of the straight line gives the apparent rate constant. Table 6.1. shows the pseudo first order rate constants for the degradation of CZ-F at the selected concentrations. A decreasing tendency in the rate constant with increase in concentration is observed. Compared to CZ, the rate constant values for CZ-F are lower at all selected concentrations (Table 6.1).

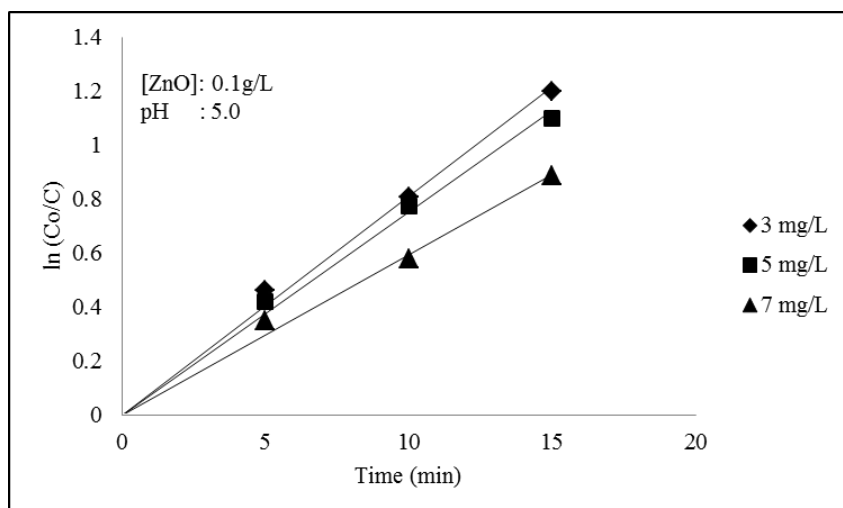


**Fig. 6.5:** Logarithmic plot of pseudo first order kinetics for the degradation of carbendazim formulation

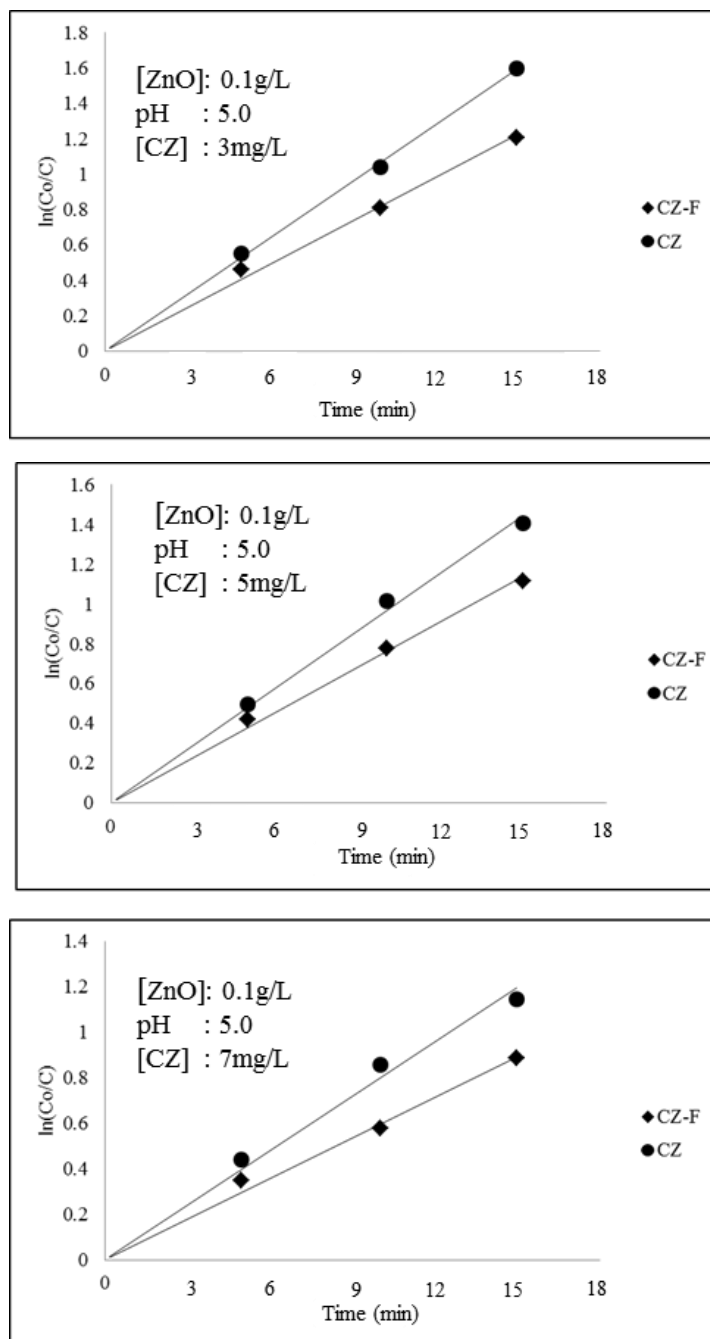


**Fig. 6.6:** Comparative logarithmic plot of pseudo first order kinetics for the degradation of carbendazim formulation and technical forms

**Table 6.1:** Pseudo first order rate constants for the photocatalytic degradation of CZ and CZ-F over ZnO. pH: 5.0 Temp: 29 ± 1°C

| Experiment | ZnO (g/L) | Carbendazim (mg/L) | CZ-F (k' h <sup>-1</sup> ) | CZ (k' h <sup>-1</sup> ) |
|------------|-----------|--------------------|----------------------------|--------------------------|
| 1          | 0.1       | 3                  | 4.42                       | 6.29                     |
| 2          | 0.1       | 5                  | 4.07                       | 5.44                     |
| 3          | 0.1       | 7                  | 3.22                       | 4.22                     |

The effect of some of the formulation ingredients on the degradation of carbendazim is evaluated by adding the respective ingredients (as declared by the manufacturer) at comparable concentrations to the technical sample and investigating the degradation rate. The carbendazim formulation used for the current study contains alkyl aryl sulphonate 2% w/w, alkyl naphthyl sulphonate 2% w/w, and CMC 2%. In order to study the effect of these adjuvants, a mixture of alkyl aryl sulphonate and alkyl naphthyl sulphonate (jeemol F, received from the pesticide manufacturer) which is normally used as the wetting agent for the preparation of pesticide formulations, is mixed thoroughly with carbendazim technical at various dosages (2%, 5% and 10%). Standard solutions of the combinations are prepared as described in section 6.2.1. Similarly, in order to study the effect of CMC, various weight percentages of CMC (2%, 5% and 10%) are thoroughly mixed with carbendazim technical. Using these mixtures standard solutions were prepared for the experiments. The rate of degradation of carbendazim in presence of these adjuvants is tested under optimized conditions. The results are shown in Fig. 6.7. The results clearly show the inhibitive effect of added ingredients on the photocatalytic degradation of

carbendazim. As the concentration of adjuvants increases the degradation decreases progressively.

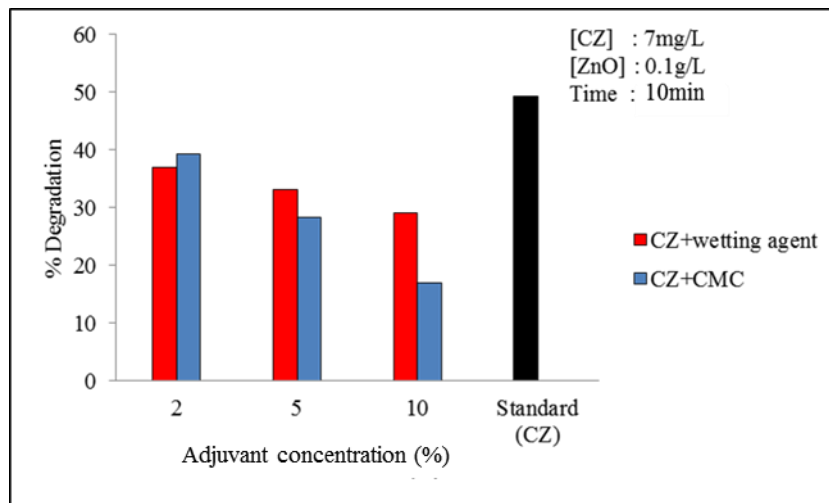


**Fig. 6.7:** Effect of various adjuvants on the photocatalytic degradation of carbendazim

Most of the photocatalytic degradation reactions involving  $\bullet\text{OH}$  radicals are non-selective. Hence, it is possible that the ROS are interacting with the carbendazim as well as the adjuvants resulting in the degradation of all, though at different rates. This in turn decreases the rate of carbendazim degradation in the formulation.

The slow but complete destruction of all organic carbon containing ingredients is illustrated from the TOC measurements. Carbendazim wetttable power formulation contains many organic compounds (adjuvants) other than carbendazim. These compounds are mainly long chain aromatic or aliphatic molecules. Even after the complete degradation of carbendazim, these relatively harmless compounds may

still be present in the system. In the case of CZ-F, the complete removal of TOC can be confirmed only after the mineralization of both carbendazim and the additives present in the system. In this context, the TOC of the system is measured at different points of irradiation. Even after 8 hr of irradiation, when the TOC has become 'nil' in the case of CZ, the formulation still contains significant amount of organic carbon (see Fig. 6.8). In the case of CZ-F, the complete mineralization is achieved only after 40 hr of irradiation time. This shows that, the mineralization of carbendazim formulation is slower. This may be due to the slow rate of degradation of the adjuvants as well as the inhibition in the degradation of CZ (by the adjuvants). Ultimately, additives also get mineralized and the TOC becomes 'nil'.

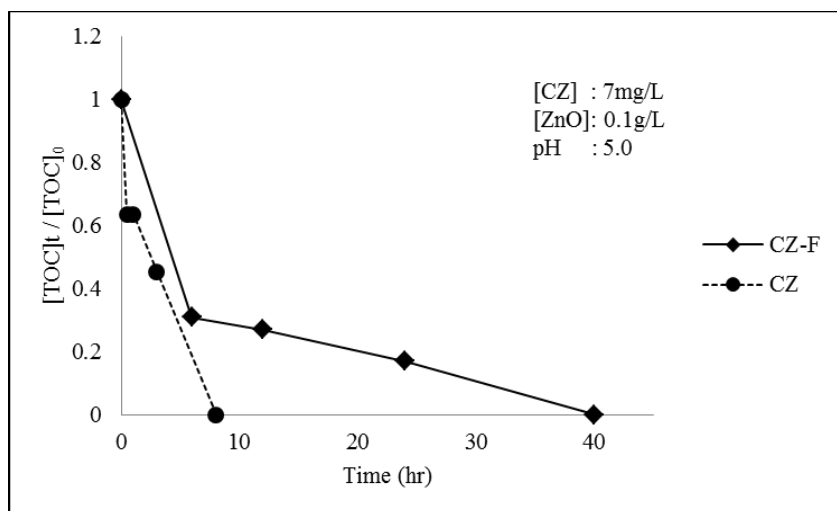


**Fig. 6.8:** Comparative depletion in the TOC content with time of irradiation during the solar photocatalytic degradation of CZ and CZ-F

### 6.3.4 Effect of pH

The effect of pH on the photocatalytic degradation of CZ-F is investigated by varying the solution pH from 3 to 11 keeping all other parameters constant. There is no degradation of carbendazim, throughout the pH range, even in presence of catalyst. In presence of sunlight and the catalyst, degradation increases as the solution pH increases, reaches a maximum at pH 5 i.e. normal pH of carbendazim formulation solution. Further increase in solution pH has no effect on degradation till pH 9. After that the degradation decreases as solution pH increases. Similar trend is observed for CZ also. The observed trend i.e. lower percentage degradation at pH>9 can be explained on the basis of zinc oxide corrosion under alkaline pH and the point of zero charge (PZC) as explained earlier. The PZC of ZnO is ~9.3 above which the surface is negatively charged. Relatively low degradation of CZ-F compared to CZ in the acidic pH may be due to the strong adsorption of the anionic surfactants on the catalyst surface thereby inhibiting the activation and formation of reactive  $\cdot\text{OH}$  radicals. This is further evident from the comparable degradation of CZ and CZ-F at extreme alkaline pH at which the anions cannot get adsorbed on the negatively charged ZnO surface. The lower degradation at pH(~3) and 12 for both forms of carbendazim may be due to the corrosion of ZnO as explained in earlier chapters. Since optimum degradation is observed at the natural pH of CZ-F suspension i.e. at pH 5, all further studies are carried out without adjusting the pH, unless indicated otherwise.

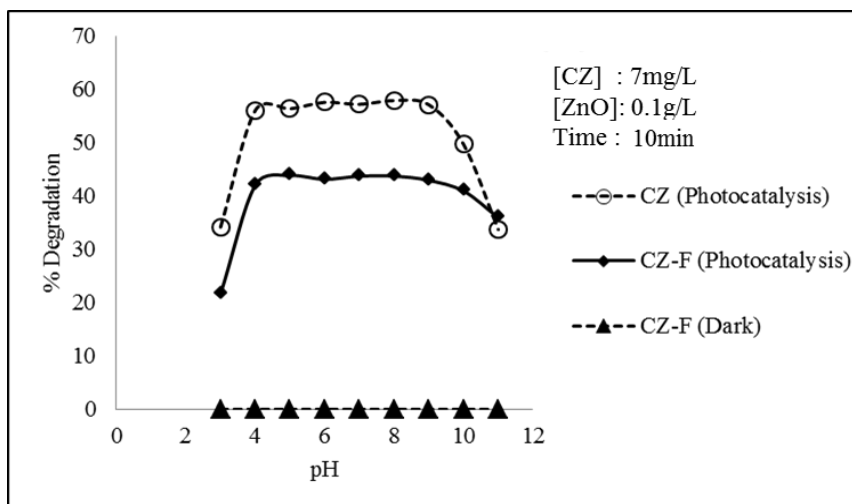


**Fig. 6.9:** Effect of pH on the degradation of carbendazim technical (CZ) and formulation (CZ-F)

### 6.3.5 Effect of oxidants

The effect of two typical oxidants i.e.  $\text{H}_2\text{O}_2$  and  $\text{S}_2\text{O}_8^{2-}$  on the photocatalytic degradation process is tested by the addition of these compounds to the reaction medium. In presence of added oxidants, slight increase in percentage degradation was observed in the case of CZ (section 3.3.6 of Chapter 3). Similar experiments were conducted for the formulation also keeping the other parameters constant.

The photocatalytic degradation processes are accompanied by the formation of  $\text{H}_2\text{O}_2$ . In the current instance also, the formation of  $\text{H}_2\text{O}_2$  is observed and measured (Fig. 6.10). The concentration of  $\text{H}_2\text{O}_2$  increases with reaction time. After reaching a critical maximum, the concentration decreases for a while and increases again. This is explained based on the concurrent formation and decomposition of  $\text{H}_2\text{O}_2$  under photocatalytic conditions.

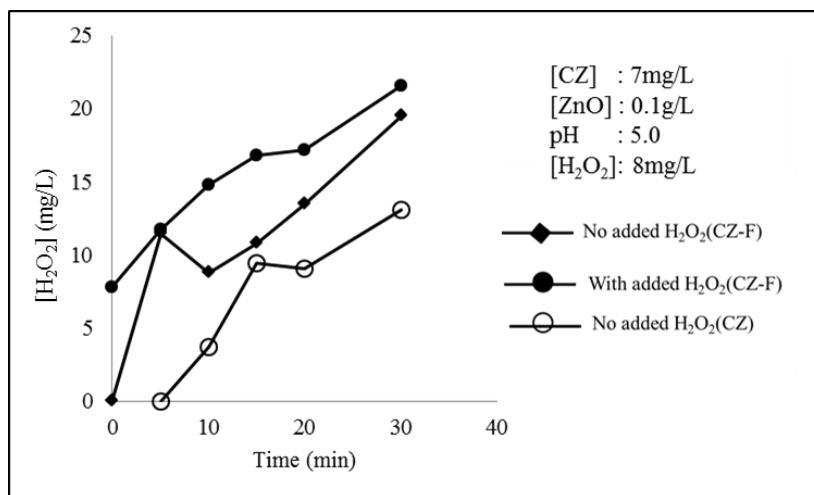


**Fig. 6.10:** Formation of H<sub>2</sub>O<sub>2</sub> during the photocatalytic degradation of carbendazim formulation

In the case of externally added H<sub>2</sub>O<sub>2</sub> also, the concentration of H<sub>2</sub>O<sub>2</sub> increases in the system with time. However, in this case the increase is not as steep as in the case of the initial in-situ formation. This may be probably because, at the higher initial concentration, the decomposition of H<sub>2</sub>O<sub>2</sub> is more facile compared to the formation. However after ~15 min the rate of increase follows similar trend in the case of the system with and without initially added H<sub>2</sub>O<sub>2</sub>.

The effect of added H<sub>2</sub>O<sub>2</sub> on the photocatalytic degradation of CZ-F is negligible as seen in Fig. 6.11. The concentration of H<sub>2</sub>O<sub>2</sub> has no effect at least in the range of 1-8mg/L. For carbendazim technical slight enhancement was observed in the selected concentration range (of H<sub>2</sub>O<sub>2</sub>) (see section 3.3.6 of Chapter 3). H<sub>2</sub>O<sub>2</sub> is known to act as an enhancer as well as inhibitor in photocatalytic systems, as discussed in section 3.3.6 of Chapter 3. The formation of less reactive HO<sub>2</sub><sup>•</sup> radical by the reaction of

$\cdot\text{OH}$  radical with the abundant  $\text{H}_2\text{O}_2$  results in reduction of reactive species in the medium and this is a major cause of the ‘nil’ effect. Similar ‘nil’ effect of  $\text{H}_2\text{O}_2$  addition is observed in the case of diquat also in both technical and formulated forms. The mechanism of the reaction leading to the ‘nil’ effect has been discussed in detail in earlier chapter.

Unlike in the case of carbendazim technical,  $\text{S}_2\text{O}_8^{2-}$  addition has negligible effect on the photocatalytic degradation of CZ-F (Fig. 6.12). Increase in the concentration of  $\text{S}_2\text{O}_8^{2-}$  also has no effect on the degradation. It is possible that the additives present in the formulation may be interacting with the persulphate and persulphate derived oxidants such as  $\text{SO}_4\cdot^-$ . More detailed investigations are needed to understand these interactions and their possible effect on various photocatalytic processes, which is beyond the scope of the current study.

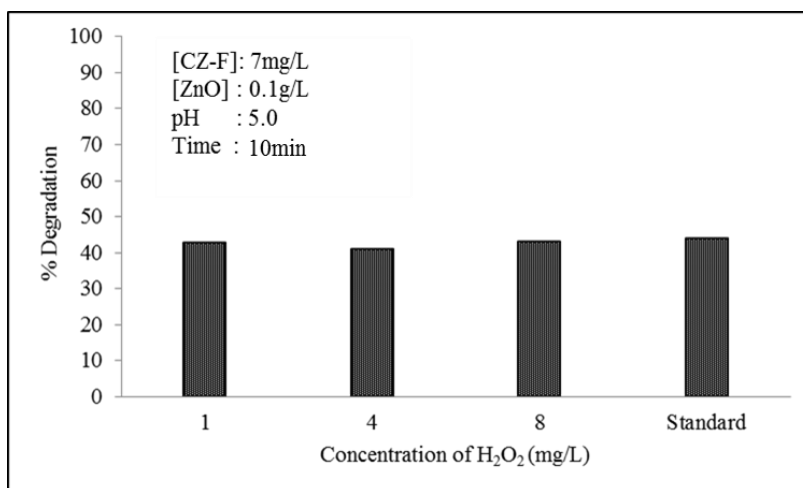


**Fig. 6.11:** Effect of  $\text{H}_2\text{O}_2$  on the photocatalytic degradation of CZ-F

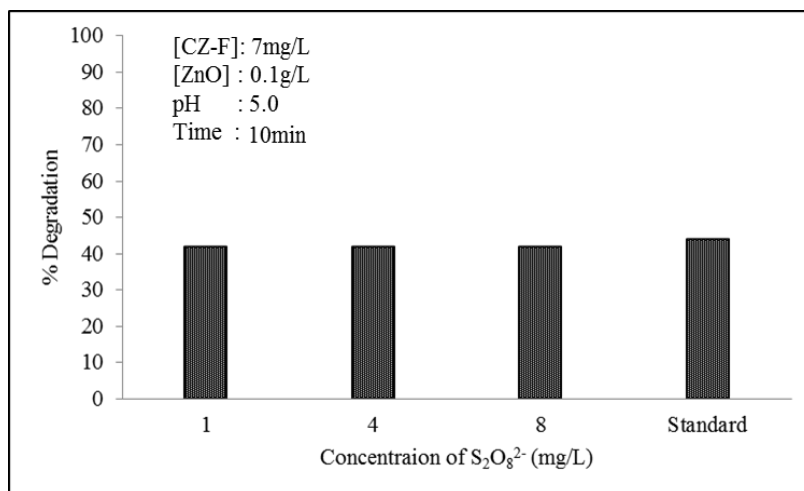


**Fig. 6.12:** Effect of persulphate on the photocatalytic degradation of CZ-F

### 6.3.6 Effect of anions and cations

A number of salts likely to be present in water, naturally and man-made, are known to affect the efficiency of photocatalytic degradation of various pollutants as demonstrated in earlier chapters. The effect of salts will often be the net effect of respective anions and cations and hence the effect of both types of ions has to be investigated separately. In this context, the effect of few typical anions, i.e.  $Cl^-$ ,  $NO_3^-$ ,  $SO_4^{2-}$  and  $PO_4^{3-}$  is investigated keeping the cation constant as  $Na^+$ . The concentration of respective ions and other parameters are kept similar to the experiments conducted with the technical form. As observed in the case of CZ, all anions except phosphate have negligible effect on the degradation of CZ-F (Fig. 6.13). In presence of  $HPO_4^{2-}$ , percentage degradation of carbendazim decreases as the concentration of the former in the reaction medium is increased. The extent of inhibition is comparable to that in the case of the technical form. Similar studies

were conducted with various cations keeping anion constant, i.e.  $\text{SO}_4^{2-}$ . The photocatalytic degradation of CZ-F was inhibited by  $\text{Al}^{3+}$  (Fig. 6.14). The inhibition increases with increase in concentration of  $\text{Al}^{3+}$  and the degradation is practically nil at 8mg/L. Other cations have only negligible effect. The observed trend is similar to that in the case of CZ also.

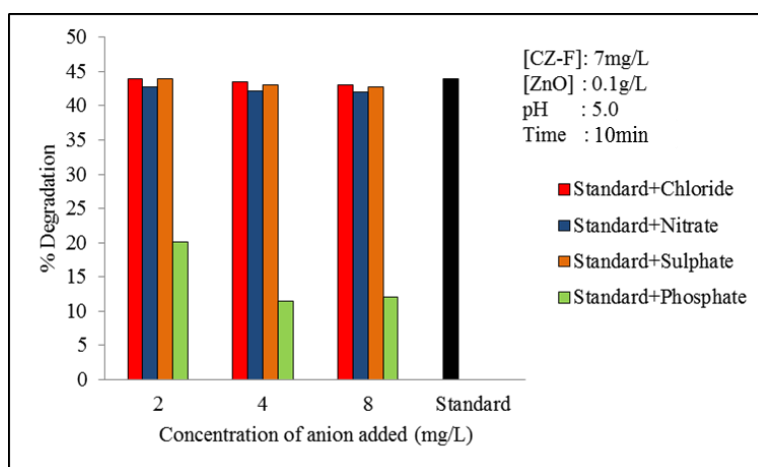


**Fig. 6.13:** Effect of anions on the photocatalytic degradation of CZ-F [Cation:  $\text{Na}^+$ ]

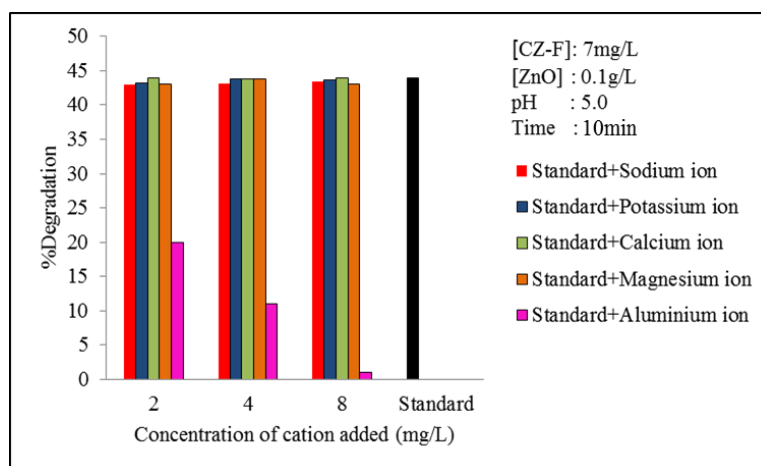


**Fig. 6.14:** Effect of cations on the photocatalytic degradation of CZ-F [Anion:  $\text{SO}_4^{2-}$ ]

For carbendazim in its pure form, the degradation in presence of  $\text{Al}^{3+}$  was ~10% when the concentration of  $\text{Al}^{3+}$  was 8mg/L. In this case, the photo-generated ROS can interact relatively more frequently with the carbendazim molecule (compared to CZ-F). In the case of CZ-F, the formulation adjuvants present along with carbendazim will also compete for the limited number of ROS resulting in complete inhibition of the degradation.

### 6.3.7 Effect of oxygen

Effect of dissolved oxygen on the photocatalytic degradation of CZ-F is tested by deaerating the reaction system with nitrogen. The photocatalytic experiments in presence of sunlight were conducted keeping other optimised parameters constant. The percentage degradation is much less in the deaerated system and a stabilization tendency is observed as the irradiation time is increased.

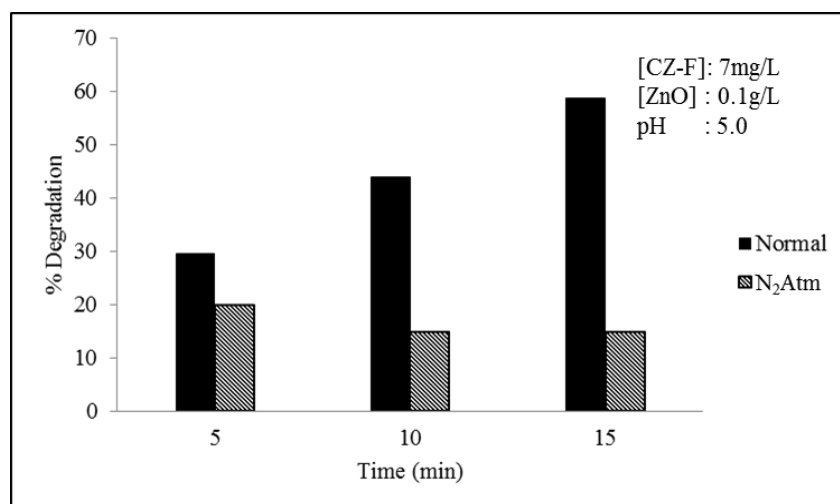
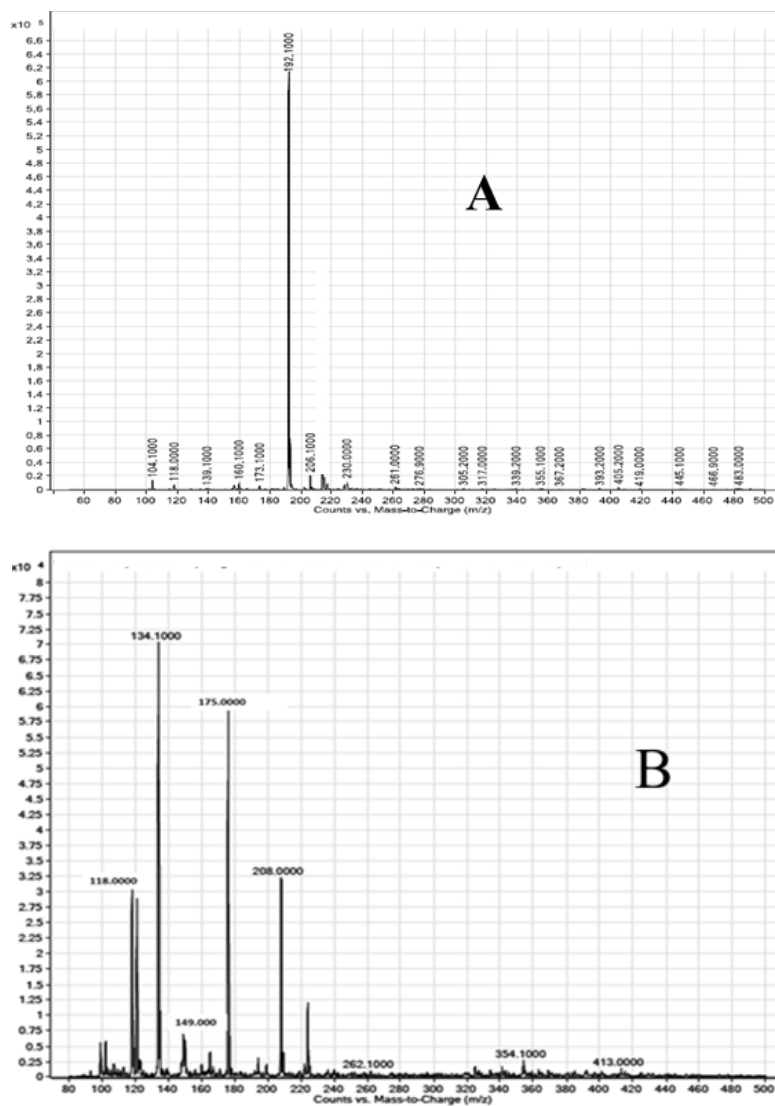


**Fig. 6.15:** Effect of deaeration with  $\text{N}_2$  on the photocatalytic degradation of CZ-F

Similar trend was observed in the case of carbendazim technical also (see section 3.3.8 of Chapter 3). The observed degradation in the deaerated system in the initial stage is due to the dissolved oxygen which is still present in the system even after nitrogen bubbling. The reasons for the inhibition of the degradation in the deaerated system have already been explained in previous chapters.

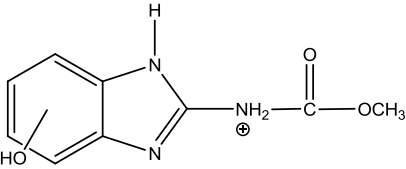
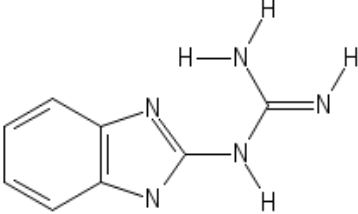
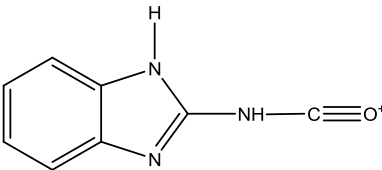
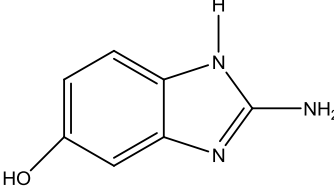
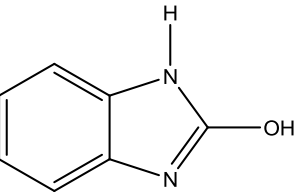
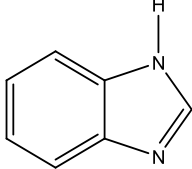
### **6.3.8 Identification of reaction intermediates**

The LC/MS spectrum of CZ-F before and after irradiation is shown in Fig. 6.16. LC/MS spectrum of CZ-F solution contains a major peak at  $m/z$  192 corresponding to carbendazim (Fig. 6.16A). But peaks corresponding to adjuvants were not observed under this condition. However, after irradiation under photocatalytic conditions, more peaks are seen under the same LC/MS conditions (Fig. 6.16B). These peaks are possibly the decomposition products of carbendazim. Some of the possible intermediates of carbendazim identified using LC/MS are shown in Table 6.2. Most of the reaction products/ intermediates found in the case of CZ-F are the same as those from CZ. Hence it can be concluded that the reaction mechanisms for the photocatalytic degradation of both carbendazim technical and formulation are identical.



**Fig. 6.16:** Mass spectra of carbendazim formulation before photocatalysis (A), and after photocatalytic degradation (B)

**Table 6.2:** List of intermediates identified during the solar photocatalytic degradation of carbendazim in the formulated form.

| Molecular or Cationic mass | Intermediates/Reaction products  |
|----------------------------|--|
| 208                        |    |
| 175                        |    |
| 160                        |   |
| 149                        |  |
| 134                        |  |
| 118                        |  |

## 6.4 Mechanism of the degradation of CZ-F

The effect of various reaction parameters, the kinetics, effect of contaminant salts and oxidants, the reaction intermediates etc. are more or less identical in the case of both CZ and CZ-F. Hence it may be inferred that the mechanism of the photocatalytic degradation is identical in the case of carbendazim in both technical and formulated forms. The mechanism is discussed in detail in section 3.4 of Chapter 3. However the extent of degradation is significantly less in the case of the formulation. This is attributed to the adsorption of the formulation adjuvants and subsequent deactivation of the catalyst, inhibition in the rate of formation of reactive free radicals ( $\cdot\text{OH}$ ), inhibition in the quanta of light reaching the catalyst surface etc. Details are discussed in respective sections in this chapter.

## 6.5 Conclusion

The sunlight induced, ZnO-mediated photocatalytic degradation is an effective tool for the complete mineralization of carbendazim even in its wettable powder formulation form in water. The degradation follows pseudo first order kinetics. Studies conducted by mixing adjuvants with the carbendazim technical reveal the adverse effect of the added ingredients on the photocatalytic degradation of the active ingredient. Added oxidants such as  $\text{H}_2\text{O}_2$  and persulphate (in the selected concentration range) have little effect on the degradation. Some of the cations/anions (salts) present in the natural water systems such as  $\text{Na}^+$ ,  $\text{K}^+$ ,  $\text{Ca}^{2+}$  and  $\text{Mg}^{2+}$  (cations) as well as  $\text{Cl}^-$ ,  $\text{SO}_4^{2-}$  and  $\text{NO}_3^-$  (anions) have no effect on the

degradation. However,  $\text{Al}^{3+}$  (cation) and  $\text{HPO}_4^{2-}$  (anion) adversely affect the degradation. The reaction kinetics as well as the intermediates formed during the degradation of carbendazim in technical as well as formulated forms are more or less identical. Hence, the mechanism of the degradation will be similar. Even in presence of adjuvants, complete mineralization of carbendazim is achieved by photocatalysis, though it takes much longer time.

.....❧.....



---

**SOLAR PHOTOCATALYSIS MEDIATED BY ZnO FOR THE  
REMOVAL OF DIQUAT FORMULATION FROM WATER**

---

- 7.1 *Introduction*
  - 7.2 *Experimental*
  - 7.3 *Results and discussion*
  - 7.4 *Mechanism of the photocatalytic degradation of DQ-F*
  - 7.5 *Conclusion*
- 

**7.1 Introduction**

Normally, diquat is formulated as emulsifiable concentrate (EC) or wettable powder (WP) by the addition of required adjuvants and suitable processing. Emulsifiable concentrate of diquat is an emulsion of the technical grade diquat (10-30%) containing an emulsifier to help the concentrate mix readily and uniformly with water for spraying. The emulsifier is a kind of detergent that helps the suspension of microscopically small oil droplets in water to form an emulsion. When an emulsifiable concentrate is added to water and stirred vigorously the emulsifier causes the oil to disperse uniformly throughout the carrier (i.e. water) producing an opaque liquid.

In addition to influencing the application and dispersion characteristics, formulation also affects the environmental stability of the active ingredient.

Formulation also is likely to influence the behavior and stability of the active ingredient under AOP conditions. In this context, the photocatalytic degradation of diquat, in the form of EC formulation, is tested in order to identify the influence of additives on the rate of degradation. Various process parameters which are likely to affect the degradation (as seen from the degradation of pure diquat, explained in Chapter 4) are evaluated in detail and optimum conditions identified. Some of the major reaction intermediates are also identified.

## **7.2 Experimental**

### **7.2.1 Chemicals**

Emulsifiable concentrate of diquat is provided by a pesticide manufacturer (who did not want their identity to be revealed) and is used as such without further modification. As per the information on the leaflet and discussion with scientists from the manufacturing firm, the formulation contains 37.3% diquatdibromide and 62.7% other ingredients. All other chemicals and materials used are the same as discussed in the earlier chapter.

### **7.2.2 Analytical procedures**

The concentration of diquat in the solution was analyzed by spectrophotometry (310 nm). The formulation additives do not influence the absorbance of diquat at 310 nm at various concentrations as seen in Fig. 7.1.

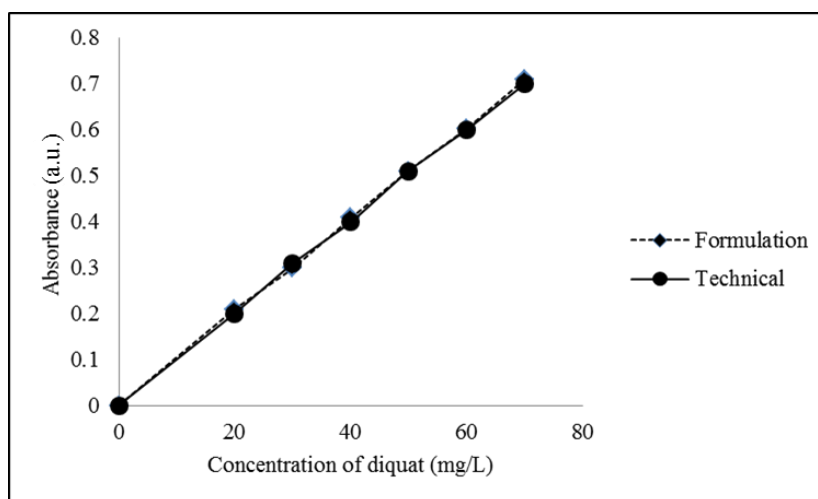


**Fig. 7.1:** Analysis of diquat 'formulation' and 'technical' at various concentrations

The mineralization of diquat is followed by analyzing the TOC content in the solution after photocatalytic treatment using Shimadzu TOC-L analyzer.

Analyses of the concentration of  $H_2O_2$ , anion and cation are done by the procedure given in section 3.2.2 of Chapter 3.

### **7.2.3 Analysis of reaction products/ intermediates**

The reaction intermediates were identified using Agilent 6460 Triple quad LC/MS equipped with an ESI interface operating in positive polarity mode. The LC column was C18 of 150 mm  $\times$  4.6 mm and 5 $\mu$ m particles (Phenomenex). The mobile phase was acetonitrile - formic acid (0.1%) in the ratio 20:80. The scanning was done by multiple reactions monitoring (MRM) in the range of 50-250 amu.

#### **7.2.4 Photocatalytic Experimental set-up**

Photocatalytic experiments in presence of sunlight were performed using a glass reactor as explained earlier. The diquat formulation solution (50 ml) of the required concentration (in terms of the active ingredient) together with ZnO was taken in the reactor. Cooling water from a thermostat ( $29 \pm 1^\circ\text{C}$ ) was continuously circulated through the water bath in which the reactor was placed. Solar experiments were performed by placing the reaction system on the roof top of our laboratory at Kochi, Kerala, India ( $9^\circ 57' 51'' \text{N}$ ,  $76^\circ 16' 59'' \text{E}$ ) on sunny days during January-May 2016.

### **7.3 Results and Discussion**

#### **7.3.1 Preliminary experiments**

Preliminary studies showed that solar photocatalysis using ZnO as catalyst is an effective tool for the removal of diquat in its emulsifiable concentrate form from water. Experiments conducted in the absence of light but in presence of catalyst and in the absence of catalyst but in presence of light show that the degradation is negligible (Fig. 7.2). Hence it is clear that, as in the case of technical diquat, both light and catalyst are essential for the degradation of diquat in the formulated form also. Diquat in pure form, i.e. technical and diquat in the formulation are represented as DQ and DQ-F respectively.

The photocatalytic percentage degradation of DQ-F increases with increase in time of irradiation (Fig. 7.3). The degradation is less in the case of formulation, especially in the early stage of reaction. However, the

difference in the degradation narrows down towards later stages when most of the diquat has already been degraded.

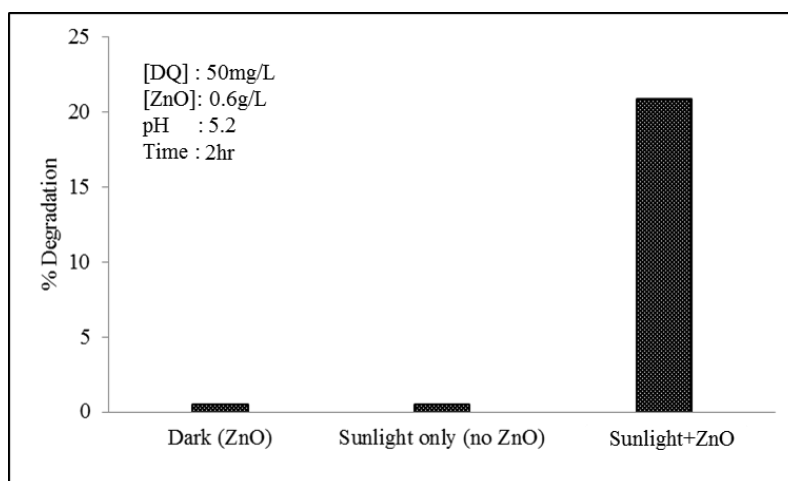


**Fig. 7.2:** Degradation of diquat in the formulated form under various conditions

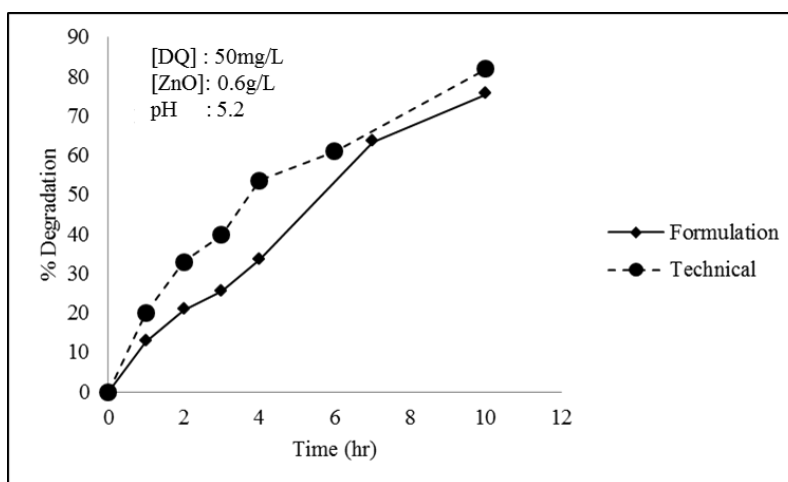


**Fig. 7.3:** Percentage degradation of diquat in the technical and formulated forms at different times of irradiation under photocatalysis

The effect of various reaction parameters on the degradation is investigated in detail as follows:

### 7.3.2 Effect of catalyst loading

The effect of catalyst loading on the degradation of DQ-F is investigated by varying the catalyst loading from 0.1-1.0g/L keeping other parameters constant (Fig. 7.4). As the catalyst loading is increased, the percentage degradation also increases and reaches an optimum at 0.6g/L and then stabilizes. Same optimum catalyst loading is observed for the degradation of diquat in pure form as well under otherwise identical conditions.

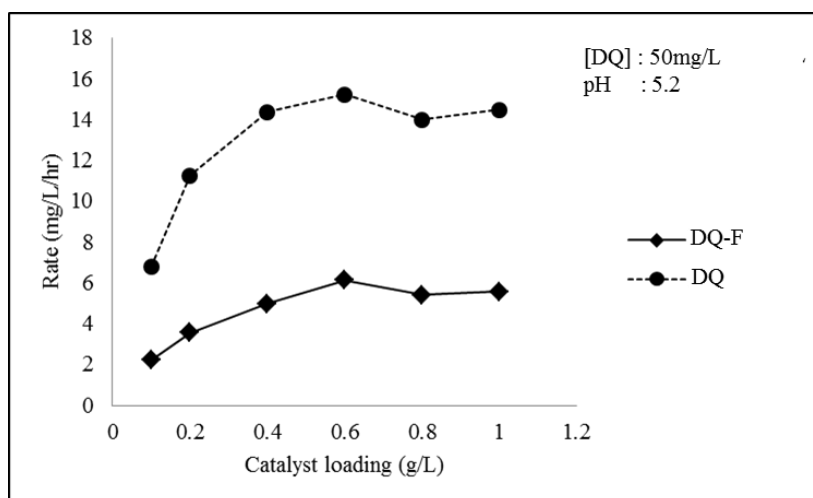


**Fig. 7.4:** Effect of catalyst dosage on the rate of degradation of diquat in technical and formulation forms

The current study is mainly focused on the degradation of diquat present in the system. The fate of the other ingredients (formulation

agents) present in the system (whose identity is not revealed by the manufacturer) is not examined due to experimental and analytical constraints. It is quite possible that these ingredients are also getting degraded or even mineralized photocatalytically. Experiment on the adsorption of diquat from the formulation on ZnO reveals that the adsorption is practically 'nil' as in the case of technical grade product. Hence it may be inferred that the emulsifying agents or other additives present in the diquat formulation do not assist the adsorption of DQ.

The degradation of diquat in water during photocatalysis is due to its interaction with the ROS generated in-situ and subsequent oxidation/mineralization. Since the interaction of the most common ROS, i.e.  $\cdot\text{OH}$  radical is non-selective, any organic species present in the system including adjuvants can undergo degradation/fragmentation and end up in numerous intermediates. This in turn can affect the overall reaction rate of the target molecule i.e. diquat. The increase in the degradation rate of DQ-F with increase in catalyst dosage can be attributed to the increase in the number of photogenerated ROS. After the optimum loading, the excess ZnO present will hinder the penetration of light or scatter the incident radiation which limits the effective utilization of incident radiation by the catalyst surface for the generation of ROS. Also the deactivation of already excited ZnO by collision with the ground state ZnO can contribute to the stabilization or even decrease in the generation of ROS. These and other possible causes for the stabilization or decrease in the rate of degradation beyond the optimum catalyst dosage are discussed in earlier chapters. Under the present experimental conditions, the optimum catalyst loading for the

degradation of DQ-F is 0.6g/L. Hence all further investigations are carried out with this dosage unless indicated otherwise.

### 7.3.3 Effect of initial concentration of DQ-F

The effect of concentration on the photocatalytic degradation of DQ is investigated in detail in Chapter 4. However, it is possible that formulation ingredients will influence the rate of degradation and hence the kinetics. The effect of diquat concentration in the formulation, i.e. DQ-F on the photocatalytic degradation is examined in the range 20-70mg/L keeping other parameters unchanged. The results are presented in Fig. 7.5. Initially the rate of reaction increases as the initial concentration increases up to 50mg/L and then stabilizes. Further increase in the concentration of diquat has little effect on the reaction rate. This indicates that after the optimum, the reaction follows zero order kinetics. Same trend is observed in the case of DQ, though the reaction rate is higher (Fig. 7.5). The lower rate of degradation in presence of formulation ingredients shows that the additives are competing with diquat for interaction with the ROS. This reduces the frequency of interaction between diquat and the ROS. It is also possible that the additives may be getting preferentially adsorbed on the surface or be in its close proximity thereby reducing the quantum of light radiation reaching the catalyst. This will reduce the efficiency of photo-activation of the catalyst and consequently the generation of reactive free radicals. The optimum concentration of DQ-F is observed to be 50mg/L which is same as in the case of the pure form.

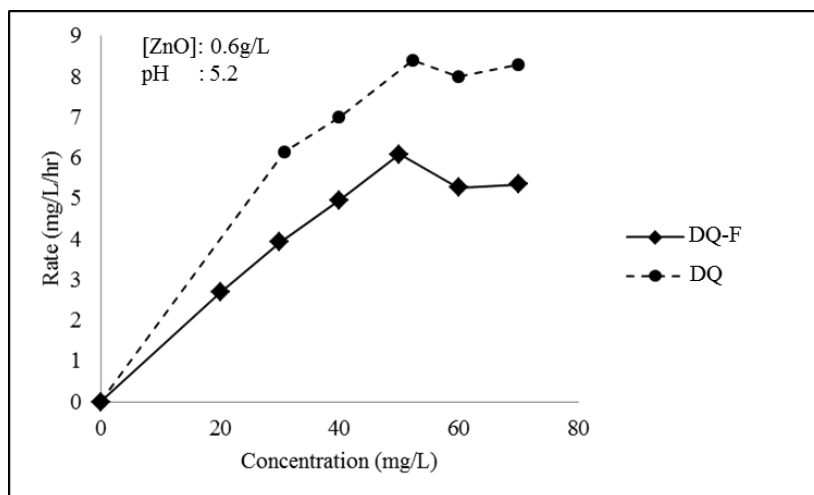


**Fig. 7.5:** Effect of initial concentration on the rate of photocatalytic degradation of diquat in technical and formulated forms

Most of the photocatalytic degradation reactions, including those described in Chapter 3 and 4 of this study follow pseudo first order kinetics and modified L-H mechanism. The applicability of pseudo first order kinetics for the degradation of diquat formulation is tested by the L-H model. Thus  $\ln(C_0/C)$  is plotted vs  $t$ . The straight line graphs in the concentration range 20-50mg/L (Fig. 7.6) show first order kinetics. The slope of the straight lines gives the pseudo first order rate constant for the respective concentrations. Comparison of the logarithmic plot for a typical concentration of DQ (50mg/L) as well as DQ-F under otherwise identical conditions shows that the rate constant for the degradation of the former is higher (Fig. 7.7). Table 7.1. shows the apparent rate constants for the degradation of DQ-F at various concentrations. As the concentration increases the rate constant decreases. Similar observations were made in the case of diquat technical and carbendazim also.

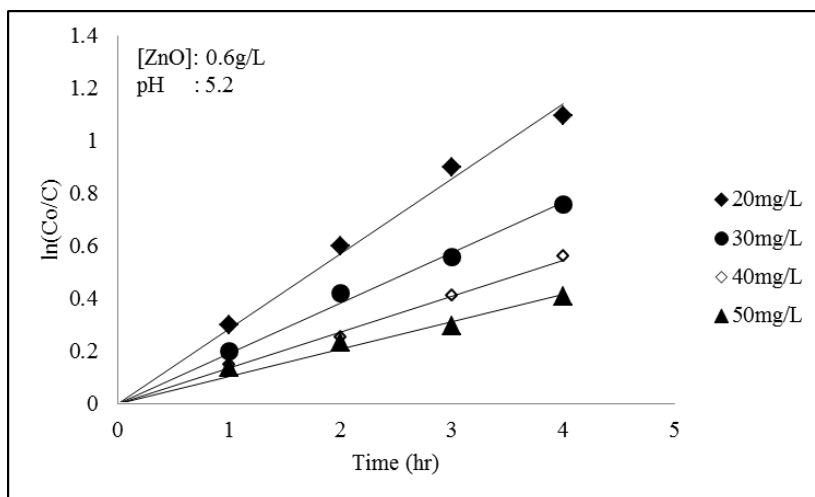


**Fig. 7.6:** Kinetics of photocatalytic degradation (linear transform  $\ln Co/C$  vs time) of diquat formulation over ZnO

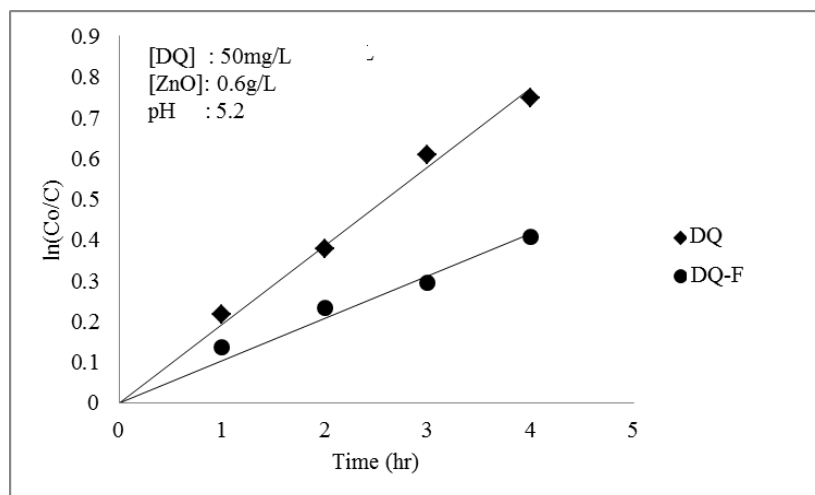


**Fig. 7.7:** Comparative kinetics of photocatalytic degradation of diquat formulation and technical over ZnO

**Table 7.1:** Pseudo first order rate constants for the photocatalytic degradation of DQ-F at various concentrations over ZnO. pH: 5.2 Temp:  $29 \pm 1^\circ\text{C}$

| Experiment | ZnO (g/L) | Diquat (mg/L) | $k' \times 10^{-2} (\text{h}^{-1})$ |
|------------|-----------|---------------|-------------------------------------|
| 1          | 0.6       | 20            | 26.9                                |
| 2          | 0.6       | 30            | 18.2                                |
| 3          | 0.6       | 40            | 15.7                                |
| 4          | 0.6       | 50            | 8.8                                 |
| 5*         | 0.6       | 50            | 18.3                                |

\* Diquat technical

The decrease in the rate constant with increase in concentration can be explained as in earlier chapters. The overall decrease in the rate of reaction compared to the technical form may be due to the interaction of added ingredients (such as emulsifiers) with the ROS which limits the availability of the reactive free radicals for interaction with diquat. Emulsifiers used in the formulation generally consist of non-aqueous mixtures containing amine alkylbenzene sulfonates (surfactants) with a poly-alkylene glycol, alkyl or alkyl aryl ether or ester. When these emulsifiers are added to water, they form small droplets. Depending on the charge on these species they can interact with the ZnO surface also thereby inhibiting the photo-activation. Thus the generation of free radicals also will be inhibited. The shielding effect of these bulky groups may reduce the overall rate of interaction between ROS and the substrate and thus inhibit the degradation.

The adsorption of diquat on ZnO is negligible. So the interaction between the ROS and diquat occurs in the bulk or in the vicinity of catalyst surface. For a particular amount of catalyst loading, the ROS

generated will be finite and at least some of the long chain emulsifier molecules present in formulation will interact with these reactive species. Also these molecules may have tendency to absorb at least a part of the incident radiation. The combined effect of these possibilities may be the reasons for the reduction in the overall rate of degradation of DQ-F. The nature of the interaction as well as the photocatalytic reactions of emulsifiers and other ingredients need an in-depth study which deserves to be taken up separately as another major research project.

#### **7.3.4 Effect of pH**

The effect of pH on the photocatalytic degradation of DQ-F is investigated by varying the solution pH under the optimized conditions. The presence of added ingredients may have significantly different role and behavior when the pH is varied. The additives are mainly charged species or neutral compounds. The nature of their interaction with the ZnO surface will vary with the surface charge of the catalyst which in turn depends on the solution pH. This can also affect the degradation of diquat. At higher solution pH, degradation of DQ is observed even in the absence of catalyst or irradiation (see section 4.3.4 of Chapter 4). Similar trend is observed in the case of DQ-F also. Above pH 8, both the technical and formulated forms of diquat are not stable. Fig. 7.8 shows the effect of pH on the degradation of DQ-F in the dark and under the photocatalytic reaction conditions. In the lower pH range, the percentage degradation is less. As the pH of the solution increases, the degradation also slowly increases and reaches a maximum at pH 5. Thereafter,

stabilization in the percentage degradation is noticed up to pH 8. Corrosion of ZnO at extremely acidic pH is already reported in the case of many photocatalytic reaction studies and is applicable in the current system also.

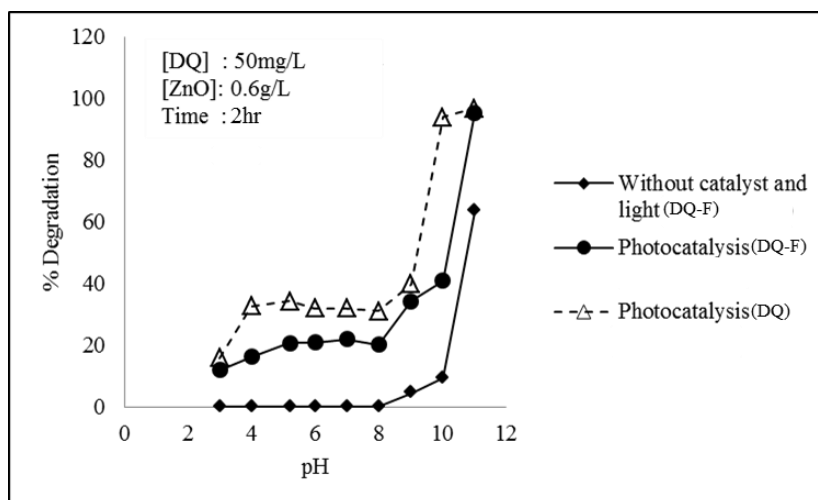


**Fig. 7.8:** Effect of pH on the degradation of diquat formulation in dark and under photocatalysis

Variation in the solution pH does not change the adsorption of diquat on the ZnO surface even in the case of formulation also as explained earlier. At higher pH (above pH 9) the ZnO surface is negatively charged (PZC of ZnO is  $\sim 9.3$ ) and the doubly positively charged diquat will have a tendency to approach the catalyst surface which may contribute to the fast removal of diquat. But the natural degradation of diquat (in the absence of catalyst and light) is also predominant at alkaline pH. The faster removal of diquat observed in the alkaline pH ( $> \text{pH } 9$ ) is the combined effect of better interaction of diquat with the ROS species generated by the surface and its natural degradation in this pH range. The current study further shows that the various additives present in the formulation have only

moderate effect on the photocatalytic degradation of diquat. The maximum percentage degradation is observed at the normal pH of 5.2. Further increase in the pH has less effect on the degradation, except at the alkaline pH as explained above. Since the optimum degradation is observed at the normal solution pH itself all further investigations are carried out at this pH unless indicated otherwise.

### **7.3.5 Effect of oxidants**

#### **7.3.5.1 Effect of H<sub>2</sub>O<sub>2</sub>**

As identified in many studies, H<sub>2</sub>O<sub>2</sub> is also one of the major intermediates/ byproducts formed during the photocatalytic reaction. In the current study also, formation of H<sub>2</sub>O<sub>2</sub> is observed. However the concentration of H<sub>2</sub>O<sub>2</sub> almost stabilizes in 3 hr even though the degradation of diquat continues unaffected (Fig. 7.9). Hence the H<sub>2</sub>O<sub>2</sub> formed in the system may be consumed in the process either by self-decomposition or by interaction with some reactive species. The concurrent formation and decomposition of H<sub>2</sub>O<sub>2</sub> and resulting oscillation in its concentration is reported in many photocatalytic systems [133].

In the case of an identical experiment in which extra H<sub>2</sub>O<sub>2</sub> is added to the system initially, the trend in the H<sub>2</sub>O<sub>2</sub> concentration remains fairly the same. However in this case the stabilization of H<sub>2</sub>O<sub>2</sub> does not happen after 3 hr. This is also consistent with the unpredictability in the net concentration of H<sub>2</sub>O<sub>2</sub> at any point of time due to the fluctuating domination of formation or the decomposition process which depends on a number of factors. The presence of adjuvants in the formulation and their interaction are complicating the inconsistency further.

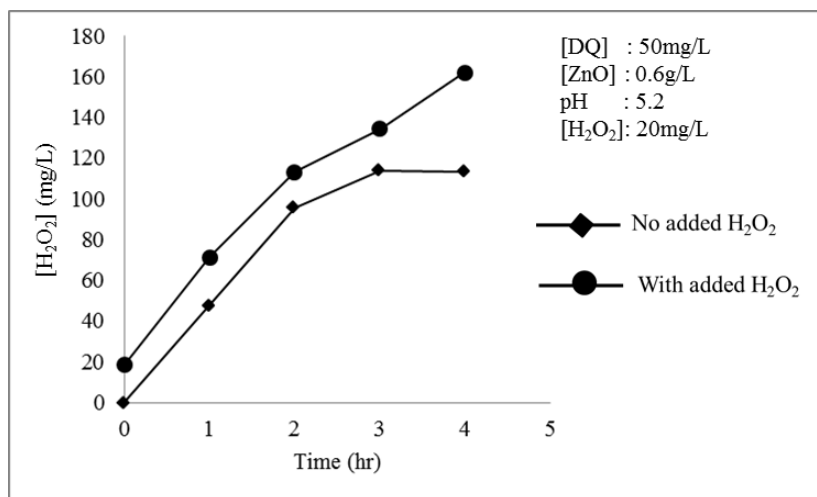


**Fig. 7.9:** Fate of in-situ formed and externally added H<sub>2</sub>O<sub>2</sub> during the photocatalytic degradation of diquat (formulation)

The effect of concentration of externally added H<sub>2</sub>O<sub>2</sub> on the photocatalytic degradation of DQ-F is tested by varying the concentration of H<sub>2</sub>O<sub>2</sub> in the system keeping the other parameters constant. Moderate inhibition in the percentage degradation is observed in the concentration range tested here (Fig. 7.10). Similar trend was observed in the case of DQ also. The detrimental effect of added H<sub>2</sub>O<sub>2</sub> has already been explained based on its ability to act as scavenger for the reactive  $\cdot\text{OH}$  radicals (Chapter 3 section 3.3.6).

There may be competition for the ROS, especially for the highly reactive  $\cdot\text{OH}$ , between the diquat and the added H<sub>2</sub>O<sub>2</sub> in the initial stage of the photocatalytic reaction. As the reaction proceeds more H<sub>2</sub>O<sub>2</sub> is formed in the system and more ROS will be scavenged. Hence the degradation of diquat slows down. However eventually the H<sub>2</sub>O<sub>2</sub> concentration also decreases due to self-decomposition and there may be

some kind of balancing between the consumption of ROS by the substrate and the  $\text{H}_2\text{O}_2$ . Hence the degradation of diquat is steady even with increased concentration of  $\text{H}_2\text{O}_2$ . In the case of diquat formulation the possibility of consumption of ROS by the added ingredients also cannot be ruled out.

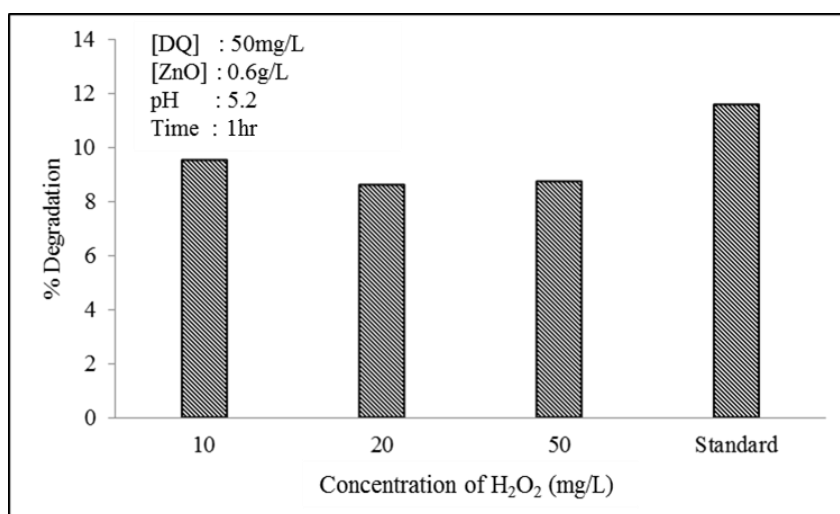


**Fig. 7.10:** Effect of added  $\text{H}_2\text{O}_2$  on the photocatalytic degradation of diquat formulation

### 7.3.5.2 Effect of persulphate (PS)

The effect of PS at various concentrations on the photocatalytic degradation of diquat is shown in the Fig. 7.11. The effect is negligible even at higher concentration of the oxidant. This is contrary to many reports in which PS acts as an enhancer for photocatalytic degradation of organic pollutants. The 'nil' effect of added oxidant PS on the degradation of DQ-F is similar to its effect on the photocatalytic degradation of DQ. The organic additives in the formulation can also act as ROS scavengers thereby preventing the effective utilization of reactive species by diquat

molecule. The absence of any enhancement by persulphate shows that the formation of the highly reactive  $\text{SO}_4^{\cdot-}$  radicals is not facilitated by sunlight. This is in line with the observations made and explanations given in the case of carbendazim in Chapter 3.

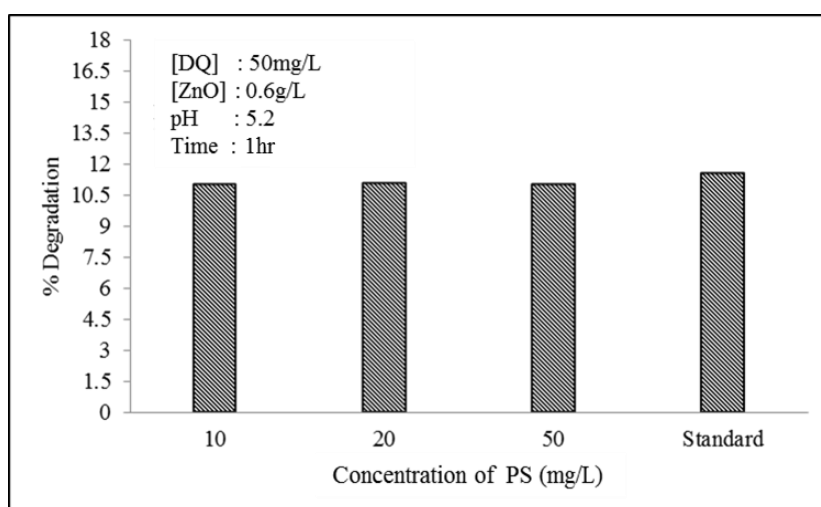


**Fig. 7.11:** Effect of added persulphate on the photocatalytic degradation of diquat formulation

### 7.3.6 Effect of common inorganic anions and cations

#### 7.3.6.1 Effect of anions

The inhibiting as well as enhancing effect of inorganic ions is already reported in many studies. Most of the inorganic ions interact with the ROS thereby affecting the availability of these species for the substrate. Hence the overall efficiency of the photocatalytic system will be affected. In this context, the effect of selected anions ( $\text{Cl}^-$ ,  $\text{SO}_4^{2-}$ ,  $\text{NO}_3^-$  and  $\text{HPO}_4^{2-}$ ) on the photocatalytic degradation of DQ-F is studied at different anion concentrations by keeping other parameters unchanged.

The results are presented in Figs. 7.12 and 7.13. The sodium salts are used for the study. In presence of chloride ions at various concentrations the percentage degradation is more or less same as the standard (without added anion). In the case of nitrate also, the effect is negligible. However, for sulphate ions, a slight increase in the percentage degradation is observed as the concentration increased from 5 to 10mg/L. But thereafter a stabilizing tendency is seen with increase in concentration.

The detrimental effect of  $\text{HPO}_4^{2-}$  on the ZnO mediated photocatalytic process has been already reported. The high adsorption of  $\text{HPO}_4^{2-}$  on the surface of ZnO was proven to be the cause of the inhibition. The preferential adsorption is confirmed by the adsorption studies (Chapter 3, section 3.3.7). However, as observed in the case of diquat technical, the degradation appears to be enhanced in presence of  $\text{HPO}_4^{2-}$  (Fig. 7.13).

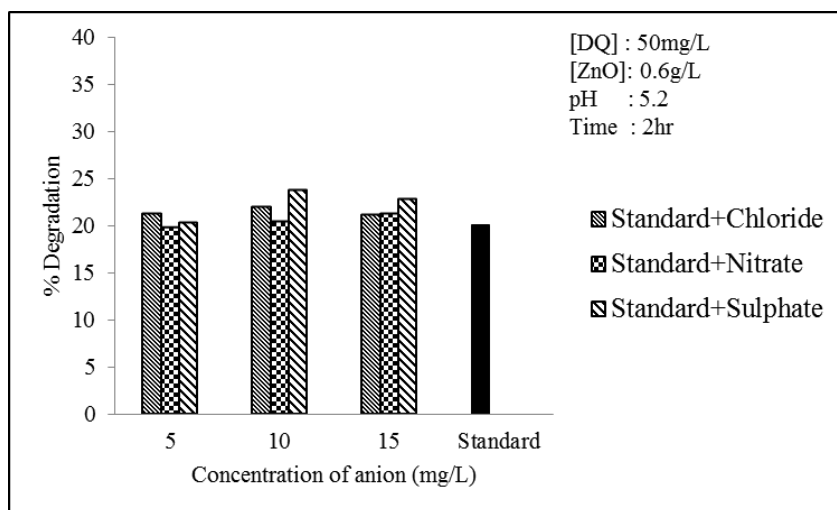


**Fig. 7.12:** Effect of anions on the photocatalytic degradation of diquat in the formulation [Cation: $\text{Na}^+$ ]

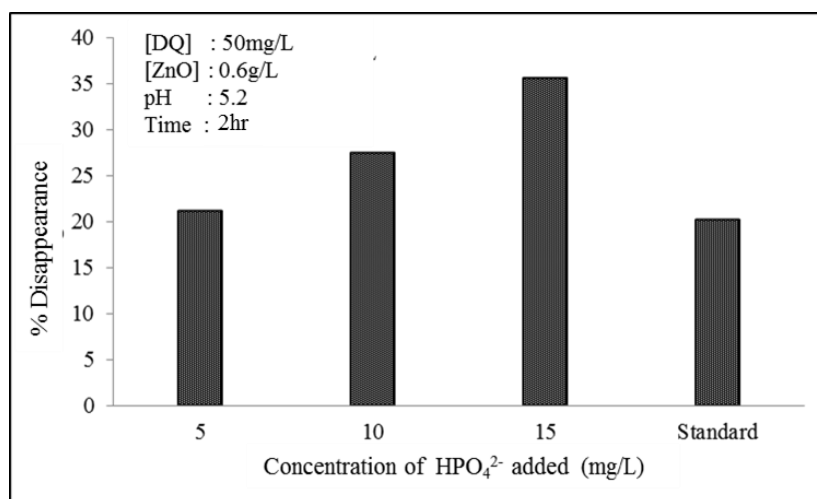


**Fig. 7.13:** Effect of  $\text{HPO}_4^{2-}$  on the photocatalytic degradation of diquat in the formulation [Cation: $\text{Na}^+$ ]

As demonstrated in Chapter 4, section 4.3.8, the apparent disappearance of diquat is not due to degradation but due to the formation of a coloured transient intermediate complex with  $\text{HPO}_4^{2-}$ . However, the precise effect of  $\text{HPO}_4^{2-}$  on the photocatalytic degradation of diquat cannot be evaluated for reasons already explained in Chapter 4 section 4.3.8. Eventually the diquat as well as the intermediates get degraded and mineralized as seen from the complete elimination of TOC (section 7.3.8).

### 7.3.6.2 Effect of cations

In this context, as done in the case of DQ, the effect of inorganic cations like  $\text{Na}^+$ ,  $\text{K}^+$ ,  $\text{Ca}^{2+}$ ,  $\text{Mg}^{2+}$  and  $\text{Al}^{3+}$  on the degradation of DQ-F is also studied. The  $\text{SO}_4^{2-}$  is the common anion used in this case. Fig. 7.14 shows the effect of selected cations at different concentrations on the degradation. Slight increase in the percentage degradation is observed in the case of  $\text{Na}^+$ ,  $\text{Ca}^{2+}$  and  $\text{Mg}^{2+}$ .

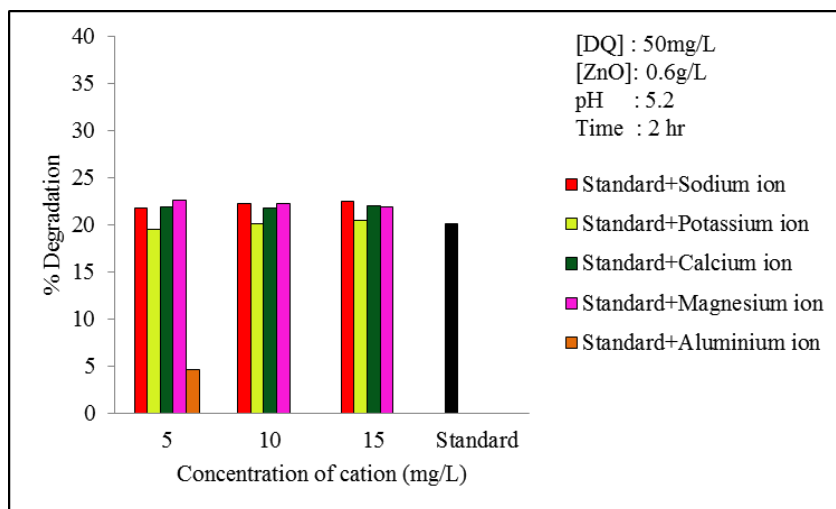


**Fig. 7.14:** Effect of cations on the photocatalytic degradation of diquat in the formulation [Anion:SO<sub>4</sub><sup>2-</sup>]

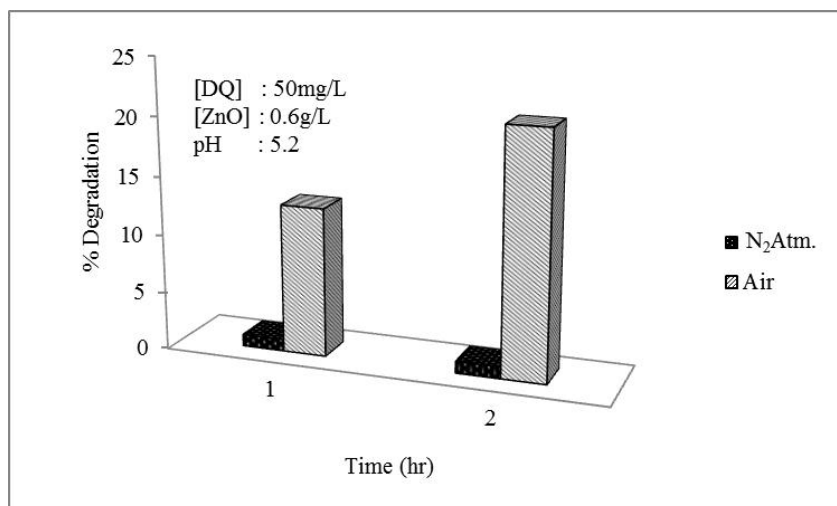
However, the effect of increasing concentration of these cations on the percentage degradation is negligible at least in the selected concentration range. The effect of K<sup>+</sup> is not much pronounced. As observed in the case of diquat technical, Al<sup>3+</sup> is inhibiting the photocatalytic reaction significantly in the case of its formulation also. The effect is more pronounced in the case of the formulation compared to the pure form. For the same catalyst loading and Al<sup>3+</sup> concentration, ~50% inhibition is observed for DQ while the degree of inhibition is much higher (>75%) for DQ-F. The degradation is almost fully inhibited in the case of DQ-F at Al<sup>3+</sup> concentration of >10mg/L.

Al<sup>3+</sup>, in the concentration range selected here, is known to get strongly adsorbed on the ZnO surface (Chapter 4 section 4.3.8). But in this concentration range the surface may not be fully covered and there

may be vacant ZnO sites which can get activated by light irradiation. The exposed ZnO surface has contributed to the moderate degradation of diquat in the pure form even in the presence of  $\text{Al}^{3+}$ , which is evident from the generation of  $\cdot\text{OH}$  radicals as measured by the photoluminescence spectrum (see section 4.3.8 of Chapter 4). However, for diquat formulation at the same catalyst loading, the inhibition is almost complete at  $\text{Al}^{3+}$  concentration  $>10\text{mg/L}$  suggesting that the surface is getting fully blocked and the  $\cdot\text{OH}$  formation is inhibited. It is possible that the added formulation ingredients such as emulsifiers are also getting adsorbed on the catalyst surface along with the  $\text{Al}^{3+}$ . Thus the active sites on ZnO surface are fully blocked from the incident radiation and the photocatalytic activity is completely inhibited.

### **7.3.7 Effect of oxygen**

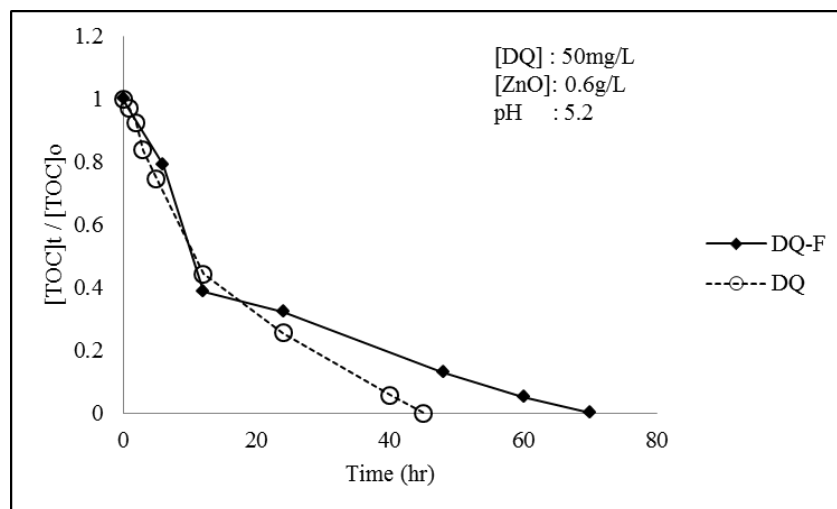
The effect of dissolved oxygen on the photocatalytic degradation of DQ-F is investigated by deaerating the system with  $\text{N}_2$  and carrying out the photocatalytic experiment under the optimized conditions. In the absence of  $\text{O}_2$ , less than 1% degradation is observed (Fig. 7.15). No change in percentage degradation was noticed as the irradiation time is increased in the case of the deaerated system. The observed inhibition in photocatalytic degradation may be due to the fast electron-hole recombination in the absence of dissolved oxygen, since it plays key role as electron scavenger. In the absence of  $\text{O}_2$ , the formation of ROS, in particular  $\cdot\text{OH}$  radicals is also inhibited as explained in earlier chapters. This is identical to the results in the case of DQ thereby indicating that the formulation adjuvants do not make any difference as far as the role of  $\text{O}_2$  is concerned.



**Fig. 7.15:** Effect of deaeration by N<sub>2</sub> on the photocatalytic degradation of diquat in the formulation

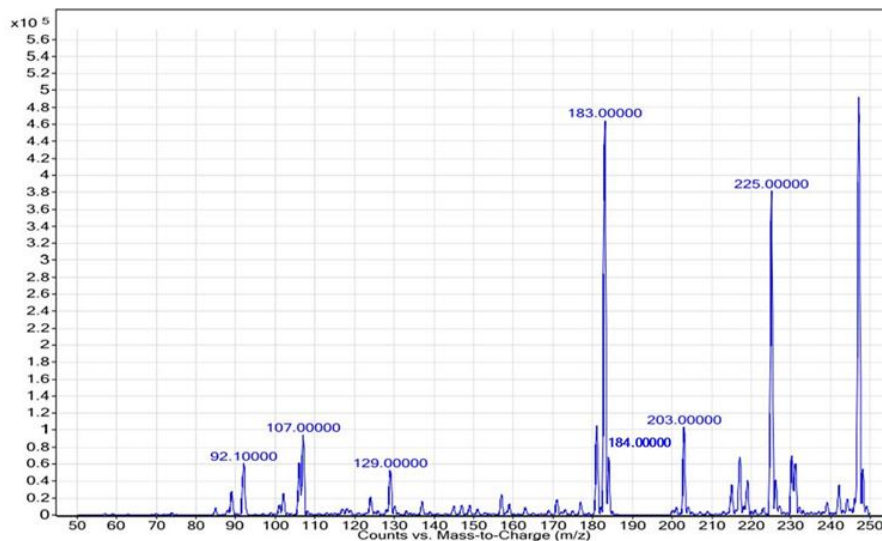
### 7.3.8 Mineralization of diquat in the formulation

Complete mineralization of organic pollutants in water is the real measurement of the efficiency of the treatment process. Along with the active ingredient, DQ-F also contains many added ingredients such as emulsifiers and stabilizing agents. Most of the data discussed above confirms that the degradation process of diquat proceeds unaffected even in the formulated form though the rate is moderately less. The ROS can also interact with the adjuvants and the intermediates formed from them which may ultimately influence the mineralization of diquat. This is verified by measuring the TOC content at different times of irradiation as shown in Fig. 7.16.

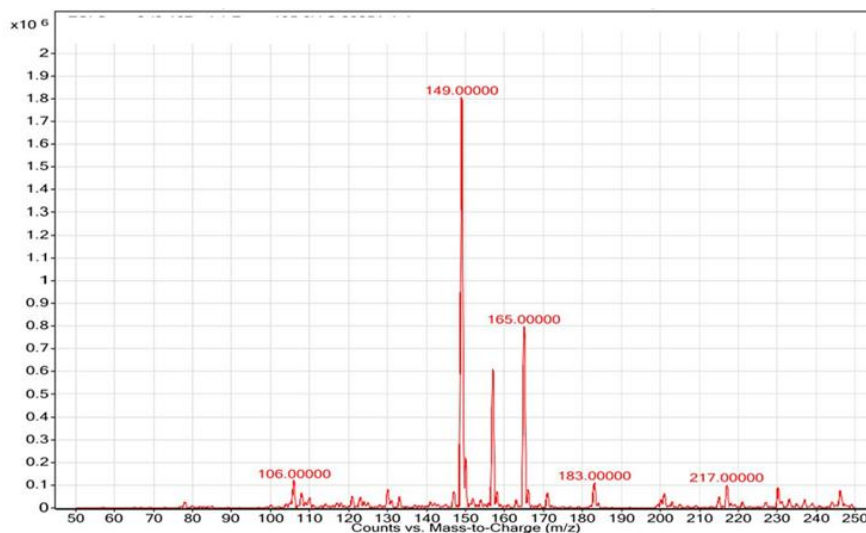


**Fig. 7.16:** Depletion in the TOC content with time of irradiation during the solar photocatalytic degradation of diquat

In the early stages of irradiation, sudden decrease in TOC content is observed in the case of both technical and formulated diquat. After 10 hr the TOC removal becomes slow. The steep initial decrease in TOC shows that the reaction proceeds through multiple intermediates and some of the intermediates may be undergoing faster degradation and mineralization. However, there may be other intermediates which mineralize slowly and hence the decrease in TOC after 10 hr irradiation is slower. Comparison of the rates of TOC removal in the case of DQ and DQ-F shows that the rate is slower in the latter case at later stages of the reaction. As explained above this may be because some of the ROS are consumed for the degradation and mineralization of the adjuvants also. The LC/MS spectrum of the diquat formulation before irradiation (Fig. 7.17) shows extra peaks at  $m/z$  225 and 247, which are not present in the technical compound indicating that they are from the added ingredients. Many of the peaks present before irradiation disappear in the LC/MS spectra after irradiation for 10 hr (Fig. 7.18).



**Fig. 7.17:** Mass spectrum of diquat formulation before photocatalytic reaction

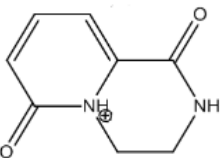
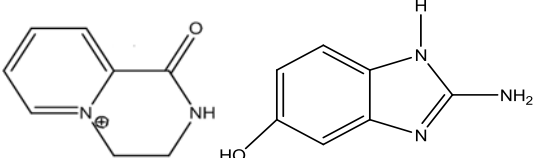
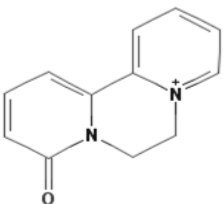
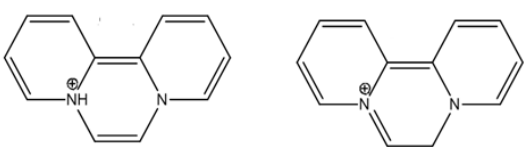


**Fig. 7.18:** Mass spectrum showing various intermediates formed during the photocatalytic degradation of diquat formulation over ZnO after 10hr of irradiation

This confirms that at least some of the added ingredients get degraded faster than diquat under the photocatalytic conditions. Major

intermediates of degradation formed during the photocatalytic reaction are identified using LC/MS and are shown in the Table 7.2. It is found that most of the intermediates formed during the photocatalytic degradation of diquat formulation are similar to those formed during the degradation of diquat technical (refer Table 4.2 in Chapter 4).

**Table 7.2:** Comparative list of intermediates identified during the photocatalytic degradation of diquat technical and diquat formulation

| Molecular/<br>Cationic<br>mass | Intermediates/ Reaction products  | Comment   |
|--------------------------------|---|---|
| 165                            |                   | Present in both diquat technical and diquat formulation |
| 149                            |                 | Present in both diquat technical and diquat formulation |
| 217                            | <br>(hydrolysed) | Present in both diquat technical and diquat formulation |
| 183                            |                 | Present in both diquat technical and diquat formulation |

#### 7.4 Mechanism of the photocatalytic degradation of diquat formulation

The intermediates formed during the degradation of DQ-F and DQ are more or less the same. The effect of various parameters on the degradation also is identical in both cases. Hence it may be inferred that the mechanism of degradation and mineralization is same in the case of both technical and formulated diquat. Since the formulation adjuvants also get mineralized under the same reaction conditions, it may be concluded that photocatalysis is a powerful tool for the purification of water contaminated with the field application of diquat.

The simple mechanism explained in detail in earlier chapters can be summarized as follows:



vb:Valence band, cb:Conduction band

The photo induced hole can oxidize a donor molecule (D) [diquat (DQ), and adjuvants in this case].



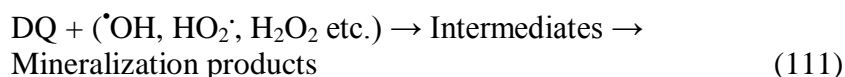
The strong oxidation power of the  $h^+$  oxidizes the water to produce hydroxyl radical ( $\cdot\text{OH}$ ).



The electron can reduce the O<sub>2</sub> present in the system to produce superoxide radical, which results in the formation of more ROS as follows:



Reduction of H<sub>2</sub>O<sub>2</sub> produces hydroxyl radical ( $\cdot\text{OH}$ ).



The  $\cdot\text{OH}$  radicals which are strong oxidants ( $E^o=2.8$  eV) can oxidize diquat and other organic molecules present in the reaction medium to various intermediate products as identified earlier. Ultimately these intermediates also get completely mineralized, leading to a COD of zero as observed in this study.

## 7.5 Conclusion

The sunlight induced photocatalytic degradation in presence of ZnO catalyst is an effective tool for the complete mineralization of diquat (in formulation form) present in water. The degradation follows pseudo first order kinetics. Added oxidants such as H<sub>2</sub>O<sub>2</sub> and persulphate (in the selected concentration range) have little effect on the degradation. Some of the cations/anions (salts) present in natural water such as Na<sup>+</sup>, K<sup>+</sup>, Ca<sup>2+</sup> and Mg<sup>2+</sup> (cations) as well as Cl<sup>-</sup>, SO<sub>4</sub><sup>2-</sup> and NO<sub>3</sub><sup>-</sup> (anions) have no effect on the degradation. However Al<sup>3+</sup> adversely affects the degradation. In

presence of  $\text{HPO}_4^{2-}$  as noticed in the case of the technical form also, diquat is forming a coloured complex which follows a different mechanism for the degradation. The kinetics as well as the intermediates formed during the degradation of diquat in technical as well as formulated form is more or less identical. Hence, the mechanism of the degradation is fairly the same. Even in presence of adjuvants, complete mineralization of diquat is achieved by photocatalysis, though the mineralization takes a longer time.

*.....✻.....*

---

**SOLAR PHOTOCATALYSIS MEDIATED BY ZnO FOR THE  
REMOVAL OF DIQUAT AND CARBENDAZIM POLLUTANTS  
FROM NATURAL WATER SYSTEMS**

---

- 8.1 *Introduction*
  - 8.2 *Experimental*
  - 8.3 *Results and discussion*
  - 8.4 *Conclusion*
- 

**8.1 Introduction**

Fertilizers and pesticides used for agricultural purposes are ultimately polluting the natural water resources. Removal of these contaminants from the polluted water requires complex treatment processes since they consist of different kinds of organic and inorganic materials. The efficiency of the treatment process depends upon various parameters such as pH, concentration and type of inorganic ions, organic loading, suspended solids etc. present in the polluted water.

In this context, the possibility of application of the solar photocatalytic technique discussed in earlier chapters for the removal of pesticide pollutants from actual field water is examined. For this purpose, the test pollutants carbendazim and diquat are dissolved in water collected from different natural water resources such as sea, river and well and the same is used as the polluted experimental water samples. Natural water, after

filtration to remove suspended matters, contains various soluble salts which can affect the photocatalytic degradation of both diquat and carbendazim in presence of ZnO as demonstrated in earlier chapters.

## 8.2 Experimental

### 8.2.1 Chemicals

Materials and their specifications are the same as shown in sections 3.2.1 and 4.2.1 of Chapters 3 and 4. The water samples used in the study are collected from well, river and sea in the neighborhood of our laboratory. The sea water was collected from the Arabian Sea in Cherai (Kochi-Kerala-India) area, and is designated as SW. The river water samples were collected from Periyar at three locations and are termed as R1, R2, R3. The well water samples were collected from three locations and are termed as W1, W2, W3. The locations from where water samples were collected shown in Fig. 8.1.

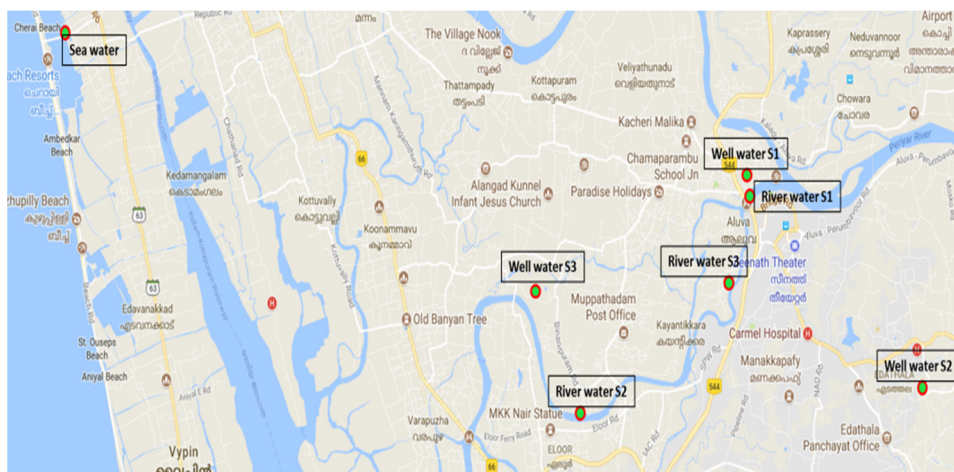


Fig. 8.1: The locations from where the water samples were collected

Standard solutions of the pollutants are prepared by dissolving the required quantity of diquat and carbendazim in the water collected from different sources.

### **8.2.2 Analytical procedures**

The concentration of diquat and carbendazim remaining in solution after photocatalytic treatment was analyzed by spectrophotometry at 310 nm and 284 nm respectively. The dissolved substances in the water collected from different sources do not interfere during the analysis of carbendazim and diquat, as verified by relevant analytical tests using distilled water and natural water under identical conditions.

The anion and cation concentrations are measured by the procedure given in Chapter 3 section 3.2.2.

Total dissolved solids in the water samples were analysed using Eutech Instruments Ion 2700 TDS analyser and turbidity was measured using ELICO CL52 D Nephelometer.

### **8.2.3 Photocatalytic Experimental set up**

The experimental setup is similar to that mentioned in Chapter 3 section 3.2.6. All other procedures are also same as mentioned in the previous chapters, unless indicated otherwise.

## 8.3 Results and discussion

### 8.3.1 Preliminary experiments

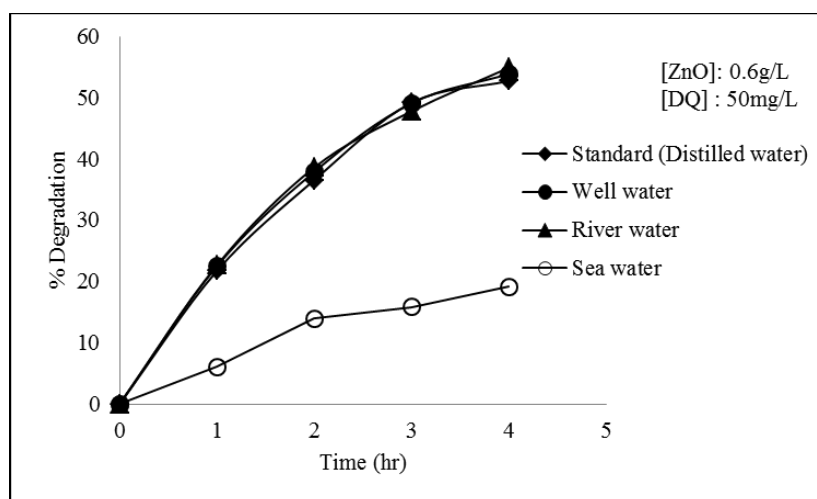
The water samples collected from different natural resources were analysed for different parameters and the results are given in Table 8.1. It is seen that the well and river water samples do not contain considerable amount of ions such as aluminium and phosphate which are known to drastically inhibit the photocatalytic degradation of diquat and carbendazim. As expected, comparatively higher concentration of ions such as chloride, sulphate, sodium, potassium, calcium and magnesium was observed in the sea water. In well-water, the concentration of most of the ions is higher than that selected for the studies conducted in the previous chapters. Compared to well water and sea water, the concentration of ions present in the river water is much less. Also the pH of the samples is in the range that has been already proven to have no effect on the photocatalytic degradation of carbendazim and diquat. The characteristics of well water and river water from various sources were more or less the same. Hence, well water (W1), river water (R1) and sea water (SW) were chosen for the study.

Table 8.1. Different Parameters and the results

| Serial<br>No. | Parameters                    | Well     |          | Well     |          | River    |          | River    |  | Sea |  |
|---------------|-------------------------------|----------|----------|----------|----------|----------|----------|----------|--|-----|--|
|               |                               | water-W1 | water-W2 | water-W3 | water-R1 | water-R2 | water-R3 | water-SW |  |     |  |
| 1             | pH                            | 8.16     | 6.48     | 5.93     | 7.75     | 7.19     | 7.05     | 7.91     |  |     |  |
| 2             | Total dissolved solids (mg/L) | 243      | 206      | 88       | 33.74    | 113      | 36       | 36050    |  |     |  |
| 3             | Turbidity (NTU)               | 1        | 1        | 1        | 2        | 2        | 3        | 12       |  |     |  |
| 4             | Chloride (mg/L)               | 19.19    | 16.7     | 16.98    | 2.63     | 22       | 2.96     | 18600    |  |     |  |
| 5             | Sulphate (mg/L)               | 22.4     | 23       | 1.88     | 1.43     | 4.7      | 1.42     | 5320     |  |     |  |
| 6             | Nitrate (mg/L)                | 43.79    | 0.42     | 14.59    | 1.11     | 2.29     | 2.46     | 10       |  |     |  |
| 7             | Phosphate (mg/L)              | ND       | ND       | ND       | ND       | ND       | ND       | 4        |  |     |  |
| 8             | Sodium (mg/L)                 | 145      | 74       | 55       | 26.44    | 26       | 17       | 9800     |  |     |  |
| 9             | Potassium (mg/L)              | 24       | 11.8     | 9.9      | 4.2      | 3.56     | 2.6      | 1571     |  |     |  |
| 10            | Calcium (mg/L)                | 71       | 35       | 5.9      | 9.72     | 22.68    | 8.8      | 1236     |  |     |  |
| 11            | Magnesium (mg/L)              | 43.3     | 20       | 5        | 7.33     | 6.26     | 4.2      | 8759     |  |     |  |
| 12            | Aluminium (mg/L)              | 0.11     | ND       | ND       | ND       | 1        | ND       | 0.16     |  |     |  |
| 13            | Silica (mg/L)                 | 76       | 20       | 9.5      | 46       | 10       | 9        | 56       |  |     |  |
| 14            | COD (mg/L)                    | 1.9      | 1.95     | 1.8      | 1.2      | 1.9      | 1.85     | 3.8      |  |     |  |

ND-Not detected

Comparison of the photocatalytic degradation of diquat and carbendazim prepared in different water samples is given in Figs. 8.2 and 8.3 respectively. For diquat and carbendazim, the percentage degradation in well and river water is comparable to that under standard conditions in distilled water. However, the degradation is much less in sea water. But in all cases, the percentage degradation increases with time, though the rate of increase is low in the case of sea water. The inhibition in sea water is due to the high ion concentration resulting in low generation of ROS and unproductive interactions. Further, the ions can get adsorbed on the surface of the catalyst, thereby inhibiting various surface initiated processes which are important in photocatalysis. Details are discussed in earlier chapters.



**Fig. 8.2:** Degradation of diquat in different water matrices

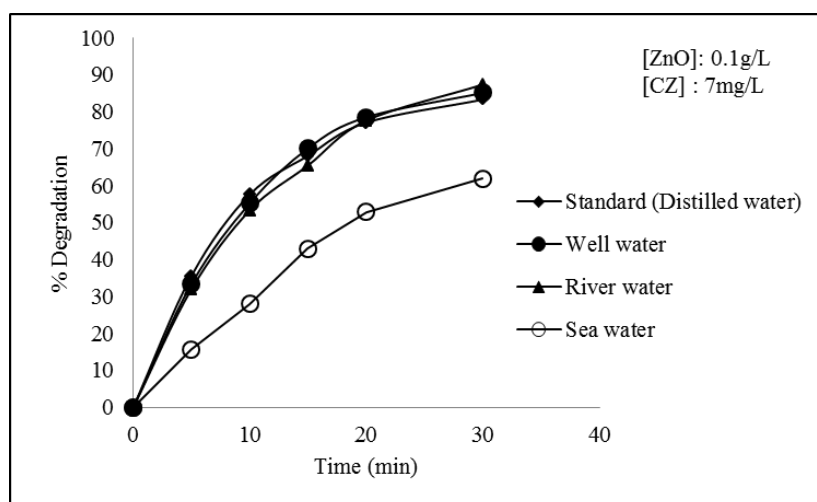


**Fig. 8.3:** Degradation of carbendazim in different water matrices

The experimental results further indicate that small amount of various of inorganic ionic species present in river and well water have less effect on the photocatalytic degradation of carbendazim and diquat. But in the case of sea water, the inhibition may be due to the presence of relatively higher amount cations and anions. In order to verify this, the effect of various salts at higher concentrations on the degradation, is tested by varying the concentration of salts from 0.1 to 3.0% in distilled water. Analysis shows that the sea water contains ~3.0% NaCl and hence the maximum concentrations of all the selected salts are kept at 3.0%. The catalyst loading and other reaction parameters are kept the same as the optimized conditions for diquat and carbendazim. The effect of different salts on the photocatalytic degradation of carbendazim and diquat is shown in Figs. 8.4 and 8.5.

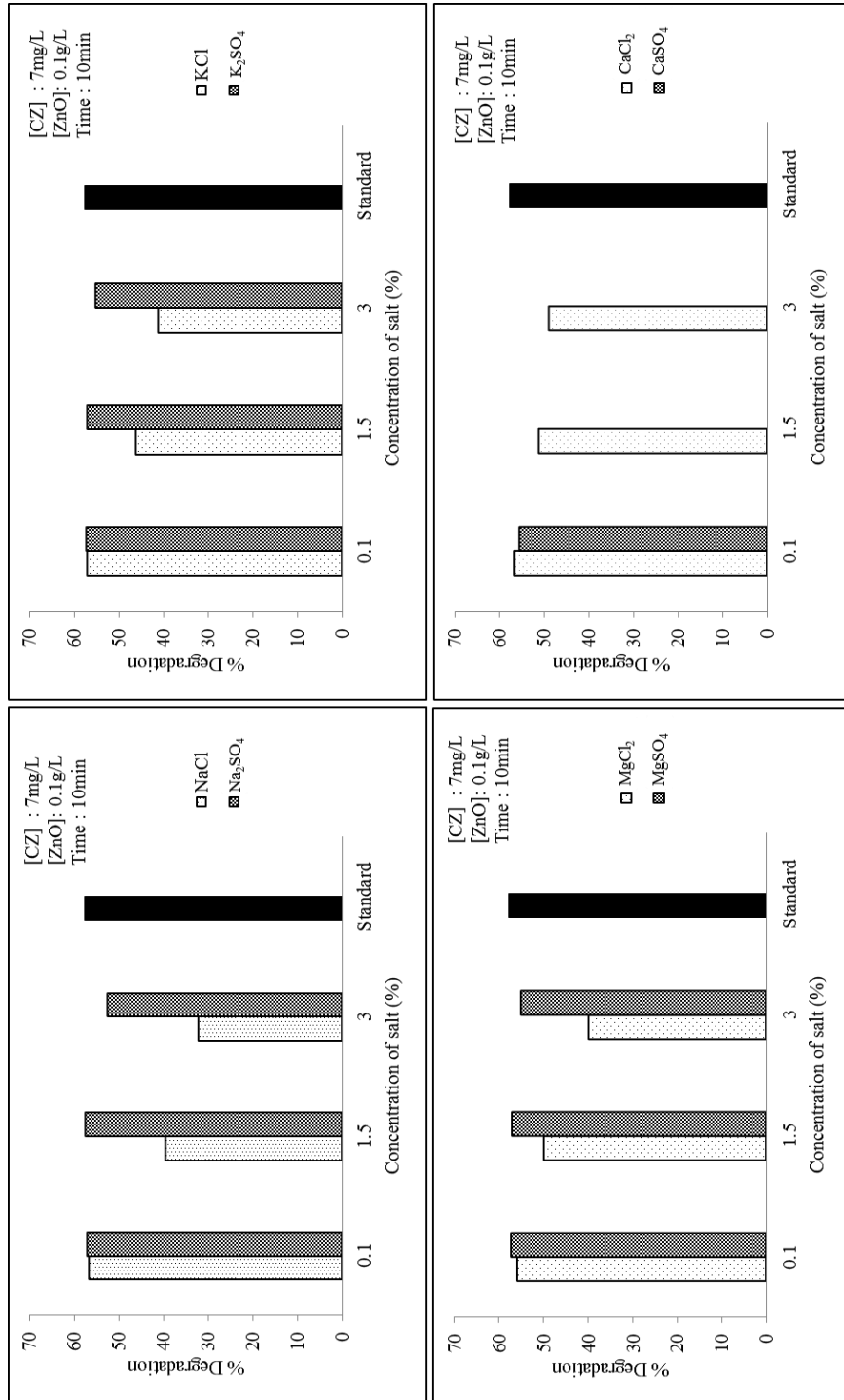


Fig. 8.4: Effect of selected salts at various concentrations on the degradation of carbendazim

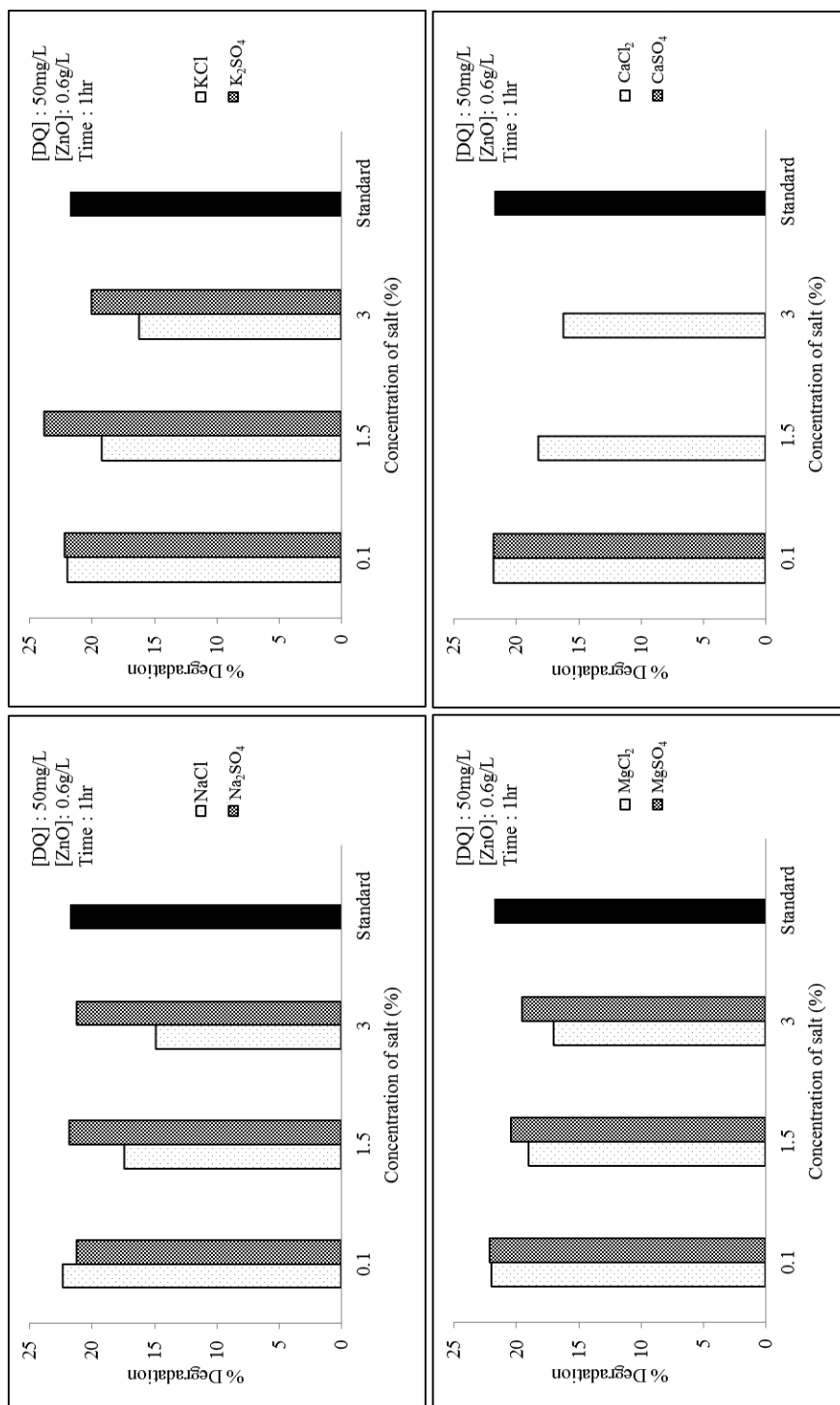


Fig. 8.5: Effect of selected salts at various concentrations on the degradation of diquat

At 0.1% all the selected salts have no effect on the degradation of both carbendazim and diquat. Moderate inhibition in the percentage degradation was observed in the case of all chloride salts at 1.5%, with the extent of inhibition varying according to the nature of cation. Thus the inhibition is in the order  $\text{NaCl} > \text{KCl} > \text{MgCl}_2 \approx \text{CaCl}_2$  for carbendazim degradation. The same order, i.e.,  $\text{NaCl} > \text{KCl} > \text{CaCl}_2 \approx \text{MgCl}_2$  is maintained in the case of diquat degradation also. The inhibition is further enhanced at 3% of chloride salt and the comparative trend remains more or less the same. But for  $\text{Na}_2\text{SO}_4$ ,  $\text{K}_2\text{SO}_4$  and  $\text{MgSO}_4$ , the inhibition is only moderate/less significant even at 3% (salt concentration). Hence it may be inferred that for  $\text{SO}_4^{2-}$  anion there is no significant effect on the degradation as the concentration is increased at least up to 3%. In the case of  $\text{Ca}^{2+}$ , only one concentration is tested for the  $\text{CaSO}_4$  (0.1%), due to solubility constraints, while for other salts the selected concentration range is 0.1-3.0%. From the study it may be inferred that the selected cations have relatively less effect on the percentage degradation of carbendazim and diquat in the selected concentration range and the inhibition is primarily due to the anions. The observed decrease in percentage degradation in sea water is primarily due to the presence of  $\text{Cl}^-$  inherent in it. In order to verify this, the major salts present in sea water were added to distilled water one by one and the effect on the degradation is tested in the case of both diquat and carbendazim. The results are presented in Figs. 8.6 and 8.7. In presence of 3.0%  $\text{NaCl}$  added to the distilled water, the percentage degradation of diquat after 1 hr irradiation is decreasing from ~22% to ~15%. For carbendazim the degradation in

presence of 3% NaCl after 10 min was ~32% compared to ~60% in pure distilled water.

The observed percentage degradation for diquat in presence of 3% NaCl in distilled water was much higher compared to that in real sea water, i.e. 15% vs 6% in 1 hr. In the case of carbendazim also, the degradation is moderately less in sea water compared to distilled water with 3% NaCl dissolved in it (28% vs 32% in 10 min) (Compare Figs. 8.2 vs 8.5 for diquat and 8.3 vs 8.4 for carbendazim). Hence it is clear that other ions present in sea water also contribute substantially to the inhibition. To study the effect of other anions and cations present in the sea water, experiments were conducted by adding definite quantities of different salts one by one to the solution of diquat and carbendazim in distilled water in the following sequence and measuring the photocatalytic degradation at definite time interval after the addition of each component. The salts are added as follows, in sequence:

NaCl ( $\text{Na}^+ = 0.98\%$ )

$\text{K}_2\text{SO}_4$  ( $\text{K}^+ = 0.15\%$ )

$\text{MgSO}_4$  ( $\text{Mg}^{2+} = 0.85\%$ )

$\text{CaSO}_4$  ( $\text{Ca}^{2+} = 0.15\%$ )

The effect of addition of each salt on the percentage degradation of diquat and carbendazim is clearly evident in Figs. 8.6 and 8.7.

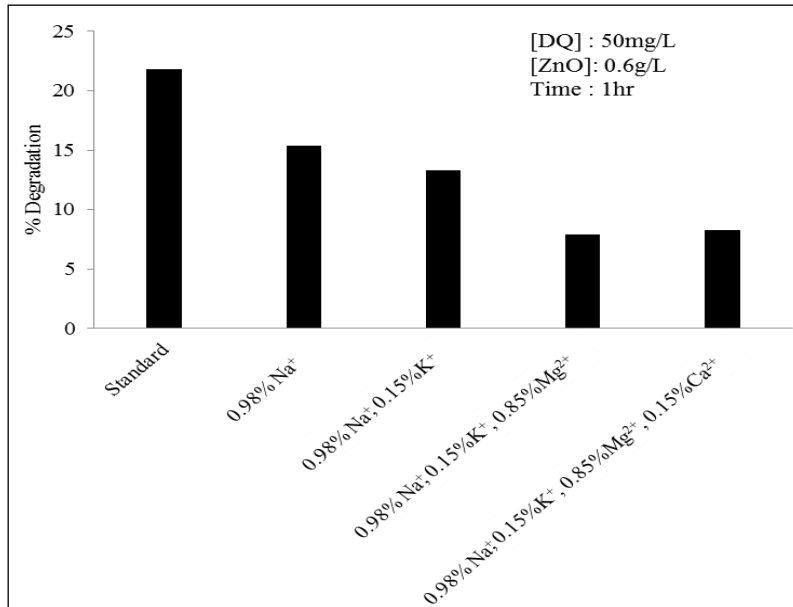


**Fig. 8.6:** Decrease in percentage degradation of diquat in presence of sequentially added salts

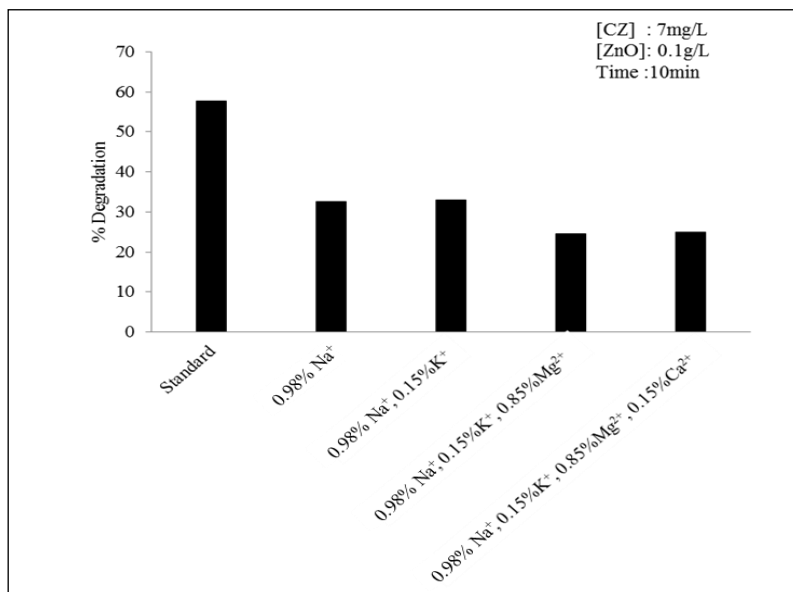


**Fig. 8.7:** Decrease in percentage degradation of carbendazim in presence of sequentially added salts

It is found that with the addition of each salt to the system, the degradation is inhibited and finally a stage is reached in which the percentage degradation is comparable to the value observed in sea water medium. In the case of both diquat and carbendazim, a sudden decrease in percentage degradation was observed when 0.85%  $\text{Mg}^{2+}$  is added (Figs. 8.6 and 8.7). But when the effects of ions are individually tested it is observed that  $\text{Mg}^{2+}$  has only little effect on the percentage degradation. Hence it is possible that the inhibition by  $\text{Mg}^{2+}$  is enhanced in presence of other anions/salts. In order to verify this, experiments were conducted by changing the sequence of salt addition in the following manner and the degradation is measured at definite time interval after the addition of each component.

NaCl ( $\text{Na}^+ = 0.98\%$ )  
MgSO<sub>4</sub> ( $\text{Mg}^{2+} = 0.85\%$ )  
K<sub>2</sub>SO<sub>4</sub> ( $\text{K}^+ = 0.15\%$ )  
CaSO<sub>4</sub> ( $\text{Ca}^{2+} = 0.15\%$ )

The results are presented in Figs. 8.8 and 8.9. It is found that the effect of addition of magnesium salt on the percentage degradation of both diquat and carbendazim is negligible when the sequence of addition is changed. The observed decrease in percentage degradation when  $\text{Mg}^{2+}$  is added at later stage may be due to the sudden increase in the total dissolved ion concentration rather than the specific effect of  $\text{Mg}^{2+}$  ion (see the results in Figs. 8.6 and 8.8). This observation is fairly similar in the case of carbendazim also (inhibition being more evident after the addition of the third salt, irrespective of  $\text{Mg}^{2+}$  or  $\text{K}^+$ ). This is further evident from the observation that the degradation does not decrease further even after the addition of  $\text{Ca}^{2+}$ , because the optimum salt concentration for maximum inhibition has already reached with the addition of  $\text{Mg}^{2+}$  (in Fig. 8.6) and  $\text{K}^+$  (in Fig. 8.8).

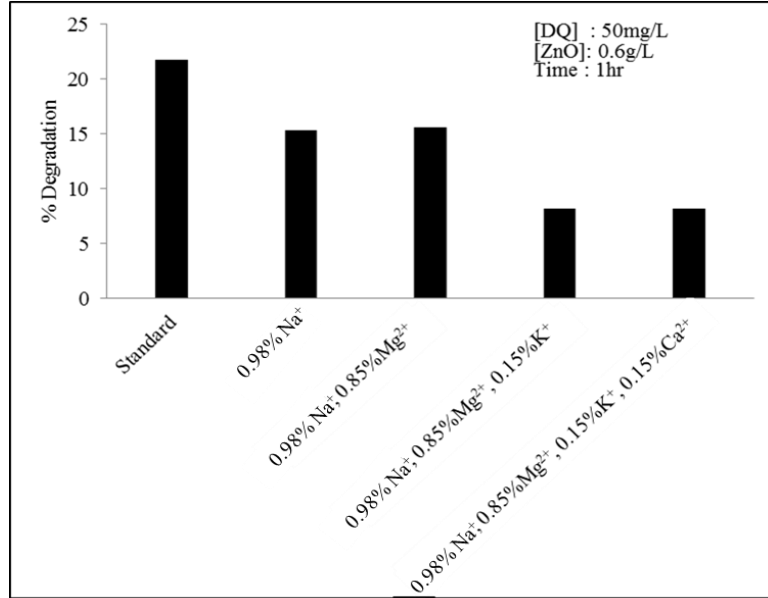


Fig. 8.8: Effect of changing the salt addition sequence on the percentage degradation of diquat

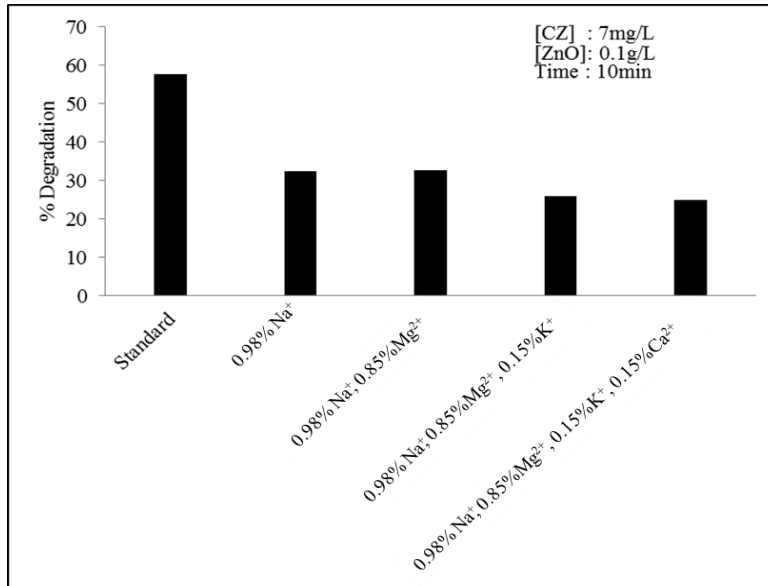
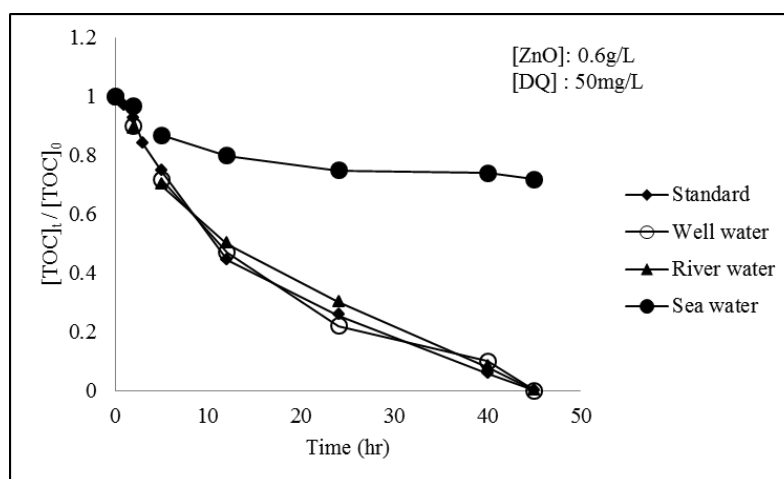


Fig. 8.9: Effect of changing the salt addition sequence on the percentage degradation of carbendazim

### 8.3.2 Mineralization

To study the mineralization process of diquat and carbendazim in the real field water, different water samples containing the pollutants are irradiated for longer time under the optimized conditions. TOC measurements were made to follow the mineralization. The results are shown in Figs. 8.10 and 8.11. It is found that, for well and river waters, the mineralization process follows the same trend as observed in the case of distilled water. In both cases, i.e. for diquat and carbendazim the mineralization is complete in ~45 hr and ~8 hr respectively. But in sea water the mineralization process is very slow in both cases. The detrimental effect of high ion concentration on the removal of organic pollutants in sea water is already reported by Martinez et al. [151]. The high concentration of chloride ion present in sea water can act as a hole and  $\cdot\text{OH}$  radical scavenger thereby substantially reducing the photocatalytic degradation efficiency. Similar deactivation of catalyst in sea water is also reported in the case of both  $\text{TiO}_2$  and  $\text{ZnO}$  [152,153].



**Fig. 8.10:** Mineralization of diquat in different water matrices

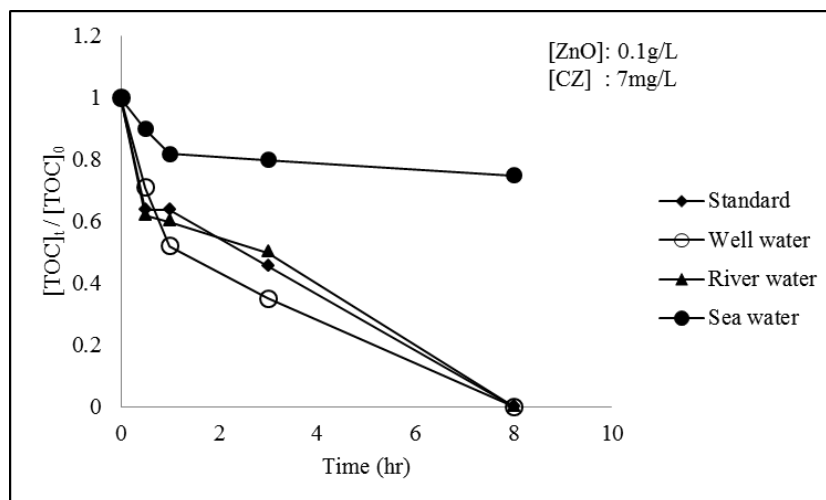
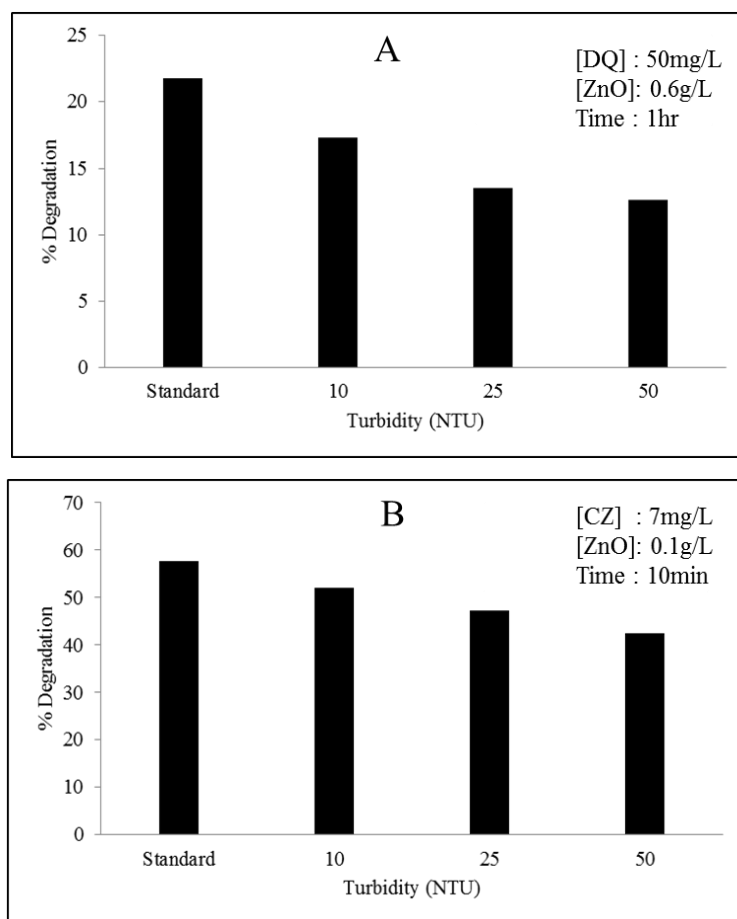


Fig. 8.11: Mineralization of carbendazim in different water matrices

### 8.3.3 Effect of solution turbidity

The water from natural resources may contain suspended solids which affect the solution clarity. During the photocatalytic reaction, the suspended solids will interfere with the light penetration thereby decreasing the efficiency of the reaction system. Also, these solids may get adsorbed on the catalyst and decrease the availability of active sites for better interaction with the contaminants. To study the effect of solution turbidity on the photocatalytic degradation of diquat and carbendazim, experiments were conducted at various turbidity levels (10-50 NTU) keeping other parameters constant. The turbidity of the solution is adjusted by adding clay into the test solution. It is found that as the solution turbidity increases percentage degradation of both carbendazim and diquat decreases. This may be due to the scattering of light by the suspended particles which hinders the penetration of light through the reaction medium thereby reducing the generation of ROS.



**Fig. 8.12:** Effect of solution turbidity on the photocatalytic degradation of (A) diquat and (B) carbendazim

## 8.4 Conclusion

The photocatalytic degradation of diquat and carbendazim in natural waters from different sources is tested. It is found that the degradation is comparable under the optimized conditions in both well water and river water. In sea water matrix, the percentage degradation is low, but the degradation increases slowly with time of irradiation. Since the inhibiting

ions such as phosphate and aluminium are not present in the water samples collected, the observed decrease in percentage degradation is due to the comparatively higher concentrations of other ions such as  $\text{Cl}^-$ ,  $\text{SO}_4^{2-}$ ,  $\text{Na}^+$ ,  $\text{K}^+$ ,  $\text{Mg}^{2+}$  and  $\text{Ca}^{2+}$ . Chloride ion is inhibiting the degradation as the concentration increases, while sulphate ion has only little effect. Similarly cations such as sodium, potassium, magnesium and calcium are not interfering with the photocatalytic degradation in the tested concentration range. However, when their cumulative concentration reaches critical level, enhanced inhibition is observed, irrespective of the nature of the salt. The degradation as well as mineralization of both diquat and carbendazim is extremely slow in sea water. This highlights the need for keeping marine resources free from pollution of pesticides and other organic contaminants.

.....❧.....

Semiconductor mediated photocatalysis has been one of the most widely investigated Advanced Oxidation Processes (AOP) for the decontamination of water from chemical and bacterial pollutants. The potential for using the renewable solar energy as the source of activation makes the technique more attractive environmentally and economically. Recently it has been proven that the wide light absorption range of ZnO including a part of the visible spectrum of sunlight makes it a favorable solar photocatalyst. Current study is an investigation on the possibility of application of solar photocatalysis mediated by ZnO for the mineralization of two pesticides, i.e. diquat (herbicide) and carbendazim (fungicide) in contaminated water. The study also explored the effect of various formulation additives on the degradation and mineralization of these active ingredients. The mutual effect of diquat and carbendazim when they are simultaneously present in water on the photocatalytic degradation of respective components is also evaluated. The effect of naturally occurring contaminants in water, in particular dissolved salts and turbidity on the photocatalytic degradation of the pollutants is also investigated. The laboratory optimized parameters for the solar photocatalytic removal of

carbendazim and diquat are further verified using real field water samples from well/river/sea as the matrix.

The catalyst ZnO used for the study was characterized by various techniques such as SEM, TEM, XRD, surface area, adsorption etc. to identify the phase, porosity, particle size and morphology. The selected pollutants, carbendazim and diquat were analyzed by UV-Visible spectrophotometry. Various anion and cation concentrations in the photocatalytic system were analyzed by Ion Chromatography and ICP/MS technique respectively. For each pollutant, various reaction parameters such as pH, catalyst loading, pollutant concentration, presence of contaminants, O<sub>2</sub> etc. were optimized. Some of the transient intermediates formed during the degradation were also identified using LC/MS technique.

Major findings and the conclusions from the study are as follows:

Sunlight induced photocatalysis in presence of ZnO catalyst is an effective tool for the complete mineralization of traces of carbendazim and diquat present in water. The degradation and mineralization of both pollutants are achieved even in their formulated form as well. The photocatalytic degradation of carbendazim and diquat follows pseudo first order kinetics. The kinetics is similar irrespective of whether they are in combination or in their formulated form. The adjuvants present in the formulation decrease the rate of photocatalytic degradation of carbendazim and diquat. This decrease is attributed to the preferential adsorption of the adjuvants on the surface sites of the catalyst and

consequent decrease in the efficiency of light absorption and the generation of reactive oxygen species (ROS) such as  $\cdot\text{OH}$ .

The degradation of both pollutants is mutually inhibited when they are simultaneously present in water. Carbendazim inhibits the degradation of diquat more than the other way. Added oxidants such as  $\text{H}_2\text{O}_2$  and persulphate (in the selected concentration range) have little effect on the degradation of both carbendazim and diquat. Some of the cations/anions (salts) present in the natural water systems such as  $\text{Na}^+$ ,  $\text{K}^+$ ,  $\text{Ca}^{2+}$  and  $\text{Mg}^{2+}$  (cations), as well as  $\text{Cl}^-$ ,  $\text{SO}_4^{2-}$  and  $\text{NO}_3^-$  (anions) have very little effect on the degradation. However  $\text{Al}^{3+}$  adversely affects the degradation of both. The photocatalytic degradation of carbendazim gets strongly inhibited in presence of  $\text{HPO}_4^{2-}$ . However, in presence of  $\text{HPO}_4^{2-}$ , diquat (both technical and formulation) forms a coloured complex which alters the mechanism for the degradation. The solution turbidity is also a major factor that affects the photocatalytic degradation in presence of ZnO. As the solution turbidity increases the degradation rate decreases.

The kinetics of the photocatalytic degradation as well as the intermediates formed during the degradation of diquat in technical and formulated forms are more or less identical. Hence it may be presumed that the mechanism of the degradation is not affected by the formulation adjuvants. Similar observations are made in the case of both carbendazim technical and formulation also. The intermediates in both cases are identified by LC/MS. Even in presence of adjuvants, complete mineralization of diquat and carbendazim is achieved by photocatalysis as seen from the decreasing COD and TOC values. Mineralization takes

longer time in the case of formulation. The degradation is facile in well water and river water showing that mild variations in the characteristics of water do not affect the degradation significantly. But the degradation is slow in sea water which is confirmed to be due to its high salt content. This clearly illustrates that chemical pollutants of all types will remain for much longer time in the ocean water which can detrimentally affect all marine organisms in the short term as well as long term. The mechanism of the process is proposed and discussed in detail.

The study shows that the pesticides diquat and carbendazim applied in the field can get eventually mineralized leaving no chemical residues in water or soil, if ZnO is incorporated as an additive to the formulation at an appropriate dosage. Since ZnO is also a micronutrient, it may not adversely affect the crops at lower concentration. However, its impact on the production process, shelf life, stability etc. has to be confirmed by each manufacturer, depending on their product specification. In any case, the study confirms that solar photocatalysis mediated by ZnO is a powerful, economical and environment-friendly technology for the mineralization of recalcitrant pollutants such as diquat and carbendazim in aquatic environment.

.....❧.....

## References

- [1] R.Connor, J.M.Faures, J.Kuylenstierna, Evaluation of water use, Water in a changing world, The United Nations world water development report 3 (2009).
- [2] Water a shared responsibility, The United Nations world water development report 2 (2006).
- [3] The human right to water and sanitation, frequently asked questions on water quality - UN-Water (2010).
- [4] L.Lam, Water pollution - human nature, Technology & the environment, *fubini.swarthmore.edu/~ENVS2/S2007/llam1/water4.html*
- [5] J.L.Cook, P.Baumann, J.A.Jackman and D.Stevenson, Pesticides characteristics that affect water quality?'. *http://insects.tamu.edu/extension/bulletins/water/water\_01.html*
- [6] M.Sarwar, M.Salman, The paramount benefits of using insecticides and their worldwide importance in food production, *International Journal of Bioinformatics and Biomedical Engineering*, 3(1) (2015) 359-365.
- [7] W.Mnif, A.I.H.Hassine, A.Bouaziz, A.Bartegi, O.Thomas, B.Roig, Effect of endocrine disruptor pesticides: A Review, *Int. J. Environ. Res. Public Health*, 8 (2011) 2265-2303.
- [8] Global market for pesticides to reach \$65.3 billion in 2017, BCC research, Market research report (2012).
- [9] D.Workman, Top pesticides exporters - World's top exports *www.worldstopexports.com/top-pesticides-exporters/*
- [10] W.J.Zhang, F.B.Jiang, J.F.Ou, Global pesticide consumption and pollution: with China as a focus, Proceedings of the *International Academy of Ecology and Environmental Sciences*, 2 (2011) 125-144.

- [11] S.K.Gupta, J.P.Jani, H.N.Saiyed, S.K.Kashyap, Health hazards in pesticide formulators exposed to a combination of pesticides. *Indian J Med Res*, 79 (1984) 666.
- [12] G.S.Toteja, J.Dasgupta, B.N.Saxena, R.L. Kalra, Surveillance of food contaminants in India, Report of an ICMR Task Force Study (Part 1), Indian Council of Medical Research, New Delhi (1993).
- [13] R.Pala, K.Chakrabartia, A.Chakraborty, A.Chowdhurya, Pencycuron application to soils: Degradation and effect on microbiological parameters, *Chemosphere*, 60 (2005) 1513 - 1522.
- [14] Environmental effects of pesticides. An impression of recent scientific literature, Pesticide action Network Europe (2010).
- [15] S.Islam, M.Tanaka, Impacts of pollution on coastal and marine ecosystems including coastal and marine fisheries and approach for management: A review, *Marine Poll. Bull.*, 48 (2004) 624 - 649.
- [16] Joint Group of Experts on the Scientific Aspect of Marine Pollution (GESAMP): The State of the Marine Environment UNEP Regional Seas Report and Studies No.115, UNEP (1990).
- [17] S.Tanabe, S.Watanabe, H.Kan, R.Tatsukawa, Capacity and mode of PCB metabolism in small cetaceans, *Mar. Mammal Sci.*, 4 (1988) 103 - 124.
- [18] A.Mitra, C.Chatterjee, F.B.Mandal, Synthetic chemical pesticides and their effect on birds, *Res. J. Environ. Toxicology*, 5 (2011) 81 - 96.
- [19] Health implications from monocrotophos use: A review of the evidence in India, World Health Organization (2013).
- [20] A.Agrawal, R.S.Pandey, B.Sharma, Water pollution with special reference to pesticide contamination in India, *J. Water Resource and Protection*, 2 (2010) 432 - 448.

- [21] W.F.Perrin, R.L.Brownell Jr, Z.Kaiya, L.Jiankang, Conservation and management of the Ganges river dolphin, *Platanista gangetica*, in India. Proceedings of Workshop on Biology and Conservation of the Platanistoid Dolphins, Wuhan, China (1986) 64 - 69.
- [22] S.Samanta, Metal and pesticide pollution scenario in Ganga River system, *Aquat. Ecosyst Health Manag.*, 16 (2013) 454 - 464.
- [23] E.Maloschik, A.Ernst, G.Hegedűs, B.Darvas, A.Székács, Monitoring water-polluting pesticides in Hungary, *Microchem. J.*, 85 (2007) 88 - 97.
- [24] I.K.Konstantinou, D.G.Hela, T.A.Albanis, The status of pesticide pollution in surface waters (rivers and lakes) of Greece. Part I. Review on occurrence and levels, *Environ. Pollut.*, 141 (2006) 555 - 570.
- [25] R.C.Martínez, E.R.Gonzalo, M.E.F.Laespada, F.J.S.San Román, Evaluation of surface and ground water pollution due to herbicides in agricultural areas of Zamora and Salamanca (Spain), *J. Chromatogr A*, 869 (2000) 471 - 480.
- [26] Continuing disaster of endosulfan in Kasargod and Kannur districts of Kerala. <https://endosulfan.wordpress.com/2011/02/01/disaster-of-endosulfan-in-kasargod-and-kannur>
- [27] S.N.Meijer, M.Shoib, L.M.M.Jantunen, K.C.Jones, T.Harner, Air-soil exchange of organochlorine pesticides in agricultural Soils, field measurements using a novel in-situ sampling device, *Environ. Sci. Technol.* 37 (2003) 1292 - 1299.
- [28] K.Pozo, T.Harner, M.Shoib, R.Urrutia, R.Barra, O.Parra, S.Focard, Passive-sampler derived air concentrations of persistent organic pollutants on a North-South transect in Chile, *Environ. Sci. Technol.* 38 (2004) 6529 - 6537.

- [29] Y.Deng, R.Zhao, Advanced oxidation processes (AOPs) in waste water treatment, *Curr. pollution rep.* 1 (2015) 167 - 176.
- [30] Photoelectrochemistry, Photocatalysis and Photoreactor, M.Schiavello (ed.), Reidel Publishing Co., Dordrecht, (1985) 457.
- [31] R.Munter, Advanced oxidation processes-Current status and prospects, *Proc. Estonian Acad. Sci. Chem*, 50 (2001) 59 - 80.
- [32] O.Legrini, E.Oliveros, A.M.Braun, Photochemical processes for water treatment, *Chem. Rev.*, 93 (1993) 671 - 698.
- [33] P.D.Francis, The use of ultraviolet light and ozone to remove dissolved organic contaminants in ultra-pure water, Report, M 2221, Electricity Council Research Centre, Capenhurst: Chester, England (1988).
- [34] Y.Sun, J.J.Pignatello, Photochemical reactions involved in the total mineralization of 2,4-D by  $\text{Fe}^{3+}/\text{H}_2\text{O}_2/\text{UV}$ , *Environ. Sci. Technol.*, 27 (1993) 304 - 310.
- [35] C.Kittle, Introduction to solid state physics, Wiley Eastern Limited, New Delhi (1976).
- [36] B.Viswanathan, S.Sivasanker, A.V.Ramaswamy, Catalysis Principles and applications, Narosa publishing house, New Delhi (2002).
- [37] J.M.Herrmann, Heterogeneous photocatalysis: an emerging discipline involving multiphase systems, *Catal. Today*, 24 (1995) 157 - 164.
- [38] J.M.Herrmann, Heterogeneous photocatalysis: fundamentals and applications to the removal of various types of aqueous pollutants, *Catal. Today*, 53 (1999) 115 - 129.
- [39] J.M.Herrmann, C.Guillard, P.Pichat, Heterogeneous photocatalysis: an emerging technology for water treatment, *Catal. Today* 17 (1993) 7 - 20.

- [40] G.Rothenberger , J.Moser, M.Grazel, N.Serpone, D.K.Sharma, Charge carrier trapping and recombination dynamics in small semiconductor particles, *J. Am. Chem. Soc.*, 107 (1985) 8054 - 8059.
- [41] M.Gratzel, Heterogeneous Photochemical Electron Transfer. CRC Press, BocaRaton, FL (1989).
- [42] A.L.Linsebigler, G.Lu, J.T.Yates, Photocatalysis on TiO<sub>2</sub> surfaces: Principles, Mechanisms, and selected results, *Chem. Rev.*, 95 (1995) 735 - 758.
- [43] M.R.Hoffmann, S.T.Martin, W.Choi, D.W.Bahnmann, Environmental applications of semiconductor photocatalysis, *Chem. Rev.*, 95 (1995) 69 - 96.
- [44] J.Peral, X.Domonech, D.H.Ollis, Heterogeneous photocatalysis for purification, decontamination and deodorization of air, *J. Chem. Technol. Biotechnol.*, 70 (1997) 117 - 140.
- [45] M.N.Chong, B.Jin, C.W.K.Chow, C.Saint, Recent developments in photocatalytic water treatment technology: A review, *Water Res.*, 44 (2010) 2997 - 3027.
- [46] S.Malato, P.Ferna´ndez-Iba´n˜ez, M.I.Maldonado, J.Blanco, W.Gernjak, Decontamination and disinfection of water by solar photocatalysis: Recent overview and trends, *Catal. Today*, 147 (2009) 1 - 59.
- [47] S.Sakthivel, B.Neppolian, M.V.Shankar, B.Arabindoo, M.Palanichamy, V.Murugesan, Solar photocatalytic degradation of azo dye: Comparison of photocatalytic efficiency of ZnO and TiO<sub>2</sub>, *Sol. Energy Mater. Sol. Cells*, 77 (2003) 65 - 82.
- [48] Y.Nosaka, M.Nishikawa, A.Y.Nosaka, Spectroscopic Investigation of the Mechanism of Photocatalysis, *Molecules*, 19 (2014) 18248 - 18267.

- [49] A.Mills, S. L.Hunte, An overview of semiconductor photocatalysis, *J. Photochem. Photobiol A: Chemistry*, 108 (1997) 1 - 35.
- [50] A.E.Pirbazari, Photocatalytical treatment of synthetic waste water containing chlorophenols by TiO<sub>2</sub> nanoparticles sensitized with cobalt phthalocyanine under visible light, *J. Chem. Eng. Process Technol.*, 8 (2017), doi:10.4172/2157-7048.1000333.
- [51] D.Robert, S.Malato, Solar photocatalysis: a clean process for water detoxification, *Sci. Total Environ.*, 291 (2002) 85 - 97.
- [52] M.Saquib, M.Muneer, Semiconductor mediated photocatalysed degradation of an anthraquinone dye, Remaol Brilliant Blue R under sunlight and artificial light source, *Dyes Pigm.*, 53 (2002) 237 - 249.
- [53] M.Izadifard, G.Achhari, C.H.Langford, Application of photocatalysts and LED Light sources in drinking water treatment, *Catalysts*, 3 (2013) 726 - 743.
- [54] Y.Lu, Y.Lin, T.Xie, L.Chen, S.Yi, D.Wang, Effect of photogenerated charge transfer on the photocatalysis in high performance hybrid Pt-Co-ZnO nano structure photocatalyst, *Appl. Mater. Interfaces*, 5 (2013) 4017 - 4020.
- [55] Priyanka, V.C.Srivastava, Photocatalytic oxidation of dye bearing waste water by Fe doped ZnO, *Ind. Eng. Chem. Res.*, 52 (2013) 17790 - 17799.
- [56] R.Ullah, J.Dutta, Photocatalytic degradation of organic dyes with manganese doped ZnO nanoparticles, *J. Hazard. Mater.*, 156 (2008)194-200.
- [57] J.J.Wu, C.H.Tseng, Photocatalytic properties of nc-Au/ZnO nanorod composites, *Appl. Catal. B: Environmental*, 66 (2006) 51 - 57.
- [58] S.Anandan, A.Vinu, T.Mori, N.Gokulakrishnan, P.Srinivasa, V.Murugesan, K.Ariga, Photocatalytic degradation of 2,4,6 trichlorophenol using La doped ZnO in aqueous suspension, *Catal. Commun.*, 8 (2007) 1377 - 1382.

- [59] Y.Chang, J.Xu, Y.Zhang, S.Ma, L.Xin, L.Zhu, C.Xu, Optical properties and photocatalytic performance of Pd modified ZnO samples, *J. Phys. Chem. C*, 113 (2009) 18761 - 18767.
- [60] A.Khatee, R.D.C.Soltani, Y.Hanifehpour, M.Safarpour, H.G.Ranjadar, S.W.Joo, Synthesis and characterization of dysprosium doped ZnO nanoparticles for photocatalysis of textile dye under visible light irradiation, *Ind. Eng. Chem. Res.*, 53 (2014) 1924 - 1932.
- [61] J.C.Sin, S.M.Lam, I.Saroshi, K.T.Lee, A.R.Mohammed, Sunlight photocatalytic activity enhancement of novel europium doped ZnO hierarchical micro/nanospheres for degradation of phenol, *Appl. Catal. B: Environmental*, 148 (2014) 258 - 268.
- [62] K.Maeda, T.Takata, M.Hara, N.Saito, Y.Inone, H.Kobayashi, K.Domen, GaN: ZnO solid solution a photocatalyst for visible-light driven overall water splitting, *J. Am. Chem. Soc.*, 127 (2005) 8286 - 8287.
- [63] S.Martha, K.M.Parida, Fabrication of nano N doped  $\text{In}_2\text{Ga}_2\text{ZnO}_7$  for photocatalytic hydrogen production under visible light, *Int. J. Hydrog. Energy*, 37 (2012) 17936 - 17946.
- [64] A.Mclaren, T.V.Solis, G.Li, S.C.Tsang, Shape and size effect of ZnO nanocrystals on photocatalytic activity, *J. Am. Chem. Soc.*, 131 (2009) 12540 - 12541.
- [65] G.D.Mihai, V.Meynen, M.Mertens, N.Bilba, P.Cool, E.F.Vasant, ZnO nanoparticle supported on mesoporous MCM-41 and SBA-15 a comparative physicochemical and photocatalytic study, *J. Mater. Sci.*, 45 (2010) 5786 - 5794.
- [66] A.N.Ejhihi, F.K.Chermahini, Incorporated ZnO onto nano clinoptilolite particle as the active centers in the photodegradation of phenylhydrazine, *J. Ind. Eng. Chem.*, 20 (2013) 695 - 704.

- [67] A.Omidi, A.H.Yangjeh, M.Pirhashemi, Application of ultrasonic irradiation method for preparation of ZnO nanostructures doped with Sb<sup>3+</sup> ions as a highly efficient photocatalyst, *Appl. Sur. Sci.*, 276 (2013) 468 - 475.
- [68] A.B.Patil, K.R.Patil, S.K.Pardeshi, Ecofriendly synthesis and solar photocatalytic activity of S-doped ZnO, *J. Hazard. Mater.*, 183 (2010) 315 - 323.
- [69] M.Pirhashemi, A.H.Yangjeh, Simple and large scale one pot method for preparation of AgBr-ZnO nano composite as highly efficient visible light photocatalyst. *Appl. Sur. Sci.*, 283 (2013) 1080 - 1088.
- [70] Y.Qiu, M.Yang, H.Fan, Y.Xu, Y.Shao, X.Yang, S.Yang, Synthesis and characterization of nitrogen doped ZnO tetrapods and application in photocatalytic degradation of organic pollutants under visible light, *Mater. Lett.*, 99 (2013) 105 - 107.
- [71] C.Shifu, Z.Wei, Z.Sujnan, L.Wei, Preparation, characterization and photocatalytic activity of N-containing ZnO powder, *Chem. Eng. J.*, 148 (2009) 263 - 269.
- [72] J.X.Sun, Y.P.Yuan, L.G.Qiu, X.Jiang, A.J.Xie, Y.H.Shen, J.F.Zhu, Fabrication of composite photocatalyst g-C<sub>3</sub>N<sub>4</sub>-ZnO and enhancement of photocatalytic activity under visible light, *Dalton Trans.*, 41 (2012) 6756 - 6763.
- [73] Y.Wang, X.Li, N.Wang, X.Quan, Y.Chen, Controllable synthesis of ZnO flowers and their morphology dependent photocatalytic activities, *Sep. Purif. Technol.*, 62 (2008) 727 - 732.
- [74] W.Yan, H.Fan, C.Yang, Ultra-fast synthesis and enhanced photocatalytic properties of alpha-Fe<sub>2</sub>O<sub>3</sub>/ZnO core shell structure, *Mater. Lett.*, 65 (2011) 1595 - 1597.

- [75] X.Zhang, J.Qin, Y.Xne, P.Yu, B. Zhang, L.Wang, R.Liu, Effect of aspect ratio and surface defects on the photocatalytic activity of ZnO nanorods, *Sci. Rep.*, 4 (2014) 4596.
- [76] M.L.M.Trevino, J.L.G.Mar, L.H.Reyes, N.A.R. Delgado, M.I. Maldonado, A.H.Remirez, Activity of the ZnO- Fe<sub>2</sub>O<sub>3</sub> catalyst on the degradation of dicamba and 2,4-D herbicides using simulated solar light, *Ceram. Int.*, 40 (2014) 8701 - 8708.
- [77] S.Navarro, J.Fenoll, N.Vela, E.Ruiz, G.Navarro, Photocatalytic degradation of eight pesticides in leaching water by use of ZnO under natural sunlight, *J. Hazard. Mater.*, 172 (2009) 1303 - 1310.
- [78] M.Mahalakshmi, B.Arabindoo, M.Palanichamy, V.Murugesan, Photocatalytic degradation of carbofuran using semiconductor oxides, *J. Hazard. Mater.*, 143 (2007) 240 - 245.
- [79] J.Fenoll, P.Hellin, P.Flores, C.M.Martinz, S.Navarro, Degradation intermediates and reaction pathway of carbofuran in leaching water using TiO<sub>2</sub> and ZnO as photocatalyst under natural sunlight, *J. Photochem. Photobio. A: Chemistry*, 251 (2013) 33 - 40.
- [80] V.G.G.Kanmoni, S.Daniel, G.A.G.Raj, Photocatalytic degradation of chlorpyrifos in aqueous suspension using nanocrystals of ZnO and TiO<sub>2</sub>, *Reac. Kinet. Mech. Cat.*, 106 (2012) 325 - 339.
- [81] M.V.Pinna, A.Pusino, Direct and indirect photolysis of cyhalofop in aqueous systems, *Chemosphere*, 82 (2011) 817 - 821.
- [82] J.Fenoll, E.Ruiz, P.Hellín, P.Flores, S.Navarro, Heterogeneous photocatalytic oxidation of cyprodinil and fludioxonil in leaching water under solar irradiation, *Chemosphere*, 85 (2011) 1262 - 1268.
- [83] J.Fenoll, F.Pilar, H.Pilar, C.M.Martínez, S.Navarro, Photodegradation of eight miscellaneous pesticides in drinking water after treatment with semiconductor materials under sunlight at pilot plant scale, *Chem. Eng. J.*, 204 - 206 (2012) 54 - 64.

- [84] J.Fenoll, P.Hellin, C.M.Martinez, P.Flores, S.Navarro, Semiconductor oxides-sensitized photodegradation of fenamiphos in leaching water under natural sunlight, *Appl. Catal. B: Environmental*, 115 - 116 (2012) 31 - 37.
- [85] J.Fenoll, P.Sabater, G. Navarro, G.P.Lucas, S.Navarro, Photocatalytic transformation of sixteen substituted phenyl urea herbicides in aqueous semiconductor suspensions: Intermediates and degradation pathways, *J. Hazard. Mater.*, 244 - 245 (2013) 370 - 379.
- [86] J.Fenoll, P.Sabater, G.Navarro, N.Vela, G.P.Lucas, S.Navarro, Abatement kinetics of 30 sulfonylurea herbicide residues in water by photocatalytic treatment with semiconductor materials, *J. Environ. Manage.*, 130 (2013) 361 - 368.
- [87] N.Daneshvar, S.Aber, M.S.Seyed Dorraji, A.R.Khataee, M.H.Rsouliard, Photocatalytic degradation of the insecticide diazinon in the presence of prepared nano crystalline ZnO powders under irradiation of UV-C light, *Sep. and Purif. Technol.*, 58 (2007) 91 - 98.
- [88] S.A.Naman, Z.A.A.Khammas, F.M.Hussein, Photo-Oxidative degradation of insecticide dichlorovos by a combined semiconductors and organic sensitizers in aqueous media, *J. Photochem. Photobiol. A: Chemistry*, 153 (2002) 229 - 236.
- [89] E.Evgenidou, K.Fytianos, I.Poulios, Semiconductor-sensitized photodegradation of dichlorovos in water using TiO<sub>2</sub> and ZnO as catalysts, *Appl. Catalysis B: Environmental*, 59 (2005) 81 - 89.
- [90] E.Evgenidou, K.Fytianos, I.Poulios, Photocatalytic oxidation of dimethoate in aqueous solutions, *J. Photochem. Photobiol. A: Chemistry*, 175 (2005) 29 - 38.
- [91] S.Sathiyarayanan, P.E.Ravi, A.Ramesh, Applications of ZnO nanorods as photocatalyst for the decontamination of imdacloprid and spirotetramat residue in water, *The open catalysis journal*, 2 (2009) 24 - 32

- [92] F.C.Doria, A.C.Borges, J.K.Kim, A.Nathan, J.C.Joo, L.C.Campos, Removal of metaldehyde through photocatalytic reaction using nano sized ZnO composites, *Water Air Soil pollut.*, 224 (2013) 1434.
- [93] D.Mijin, M.Savic, P.Snezana, A.Smiljanic, O.Glavaski, M.Jovanovic, S.Petrovic, A study of the photocatalytic degradation of met amitron in ZnO water suspension, *Desalination*, 249 (2009) 286 - 292.
- [94] P.V.Korake, R.S.Dhabbe, A.N.Kadam, Y.B.Gaikwad, K.M.Garadkar, Highly active lanthanum doped ZnO nanorods for photodegradation of metasytox, *J. Photochem. Photobiol. B: Biology*, 130 (2014) 11 - 19.
- [95] A.Tomasevic, J.Daja, S.Petrovic, E.Kiss, D.Mijin, A study of the photocatalytic degradation of methomyl by UV light, *Chem. Ind. Chem. Eng. Q.*, 15 (2009) 17 - 19.
- [96] E.Evgenidou, I.Konstantinou, K.Fytianos, I.Poulios, T.Albanis, Photocatalytic oxidation of methyl parathion over TiO<sub>2</sub> and ZnO suspension, *Catal. Today*, 124 (2007) 156 - 162.
- [97] S.Anandan, A.Vinu, K.L.P.S.Lovely, N.Gokulakrishnan, P.Srinivasu, T.Mori, V.Murugesan, V.Sivamurugan, K.Ariga, Photocatalytic activity of La doped ZnO for the degradation of monocrotophos in aqueous suspension, *J. Mol. Catal. A: Chem.*, 266 (2007) 149 - 157.
- [98] S.Anandan, A.Vinu, N.Venkatachalam, B.Arabindoo, V.Murugesan, Photocatalytic activity of ZnO impregnated H $\beta$  and mechanical mix of ZnO/H $\beta$  in the degradation of monocrotophos in aqueous solution, *J. Mol. Catal. A: Chem.*, 256 (2006) 312 - 320.
- [99] S.Rabindranathan, S.Devipriya, S.Yesodharan, Photocatalytic degradation of phosphamidon on semiconductor oxides, *J. Hazard. Mater.*, 102 (2003) 217 - 229.
- [100] P.V.Korake, R.Sridhakrishna, P.P.Hankare, K.M.Garadkar, Photocatalytic degradation of phosphamidon using Ag doped ZnO nanorods, *Toxicol. Enviro. Chem.*, 94 (2012) 1075 - 1085.

- [101] P.Kaur, P.Bansal, D.Sud, Heterostructured nanophotocatalysts for degradation of organophosphate pesticides from aqueous streams, *J. Korean Chem. Soc.*, 57 (2013) 382 - 388.
- [102] M.Muneer, B.Abbad, M.S.Takriff, M.Said, A.Benamor, M.S.Nasser, A.W.Mohammad, Photocatalytic degradation of pentachlorophenol using ZnO nanoparticle: Study of intermediates and toxicity, *Int. J. Environ. Res.*, 11 (2017) 461 - 473.
- [103] P.Mazellier, É.Leroy, J.De Laat, B.Legube, Degradation of carbendazim by UV/H<sub>2</sub>O<sub>2</sub> investigated by kinetic modeling, *Environ. Chem. Lett.*, 1 (2003) 68 - 72.
- [104] M.S.Siboni, A.J.Jafari, M.Farzadkia, A.Esrafil, M.Gholami, Enhanced photocatalytic activity of Cu-doped ZnO nanorods for the degradation of an insecticide: Kinetics and reaction pathways, *J. Environ. Manage.*, 186 (2017) 1 - 11.
- [105] A.Bojanowska-Czajka, H.Nichipor, P.Drzewicz, B.Szostek, A.Gałęzowska, S.Męczyńska, M.Kruszewski, Z.Zimek, G.Nałęcz-Jawecki, M.Trojanowicz, Radiolytic decomposition of pesticide carbendazim in waters and wastes for environmental protection, *J. Radioanal. Nucl. Chem.*, 289 (2011) 303 - 314.
- [106] A.Kalwaslińska, J.Kesy, W.Donderski, Biodegradation of carbendazim by epiphytic and neustonic bacteria of eutrophic Chelmszyńskie Lake. *Pol. J. Microbiol.*, 57 (2008) 221 - 230.
- [107] J.Saien, S.Khezrianjoo, Degradation of the fungicide carbendazim in aqueous solution with UV/TiO<sub>2</sub> process: Optimization, Kinetics and toxicity studies, *J. Hazard. Mater.*, 157 (2008) 269 - 276.
- [108] N.A.Ghalwa, H.M.A.Shawish, M.Hamada, K.Hartani, A.A.H.Basheer, Studies on degradation of diquat pesticide in aqueous solution using electrochemical method, *Am. J. Analyt. Chem.*, 3 (2012) 99 - 105.

- [109] M.H.Florencio, E.Pires, A.L.Castro, M.R.Nunes, C.Borges, F.M.Costa, Photodegradation of diquat and paraquat in aqueous solutions by titanium dioxide: Evolution of degradation reactions and characterisation of intermediates, *Chemosphere*, 55 (2004) 345 - 355.
- [110] H.Morkoc, U.Ozgun, Zinc Oxide, Fundamentals Materials and Device Technology, Wiley-VCH, Verlag GmbH & Co. (2009)
- [111] C.Klingshirn, The luminescence of ZnO under high one and two quantum excitation, *Physica. Status. Solidi (b)* 71 (1975) 547 - 556.
- [112] M.Ahmad, S.Yingying, A.Nisar, H.Sun, W.Shen, M.Wei, J.Zhu, Synthesis of hierarchical flower like ZnO nanostructures and their functionalization by Au nanoparticles for improved photocatalytic and high performance Li-ion battery anodes, *J. Mater. Chem.*, 21 (2011) 7723 - 7729.
- [113] T.Jia, W.Wang, F.Long, Z.Fu, H.wang, Q.Zhang, Fabrication, characterization and photocatalytic activity of La doped ZnO, *J. Alloys Compd.*, 484 (2009) 410 - 415.
- [114] F.Liu, Y.H.Leung, A.B.Djurisic, A.M.Ching Ng, W.K.Chan, Native defects in ZnO, Effect on dye adsorption and photocatalytic degradation, *J. Phys. Chem.*, 117 (2013) 12218 - 12228.
- [115] Carbendazim - Fact sheet - Pesticide Action Network UK, *Pesticides News*, 57 (2002) 20-21.
- [116] Pesticide information profile, Diquat dibromide, <http://pmep.cce.cornell.edu/profiles/extoxnet/dienochlor-glyphosate/diquat-ext.html>
- [117] F.M.Fishel, Pesticide formulations, IFAS Extension, University of Florida, <http://edis.ifas.ufl.edu/pdffiles/PI/PI23100.pdf>
- [118] T.Gouge, Understanding pesticide formulations, Formulations development, Bayer ES. [http://www.cdpr.ca.gov/docs/emon/surfwtr/presentations/gouge\\_formulation\\_050510.pdf](http://www.cdpr.ca.gov/docs/emon/surfwtr/presentations/gouge_formulation_050510.pdf)

- [119] T.Kaur, A.P.Toor, R.K.Wanchoo, Parametric study on degradation of fungicide carbendazim in dilute aqueous solution using nano TiO<sub>2</sub>, *Desalin. Water Treat.*, 54 (2015) 122 - 131.
- [120] R.Rajeswari, S.Kanmani, TiO<sub>2</sub> based heterogeneous photocatalytic treatment combined with ozonation for carbendazim degradation, *Iran. J. Environ. Health. Sci. Eng.*, 6 (2009) 61 - 66.
- [121] A.D.Eaton, L.S.Clesceri, E.W.Rice, A.E.Greenberg, Standard methods for the examination of water and waste water, American Public Health Association, Washington, (2005).
- [122] J.Yu, W.Wang, B.Cheng, B.L.Su, Enhancement of photocatalytic activity of mesoporous TiO<sub>2</sub> powders by hydrothermal surface fluorination treatment, *J. Phys. Chem. C*. 113 (2009) 6743 - 6750.
- [123] M.Sayed, F.Pingfeng, H.M.Khan, P.Zhang, Effect of isopropanol on microstructure and activity of TiO<sub>2</sub> films with dominant {110} facets for photocatalytic degradation of bezafibrate, *Int. J. Photoenergy*, 2014 (2014), doi: 10.1155/2014/490264
- [124] P.Pichat, Photocatalysis and Water Purification: From Fundamentals to Recent Applications; Wiley-VCH, Verlag GmbH and Co. (2013).
- [125] A.Jamali, R.Vanraes, P.Hanselaer, T.V.Gerven, A batch LED reactor for the photocatalytic degradation of phenol, *Chem. Eng. Process.: Process Intensification*, 71 (2013) 43 - 50.
- [126] I.K.Konstantiinou, T.A.Albanis, Photocatalytic transformation of pesticides in aqueous titanium dioxide suspensions using artificial and solar light: intermediates and degradation pathways, *Appl. Catal. B: Environmental*, 42 (2003) 319 - 335.
- [127] S.Jain, R.Yamgar, R.V.Jayram, Photolytic and photocatalytic degradation of atrazine in the presence of activated carbon, *Chem. Eng. J.*, 148 (2009) 342 - 347.

- [128] H.Al-Ekabi, N.Serpone, Kinetic studies in heterogeneous photocatalysis: photocatalytic degradation of chlorinated phenols in aerated aqueous solution over TiO<sub>2</sub> supported on glass matrix, *J. Phys. Chem.*, 92 (1988) 5726 - 5731.
- [129] E.Evgenidou, I.Konstantinou, K.Fytianos, I.Poulios, T.Albanis, Photocatalytic oxidation of methyl parathion over TiO<sub>2</sub> and ZnO suspensions, *Catal. Today*, 124 (2007) 156 - 162.
- [130] S.Kaniou, K.Pitarakis, I.Barlagianni, I.Poulios, Photocatalytic oxidation of sulfamethazine, *Chemosphere*, 60 (2005) 372 - 380.
- [131] P.Mazellier, E.leroy, B.Legube, Photochemical behavior of the fungicide carbendazim in dilute aqueous solution, *J. Photochem. Photobiol. A: Chemistry*, 153 (2002) 221 - 227.
- [132] S.G.Anju, S.Yesodharan, E.P.Yesodharan, Zinc oxide mediated sonophotocatalytic degradation of phenol in water, *Chem. Eng. J.*, 189-190 (2012) 84 - 93.
- [133] K.P.Jyothi, S.Yesodharan, E.P.Yesodharan, Ultrasound, Ultraviolet light and combination assisted semiconductor catalysed degradation of organic pollutants in water: Oscillation in the concentration of H<sub>2</sub>O<sub>2</sub> formed *in-situ*, *Ultrason. Sonochem.*, 21 (2014) 1782 - 1796.
- [134] S.Ahmed, M.G.Rasul, R.Brown, M.A.Hasib, Influence of parameters on the heterogeneous photocatalytic degradation of pesticides and phenolic contaminants in waste water, *J. Environ. Manage.*, 92 (2011) 311 - 330.
- [135] M.Abdullah, G.K.C.Low, R.W.Matthews, Effects of common inorganic anions on rate of photocatalytic oxidation of organic carbon over illuminated titanium dioxide, *J. Phys. Chem.*, 94 (1990) 6820 - 6825.
- [136] C.Guillard, E.Puzenat, H.Lachheb, A.Houas, J.M.Herrmann, Why inorganic salts decrease the TiO<sub>2</sub> photocatalytic efficiency?, *Int. J. Photoenergy*, 7 (2005) 1 - 9.

- [137] K.P.Jyothi, S.Yesodharan, E.P.Yesodharan, Contaminant salts as enhancers of sonocatalytic degradation of organic water pollutants: Effect of concentration, reaction time and adsorption on the efficiency of enhancement and the fate of concurrently formed H<sub>2</sub>O<sub>2</sub>, *J. Environ. Chem. Eng.*, 10.1016/j.jece.2016.12.053
- [138] L.Zhen, Z.Suiyi, L.Zhongmou, L.Jiancong, H.Migxintuo, W.Yang, Study of phosphate removal from aqueous solution by zinc oxide, *J. Water and Health*, 13 (2015) 704 - 713.
- [139] K.E.O'Shea, I.Garcia, M.Aguilar, Titanium dioxide photocatalytic degradation of dimethyl and diethyl methyl phosphonate: effect of catalyst and environmental factors, *Res. Chem. Intermed.*, 23 (1997) 325 - 339.
- [140] G.A.Parks, The isoelectric points of solid oxides, solid hydroxides and aqueous hydroxo complex systems, *Chem. Rev.*, 65 (1965) 177 - 198.
- [141] J.Saien, A.R.Soleymani, Degradation and mineralization of Direct blue 71 in a circulating up-flow reactor by UV/TiO<sub>2</sub> process and employing a new method in kinetic study, *J. Hazard. Mater.*, 144 (2007) 506 - 512.
- [142] R.Comparelli, E.Fanizza, M.L.Curri, P.D.Cozzoli, G.Mascolo, A.Agostiano, UV induced photocatalytic degradation of azo dyes by organic capped ZnO nano crystals immobilized onto substrate, *Appl. Catal B: Environmental*, 60 (2005) 1 - 11.
- [143] C.Karunakaran, R.Dhanalakshmi, Semiconductor catalysed degradation of phenols by sunlight, *Solar Energy Mater. Solar Cells*, 92 (2008) 1315 - 1321.
- [144] K.P.Jyothi, S.Joseph, S.Yesodharan, E.P.Yesodharan, Periodic change in the concentration of H<sub>2</sub>O<sub>2</sub> formed during the semiconductor mediated sonocatalytic treatment of wastewater: Investigations on pH effect and other operational variables, *Res. J. Recent Sci.*, 2 (2012) 1-14.

- [145] J.R.Harbour, J.Tromp, M.L.Hair, Photogeneration of hydrogen peroxide in aqueous TiO<sub>2</sub> dispersions, *Can. J. Chem.*, 63 (1985) 204 - 208.
- [146] M.Muruganandham, M.Swaminathan, Photocatalytic decolourization and degradation of reactive orange 4 by TiO<sub>2</sub>-UV process. *Dyes Pigments*, 68 (2006) 133 - 142.
- [147] E.Kudlek, M.Dudziak, J.Bohdziewicz, Influence of Inorganic Ions and Organic Substances on the Degradation of Pharmaceutical Compound in Water Matrix, *Water*, 8 (2016) 532, doi:10.3390/w8110532
- [148] J.Fenoll, P.Hellin, P.Flores, C.M.Martinez, S. Navarro, Photocatalytic degradation of five sulfonylurea herbicides in aqueous semiconductor suspensions under natural sunlight, *Chemosphere*, 87 (2012) 954 - 961.
- [149] L.Rimoldi, D.Meroni, E.Falletta, V.Pifferi, L.Fulciola, G.Cappelletti, S.Ardizzone, Emerging pollutant mixture mineralization by TiO<sub>2</sub> photocatalysts. The role of the water medium, *Photochem. Photobiol. Sci.*, 16 (2017) 60 - 66.
- [150] B.Gozmen, M.Turabik, A.Hesenov, Photocatalytic degradation of Basic Red 46 and Basic Yellow 28 in single and binary mixture by UV/TiO<sub>2</sub> / periodate system, *J. Hazard. Mater.*, 164 (2009) 1487 - 1495.
- [151] L.M.P.Martinez, S.M.Torres, J.L.Figueiredo, J.L.Faria, A.M.T.Silva, *J. Water Res.*, 77 (2015) 179 - 190.
- [152] A.J.Albrbar, A.Bjelajac, V.Djokic, J.Miladinovic, D.Janackovic, R.Petrovic, *J. Ser. Chem. Soc.*, 79 (2014) 1127 - 1140.
- [153] X.Yu, Q.Ji, J.Zhang, Z.Nie, J.Liu, L.Wang, *IOP Conf. Series: Earth and Environmental Science*, 81 (2017), doi: 10.1088/1755-1315/81/1/012079.

.....✂.....



# ANNEXURES

## Annexure 1

### List of Abbreviations and Symbols

|        |  |
|--------|--|
| A.I.   | Active Ingredient                            |
| amu    | Atomic mass unit                             |
| AOPs   | Advanced Oxidation Processes                 |
| BET    | Brunauer-Emmett-Teller                       |
| BOD    | Biochemical oxygen demand                    |
| COD    | Chemical oxygen demand                       |
| DDT    | Dichlorodiphenyltrichloroethane              |
| EDTA   | Ethylenediaminetetraacetic acid              |
| ESI    | Electrospray ionization                      |
| eV     | electron-volt                                |
| FAS    | Ferrous ammonium sulphate                    |
| FTIR   | Fourier Transform-Infrared Spectroscopy      |
| g/L    | grams per Litre                              |
| HCH    | Hexachlorocyclohexane                        |
| HTPA   | 2-hydroxy terephthalic acid                  |
| IC     | Ion chromatography                           |
| ICP/MS | Inductively Coupled Plasma Mass Spectrometry |
| LC/MS  | Liquid Chromatography Mass Spectrometry      |
| LED    | Light Emitting Diode                         |
| Lux    | Luminous flux per unit area                  |
| M      | Molar  |
| mg/L   | milligrams per Litre                         |
| mM     | milli Molar                                  |
| MRLs   | Maximum Residual Limits                      |

|               |   |
|---------------|---|
| MRM           | Multiple Reaction Monitoring                  |
| NHE           | Normal Hydrogen Electrode                     |
| nm            | Nano Meter                                    |
| NTU           | Nephelometric Turbidity Unit                  |
| PL            | Photoluminescence                             |
| POPs          | Persistent Organic Pollutants                 |
| PS I          | Photosystem I                                 |
| ROS           | Reactive Oxygen Species                       |
| SCE           | Saturated Calomel Electrode                   |
| SEM           | Scanning Electron Microscopy                  |
| $t_{1/2}$     | Half-life                                     |
| TEM           | Transmission Electron Microscopy              |
| TOC           | Total Organic Carbon                          |
| TPA           | Terephthalic acid                             |
| US EPA        | United States Environmental Protection Agency |
| UV            | Ultraviolet                                   |
| V             | Volt  |
| XRD           | X-Ray Diffractogram                           |
| $\mu\text{m}$ | Micro meter                                   |
| $2\theta$     | 2 theta                                       |
| Å             | Angstrom                                      |

.....✂.....

## Annexure 2

### ||| List of Publications |||

#### A. Published in peer reviewed journals

- [1] O. M Shibin, B. Rajeev, V. Veena, E. P Yesodharan Suguna Yesodharan, Zinc oxide photocatalysis using solar energy for the removal of trace amounts of Alpha-methyl styrene, Diquat and Indigo Carmine from water, *J. Adv. Oxid. Technol.*, 17 (2014) 297-304
- [2] O. M Shibin, E. P. Yesodharan, Suguna Yesodharan, Sunlight induced photocatalytic degradation of herbicide diquat in water in presence of ZnO, *J. Env. Chem. Eng.* 3 (2015) 1107-1116.
- [3] O. M Shibin, E. P. Yesodharan, Suguna Yesodharan, Green technology in wastewater treatment: Solar photocatalysis mediated by ZnO for the removal of trace amounts of carbendazim fungicide from water, *IOSR Journal of Applied Chemistry*, e-ISSN:2278-5736 (2016) 71-86.

#### B. Presented in conferences

- [1] O. M Shibin, B. Rajeev, V. Veena, E. P Yesodharan Suguna Yesodharan, "Zinc oxide photocatalysis using solar energy for the removal of Alpha Methylstyrene, Diquat, Indigocarmine", in the 18<sup>th</sup> International conference on Semiconductor Photocatalysis and Solar Energy Conversion (SPASEC-18), San Diego, USA, November 2013; P-179.

- [2] B. Rajeev, O. M. Shibin, Suguna Yesodharan, E. P. Yessodharan, “Green technology based on solar photocatalysis for the removal of recalcitrant toxic pollutants from water: Application of LC/GC/MS for the identification of reaction intermediates” in the Third International Conference on Frontiers of Mass Spectrometry (ICMS 2017), Kottayam, Kerala ,December 2017, proceedings page no. 76.
- [3] O. M Shibin, E. P. Yesodharan, Suguna Yesodharan “Green technology in wastewater treatment: Solar photocatalysis mediated by ZnO for the removal of trace amounts of carbendazim fungicide from water”, International Conference on Emerging Trends in Engineering & Management (ICETEM-2016)”, held at Kadayirippu, Ernakulam (2016).

.....☪☪.....

## Annexure 3

### Reprints of Paper Published

- [1] Zinc oxide photocatalysis using solar energy for the removal of trace amounts of Alpha-methyl styrene, Diquat and Indigo Carmine from water, *J. Adv. Oxid. Technol.*, 17 (2014) 297-304
- [2] Sunlight induced photocatalytic degradation of herbicide diquat in water in presence of ZnO, *J. Env. Chem. Eng.* 3 (2015) 1107-1116.
- [3] Green technology in wastewater treatment: Solar photocatalysis mediated by ZnO for the removal of trace amounts of carbendazim fungicide from water, *IOSR Journal of Applied Chemistry*, e-ISSN:2278-5736 (2016) 71-86.